Empirical Studies on the Evaluation of Current Embryo Selection Techniques in Human *in-vitro* Fertilization

A thesis submitted to the University of Kent for the degree of

DOCTOR OF PHILOSOPHY

in the Division of Natural Sciences

July 18th, 2022

Andrea R Victor

Department of Biosciences

1. Declaration

No part of this thesis has been submitted in support of an application for any degree or qualification of the University of Kent or any other University or Institute of Learning.

Andrea Victor

July 10th, 2022

2. Acknowledgements

Without the extraordinary support of my advisors, friends and family, there is no way I could have accomplished the monumental task of (hopefully) getting a PhD while working full time and having two children (somewhere in there). Over the past five years, there are innumerable moments in which I felt completely overwhelmed; and now, looking back, I find myself completely overwhelmed at the generosity of time, love and support that was given to me to accomplish this goal. It's easy to think of all the people I need to thank – but what's much harder is finding the words to do so.

Professor Griffin – thank you for taking me on as one of your students. This was an incredible opportunity and I feel I've grown so much under your supervision. I'll forever be grateful for all your support. I must add – I'll never be happy with what COVID did to our world, but if there is one silver lining, it made virtual meetings the norm; this afforded me even more access to you and allowed me to feel like a real member of your Kent-based lab team.

I'd like to thank Dr. Zouves, Dr. Barnes and all ZFC lab members past and present for providing me a forum by which to perform the research that forms the bulk of this thesis.

I am forever indebted to my parents for flying cross country way too many times to help care for my daughters and keeping us fed and financially afloat. And of course, for never

forgetting to ask "how much longer until I graduate" – payback I suppose for all of the times I asked "are we there yet?"

I am grateful for my little girls, Amelie and Eloise. They both have attended their fair share of Griffin lab meetings at the breakfast table and at the ripe age of 3 and 6 have some working knowledge of embryonic mosaicism. They have taught me how to focus amongst massive distraction, and thanks to them, I strive to be better and work harder – thank you both for the inspiration.

And lastly, I truly have no words for my husband and partner in both crime and research, Mano. I am so fortunate to have a scientific mentor that I have unlimited access to (even at two in the morning) should I have questions or require clarity on a concept or idea. Supporting me at my best and always at my worst, I have leaned on him in so many ways, and this PhD would have been an impossible task without him. I am forever grateful.

3. Incorporation of Published Work

This thesis incorporates the following body of work.

Book Chapter/Review:

Victor AR, Ogur C, Thornhill A, Griffin DK.
Preimplantation Genetic Testing for Aneuploidies: Where We Are and Where We're Going. Preimplantation Genetic Testing: Recent Advances in Reproductive Medicine, Editors D. Griffin and G. Harton, 2020, CRC Press.

Peer-Reviewed Journal Articles:

Victor AR, Griffin DK, Brake AJ, Tyndall JC, Murphy AE, Lepkowsky LT, Lal A, Zouves CG, Barnes FL, McCoy RC, Viotti M.
Assessment of aneuploidy concordance between clinical trophectoderm biopsy and blastocyst.
Hum Reprod. 2019 Jan 1;34(1):181-192.

Victor AR, Tyndall JC, Brake AJ, Lepkowsky LT, Murphy AE, Griffin DK, McCoy RC, Barnes FL, Zouves CG, Viotti M.
One hundred mosaic embryos transferred prospectively in a single clinic: exploring when and why they result in healthy pregnancies.
Fertil Steril. 2019 Feb;111(2):280-293.

Viotti M, **Victor AR**, Barnes FL, Zouves CG, Besser AG, Grifo JA, Cheng EH, Lee MS, Horcajadas JA, Corti L, Fiorentino F, Spinella F, Minasi MG, Greco E, Munné S.
Using outcome data from one thousand mosaic embryo transfers to formulate an embryo ranking system for clinical use.
Fertil Steril. 2021 May;115(5):1212-1224.

Victor AR, Brake AJ, Tyndall JC, Griffin DK, Zouves CG, Barnes FL, Viotti M.
Accurate quantitation of mitochondrial DNA reveals uniform levels in human blastocysts irrespective of ploidy, age, or implantation potential.
Fertil Steril. 2017 Jan;107(1):34-42.e3.

Victor AR, Griffin DK, Gardner DK, Brake A, Zouves CG, Barnes FL, Viotti M.
Births from embryos with highly elevated levels of mitochondrial DNA.
Reprod Biomed Online. 2019 Sep;39(3):403-412.

Viotti M, **Victor AR**, Griffin DK, Groob JS, Brake AJ, Zouves CG, Barnes FL.
Estimating Demand for Germline Genome Editing: An In Vitro Fertilization Clinic Perspective.
CRISPR J. 2019 Oct;2(5):304-315.

Victor AR*, Mauricio M*, Griffin DK, Duong T, Bolduc N, Farmer A, Garg V, Hadjantonakis AK, Coates A, Barnes FL, Zouves CG, Greene WC, Viotti M.
SARS-CoV-2 Can Infect Human Embryos.
bioRxiv 2021.01.21.427501. Under revision with Scientific Reports.

Abstracts:

Victor AR, Griffin DK, Zouves CG, Barnes FL, Viotti M.
SARS-CoV-2 and the Human Embryo
Northern California Association of Reproductive Biologists Webinar, March 2021

Victor AR, Griffin DK, Zouves CG, Barnes FL, Viotti M.
Chromosomal profiling of preimplantation embryos: where we are and where we are going
International IVF Initiative (I3) Webinar, August 2020

Victor AR
PGT-A: The Future
Carlsbad Embryo Biopsy Workshop
Carlsbad USA 2019

Victor AR, Griffin DK, Zouves CG, Barnes FL, Viotti M.
ICM, TE and Mosaicism – Does it Matter?
South West Embryology Summit
Pheonix, USA 2018

Victor AR, Griffin DK, Zouves CG, Barnes FL, Viotti M.
Aneuploidy Concordance Between Trophectoderm And Inner Cell Mass By Next-Generation Sequencing.
Cambridge Healthtech Institute's Advances in Reproductive Genetic Diagnostics, Boston, USA 2017

Victor AR, Griffin DK, Zouves CG, Barnes FL, Viotti M.
The Effects Of Laser Manipulation On Biopsy Karyotype In PGS
Preimplantation Genetic Diagnosis International Society (PGDIS),
Valencia, Spain 2017

Victor AR, Viotti M.
Mitochondrial DNA As A Marker For Ploidy And Implantation In IVF
Fertility and Sterility Journal Club Global, 2017

4. Table Of Contents

5. Abbreviations

ACE2   Angiotensin Converting Enzyme 2

ADO   Allele Drop Out

AMA   Advanced Maternal Age

AMH   Anti-Müllerian Hormone

ANOVA   Analysis of variance

ART   Assisted Reproductive Technology

ATP   Adenosine triphosphate

Avg   Average

BF   Blastocoel Fluid

BSA   Bovine Serum Albumin

CDC   Centers for Disease Control and Prevention

cfDNA   Cell-free DNA

CGH   Comparative genomic hybridization

CNV   Copy Number Variation

COVID   Coronavirus Disease

CPM   Confined Placental Mosaicism

Ct   Cycle threshold

CVS   Chorionic Villus Sampling

DNA   Deoxyribonucleic Acid

DOR   Diminished Ovarian Reserve

FISH   **Fluorescence In Situ Hybridization**

FSH   **Follicle Stimulating Hormone**

GGE   **Germline Genome Editing**

hESC   **Human Embryonic Stem Cell**

ICM   **Inner Cell Mass**

ICSI   **Intra-Cytoplasmic Sperm Injection**

IRB   **Institutional Review Board**

IVF   **In-Vitro Fertilization**

LD   **Linkage Disequilibrium**

MF   **Male Factor**

mRNA   **Messenger Ribonucleic Acid**

mtDNA   **Mitochondrial DNA**

nDNA   **Nuclear DNA**

NGS   **Next Generation Sequencing**

NIPT   **Non-invasive Prenatal Testing**

ns   **Not Significant**

OP/B   **Ongoing Pregnancy/Birth**

PB   **Polar Body**

PBS   **Phosphate-Buffered Saline**

PCA   **Principal Component Analysis**

PCOS   **Polycystic Ovarian Syndrome**

PCR   **Polymerase Chain Reaction**

PGC	**Primordial Germ Cell**
PGT	**Pre-implantation Genetic Testing**
PGT-A	**PGT - Aneuploidies**
PGT-M	**PGT - Monogenic**
PGT-P	**PGT - Polygenic**
PGT-SR	**PGT - Structural Rearrangements**
POC	**Product of Conception**
qPCR	**Quantitative Polymerase Chain Reaction**
RIF	**Repeat Implantation Failure**
RM	**Repeat Miscarriage**
RNA	**Ribonucleic Acid**
RT-qPCR	**Reverse Transcription Polymerase Chain Reaction**
S	**Spike Protein**
SARS	**Severe Acute Respiratory Syndrome**
SM	**Spent Media**
SNP	**Single Nucleotide Polymorphism**
STDEV	**Standard Deviation**
TE	**Trophectoderm**
UPD	**Uniparental Disomy**
WGA	**Whole Genome Amplification**

6. Abstract

In vitro fertilization (IVF) is an assisted reproductive technology (ART) that aims to assist intended parents overcome fertility issues, including an infertility diagnosis and other barriers to conception. It involves harvesting gametes from a male and female provider to generate embryos, with the subsequent transfer of these embryos into a uterus with the goal of establishing a viable pregnancy and a healthy take home baby.

Technological advances in the field have led to drastic improvements in outcomes over the years, including selection methods of the most competent embryo for transfer within a cohort. Embryo selection tools include evaluating an embryo's chromosomal composition (preimplantation genetic testing for aneuploidy, or PGT-A) and other biomarkers/conditions that may have an impact on implantation and the ensuing pregnancy. Notably, many such methodological innovations (even some routinely used in the industry) still lack appropriate validation and are in dire need of unbiased vetting. The primary goal of this thesis is to evaluate current embryo selection techniques. This work encompasses the following items:

(1) Evaluating if current DNA sampling techniques (biopsy) of an embryo is an adequate predictor of the remaining embryo, which is a central premise of preimplantation genetic testing for aneuploidy (PGT-A); I conclude that a clinical trophectoderm (TE) biopsy correctly predicts aneuploidy in the inner cell mass (ICM) in the vast majority of cases

when one or several chromosomes are abnormal, but aneuploidy of segmental (sub-chromosomal) nature is not well correlated in paired TE-ICM samples.

(2) Assessing of clinical outcomes of embryos classified as mosaic by routine clinical biopsy; I conclude that embryos classified as mosaic by PGT-A are associated with different clinical outcomes when compared to embryos diagnosed as euploid by PGT-A, namely reduced rates of implantation, ongoing pregnancy, and live birth.

(3) Defining features of mosaicism to rank embryos by their potential for a positive outcome; I conclude that mosaic level (putative percent aneuploid cells in the biopsied sample) and mosaic type (aneuploidy involved in the mosaicism) correlate with specific clinical outcomes and can be used to prospectively rank mosaic embryos in the clinical setting.

(4) Evaluating mitochondrial DNA (mtDNA) levels determined from a clinical trophectoderm biopsy as a potential predictor of implantation; I conclude that accurate calculation of mtDNA levels shows there is no association with embryo ploidy or implantation potential.

(5) Studying the health of babies from embryos reported to have high mtDNA levels; I conclude that unusually high mtDNA levels did not preclude blastocyst implantation and healthy births.

(6) Performing a theoretical evaluation on the potential application of genome editing to human embryos such that abnormal embryos may be repaired and reclassified as transferable; I conclude that demand for germline genome editing (GGE) to cure heritable genetic diseases is grossly over estimated, mainly due to the role of preimplantation genetic testing, but nevertheless future applications may exist to correct chromosomal abnormalities and rescue aneuploid embryos.

(7) Exploring SARS-CoV-2 infection and its implications on embryo viability and its potential effect on strategies for embryo selection; I conclude that preimplantation embryos are vulnerable to SARS-CoV-2 infection, which can compromise their health and viability.

The data presented in this thesis empirically evaluates the utility of several embryo selection techniques on the IVF cycle. The array of methods available is certain to grow in time; to ensure that new instruments of selection or refinements to current tools continue to have a positive effect on outcomes and success rates, they must be evaluated thoroughly before being applied in the clinic in full force.

7. List Of Figures

Main Figures

Supplementary Figures

8. List Of Tables

Main Tables

Supplementary Tables

9. Introduction

9.1. The ART of embryo selection

In-vitro fertilization (known more commonly by its acronym "IVF") has a long and distinguished history as a clinical approach to assisted reproduction technology (ART) (Figure 1). Its first clinical introduction in 1978 (Steptoe and Edwards, 1978) preceded decades of basic research and led to the award of a Nobel Prize for Medicine to Bob Edwards in 2010. The details of the technical developments and practices of how IVF works are beyond the scope of this thesis however contemporary approaches are dealt with in the Materials and Methods section(s) later. In essence however the procedure involves a couple presenting in a fertility clinic with a reproductive issue, and counselled as to the right course of action in order that they may ultimately conceive a healthy child. IVF is one of many courses of action and involves ovarian stimulation of the female partner to produce a large number of eggs. Exposure to the sperm, either through putting both sets of gametes (including a selected motile fraction) together, or intracytoplasmic sperm injection (ICSI) directly introducing a single sperm into the egg has the intention of forming single cell zygotes. From this, the skill of the embryologist comes into play to select only embryos that are thought to have one pro-nucleus form each parent (2PN). As the embryo develops, the embryologist is also called upon to rank those embryos thought more likely (on the basis of morphology) to develop into pregnancies and healthy live births. Multiple embryo transfer strategies (i.e. implanting more than one embryo) are largely giving way to the notion of transferring only one embryo per treatment cycle, to

avoid the obstetric complications of multiple live births (twins, etc.). If all goes well, a normal live birth ensues, with success rates varying around the world from country to country and from clinic to clinic. The ultimate aim is "one egg, one embryo, one baby" per treatment cycle however even the best clinics are far from that. IVF is still, at its heart, an unsuccessful procedure and success rates of over 50% per treatment cycle is impressive for any clinic (with most not achieving this). To this end, there is much to do in order that IVF may be improved, and couples have their own genetic children.

Figure 1. The IVF Cycle.
After the female patient undergoes ovarian stimulation, eggs are retrieved and fertilized in vitro with the male's sperm, ideally resulting in a group of embryos. A selection process occurs to prioritize the transfer of one embryo from those amongst the cohort. If no pregnancy is achieved or an additional pregnancy is desired, the next embryo in the prioritization list is used, and so forth. Evaluation of current techniques of embryo selection is the central theme of this thesis.
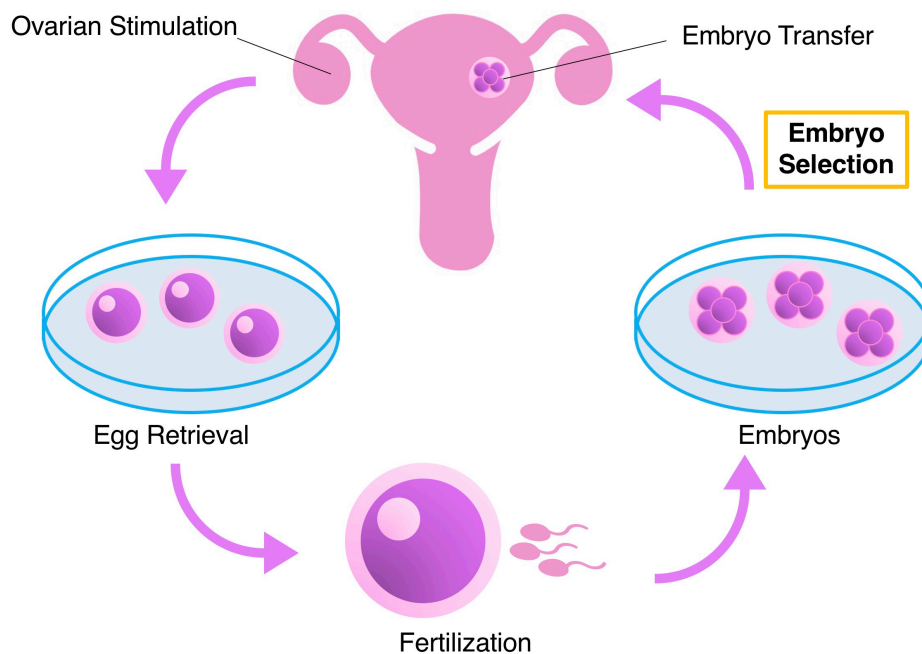
The concept of determining the genetic status of the embryo was also introduced by Bob Edwards (Gardner and Edwards 1968). They applied IVF technology in rabbits, detecting the presence of Barr Bodies – inactive sex chromosomes (their presence being indicative of female genetic sex). This was the first chronicled example of preimplantation genetic testing (PGT) (1). The first reported use of PGT clinically however was by Alan Handyside and colleagues (Handyside et al 1990). PGT is an adjunct treatment to IVF, designed either to prevent the transmission of heritable disorders, or to improve IVF success. It can be broken down into four types:

- For monogenic disorders (PGT-M)

- For inherited structural chromosome rearrangements (PGT-SR)

- For polygenic traits (PGT-P)

- For *de-novo* chromosome disorders such as aneuploidy (PGT-A)

The latter (PGT-A) is controversial and the topic of this thesis. In addition to the detection of whole chromosome aneuploidy, it can be used to detect partial chromosome gains and losses that also arise *de-novo* (in this way it is distinct from PGT-SR in that the parents are not known carriers of a balanced rearrangement) and has recently been expanded to examine the relevance of mitochondrial DNA content, its relationship to aneuploidy and whether it can be used as a measure to rank embryos for transfer. Moreover, it has recently been suggested that gene editing may be used as an adjunct or alternative to PGT. Finally, the spectre of Covid has entered all our consciousness and lives – whether the virus can actually enter the life of a preimplantation embryo however has not been determined.

With the above in mind, this thesis deals substantively with the concept of improving IVF through PGT-A, and mitochondrial assays, then latterly considers gene editing and the possibility of Covid infection. Essentially, PGT and some aspects of gene editing, as well as any future assay for Covid infection, all involve two steps in addition to the regular IVF procedure: **Sampling** (taking cellular material to make the diagnosis) and **diagnosis** (determination of genomic content on the assumption that the sample is representative of the whole embryo).

9.2. Sampling Methods for PGT

Traditionally, there are three sources from which cells can be biopsied for use in PGT. These are polar bodies from oocytes, blastomeres from cleavage-stage embryos and trophectoderm cells from blastocysts. In an ideal world, the timing of biopsy should be to ensure the most accurate identification of chromosome imbalance and the result on the biopsied cell(s) should correlate to an identical abnormality in the remainder of the embryo.

9.2.1. Polar body biopsy

Polar body (PB) biopsy was first introduced to identify oocytes that carry disease alleles in women heterozygous for a genetic disease (2). Polar bodies are the by-products of meiosis I and II and their biopsy is not likely to negatively impact an embryo's future development. Polar bodies may be removed either one at a time or simultaneously

following fertilization (Figure 2) (3), but because they might undergo rapid fragmentation, any delay in biopsy could result in misdiagnosis or no result. The primary advantages of polar body biopsy are that it is less invasive than other forms of biopsy and it inherently creates a greater time window for analysis when performing transfer for a fresh cycle. Disadvantages lie in the fact that polar bodies cannot be used to detect paternal chromosomes, nor post zygotic errors. Consequently, polar body biopsy is limited in PGT to the diagnosis of meiotic abnormalities, monogenic traits and chromosome translocations of maternal origin. Polar body gained popularity when it was proposed as an alternative to cleavage stage biopsy (4, 5), which after randomized controlled trials (RCTs) (6, 7) demonstrated limited applicability of PGT-A. Indeed, the first successful live birth following 24 chromosome screening (see later sections) was performed following polar body biopsy (8).

Figure 2. Polar Body Biopsy Pre- or Post- Fertilization.
Polar bodies (PBs) are removed using a fine needle, either pre-fertilization when only PB1 is present, or after fertilization when both PB1 and PB2 are present.
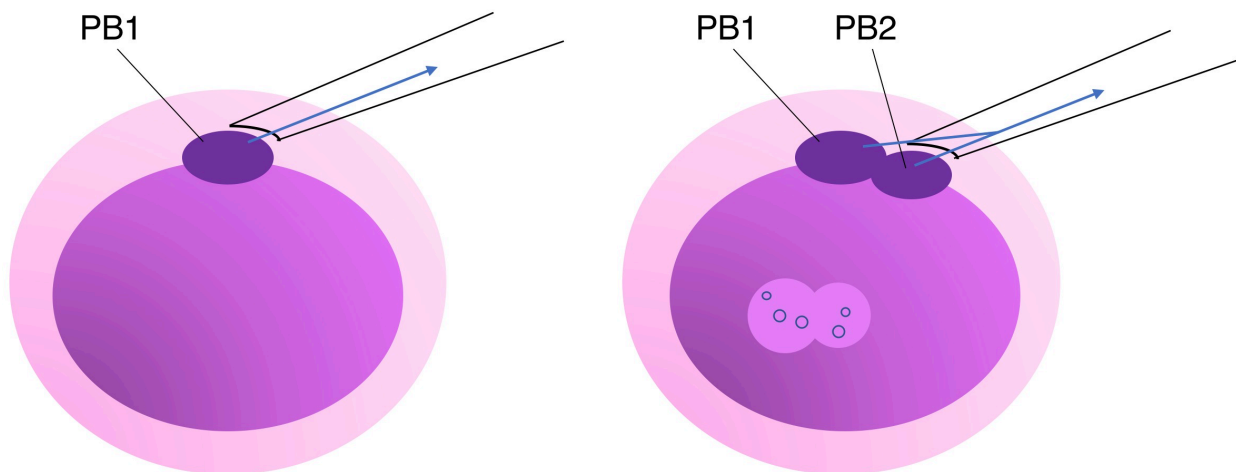
Detecting chromosome segregation errors following polar body biopsy is limited to meiotic abnormalities. This is important because analysis on serial biopsies of embryos have demonstrated that approximately half the embryos (47.6%) found to have an abnormality carry aneuploidies other than female meiotic-derived ones (9). Indeed, analysis of polar body biopsy material has the least predictive value for whole embryo ploidy and implantation potential compared to the other two methods (10). Moreover, prediction of the ploidy status of PBs with reciprocal aneuploidies (e.g. where the first polar body has disomy 21 and the second has nullisomy 21) raises another issue: That is, reciprocal aneuploidies of the same chromosomes are nearly always euploid (11). A further consideration is the differentiation between single chromatid and whole chromosome losses and gains, when single chromosome losses are the most prevalent. It has been suggested that pooling first and second polar body ahead of DNA amplification could alleviate this problem and reduce costs (12).

A recent multicentre RCT involving 23 chromosome testing of polar bodies for PGT-A (using the array CGH platform – see below) was performed (ESTEEM – the ESHRE Study into The Evaluation of oocyte Euploidy by Microarray analysis) (13) involving women aged 36-41. Primary results were deemed "disappointing" because the likelihood of a live birth within one year did not increase. One positive result however was that the miscarriage rate was significantly lower than the no intervention group (14), which may provide a sufficient incentive for some patients.

9.2.2. Cleavage-stage (blastomere) biopsy

Blastomere (cleavage stage) biopsy is performed by the removal of one or two cells from a day-three embryo that has at least six (Figure 3). Calcium and Magnesium -free media is commonly used. In order to open the zona pellucida chemical (acid Tyrode's), mechanical or, most commonly, laser assisted approaches may be used. This approach assesses both maternal and paternal contributions to the embryo and allows sufficient time for analysis to be performed before transfer of a fresh embryo, even if transport PGT (i.e. sending samples to specialist diagnostic labs) is used. This technique is the oldest and, until recently, the most widely applied method for PGT (15), but nonetheless is prone to technical and biological drawbacks: Firstly, the mosaicism rate is at its highest level in cleavage stage embryos (see discussion of chromosome mosaicism in later sections), regardless of maternal age; moreover, the potential damage of significantly decreasing cell number on further development is significant (16).

Figure 3. Blastomere (Cleavage Stage) Biopsy.
A broad needle is used to collect one (or two) blastomeres.
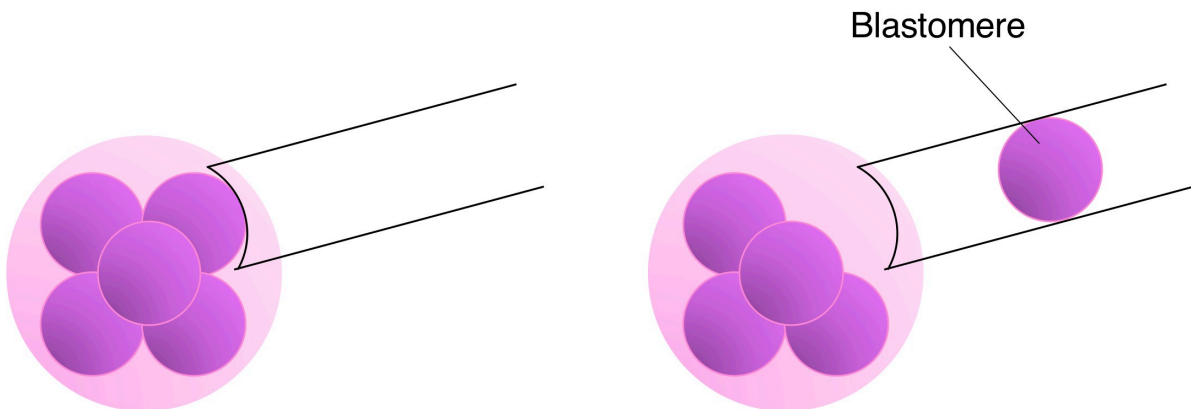
Cleavage stage biopsy was, quite probably, behind the biggest controversies surrounding PGT-A. Some initial, retrospective, studies proved positive (17, 18) but later RCTs demonstrated either no improvement or an adverse effect on IVF outcome (7, 19). The subsequent melee that ensued shows little sign of abating with some arguing PGT-A in its entirety should be discontinued on the basis of these results, but others making the point that it is cleavage stage biopsy that is the problem. With a mean of eight cells, removing one or two incurs the serious risk of impeding an embryo's developmental potential, and could be operator dependent. The initial RCTs were in fact severely criticized on the basis that one interpretation of the Mastenbroek et al (2007) data is that there was a third group in the manuscript (briefly mentioned) that had biopsy but no PGT-A. A 6% live birth rate in this group compared to 16.8% in the PGT-A cohort (and 14.7% in controls) provides evidence, some argue, that cleavage stage biopsy in the hands of these particular authors may be the root cause of these adverse outcomes.

The effect of cleavage stage biopsy on developing embryos was assessed in a RCT using a paired design (20). That study demonstrated a relative 39% reduction in implantation rates as a result of cleavage stage biopsy, but no measurable adverse effect after trophectoderm biopsy (20). There is also some evidence from morphokinetic analysis that developmental dynamics are impaired after blastomere biopsy, causing delayed compaction and altered hatching (21, 22). A further drawback of blastomere biopsy is that with only one cell to analyse, the process is prone to false positive and negative results.

Taking all these things into account, cleavage stage biopsy has largely been discontinued and replaced by blastocyst stage (trophectoderm) biopsy for all forms of PGT.

9.2.3. Blastocyst stage (trophectoderm) biopsy

Blastocyst-stage (trophectoderm) biopsy became the most commonly used form after improved culture conditions have led to much higher blastulation rates (Figure 4)(23). Trophectoderm biopsy can either be performed directly on a day 5-6 blastocyst or by the biopsy of a small part of the trophectoderm, that had herniated through the opening previously created on day three.

Figure 4. Blastocyst-Stage Trophectoderm Biopsy.
A group of 5-10 cells is isolated from the trophectoderm (TE) layer.
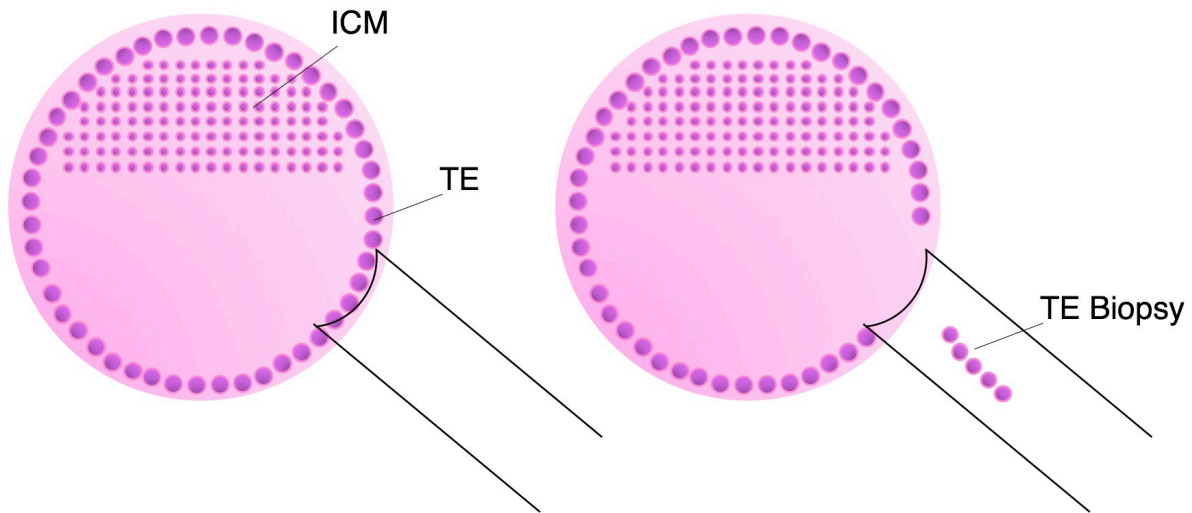
Trophectoderm biopsy has many advantages. First, the blastocyst has >100 cells, and thus the removal of between two and ten is less likely to have an adverse effect on future

embryo development. Amplification failure, misdiagnosis and allele dropout (ADO) is lower compared to cleavage stage biopsy (24) and there is evidence that mosaicism is lower in blastocysts compared to cleavage stage IVF embryos (25). Using this natural selective advantage, the cytogenetic analysis of blastocysts not only reduces the relative cost of PGT-A, but also reportedly increases implantation rate and multiple pregnancy risk as a result of single euploid blastocyst transfer (26, 27). Moreover, there has been a suggestion that the trophectoderm biopsy technique is possibly less operator dependent thus reproducible across various IVF clinics (28). For this reason, RCTs demonstrating benefits of PGT-A, were carried out using trophectoderm (26, 29-31) apart from one that used cleavage stage biopsy (32), which also demonstrated the benefits of PGT-A.

While losing 5-10 cells of the TE in a biopsy for PGT-A has largely been shown to be inconsequential to the viability of a blastocyst (20), the physical process of collecting a TE biopsy can be damaging to the embryo if done incorrectly. It is also a cumbersome technique that requires highly skilled embryologists. As a result, there is great interest in developing methods of non-invasive PGT-A.

9.2.4. Blastocentesis

Blastocentesis refers to the extraction of blastocoelic fluid (BF) for subsequent analysis (Figure 5). BF is known to contain DNA originating from embryonic cells as well as proteins involved in embryonic development (33, 34). In this technique, BF is aspirated through an ICSI pipette, a process of limited invasiveness. Each blastocysts yields

approximately 0.01μL BF, which is subsequently amplified by WGA (35). In a study performed to investigate the potential of blastocoelic fluid as a diagnostic sample, the DNA could be obtained in 82% of the sampled fluids, 97.1% of the diagnosis results were in concordance with trophectoderm cells (36). Other studies have failed to replicate these rates of concordance, as highlighted in a report in which only 40% of blastocoelic fluid cases reflected the ploidy of the embryo (37). Recently, it was shown that aneuploid embryos contained significantly higher overall quantities of DNA than euploids in the blastocoelic fluid, likely due to higher rates of apoptosis in aneuploid cells (38). This could lead to a minimally-invasive PGT-A method that simply quantifies DNA amounts in the BF. Future studies with large sample sizes will be needed to validate this proposed method.

Figure 5. The Blastocentesis Procedure.
A fine needle is inserted through the zona pellucida and between junctions of neighboring TE cells to access the blastocyst cavity, from where the BF is sucked into the needle.
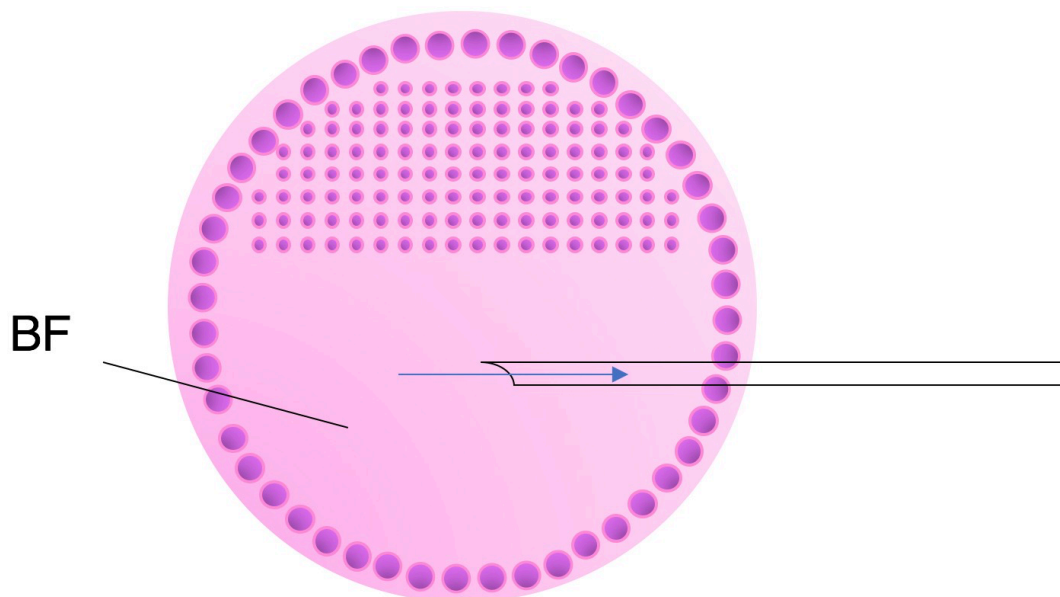
9.2.5. Analysis of spent culture medium

True non-invasive PGT-A (niPGT-A) would mean letting the embryo grow undisturbed until vitrification or fresh transfer and still somehow gain knowledge on its viability. Efforts are currently focused on analysis of spent medium (SM) for biomarkers predictive of embryo state and clinical outcome, including DNA, RNA, protein, metabolites, and exosomes. Initial efforts mainly focused on amino acid analysis in the SM but showed limited potential for routine application (39, 40).

More recently, research has focused on DNA in SM. Cell-free DNA (cfDNA) derived from the embryo is present in the SM through processes that are yet to be understood, but likely involve apoptosis and other cell death pathways or DNA-based signalling. Whether the cfDNA is of sufficient quantity and quality to reliably be analysed, and whether it is truly reflective of the embryo's karyotype, are questions currently being investigated in a fast-moving field. A flurry of recent reports using state-of-the-art NGS platforms observed ploidy concordance rates between SM and blastocyst cells in the 80-95% range (37, 41-44). Nevertheless, it is crucial to note that the SM analysed in those studies might not have been pristine; in every instance the authors performed some procedure that could artificially increase the abundance of cfDNA in the SM, such as assisted hatching, freeze-thaw cycle, or invasively isolating a TE biopsy before collecting the SM. Only one recent publication has avoided such confounding procedures altogether in addition to having been conducted blindly and prospectively, and it reports 78.7% concordance rate for ploidy and sex between SM and TE (45). Various efforts are underway to modify the

culture methods, spent medium collection method, WGA chemistry, and NGS process and analysis to continue inching up the concordance rates. It is important to note that 100% concordance between SM and TE may not be realistic and this could be because SM turns out to be a more accurate representation of the embryonic genotype for reasons that are not yet well understood. Better rates of concordance are observed in embryos cultured to embryonic day 6 or 7, over those cultured only to day 5; but the most successful blastocysts are typically those vitrified on developmental day 5 (46). Maternal DNA contamination in the medium, mainly through cumulus cells, can affect the ploidy as well as the sex in the PGT-A results (47). How sensitive is niPGT-A regarding segmental deletions/duplications, and mosaicism?

Interestingly, niPGT might not need to be regarded as a one-to-one substitute of TE biopsy-based PGT-A. It might serve as a low-resolution screening tool for laboratories that choose not to perform TE biopsy. Or it can be done in parallel with the TE analysis. One study shows that concordant euploidy in paired BM-TE samples predicts better likelihood of implantation for an embryo than when its TE biopsy is euploid but its BM shows aneuploidy (52.9% vs. 16.7%, respectively)(45).

Due to mosaicism, some might argue that looking at the content of SM may be a better evaluation of the embryo than an individual trophectoderm biopsy. This is a rapidly evolving field and, if successful, will revolutionize the PGT-A landscape.

9.2.6. Morphokinetics and time-lapse for aneuploidy detection

Another avenue being explored to evaluate embryos in a non-invasive way is the continuous monitoring via time-lapse imaging technology during culture. Some studies have indicated that embryos exhibit different kinetic behavior in cell division patterns according to their ploidy (48-51). Other reports have refuted that claim (52-54).

Another set of studies have explored the correlation between morphokinetic patterns and implantation potential, rather than strict ploidy state with promising results (55, 56).

Time-lapse monitoring must not necessarily need to replace PGT-A altogether but might instead offer an added benefit as the two technologies can be performed in parallel. For instance, morphokinetic patterns might help rank embryos classified by PGT-A as euploid with highest chance of implantation and decreased chance of miscarriage, as has recently been attempted with some success (57, 58). Future work will need to address this point.

9.3. Vitrification and "freeze-all" strategies

Biopsy timing also affects the decision of whether to vitrify all of the embryos ("freeze all") embryos or perform embryo transfer using fresh embryos in the first cycle.

In fresh cycles, the time for analysis is limited by the implantation window of the blastocyst. Cryopreservation is thus an attractive option, at least for subsequent cycles, and this was initially thought to be a major drawback. Despite this, the development of

enhanced culture conditions and improved vitrification techniques led to improved blastulation rates, more embryos available for trophectoderm biopsy and improved survival post-thawing (59). Indeed IVF (regardless of PGT) has seen improvement in embryo cryopreservation techniques and, recently, there has been a change in emphasis towards embryo vitrification with a view to a later transfer ("freeze-all") possibly associated with milder, or no ovarian stimulation. Therefore, while to some degree increased pregnancy success rates have been associated with PGT-A technologies getting better (i.e. improved blastocyst biopsy and 24 chromosome screening) improved vitrification and "freeze all" may play a part. The transfer of previously vitrified single blastocysts reportedly leads to equivalent live-birth rates and improved neonatal outcomes compared to fresh transfers (60). An additional factor is the improved knowledge of the endometrium in determining the window of implantation through studies of the endometrial transcriptome (61, 62). Natural, or low stimulation cycles appear to be preferable over traditional stimulation regimes, when gene expression profiles are used to determine implantation window (63). Moreover, transfer in subsequent cycles may also allow for preparation of a more physiological and receptive endometrium e.g. through consideration of the microbiome.

9.4. Using IVF technology to detect chromosomes – PGT-A

As mentioned above, the first clinical PGT was performed by Handyside et al (1990). It involved polymerase chain reaction (PCR) of a Y-chromosome-specific repeat sequence in order to detect the presence of the male determining chromosome and thereby

determine genetic sex. By only transferring female embryos, the transmission of X-linked conditions in which the mother was a carrier (64) could be controlled, such that none of the progeny would be affected. The detection of a Y specific sequence was however incredibly prone to both false positive and false negative results and was soon replaced by fluorescence in-situ hybridization (FISH) technology (65, 66) detecting X and Y specific probes in a dual colour strategy. Cytogenetic detection of sex chromosomes preceded the practice of testing embryos for monogenic disorders directly (in the case of sex-linked disorders, unaffected males could be identified) and also for chromosomal aneuploidies extra or missing chromosomes.

As this thesis rarely deals directly with PGT-M, PGT-SR and PGT-P, detection methods for these approaches are only touched upon in this thesis when relevant to PGT-A (in reality the methods are common for PGT-SR). Indeed, PGT's most prominent and controversial use is for aneuploidy testing of oocytes and embryos - PGT-A and that forms the basis of the bulk of this thesis. PGT-A serves a threefold purpose. First, it tests for chromosomal aneuploidies that can lead to the birth of babies with chromosomal copy number syndromes (e.g. Down Syndrome – trisomy 21). Second, it has the potential to reduce miscarriage rates as approximately half of all first trimester abortions are chromosomally abnormal. Finally, it is often prescribed with the intention of improving IVF outcomes e.g. by reducing time to pregnancy.

At its inception, the goal of PGT-A was to reduce the risk of offspring with live-born chromosomal syndromes. Fluorescence in-situ hybridization (FISH) technology was used to obtain copy number information of high-risk chromosomes 13, 18, 21, X and Y (67) (17). Embryos that did not have the normal complement of targeted chromosomes could then be deselected for transfer (see technical section below for FISH).

The panel of screened chromosomes soon grew to include chromosomes 16 and 22, both of which are common in spontaneous abortions (68). Notably, screening of chromosomal abnormalities associated with increased miscarriage prior to implantation marked a seminal shift in the previously limited uses of PGT. Such studies signified the first instances of harnessing this technology beyond reducing the risk of disease in offspring and broadened its application to improving IVF outcomes. As such, exploiting this technology in this manner facilitated achieving viable pregnancies more likely to result in healthy live-births whilst reducing the risk of miscarriage. Referral categories, therefore, included treatment of patients experiencing recurrent miscarriage (RM) and recurrent implantation failure (RIF) (69). Additionally, cited uses include the treatment of patients of advanced maternal age (AMA) (69) – the most common use of PGT-A - and severe male factor infertility (70, 71) both of which result in increased levels of embryonic aneuploidy.

Although 24 chromosome FISH was eventually reported (72, 73), technical limitations prevented FISH from expanding its screening panel much beyond 12-chromosomes for routine use, establishing a detection ceiling of 60-80% of all aneuploid embryos (74).

Given that aneuploidy can affect all twenty-four chromosomes in the early human embryo (75), this could be a contributing factor as to why randomized controlled trials failed to show improvements in live birth rates utilizing this technology (7, 76). Other reasons might be sub-optimal (cleavage stage) biopsy protocols that led to embryo damage. A more comprehensive PGT-A test was thus needed if PGT-A were to be taken seriously as a means of improving IVF outcomes. Genome-wide molecular methodologies like quantitative PCR, array comparative genomic hybridization (aCGH) and next-generation sequencing (NGS) were thus introduced.

Twenty-four chromosome screening methodologies brought with them increased resolution, offering information on the karyotype of an embryo beyond uniform whole chromosome aneuploidy. This included the possibility of gaining insight into embryonic mosaicism and segmental aneuploidies. Such in depth information offers practitioners and patients additional ways to select chromosomally normal embryo(s) for transfer within a cohort. Concurrently, continued advancement in the IVF laboratory has meant improved fertilization, better embryo culture systems, less damaging biopsy protocols and higher quality embryos. In addition, improved implantation rates and refinements in cryopreservation methods have made the transfer of fewer embryos (preferably a single embryo) a categorical requirement to prevent high-risk multiple pregnancy. Taken together, these technological advancements further underscore the need for more refined, objective embryo selection methods such as those provided by PGT-A.

One of the biggest challenges in PGT is the small amount of starting material available for analysis. Depending on the developmental stage at which the biopsy is performed, between one and ten (but typically no more than five from a blastocyst) are removed from the embryo and used for testing. Like most diagnostic tests, a high level of accuracy is required given the potential ramifications of a misdiagnosis. A false negative result would mean an abnormal embryo is diagnosed as normal and could result in miscarriage, ongoing pregnancy or live birth of a chromosomally abnormal baby. Alternatively, a false positive may result in a chromosomally normal embryo being misdiagnosed and discarded.

9.4.1. Fluorescence in-situ Hybridization (FISH)

FISH utilizes fluorescently labeled DNA sequences (probes) to visualize specific chromosomal regions. The probes contain complementary sequences that bind to a region of interest and can be visualized using fluorescent microscopy. When applied in the context of PGT-A, biopsied cell(s) from gametes/embryos are fixed to a slide. Probes are hybridized to the fixed material, and the presence or absence of each target chromosomal region is indicated by whether or not the fluorescent tags/signals are present under a fluorescent microscope (Figure 6). It is inferred that the presence of a signal indicates the chromosome is present, while its absence indicates it is missing.

Though the technique was developed in the 1980s, its first use in the IVF clinic was not until 1992, when it was used as an alternative to PCR-based methods to treat families at

risk of transmitting sex-linked disorders by probing for chromosome X and Y (66, 77). Shortly thereafter, FISH was applied to assess the chromosomal copy number of an embryo, by probing for chromosomes associated with live-born syndromes (13, 18, 21, X and Y), thereby establishing the first iteration of PGT-A. Over time, FISH panels used for PGT-A increased to include up to 12 chromosomes, starting with those known to display the highest frequency of aneuploidy in material from first trimester spontaneous abortion and prenatal loss. Later additions included chromosomes associated with high levels of aneuploidy in the early developing embryo (78).

The number of chromosomes that could be targeted, however, was limited by the spectral resolution, filter sets, and the small amount of embryonic material available for testing. That is, although 24 chromosome FISH was eventually achieved (72, 73), this was more applicable as a research tool and never likely to be applied clinically. While 5 to 12-chromosome panel FISH was a widespread diagnostic technology in the IVF labs of the 1990s, as a clinically reliable diagnostic tool, it has substantial limitations and challenges. As only a single target on each chromosome is probed, any segmental abnormality outside of this region would go undiagnosed, underscoring the limited resolution of the test. In addition, cell nucleus fixation and downstream analysis are technically challenging, operator dependent and subjective. Finally, probe failures and overlapping signals are not uncommon and can significantly hinder an accurate diagnosis in an already limited chromosomal panel. These drawbacks are likely some of the principal

reasons RCTs have failed to show improved live birth rates in PGT-A IVF cycles using

this technology (7, 76).

Figure 6. FISH Process Used In PGT-A.
(A) A biopsied cell is fixed to a slide and fluorescent probes targeting specific chromosomes are hybridized to the nucleus. (B) Microscopy and image analysis is performed and targeted chromosome signals can be counted and evaluated for ploidy. Adapted from Ioannou et al, Chromosome Research 2012 20(4):447-60.
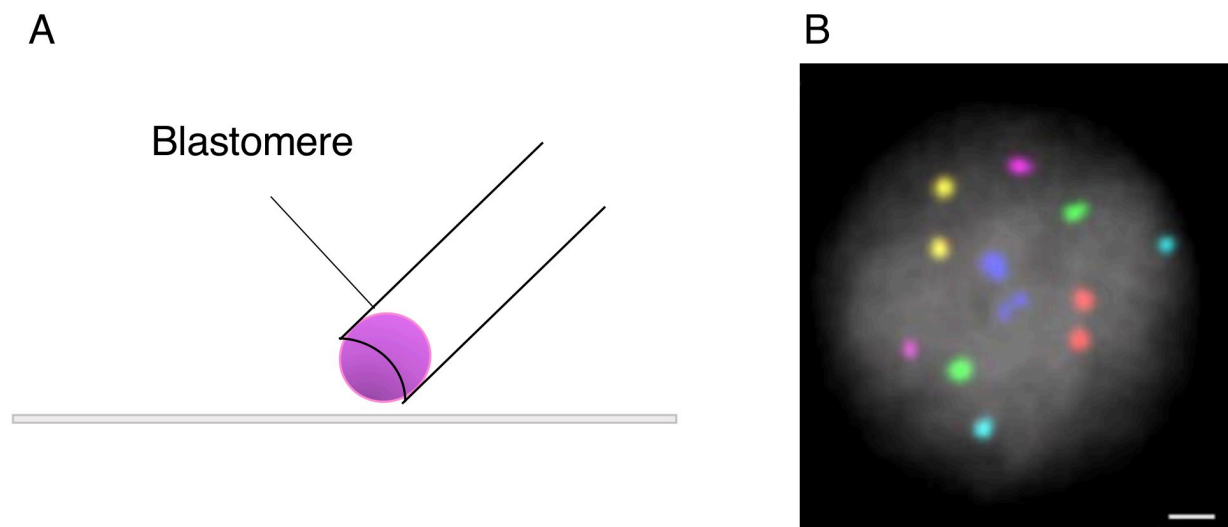
FISH is still occasionally used for chromosomal screening of human embryos in certain

clinics, but it has largely been replaced by genome-wide molecular techniques. Though it

continues to be used in instances of heritable structural rearrangements where

breakpoints cannot be adequately diagnosed using PCR-based methods, it is mostly

relegated to research practices in IVF and PGT, in the investigation of nuclear

organization and mosaicism (79).

9.4.2. The need for whole genome amplification (WGA) to facilitate 24 chromosome screening

A major limitation of preimplantation genetic testing is the limited amount of starting material – polar bodies from a mature oocyte or zygote, one or two blastomeres from a cleavage stage embryo, or five (to ten) cells from a blastocyst. With each cell containing approximately 6 pg of DNA, even a ten-cell biopsy does not yield sufficient DNA to meet the current required input quantities for molecular testing approaches like aCGH and NGS. To meet the needs of higher resolution molecular techniques, new technology was called for.

WGA methods were developed in the early 1990s as a means to increase the amount of DNA from limited samples in a sequence independent fashion. It quickly became an invaluable tool in the world of molecular genetics as it made copy number variation in single or few cell samples possible. The field of embryo testing welcomed the technology as it addressed the issue of insufficient sample size.

There are various types of WGA, which fall broadly into three categories: PCR based, Multiple Displacement Amplification (MDA) based and hybrid. Each approach has advantages and disadvantages when it comes to important features like genome coverage, representation bias, reproducibility, error rates, robustness and yield. PCR based methods include degenerate oligonucleotide primed PCR (DOP-PCR), which utilizes partially degenerate oligonucleotide sequences/primers, thermostable DNA

polymerase and slowly increasing annealing temperatures during the PCR reaction. It is a relatively short two-step protocol that can be completed in less than three hours (80). Recent modifications in the reaction chemistry have significantly improved the quality of the amplified material by providing increased genome coverage and decreased allele drop-out (ADO) (81). DOPlify, a popular commercial DOP-PCR kit, has been integrated into various downstream genome-wide PGT-A workflows.

Also loosely falling into the PCR based WGA category are linker-adapter PCR (LA-PCR) methodologies. In LA-PCR, template DNA is fragmented and tagmented, meaning linkers containing a primer binding site are enzymatically attached to the ends of the fragmented DNA. PCR is then used to amplify the tagmented DNA fragments by adding PCR primers complementary to the linker-primer binder site. While this method can be more labor-intensive than other amplification methods, it appears to offer reasonable reproducibility and genome uniformity allowing for accurate chromosome copy number assessment. This is leveraged in various downstream genome-wide workflows as various commercially available LA-PCR kits, like Sureplex and Picoplex, are currently some of the most widely used WGA chemistries for PGT-A purposes.

Multiple displacement amplification, or MDA, is a non-PCR based method for WGA. MDA uses high-fidelity bacteriophage DNA polymerase that denatures double stranded DNA and amplifies a single stranded template in an isothermal reaction. The high-fidelity polymerase reduces nucleotide errors in amplified sequences which is well suited for

single nucleotide polymorphism (SNP) detection, however its amplification uniformity across the genome appears hampered compared to PCR based methods (82). Though minimal hands-on time is required, the reaction time can be greater than eight hours.

Hybrid WGA techniques combine MDA and LA-PCR methodologies, like multiple annealing and looping based amplification cycles, or MALBAC. An initial isothermal amplification of denatured template is performed using specific MALBAC primers, followed by PCR amplification of the DNA-MALBAC primer fragments. Hybrid methods, though more labor intensive than standard MDA, offer reasonable uniformity across the genome (82-85).

WGA chemistries and the availability of more DNA from PGT samples ushered in a new era of molecular diagnostic techniques requiring starting material beyond just a few cells.

9.4.3. Comparative genomic hybridization (CGH)

CGH is a method for analyzing copy number variations of a sample by comparing it to the ploidy status of a reference sample. Applying the principles of FISH, the process of CGH also utilizes DNA hybridization. However, instead of hybridizing labeled probes to a fixed sample, CGH involves fluorescently labeling sample DNA (in red) and a known euploid reference DNA (in green) solution. These samples are then co-hybridized to a normal metaphase spread to bind to their locus of origin. With the help of a fluorescent microscope and software, the differentially colored fluorescent signals are compared

along the length of each chromosome for identification of chromosomal differences between the sample and reference. If the sample is euploid, the ratio of sample to reference DNA will be balanced and an equal mix of red and green will be seen across all chromosomes. Any chromosomal imbalance will be detected as a shift towards red or green for that specific chromosome.

CGH was first introduced as a diagnostic tool to test for chromosome copy number changes in solid tumors in the early 1990s (86). The technology was successfully applied to the field of IVF and PGT-A in 1999, using whole genome amplified material from single cells biopsied from cleavage stage embryos. Unlike limited panel FISH, CGH offered ploidy information across all 24-chromosomes (87, 88). In fact, it offered information on copy number at various loci across all 24-chromosomes, and for the first-time shed light on the incidence of segmental aneuploidies and genomic instabilities in preimplantation development (89).

While a breakthrough technology, this procedure was laborious and time consuming (90). In a clinical setting this presented challenges given the time constraints of embryo development, uterine receptivity, and window of implantation. Therefore, in order to be effectively applied in an IVF setting, CGH required embryos to be frozen and used in a future frozen embryo transfer cycle. Despite the advancements in PGT, the process of embryo freezing was not yet sufficiently advanced to support this process.

Nevertheless, this comprehensive approach provided a springboard to the development of additional genome-wide PGT-A technologies, including workflows that were more compatible with IVF cycle timing and platforms with further increased resolution, due to the new appreciation for segmental abnormalities in IVF embryos (91, 92).

9.4.4. Array-CGH (aCGH)

aCGH is similar to CGH in that it involves the fluorescent labeling of a sample to a known reference and assessment of copy number by comparative analysis (93). Instead of being hybridized to metaphase chromosomes, however, the two-colored DNA sample/reference cocktail is hybridized to bacterial artificial chromosomes (BAC) or synthetic oligonucleotides, called microarrays. Fluorescence ratios at each arrayed DNA element are analyzed and can provide a locus-by-locus measure of DNA copy number variation at an increased mapping resolution to standard CGH (Figure 7).

A fully automated aCGH solution (24Sure – BlueGnome later Illumina, Inc) was introduced in the early 2000s with a workflow that was IVF-cycle friendly and allowed for fresh embryo transfer even when biopsying advanced blastocysts. The specialized software (BlueFuse) analyzed the ratio of the fluorescent signal intensity at each chromosomal position, or clone, represented on the array, and compared these ratios to those of reference DNA. Clones with normalized intensities significantly greater than the reference intensities indicated copy number gain in the sample at that position. Similarly, significantly lower intensities in the sample are signs of copy number loss. Bluefuse

software calculates standard deviation ratios after smoothing and normalizing raw data (8, 94-96) reporting genome wide copy number information as log2 ratios. It is able to offer a mapping resolution as small as 2.5Mb (97).

aCGH technology as a tool for PGT-A has been rigorously and successfully applied in the field; including proof of principle (5), preclinical validation (98), RCT (29) and retrospective case control studies (99).

Despite its numerous strengths, aCGH does have its limitations. It cannot detect polyploidies or uniparental disomies (UPD) because the relative ratios of chromosomal DNA are the same as that of the control DNA. Another disadvantage is resolution and the limited ability to detect mosaicism (100).

9.4.5. Next-Generation Sequencing (NGS)

Sequencing is the process of determining the order of nucleotides. The 'next-generation' designation refers to the more recently developed technologies that have the ability to generate this information quickly, accurately and in a cost-effective manner. These methods started emerging in the early 2000s and catapulted the field of biological research and medical genetics into a new era. They offer a major progression towards a more comprehensive characterization of the human genome and associated genetic

Figure 7. The Process Of aCGH Used In PGT-A.
Free floating fluorescently labeled single stranded DNA (A) is hybridized to a microarray chip (B) where the ssDNA is attracted to its complimentary probe that is stationary. Fluorescent signals are compared to that of a reference to make a ploidy determination in a given region (C).
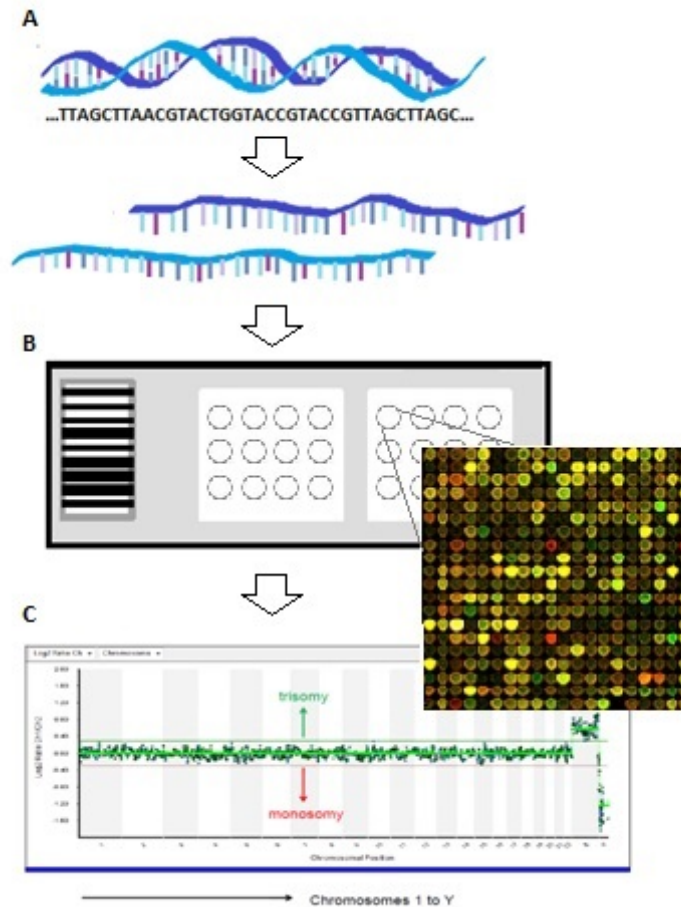
disease. The field of PGT-A began harnessing these tools for routine use a decade later

(Figure 8) (101-103). The most popular sequencing platforms utilized for PGT-A purposes

include Illumina and Ion Torrent technologies. Both systems essentially entail single

stranded DNA template being repeatedly exposed to a sequence of dNTPs. Incorporation

of bases complementary to the template can be detected in different ways. Illumina

sequencing by synthesis technology enriches DNA templates with fluorescently labeled chain terminating nucleotides, and base incorporation/calling is determined by light detection using specialized cameras. Ion Torrent/LifeTech technology, rather than utilizing optical components, detects nucleotide sequences by changes in pH, as nucleotide incorporation releases protons, changing the pH of the surrounding solution proportional to the number of incorporated nucleotides.

There are two basic approaches of these sequencing methodologies when applied for PGT-A analysis. One, a non-targeted, shot-gun sequencing of random fragmented genomic DNA from WGA biopsied embryonic material. And two, a targeted sequencing approach, which performs a highly multiplexed PCR to amplify many targeted regions across the genome.

Regardless of the approach, a barcoding step allows all fragments of a specific sample to have a unique identification sequence attached, or molecular barcode (104). The ability to label each sample with a molecular signature allows multiple samples to be processed at once, providing time and cost saving benefits. Resulting data is demultiplexed and individual samples are mapped to a known human reference genome. The number of reads at each chromosomal region can be quantified, and any potential aneuploidy can be deduced by a disproportionate number of reads in a given region.

PGT-A with NGS has shown increased resolution for small copy number variations (CNVs), structural rearrangements and mosaicism as compared to aCGH. Moreover, NGS has the ability to simultaneously detect monogenic disorders (105). Mosaicism detection of various NGS PGT-A workflows have been thoroughly explored and limits of detection have been reported to be as low as 10% (106, 107). This topic is further addressed in a later section. NGS has also increased the confidence in the detection of some polyploidy, as compared to previous technologies, although commonly used PGT-A platforms are still not able to identify this condition in all cases.

Because of these improvements, it has been suggested that NGS technology has had a positive impact on IVF outcomes by decreasing failed implantation and miscarriage rates (108).

9.4.6. Real time quantitative PCR (qPCR)

qPCR applies the same tenets as classical PCR but has the ability to offer quantitative information of PCR-targeted loci. It monitors DNA amplification as the reaction progresses by using fluorescently labelled primers such that a fluorescent signal can be recorded at each PCR cycle. Signals can be measured, and relative target abundance can be determined between template DNA and a calibrator reference sample.

Methods applying this technology to PGT-A have been described and successfully utilized in the clinic on biopsies from advanced stage embryos (109-111).

Figure 8. NGS-Based PGT-A.
Source DNA from embryo cells is fragmented, amplified, and sequenced. The sequencing reads are aligned to a reference genome and counted by genomic regions.
Adapted from Vermeesch et al, Nat Rev Genet. 2016 Sep 15;17(10):643-56.
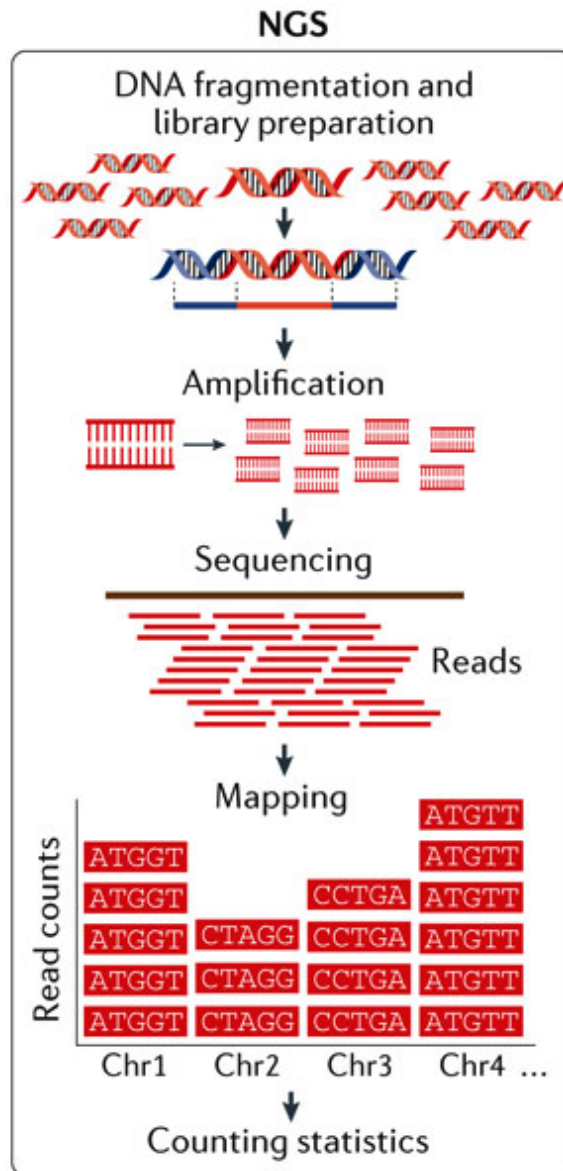
The procedure is cost effective and efficient as compared to other genome-wide PGT-A solutions and does not require the use of WGA (112, 113). This process involves a multiplexed pre-amplification reaction targeting specific loci across the genome, followed by qPCR using TaqMan copy number assay. Importantly, this method can be easily combined with testing for monogenic mutations.

One drawback, however, is its limited resolution as it only provides copy number information at a limited number of defined regions on each chromosome. This greatly reduces its ability to detect segmental abnormalities when compared to other methodologies and could thus under-report abnormalities leading to increased risk of miscarriage. This method's ability to detect mosaicism however remains to be determined.

9.4.7. SNP-arrays

A single nucleotide polymorphism (SNP) is a variation at a single site in the genome and is the most frequent type of variation found in humans. A SNP array is a technology used to detect these polymorphisms, using the same basic principles of standard microarray, including DNA hybridization, fluorescent microscopy and solid surface capture in order to detect these polymorphisms. Unlike classic microarrays that can only detect gains or losses at a probed region, SNP arrays contain two hybridization loci per SNP. Each allele is differentially labelled, allowing for the detection of hetero- and homozygosity (114), as

well as instances of allelic imbalance (115), including loss of heterozygosity (LOH) and uni-parental disomy (UPD).

Though most commonly used for genome wide association studies (GWAS) to map disease loci, SNP arrays can also be utilized to generate a virtual karyotype by using software to determine the copy number of each SNP present on the array by comparative fluorescence, and subsequent alignment of the SNPs in chromosomal order. SNP technology has been successfully applied as a chromosome copy number tool in the context of PGT-A (116-118). Benefits include comprehensive detection of polyploidy, UPD and simultaneous detection of PGT-A and M.

9.4.8. Karyomapping and Haplarythmisis

Karyomapping is a high density SNP genotyping platform that uses parental DNA to determine 'informative' loci of a parental haplotype, where four distinct sets of markers can be identified across each parental chromosome (119). Parental genotypes can be aligned with genotypes of their children and/or embryo genotypes, generating a 'karyomap' that can display homologous chromosomes and any points of genetic exchange induced by chiasmata. As such, in the event of a chromosomal abnormality, it can infer whether the abnormality has stemmed from meiosis I, meiosis II or a post zygotic error (120, 121).

In the event of a mosaic result, the source of the chromosomal error may have substantial clinical implications. For example, it is known that meiotically incurred mosaic trisomies later corrected by trisomy rescue lend themselves to poorer clinical outcomes, as compared to mosaicism resulting from post zygotic errors (122). As a SNP array, karyomapping is also able to detect polyploidy, UPD and simultaneously perform PGT-A and PGT-M testing. As such, it is a universal test for PGT-A, PGT-SR and PGT-M with potential applications for PGT-P.

9.4.9. Looking forward for PGT (and PGT-A in particular)

Over the past three decades, PGT-M has been applied to over 400 conditions (123), and credited with the birth of thousands of unaffected children (15, 123). The efficacy of PGT-A, on the other hand, despite boasting thousands of healthy live births from IVF cycles utilizing this technology, is still widely debated. As PGT-A is not like the other three forms in that its goal is not the prevention of disease by inheritance, but to maximize implantation potential while addressing patient specific needs, it deserves special attention. These individualized concerns may range from a patient's anxiety over the prospect of experiencing another miscarriage or offering a young couple peace-of-mind of having genetically competent embryos banked for future use. Unfortunately, while critical to good patient care, these benefits are harder to quantify and often overlooked.

According to the European Society of Human Reproduction and Embryology (ESHRE) PGD consortium data for 10-year period (1997-2007), out of more than 27,000 cycles that

reached oocyte retrieval, over 60% were destined for aneuploidy screening. Global figures are becoming more difficult to collate but it has been estimated that approximately 100,000 PGT cycles have been performed worldwide over the past 23 years (www.pgdis.org) and nearly 80% of these cycles have been PGT-A (personal communication from numerous meetings including PGD international society - PGDIS). The demand of IVF has been increasing due to wider accessibility and various societal trends and with it, so it seems, the use of PGT-A. Nonetheless, the efficacy of PGT-A and its clinical applicability continues to be questioned and debated. Numerous studies attest to its efficacy including retrospective analyses, randomized controlled trials and non-selection studies. Conversely, the majority of these have attracted criticism either for sample size, study design or interpretation. Most recently, a large multi-centre trial (the STAR trial) (31) provided ammunition for both proponents and opponents of PGT-A. For the later, analysis suggested no significant increase in improving first-time pregnancy rates, overall. Reanalysis of the data however for women over the age of 35 demonstrated a significant improvement. Moreover, the study provided clear evidence that procedural or technical differences between IVF centres can influence PGT-A outcomes. Perhaps the most controversial side of the PGT-A debate is what happens when it is determined that the embryo biopsy contains some cells that are aneuploid and some that are chromosomally normal.

9.5. Aneuploidy and Mosaicism

The use of FISH, aCGH, NGS and SNP technologies have all been instrumental tools as we try to better understand the basic patterns of chromosome abnormalities in early

human embryonic development. These insights may offer clinicians and patients decision-making tools for optimal clinical outcomes while giving us much needed insight into the origins of chromosome abnormality.

9.5.1. Aneuploidy

Aneuploidy is a disorder of chromosome number (Figure 9). Its classical definition in humans describes any deviation of 23 or its multiples in chromosome count. Strictly speaking, having one or two complete extra sets of chromosomes, (triploidy and tetraploidy), or only having one set of chromosomes (haploidy) are not considered examples of aneuploidy. The most commonly encountered forms of aneuploidy in embryos are trisomies, in which an individual chromosome is present in triplicate, or monosomies, where only one copy is present, resulting in 47 or 45 chromosomes per cell respectively. Chromosomes can also be present in multiple copies (tetrasomy, pentasomy, polysomy) or none at all (nullisomy), and more than one chromosome can be affected in the karyotype (double aneuploids, complex aneuploids).

Aneuploidy results from erroneous chromosome segregation during cell division, which can occur during meiosis in gametogenesis or during mitosis in embryonic development. Both meiosis and mitosis are highly complex, coordinated processes that depend on the correct formation of an intricate network of microtubules known as the spindle, responsible for physically moving chromosomal content during cell division.

Figure 9. Trisomy 21 As An Example Of Aneuploidy.
Each autosome is present twice (disomic), except for chromosome 21, which is present as three copies (trisomic) (see red box).
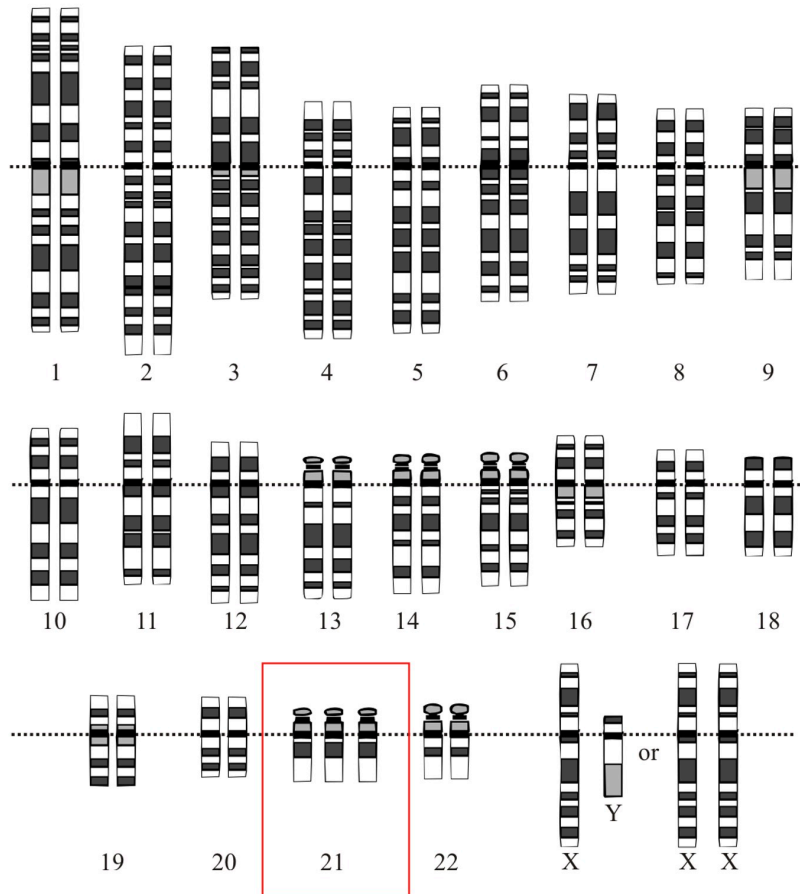
Compromised formation of the spindle can prevent correct segregation of chromosomes or chromatids to daughter cells.

Natural human embryo mortality from fertilization to live birth in normal healthy women is estimated to be no less than 40-60% (124). Aneuploidy is common in preimplantation embryos and is thought to be the leading cause of reproductive failure and pregnancy loss in natural conceptions (68, 125, 126). Embryos monosomic for any autosome often

fail to implant and invariably fail to develop to term because of the insufficient dosage of essential genes. This is also true for the majority of trisomic embryos, which experience excesses in gene dosage. However, trisomies in some autosomes, notably 13, 18, and 21, can result in live births albeit often with limited survival or lifelong medical ramifications. Sex chromosomes are more permissive of copy number abnormalities, and offspring experience clinical conditions ranging from undetectable to severe.

In IVF, some 40% of blastocyst-stage embryos contain aneuploidies, both in natural ovulation and super-ovulation cycles (127). The majority of aneuploidies are thought to originate in the oocyte (120, 128), and there is a well-documented correlation between maternal age and incidence of aneuploidy both in natural conceptions and in IVF embryos (68). The higher likelihood of conceiving a Down Syndrome fetus with increasing maternal age has long been known (129). In IVF, the proportion of embryos in a patient's embryo cohort that are aneuploid increases progressively from 30% in women in their early 30s to more than 90% when reaching the age of 44 (75). A recent large-scale analysis of over 130,000 PGT-A embryos revealed that the incidence of embryos with single chromosome aneuploidies remains relatively constant across ages, but aneuploidies involving 2-5 different chromosomes become progressively more prevalent with advancing maternal age (130). Various explanations have been proposed for this correlation. Prolonged exposure to environmental insult, the accumulation of reactive oxygen species (ROS) (131) and/or carbonyl stress that might affect mitochondrial integrity (132) might all result in abnormal spindle formation and aberrant chromosomal segregation during meiosis.

Direct observation of compromised meiotic spindles in AMA patients supports this notion (133). While this renders AMA the leading referral category for PGT-A, the significant presence of aneuploid embryos observed in some younger and donor IVF cycles provides powerful rationale for PGT-A in all IVF cycles (134).

9.5.2. Segmental Aneuploidy

Contemporary interpretations of aneuploidy in embryology also include segmental losses and gains, where there are deviations in the normal copy number of sub-chromosomal stretches affecting several megabases (Mb). Such chromosomal abnormalities in embryos were first documented in murine models using classical cytogenetic methods (135). Most present-day PGT-A platforms are validated to detect partial chromosomal abnormalities of at least 20 Mb. Segmental aneuploidies are mainly believed to originate from mitotic errors during early cell divisions in the forming embryo. This developmental period is associated with weakened cell cycle checkpoints, lax DNA damage repair mechanisms, and double strand breaks due to rapid proliferation (136, 137). Approximately 16% of IVF-generated blastocysts contain segmental losses or gains. Interestingly, of these segmental aneuploids, only 5% arrive from germ cell derived errors, particularly from the father's side (120).

Identification of segmental aneuploidies during PGT-A is important, since it is present in ~6% of established pregnancies that miscarry, and babies born with such chromosomal

errors can experience serious clinical consequences such as seen in Cri-du-chat, Wolf-Hirschhorn, or Jacobson syndromes (138, 139).

9.5.3. Chromosomal Mosaicism in Embryos

While the concept of aneuploidy operates on an individual cell level, entire embryos are referred to as 'aneuploid' suggesting that all its cells are chromosomally abnormal. Systematic "cell by cell" analysis has however yet to be performed on a large number of human blastocyst embryos and thus a prevailing supposition that when the anomaly is a consequence of meiotic errors, that all cells are affected equally, still requires validation. In other words, if the aneuploidy is present from the onset of fertilization, the zygote will pass on the chromosomal abnormality to all descendent cells over subsequent cell divisions. As with karyotypically normal embryos however a chromosome segregation error could happen during mitosis as a postzygotic event. In these cases, the result is the presence of cells with different chromosomal content- a phenomenon known as mosaicism. The different cell types could all be abnormal and contain different aneuploidies, or there could be a mix of euploid and aneuploid cells. It is the latter version (sometimes referred to as diploid-aneuploid) where it is assumed that a post-zygotic error led to the aneuploid cell, that attracts the most attention with PGT-A.

Mosaicism was first documented in human embryos with FISH (65, 66, 77, 140). Since then, a number of different mitotic error mechanisms have been proposed to explain mosaicism: mitotic non-disjunction, anaphase lagging, or formation of multinuclei and/or

micronuclei, centriole/centrosome dysregulation and endoreplication (128, 141-143). Mitotic non-disjunction means that sister chromatids of a chromosome are not correctly separated during cell division, resulting in one trisomic and one monosomic daughter cell. Anaphase lagging is an event leading to monosomy in one of the daughter cells at mitosis, because a chromatid does not become incorporated into the nucleus. In mosaic embryos, there is a documented increased incidence of monosomies compared to trisomies, suggesting that anaphase lagging is the principal mechanism creating mosaicism (73, 144, 145). Micronuclei, or small nucleus-like structures, are thought to arise when chromosomal material forms its own nuclear membrane. Since proper kinetochores are absent, the chromosomal content of micronuclei are unable to undergo regulated mitosis, likely resulting in mosaicism in daughter cells (142, 146). Finally, endoreplication without subsequent division could hypothetically result in mosaicism but has not been documented for individual chromosomes, but rather for entire chromosomal complements (141).

Mosaicism can also result from a uniformly aneuploid embryo undergoing a mitotic event that converts aneuploid cells to euploid ones. For example, in 'trisomy rescue' cells lose the extra chromosome, resulting in disomy. This mechanism for the creation of mosaicism implies that a meiotic event, responsible for the initially ubiquitous aneuploidy, is followed by a mitotic event during development. While the incidence of this mechanism is not currently known, it must be noted that this may account for some cases of uniparental

disomy (UPD) when the two chromosomes that prevail after the 'rescue' are derived from the same parent. UPD is seen in newborns at an incidence of 1 in 3500 (147).

Evidence from a mouse model for aneuploidy indicates that meiotically induced aneuploidy might trigger downstream mitotic events. Using synaptonemal complex protein 3 (SYCP3) null mice, which experience chromosomal missegregation during meiosis, a study has shown that aneuploid embryos become cytologically unstable, resulting in a rapid evolution of mosaicism and early embryonic death by apoptosis independently of p53 mechanism (148, 149). In an aneuploid background, mitotic events resulting in euploidy might be common, and the meiotic-mitotic error pathway might therefore be a substantial contributor to the incidence of mosaicism in human embryos.

In general, it is thought that cleavage-stage embryos are more prone to contain mosaicism than blastocysts (150). A systematic review indicated that three quarters of cleavage stage embryos contained two or more cell groups with different chromosomal content, the majority being of the diploid-aneuploid type of mosaicism (151), although it must be noted that most studies have relied on the limited FISH technique. One notable cleavage-stage study using PGT-A techniques on good quality IVF embryos from young patients (<35yrs) reported that 70% of cleavage stage embryos are mosaic (152). Another report, using SNP analysis on 28,052 cleavage stage embryos, indicated that at least 25% contained aneuploid errors of mitotic origin (128). During the first cell divisions, the embryonic genome is largely inactive, meaning that cell cycle progression is solely

regulated by maternally-derived factors independent of transcription. A dampened governance of the cell cycle might result in increased mitotic errors, explaining the common occurrence of mosaicism at the cleavage stage (153). This could in turn explain why cleavage stage PGT-A, in which a single cell is analyzed, has been largely presumed ineffective (7), although some RCTs have shown tangible benefits in some patient groups (32, 154).

Though not as common, blastocyst-stage mosaicism has also been demonstrated with FISH analysis of fixed whole embryos, and mosaic mixes have been documented in the inner cell mass (ICM) as well as trophectoderm (TE) tissues (155, 156). Blastocyst-stage mosaicism might be less prevalent because some mosaic embryos might arrest during development (153), especially in cases with high aneuploid cell load. Data from mouse experiments supports this notion, as it was shown that chimeric embryos composed of different ratios of euploid and aneuploid cells have different viability. In these studies, transferred embryos with a ratio of 1:3 euploid-to-aneuploid cells never resulted in a live birth, whereas those with a 1:1 ratio had a 50% chance of coming to term (157). Analysis of cell proliferation and death indicated that in surviving embryos, euploid cells tended to outcompete aneuploid ones. This means that mosaic embryos might be able to self-correct and become entirely euploid, offering an alternative explanation for why less mosaicism is observed at the blastocyst stage compared to earlier stages (153). Moreover, mosaicism rate is reported as less than 1-2 % in viable pregnancies (158), suggesting those mechanisms are still at play after implantation.

Whether a mosaic embryo is capable of implanting and its subsequent clinical fate depend on a variety of factors. These include the timing of the segregational error, the proportion and the lineage of the embryo that has been affected and the type of abnormalities and the chromosome(s) involved (122, 159). Conceptually, an embryo would be predicted to be less severely affected when the error occurs at later stages of development, most likely resulting in confined mosaicism (159). This is particularly relevant in that a meiotic error or one in the very earliest cleavage divisions would, most likely, be the most clinically significant as it would affect the majority of cells in the embryo. Whereas if the mitotic error occurs later in development when cell lineages have already segregated, the clinical consequences might be different. For example, confined placental mosaicism (CPM), in which aneuploid cells are confined to the placenta, affects 1-2% of ongoing pregnancies and can lead to intrauterine growth retardation or placental insufficiency (160).

The incidence of mitotically derived mosaicism in embryos does not increase with maternal age, in contrast to meiotic aneuploidy where there is a far clearer age correlation (79, 151-153). This indicates that age-related factors leading to increased meiotic errors do not play a role in mitotic errors, which appear to have a uniform base-line error rate across patients. This concept is markedly at odds with the notion that errors in mitosis are more common in an already aneuploid setting due to a previous meiotic event. Such discrepant hypotheses remain to be resolved, as we continue to learn more about the

biological mechanisms of mosaicism. It is probably that maternally derived factors are not solely responsible for the creation of mosaic embryos. As centrosomes are paternally inherited and are responsible for spindle formation during mitosis, there is a likely paternal contribution to mosaicism formation. In fact, disruption of centrosomes increases mosaicism rates in embryos (161). Additionally, it is thought that laboratory procedures might influence rates of mosaicism as incidence of mosaic embryos varies greatly between IVF centers (106). Culture conditions, ovarian hyperstimulation strategies, and biopsy techniques (including excessive use of laser thermal ablation) have all been hypothesized to have a significant influence on the measured rates of mosaicism, as they might influence the chance of aberrant mitosis or compromised biopsy material (162). Rates of mosaicism might therefore be a key performance indicator for quality assurance in IVF laboratories.

9.5.4. Mosaicism detection and its clinical implications

The incidence of mosaicism and how best to detect it using PGT-A are the current subjects of much debate. The reported proportion of IVF embryos that are classified as mosaic has varied widely, ranging from under 4% to over 90% (163). The estimation depends heavily on various factors such as embryo characteristics, biopsy techniques, PGT-A platform employed, and thresholds used to define mosaicism.

Detection of mosaicism during PGT-A is developmentally stage-specific; only blastocyst analysis involves the evaluation of multiple cells, which is a prerequisite to detect the

presence of different karyotypes. The PGT-A platform must be sensitive enough to detect mosaicism when present within the 5-10 cell blastocyst biopsy. Since the set of cells in the biopsy are processed in bulk, results indicate intermediate copy numbers for the chromosomal regions affected by mosaicism. Several laboratories using PGT-A with NGS have performed cell or DNA mixing experiments using cell lines with different known aneuploidies, resulting in karyotype profiles consistent with mosaicism (37, 107, 108, 164, 165). As a result, when PGT-A results display a similar profile, the embryo can be classified as mosaic (Figure 10). Furthermore, analysis of karyotype profiles makes it possible to estimate the percentage of aneuploid cells in the biopsy. Embryos can be grouped in 'high' and 'low' mosaics and characterized by type of aneuploidy involved in mosaicism: segmental, monosomy, trisomy, or multiple chromosomes.

Currently, NGS is the only PGT-A method recommended for the diagnosis of mosaicism, due to its superior resolution and accuracy compared to previous technologies (164). Reanalysis of WGA material from aCGH PGT-A runs with NGS reclassified numerous failed implantation embryos from 'euploid' to 'mosaic' (108). PGDIS (166) and CoGEN (167) have published position statements defining mosaicism in PGT-A. These were based on initial validation studies proposing that karyotype profiles deviating from disomic values by <20% should be treated as normal, those with >80% as abnormal, and the remaining ones between 20-80% as mosaic (106, 168).

Figure 10. Detecting Mosaicism Using PGT-A.
If mosaicism is present in the collected TE biopsy, the digital karyotype profile generated during PGT-A will produce an intermediate copy number for the affected chromosome. In the given example, chromosome 13 produces a value of 2.5, indicating that half the analyzed cells contained disomy 13 and the other half contained trisomy 13.
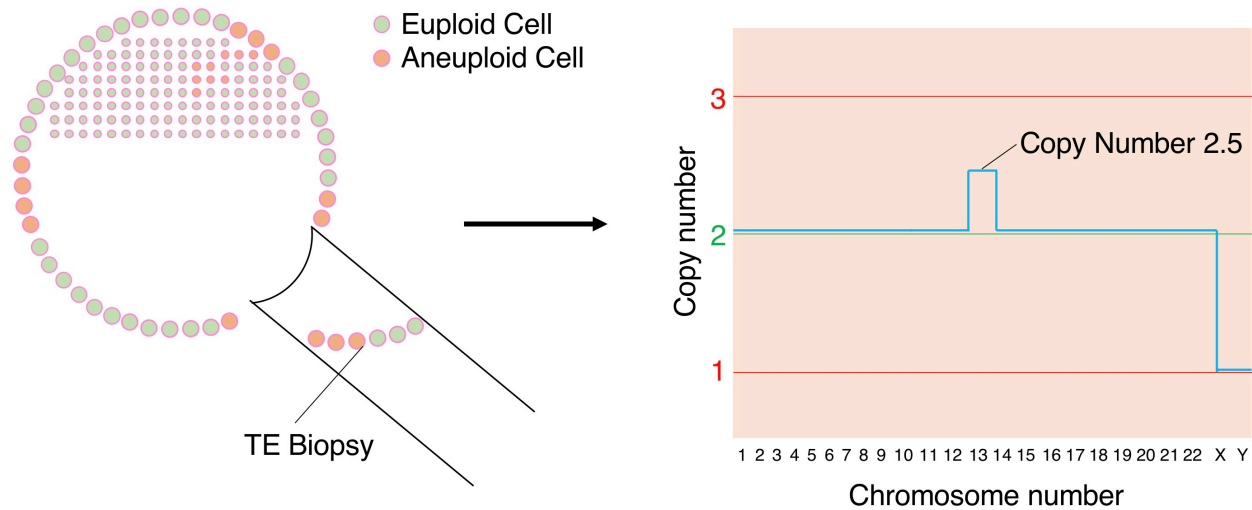
It must be noted that technical noise in PGT-A can also result in karyotype profiles with intermediate values consistent with mosaicism (163, 169). Irregularities of the WGA procedure and S-phase artifacts (potential intermediate conformations of DNA during the synthesis phase of the cell cycle) can affect the output of the process. Validation and recurrent quality control of the PGT-A platform used is paramount, and individual low quality PGT-A results should be interpreted carefully.

Interestingly, studies from different groups have repeatedly shown that blastocysts classified as mosaic with PGT-A possess a distinct set of clinical outcomes compared to blastocysts classified as fully euploid (107, 164, 170, 171). This suggests that a diagnosis

of mosaicism is not just an artifact of PGT-A, rather a reflection of something biological. Even blastocysts categorized as 'low mosaics' have poorer outcomes than the euploid group (164, 171), indicating they are not merely euploids wrongly classified as mosaics because of technical noise. Originally, the stance toward embryos with a mosaic profile was to group them with full aneuploids, since they presumably also contain abnormal cells (albeit interspersed with normal cells).

The first report of mosaic embryo transfers appeared in 2015, and showed that such embryos could implant and lead to babies that appeared normal by routine medical examination at birth (172). Since then, there have been more than 400 embryos classified as mosaic that have been transferred, leading to over 50 births. So far there have been no reports of compromised newborns. The inevitable questions are: Are children born from mosaic embryo transfers truly 'healthy'? And if so, how is it that they are not affected in any appreciable way? These questions might be difficult to answer. While there have been no reports of obvious symptoms, more subtle conditions might yet be uncovered or could appear later in life of those children. To date there have not been any studies thoroughly investigating whether a higher than usual load of abnormal cells is found in various tissues of infants that were diagnosed as mosaic at the blastocyst stage. Such questions form the basis of studies in chapter 11. Furthermore, nothing is known about potential epigenetic or transcriptomic consequences of mosaicism in embryos.

Notably, there is good reason to believe that aneuploid cells in a mosaic setting are outcompeted by euploid cells, providing mechanism by which mosaicism in embryos becomes resolved. The findings from the chimeric mouse model study firmly support such a model (157). Those embryos that at the onset of the experiment (equivalent to the cleavage stage) contained a 1:1 mix of euploid and aneuploid cells 'lost' the chromosomally abnormal cells either through direct apoptosis or decreased cell proliferation. The aneuploid fraction became progressively depleted and embryos were capable of implantation and reaching term. Notably, the chimeric mouse embryo is a contrived model of mosaic human embryos, and the aneuploidy in the study affected several chromosomes resulting in cells that are not compatible with life. Nonetheless, immunofluorescent stains for markers of cell proliferation and apoptosis in human embryos have shown distinctly different patterns of cell cycle dynamics between blastocysts classified as euploid and mosaic (107). Also, extended *in vitro* culture of human blastocysts initially classified as 'mosaic' often showed a complete switch to full normalcy when cultured until day 12, both in cells derived from the ICM and TE (165).

The phenomenon of mosaicism poses an additional challenge to PGT-A. Looking at the blastocyst as a whole, mosaicism could lead to false PGT-A results even when uniform aneuploidy or euploidy is diagnosed in the TE biopsy. Since the TE biopsy is taken from a random sample in the tissue, it is possible that the whole collection of cells in the biopsy has a different chromosomal makeup than parts or the entire remaining embryo. Studies have explored the incidence of such a situation by analyzing serial biopsies in individual

blastocysts and determining rates of concordance (173). The most recent reports, which analyze the various TE and ICM biopsies by NGS, demonstrate that non-mosaic, uniform aneuploidies or euploidies detected in a TE biopsy are excellent predictors of the chromosomal status in the remaining embryo (165, 174). For whole chromosome aneuploidies, a clinical TE biopsy is 96.4% predictive of aneuploidy in the ICM. Segmental aneuploidies appear to be less concordant between serial biopsies, but this needs to be confirmed in larger datasets (174, 175). Considering that the majority of segmental deletions/duplications originate during the initial cell divisions in embryogenesis, their frequent mosaic pattern is to be expected (136, 137). The incidence of segmental aneuploidies remains relatively constant with maternal age (130), just as is the case with embryos in the mosaic category. Intra-blastocyst mosaicism is also unsurprisingly a poor predictor of the karyotype content of the remaining cells in the conceptus (107, 165). The issue of whether a TE biopsy is an accurate predictor of the chromosomal status of the rest of the embryo requires further consideration however and this is the subject of chapter 10.

The diagnosis of mosaicism in PGT-A invariably complicates the interaction between physician and patient. Position statements set forth by PGDIS and CoGEN recommend how to prioritize mosaic embryos in the clinic. If no euploid embryos are available, patients may opt to transfer an embryo classified as mosaic, and furthermore there might be a choice between two or more mosaic embryos. In such cases, mosaic trisomies in chromosomes X, Y, 13, 18, and 21, and monosomies in X are typically not recommended

for transfer, as those aneuploidies are viable. Aneuploidies in chromosomes 14 and 15 are also considered problematic, since trisomy or monosomy rescue could lead to UPD, known to have clinical consequences in the mentioned chromosomes. Trisomies in chromosomes 2,7, and 16 can lead to intrauterine growth retardation, so mosaicisms affecting those chromosomes are low priority for transfer. The position statements also recommend follow-up with the patient if pregnancy is established, and NIPT (non-invasive prenatal testing), CVS (chorionic villus sampling), but especially amniocentesis (which tests fetus-derived cells) should be discussed during counseling. A study on the occurrence of mosaicism in products of conception has produced some guidelines for prioritizing mosaic embryos based on the likelihood of mosaicism in individual chromosomes to result in miscarriages (176). The currently published reports on mosaic embryos transfers, although numerous, are individually quite limited in sample size with none surpassing 143 transferred embryos. This has led to some contradicting observations, for example one study claiming that increasing level of mosaicism (the percentage aneuploid cells present in the TE biopsy) adversely affects clinical outcomes (171), and another refuting that finding (107). Evidence-based guidelines will solidify over the next years with increasing sample sizes and comprehensive analyses.

Suggestions that we should regard 'mosaic' as its own category in PGT-A (164, 177) are bolstered by mounting evidence that mosaics have a distinct set of clinical outcomes (107, 164, 170-172). Euploid embryos should be prioritized for transfer, but when none are available, mosaics should be considered after appropriate counselling, while aneuploids

should continue to be deselected. Failure to consider mosaic embryos separately will invariably be disadvantageous: If they are to be grouped with the euploids, overall rates of implantation and birth will decrease. Regarding mosaic embryos as 'abnormal' together with aneuploids would result in discarding viable embryos that can potentially lead to normal pregnancies. Clearly however, this is an area that required further consideration and this is the subject of chapter 12.

9.5.5. Mitochondrial DNA and its role in PGT-A

Low mitochondrial number, unfavourable cytoplasmic distribution and inadequate ATP production collectively contribute to poor fertilisation and subsequent embryo development during IVF (178, 179). Mitochondrial number increases ~45x during oogenesis, peaking in the mature (metaphase II) oocyte and coinciding with the time of fertilisation (180), at ~2.6 × 10^5 copies (~100x higher than in somatic cells) (181). However, mitochondrial complement of fully-grown but immature oocytes (i.e. those harvested prior to in vitro maturation (IVM)) are highly variable, but are lower in developmentally less competent oocytes. Unlike somatic cells, each oocyte mitochondrion is believed to contain only one to two copies of mitochondrial DNA (mtDNA) (180, 182), so that estimates of mtDNA copy number are representative of mitochondrial number in these cells. Studies with pre-pubertal pigs indicate that mtDNA copy number is reduced in developmentally less mature oocytes at the point of collection, but can undergo compensatory replication during IVM (183). This can be stimulated with the addition of factors such as neuregulin 1 leading to better post-fertilisation development

(184). Furthermore, supplementation of oocytes from pre-pubertal pig with mitochondria from older, more mature female relatives (185) or with autologous populations of mitochondria from oocytes from the same animal (186) can also improve fertilisation and embryo development. What we do not know however is whether there are threshold levels of mtDNA and ATP for optimal oocyte maturation and fertilisation (182), nor whether there are alternative means of generating ATP within the oocyte such as the adenosine salvage pathway (187). Findings to date, however, emphasise the importance of mitochondria in determining oocyte quality and highlight possibilities to modify mitochondrial number and metabolism during IVM to enhance post-fertilisation development. Often compromised mitochondrial function and aneuploidy are mechanistically linked. Adequate levels of mitochondria and ATP are required to drive energy-demanding cellular events associated with meiosis and fertilisation including polymerisation of microtubules, activation of motor proteins and segregation of chromosomes. Moreover, in the mouse, decreased levels of mitochondria-derived ATP can lead to a disassembly of metaphase II oocyte spindles (29), which in turn leads to increased levels of aneuploidy.

During PGT-A, aside from the analysis of nuclear DNA content, cellular biopsies can be evaluated for mitochondrial DNA (mtDNA) load. Two groups published independent studies in 2015 indicating that high mtDNA content per cell correlated with poor embryo viability (188, 189). They described a threshold of mtDNA copy number that if surpassed always led to failed implantation upon transfer. One of the groups published two additional studies supporting the findings, although noting that some clinics did not generate

blastocysts with greatly elevated mtDNA copy number (190, 191). Publications from other laboratories could not reproduce the results (192-195). Noting that vastly different mtDNA quantitation methods were used between studies, it was suggested that technical variability could have caused the contradictory observations. Guidelines were hence proposed with the intent to standardize mtDNA copy number analysis during PGT-A (196). Recently, a study adhering to those guidelines reported the implantation of blastocysts with highly elevated mtDNA copy number which led to subsequent healthy births (197). The use of mtDNA copy number assessment as a routine PGT-A 'add-on' to further rank euploid embryos has therefore largely been discredited. Whether it will find some use in particular settings remains to be determined.

The role of mtDNA in PGT-A forms the basis of new results in chapters 13 and 14.

9.6. Thesis perspectives

Despite the at-times heated controversy regarding the efficacy of PGT-A, it is a technology that is likely here to stay. The availability of higher resolution platforms have arguably, expanded the utility of the test. As testing platforms continue to improve, additional information will likely become available regarding the genomic, transcriptomic and epigenetic status of an embryo. As we make sense of this additional information and its relationship to downstream outcomes, one can envision a world where every IVF embryo undergoes some form of PGT. A single test may offer a comprehensive picture

regarding the absolute health of an embryo and that of the resultant fetus, offering additional refinements to the science of embryo selection. Perhaps the '-A' in PGT-A will become obsolete, as the lines between PGT-M/-SR/-P and -A will be completely blurred. In the meantime, however, improving PGT-A has become a priority and fundamental questions pertaining to the use of it going forward loom large, specifically, how predictive of mosaicism is the TE biopsy, what happens when we transfer an embryo in which mosaicism is detected and to what extent should the results be used to rank, rather than select, the embryos? In terms of mitochondrial content and its relevance, the jury is still out on whether it is a useful, or completely useless, test. Finally, as mentioned at the very beginning of this introduction, it is always worth looking beyond PGT into the wider world, the issue of gene editing and its role as an adjunct or alternative to PGT is a relevant question, as is the ubiquitous Covid-19 and whether this needs to be incorporated into our future strategies.

9.7. Specific aims of the thesis

With the above in mind, there are a number of key questions that arise in terms of improving PGT-A (including mtDNA screening). Specifically the, purpose of this thesis is to test the following hypotheses:

a) A clinical TE biopsy is an adequate predictor of the remaining blastocyst's chromosomal status; i.e. that there is concordance between biopsy and blastocyst (see chapter 10)

b) Embryos classified as mosaic by PGT-A (TE biopsy) have inferior clinical success rates than euploid embryos, but can nonetheless result in healthy pregnancies (see chapter 11)

c) Features of mosaicism detected with PGT-A are useful to rank embryos by their potential to result in pregnancy and live birth (see chapter 12)

d) Accurate quantitation of mitochondrial DNA (mtDNA) in human blastocysts serves as a biomarker of ploidy and/or predictor of implantation (see chapter 13)

e) Embryos with high mtDNA content can result in healthy births (see chapter 14)

f) PGT largely obviates the clinical need for germline genome editing (GGE), but GGE might be a useful tool to correct aneuploidies detected by PGT-A in certain instances (see chapter 15)

g) SARS-CoV-2, the virus responsible for COVID-19, can infect human embryos, affect their viability and thus impact on PGT-A strategies (see chapter 16)

Aims Of This Thesis

10. Specific Aim A: To test the hypothesis that a clinical TE biopsy is an adequate predictor of the remaining blastocyst's chromosomal status.

The following published work is presented for this specific aim:

Victor AR, Griffin DK, Brake AJ, Tyndall JC, Murphy AE, Lepkowsky LT, Lal A, Zouves CG, Barnes FL, McCoy RC, Viotti M. *Assessment of aneuploidy concordance between clinical trophectoderm biopsy and blastocyst.* Hum Reprod. 2019 Jan 1;34(1):181-192. doi: 10.1093/humrep/dey327. PMID: 30418565.

10.1. My Personal Contribution to the Work

My personal contribution to this work includes study design, oversight, and execution of experiments; this includes prepping and performing most embryo thaws, biopsies, and subsequent next generation sequencing and genetic analysis. In addition, I assisted with writing and editing the manuscript.

10.2. Chapter Summary

Due to the phenomenon of chromosomal mosaicism, concern has been expressed about the possibility of discarding blastocysts classified as aneuploid by pre-implantation genetic testing for aneuploidy (PGT-A) that in fact contain a euploid inner cell mass (ICM). Previously published studies investigating karyotype concordance between TE and ICM have examined small sample sizes and/or have utilized chromosomal analysis technologies superseded by Next Generation Sequencing (NGS). It is also known that blastocysts classified as mosaic by PGT-A can result in healthy births. TE re-biopsy of embryos classified as aneuploid can potentially uncover new instances of mosaicism, but the frequency of such blastocysts is currently unknown. We therefore asked: Is a clinical trophectoderm (TE) biopsy a suitable predictor of chromosomal aneuploidy in blastocysts?

We decided to address this question by isolating serial re-biopsies of embryos and comparing their chromosomal content. To that end, 45 patients donated 100 blastocysts classified as uniform aneuploids (non-mosaic) using PGT-A by NGS (n=93 whole chromosome aneuploids, n=7 segmental aneuploids). In addition to the original clinical TE biopsy used for PGT-A, each blastocyst was subjected to an ICM biopsy as well as a second TE biopsy. All biopsies were processed for chromosomal analysis by NGS, and karyotypes were compared to the original TE biopsy.

When one or more whole chromosomes were aneuploid in the clinical TE biopsy, the corresponding ICM was aneuploid in 90 out of 93 blastocysts (96.8%). When the clinical TE biopsy contained only segmental (sub-chromosomal) aneuploidies, the ICM was aneuploid in 3 out of 7 cases (42.9%). Blastocysts showing aneuploidy concordance between clinical TE biopsy and ICM were also aneuploid in a second TE biopsy in 86 out of 88 cases (97.7%). In blastocysts displaying clinical TE-ICM discordance, a second TE biopsy was aneuploid in only 2 out of 6 cases (33.3%).

The high rate of intra-blastocyst concordance observed in this study concerning whole chromosome aneuploidy contributes experimental evidence to the validation of PGT-A at the blastocyst stage. Concomitantly, the results suggest potential clinical value in reassessing blastocysts deemed aneuploid by TE re-biopsy in select cases, particularly in instances of segmental aneuploidies. This could impact infertility treatment for patients who only have blastocysts classified as aneuploid by PGT-A available.

10.3. Chapter Introduction

A number of clinical trials have reported improved IVF outcomes following the vetting of embryos for chromosomal abnormalities (26, 29, 30, 32), and yet the IVF community is still debating the appropriate use of preimplantation genetic testing for aneuploidy (PGT-A, previously called PGS) (198, 199). Skeptics of the technology condemn the assumption that a 5-10 cell biopsy is representative of the remaining embryo (200, 201).

Indeed, the phenomenon of mosaicism, the condition of containing two or more cell lines with distinct chromosomal content (141), provides a biological rationale for that concern. A karyotypic categorisation of the trophectoderm (TE), the precursor to the placenta, might therefore not always be predictive of the inner cell mass (ICM), which gives rise to the fetus.

One of the potential consequences of misclassification of embryos during PGT-A is the deselection of viable embryos when a blastocyst is deemed aneuploid by TE biopsy but in fact contains a euploid ICM (201-203). Some patients are only capable of producing embryos classified as aneuploid by PGT-A even after repeated IVF cycles, particularly at an advanced age (75). Such cases invariably lead to the abandonment of infertility treatment.

Previous studies investigating rates of TE-ICM chromosomal concordance (expertly reviewed by Capalbo and Rienzi), while extremely valuable, have relied on limited sample sizes or methodologies that have recently been superseded by higher resolution genetic testing platforms (173). Next Generation Sequencing (NGS), has been heralded as a PGT-A technique with superior sensitivity for chromosomal mosaicism compared to aCGH, qPCR or SNP array (106, 108, 164, 177, 204) and has also been reported as highly effective in detecting segmental (i.e. sub-chromosomal) losses and gains, with higher precision than previous methods (205).

The purpose of this study was specifically to test the hypothesis that a blastocyst embryo classified as aneuploid by NGS-based PGT-A correctly predicts the ploidy of the ICM in the majority of cases. Furthermore, by analyzing a second TE biopsy, we determined the frequency of blastocysts originally classified as aneuploid that could be redefined as mosaic by re-biopsy.

10.4. Methods and Materials

10.4.1. Embryos and Clinical PGT-A Analysis by NGS

Blastocysts derived from patients seeking infertility treatment were generated by in-vitro fertilization and embryo culture as previously described (206), and were evaluated using the Gardner system (207). As part of the embryo selection process, a clinical 5-10 cell TE biopsy was collected and blastocysts were vitrified. The clinical TE biopsies were subjected to whole genome amplification (WGA) with SurePlex reagents (Illumina) followed by NGS-based PGT-A using Illumina's VeriSeq kit (Illumina) on a MiSeq system (Illumina) according to the manufacturer's protocol and described in detail elsewhere (137). For quality control, only samples satisfying the following cutoffs were used: number of Reads Passing Filter: >0.25M; Average Q-Score: >30; Alignment Score: >30; DLR (derivative log ratio): <0.4. Karyotype profiles were evaluated independently by three analysts and a consensus was determined. Copy number variation (CNV) for each chromosome was scored in Bluefuse Multi Analysis Software (Illumina) according to guidelines defined by the Preimplantation Genetic Diagnosis International Society (PGDIS), accessible at 'http://www.pgdis.org/docs/newsletter_071816.html'. Profiles with

copy number scale values <1.2 and >2.8 were recorded as aneuploid, those with values between 1.8 and 2.2 were recorded as euploid, and all others were recorded as mosaic. These guidelines reflect the detection range of mosaicism by NGS PGT-A, validated in various cell- and DNA-mixing experiments (106, 108, 164, 204). The resolution of VeriSeq NGS is validated to detect segmental (sub-chromosomal) aneuploidies of 20Mb or larger by the manufacturer, although detection of regions down to 1.81Mb have been reported using this platform (103). In our centre, we consider 'aneuploidy' to encompass both whole and segmental chromosome abnormalities.

Supernumerary blastocysts classified as 'aneuploid' (no mosaics) by PGT-A were donated to science by signed informed consent by 45 patients (average age of 36.5 ± 5.7) and de-identified. This study was approved by the institutional review board of the Zouves Foundation for Reproductive Medicine (OHRP IRB00011505).

10.4.2. ICM and Second TE Biopsy Collection and Analysis

ICM biopsies were isolated from vitrified-warmed blastocysts as outlined in the legend for Figure 11A, basing the technique on a protocol described previously (208) but omitting the exposure of samples to Ca^{2+}/Mg^{2+}-free medium. Immediately following ICM biopsy, an additional TE biopsy was collected. All biopsies were washed three times to clear any loose cells or cellular debris, and subsequently stored at -80°C until further processing. Biopsies were subjected to NGS-based PGT-A (as detailed above), and the results were evaluated independently by three analysts blinded to the analysis profile of the original,

clinically reported TE biopsy. For transparency, all karyotype profiles of every biopsy analyzed in this study are shown in the main or supplementary figures of the manuscript.

10.4.3. Immunofluorescence

Whole blastocysts or biopsies were immersed in fixation buffer containing 4% paraformaldehyde (EMS #15710) and 10% fetal bovine serum (FBS) (Seradigm 1500-050) in phosphate buffered saline (PBS) (Corning MT21040CM) for 10 minutes (min) at room temperature (rt), followed by three 1 min washes at rt in stain buffer, composed of 0.1% Triton X-100 (TX-100) (Sigma X100-100ML) and 10% FBS in PBS. Samples were then immersed in permeabilization buffer (0.5% TX-100, 10% FBS in PBS) for 30 min at rt, followed by three washes in stain buffer. Samples were then exposed to stain buffer containing both primary antibodies each in 1:200 concentrations over night at 4°C rocking on a nutator. Primary antibodies were mouse anti-human GATA3 (Thermo Fisher MA1-028) and rabbit anti-human OCT4A (Cell Signaling #2890). The next day, after three washes in stain buffer, samples were immersed in stain buffer containing both secondary antibodies each in 1:500 concentrations for 2-3 hours at rt. Secondary antibodies were goat anti-mouse IgG AlexaFluor488 (Thermo Fisher A11029) and goat anti-rabbit IgG AlexaFluor647 (Thermo Fisher A21245). After three washes in stain buffer, samples were exposed to nuclear stain (Hoechst 33342, Thermo Fisher H3570) diluted at 1:1000 in stain buffer for 30 min at rt, followed by three more washes in stain buffer. Samples were placed in glass bottom dishes (MatTek P35G-1.5-20-C) in small drops of stain buffer

overlaid with mineral oil (Sigma M5904), and imaged with a LSM 780 Confocal microscope (Zeiss).

10.1.4. Analysis of Tissue Relatedness

In cases of clinical TE-ICM karyotype discordance, we confirmed tissue relatedness by a DNA fingerprinting method, which utilizes SNP analysis and linkage disequilibrium, known as 'Tilde' (209). The method was used to rule out sample cross-contamination or mislabeling and infer, based on low-coverage sequencing data, whether ICM and TE biopsies were derived from the same blastocyst. This method facilitates indirect comparison of low-coverage samples based on the principle that sparse observed genotypes are informative of genotypes at nearby unobserved markers due to patterns of linkage disequilibrium (LD) in the population.

Reads were mapped to the hg19 reference using the BWA (version 0.7.17) backtrack algorithm with default parameters (210). We then used the LASER method (version 2.04; (211)) to select the appropriate ethnically matched 1000 Genomes Project super-population (212) for each blastocyst, as required by Tilde. LASER combines genotype imputation with principal components analysis to infer individual ancestry based on low-coverage sequence data. Blastocyst genotypes were visualized in reference ancestry space defined by principal components analysis of the HGDP reference panel (213). Blastocysts were then assigned to corresponding 1000 Genomes super-populations based on ancestries of the K=10 nearest neighbor reference samples in principal

components space. In the case of blastocyst #97, whose ICM and TE biopsies were assigned to European and Middle Eastern reference populations, respectively, we selected the European super-population as the reference panel. We note that these populations fall close to one another in space defined by the top three principal components. Furthermore, Vohr et al. (2015) demonstrated that Tilde is relatively robust to misspecification of the reference panel.

Tilde computes a log-likelihood ratio comparing a model in which two samples are derived from the same individual (i.e., same embryo) to a model in which two samples are derived from unrelated individuals (i.e., different embryos). Positive log-likelihood ratios indicate that the data support the former model, while negative log-likelihood ratios indicate that the data support the latter model. Bootstrapping was performed to generate distributions and assess uncertainty in log-likelihood ratio estimates.

10.4.5. Statistical Analysis of Correlation Between Morphology and Karyotype Discordance

Analysis and graph preparation were performed in Prism 6 (GraphPad). Differences between groups were assessed by Chi-square test for trend with 95% confidence levels. Significance was defined when $P < 0.05$.

10.5. Results

10.5.1. Isolation of ICM and Second TE Biopsies

We adopted a modified ICM-biopsy procedure previously outlined (208), which permitted us to collect an ICM biopsy and subsequently a second TE biopsy in blastocysts (Figure 11A). Immunofluorescence was used to confirm accurate isolation of intended cells. In whole blastocysts, the pluripotency factor OCT4 was present at high levels in the ICM and at low levels in the TE, while GATA3 was exclusively expressed in cells of the TE as previously shown (214). Analysis of matched TE-ICM biopsies from 12 blastocysts indicated that both biopsy types exclusively contained cells of their intended lineage and were devoid of contamination from the other cell type (Figure 11B and Supplementary Figure 1). Nuclear counterstain by Hoechst did not reveal any cells with fragmenting or apoptotic nuclear material, suggesting that the biopsy technique did not disrupt individual cells (Figure 11B and Supplementary Figure 1). On average, TE biopsies comprised 7.6 cells (+/- 1.3 SD) while ICM biopsies comprised 7.3 cells (+/- 2.0 SD).

Figure 11. Validation Of Biopsy Methods Used In The Study.
(A) Isolation of ICM biopsy in blastocysts. The blastocyst is immobilized with a holding pipet touching the polar TE (adjacent to the ICM), and laser pulses are administered through the zona and mural TE opposite the ICM creating an opening. A biopsy pipette is introduced and guided to the ICM, which is suctioned out through the opening. Once a portion of ICM cells are extracted past the zona, they are exposed to laser pulses aimed at cell-cell junctions to isolate a 5-10 cell biopsy. (B) Nuclear counterstain (Hoechst) and immunofluorescent stains for the TE marker, GATA3, and ICM marker, OCT4, in a whole human blastocyst and isolated TE and ICM biopsies. See additional samples in Supplementary Figure 1. Scale bars = 25µm.

A

B
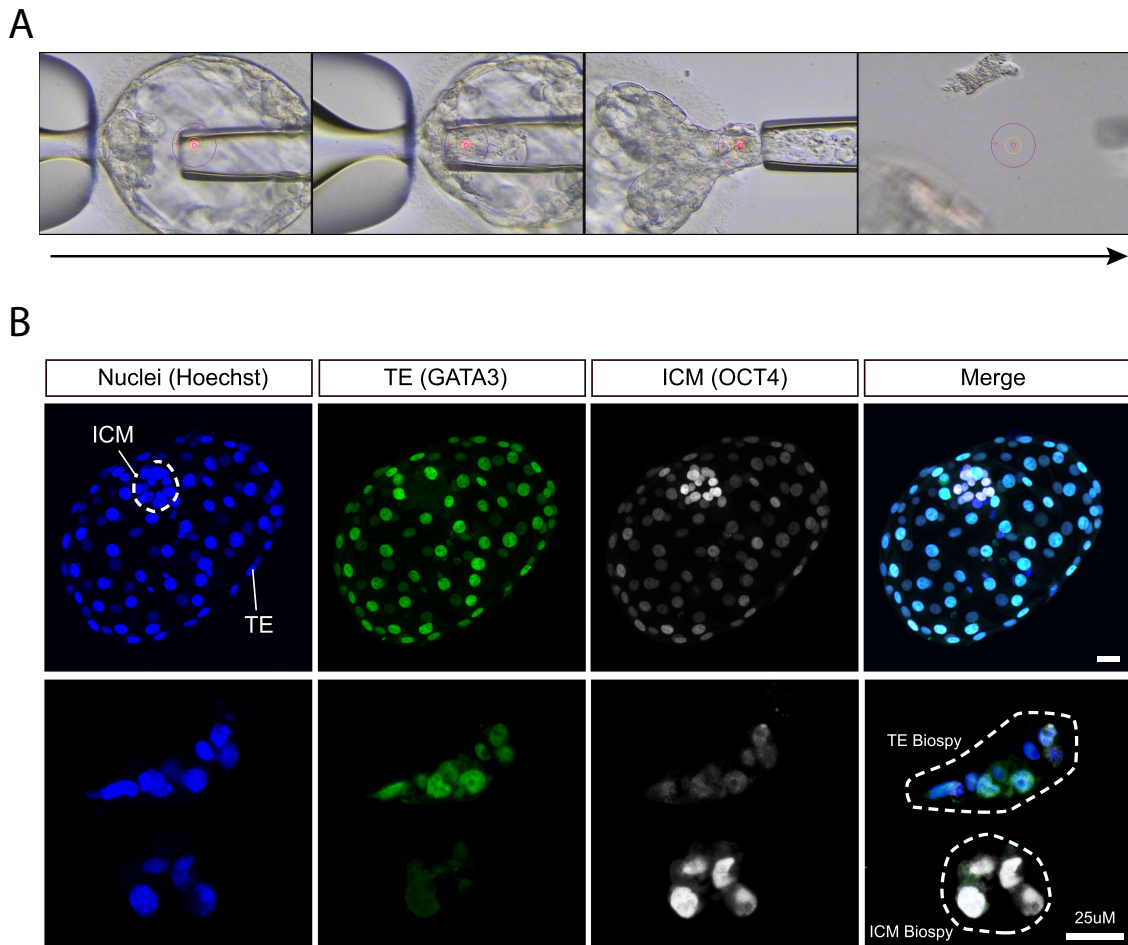
10.5.2. Clinical TE-ICM Biopsy Concordant Blastocysts

Of the 100 blastocysts originally classified as aneuploid by clinical (original) TE biopsy, 93 had ICMs that were also classified as aneuploid, which we denote as aneuploid-aneuploid concordant (Figure 12 and Table 1). Importantly, when only considering blastocysts with whole chromosomal aneuploidies (single or multiple) in their clinical TE biopsies, aneuploidy in the ICM was present in 90 out of 93 cases (96.8%). On the other hand, when considering blastocysts with only segmental (sub-chromosomal)

aneuploidies in their clinical TE biopsies, aneuploidy in the ICM was present in only 3 out of 7 cases (42.9%).

In aneuploid-aneuploid concordant blastocysts, analysis of second TE biopsies showed aneuploidy in 86 out of 88 cases, equaling 97.7% (Table 1). The remaining two samples showed a mosaic pattern in their respective second TE biopsies. In five samples, a second TE biopsy could not be retrieved.

The 93 clinical TE-ICM aneuploid-aneuploid concordant blastocysts could be further subdivided in two groups. Thus, 79 were blastocysts that had perfectly matching karyotypes in the clinical TE and ICM biopsies (i.e., all the same chromosomes possessed the same aneuploidies in both tissues), which we denoted as aneuploid-aneuploid perfect concordance (Figure 12, Table 1, and for the karyotypic profiles see Supplementary Figure 2). Such instances are likely consequences of meiotic errors, as the identical aneuploidy is present in both TE and ICM tissues.

The remaining 14 out of 93 blastocysts had dissimilar aneuploidies in the clinical TE and ICM biopsies, which we denoted as aneuploid-aneuploid imperfect concordance (Figure 12, Table 1, and for the karyotypic profiles see Supplementary Figure 2). Interestingly, most of such blastocysts (10 out of 14) showed the same aneuploid chromosome(s) in the ICM biopsy as the clinical TE biopsy (presumed consequence of meiotic error), but

contained additional mosaic events in the ICM (resulting from mitotic error), often segmental in nature.

Figure 12. Summary Of Paired Clinical TE-ICM Comparison Results.
Summary of paired clinical TE-ICM comparison results. Dot plot displays results for all blastocysts, regardless of aneuploidy type. Pie charts depict data stratified by nature of aneuploidy detected in the original TE biopsy for each blastocyst.
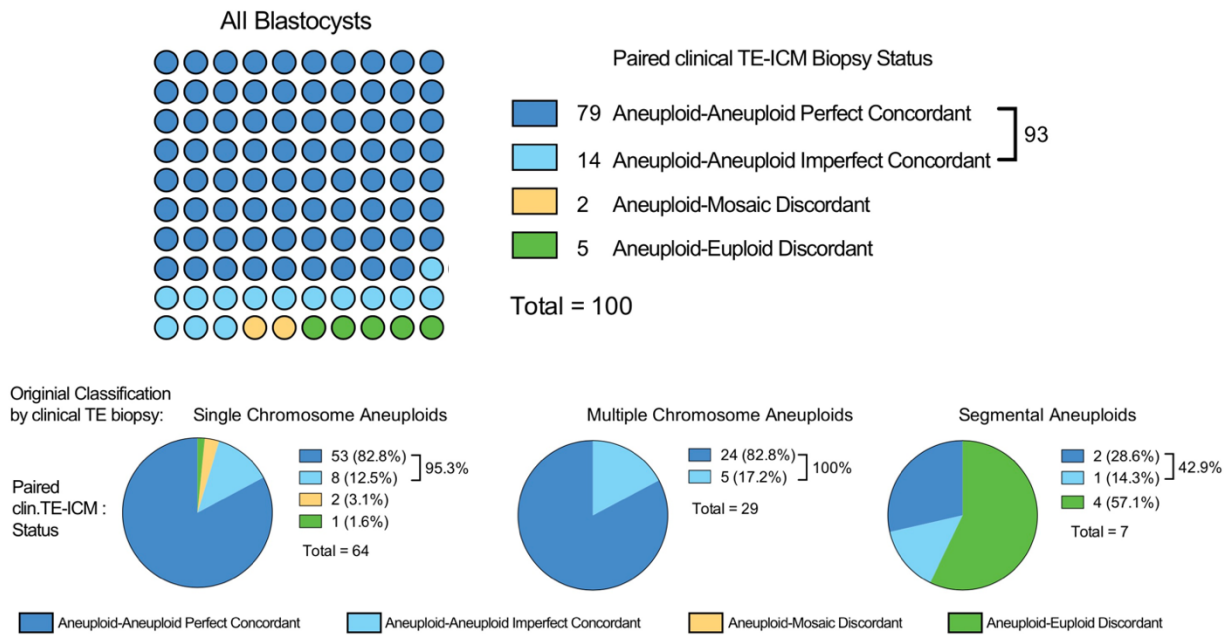
Table 1. List Of Blastocysts, Clinical TE, ICM, And Second TE Biopsies Analyzed In This Study.

Blastocyst Study id#	Gardner Grade	Clinical TE–ICM aneuploid–aneuploid perfect concordant		
		Clinical TE Biopsy	**ICM Biopsy**	**Second TE Biopsy**
1	4BB	45,XY,−4	45,XY,−4	45,XY,−4
2	4BB	45,XX,−7	45,XX,−7	45,XX,−7
3	5BB	45,XX,−8	45,XX,−8	46,XX,−8*,+15*,+20*
4	3AB	45,XY,−8	45,XY,−8	45,XY,−8
5	5BC	45,XX,−10	45,XX,−10	45,XX,−10
6	4BB	45,XY,−11	45,XY,−11	45,XY,−11
7	5BB	45,XX,−13	45,XX,−13	45,XX,−13
8	5BC	45,XY,−13	45,XY,−13	n/a
9	5BC	45,XY,−14	45,XY,−14	45,XY,−14
10	4BB	45,XY,−14	45,XY,−14	45,XY,−14
11	2BB	45,XX,−15	45,XX,−15	45,XX,−15
12	4BC	45,XX,−15	45,XX,−15	n/a
13	3BB	45,XX,−16	45,XX,−16	45,XX,−16
14	4BC	45,XX,−16	45,XX,−16	45,XX,−16
15	4BB	45,XX,−16	45,XX,−16	45,XX,−16
16	4BB	45,XY,−16	45,XY,−16	45,XY,−16
17	5CC	45,XY,−16	45,XY,−16	45,XY,−16
18	5CC	45,XX,−17	45,XX,−17	45,XX,−17
19	5AB	45,XY,−18	45,XY,−18	45,XY,−18,del(10)(q11.21q26.3)*
20	4BB	45,XX,−21	45,XX,−21	45,XX,−21
21	5BB	45,XX,−21	45,XX,−21	45,XX,−21
22	4CB	45,XY,−21	45,XY,−21	45,XY,−21
23	5BB	45,XX,−22	45,XX,−22	45,XX,−22
24	4BB	45,XX,−22	45,XX,−22	45,XX,−22
25	5BB	45,XY,−22	45,XY,−22	45,XY,−22
26	4BB	45,XY,−22	45,XY,−22	45,XY,+4*,−22
27	4AA	45,XY,−22	45,XY,−22	45,XY,−22
28	4BB	45,X	45,X	46,XX,dup(X)(p22.33p21.1),dup(X)(q22.3q25)*
29	5BC	47,XX,+1	47,XX,+1	47,XX,+1
30	4BC	47,XY,+4	47,XY,+4	47,XY,+4
31	4AB	47,XX,+13	47,XX,+13	47,XX,+13
32	3BB	47,XX,+13	47,XX,+13	47,XX,+13
33	5AA	47,XY,+15	47,XY,+15	47,XY,+15
34	4CB	47,XX,+16	47,XX,+16	47,XX,+16
35	3AB	47,XX,+16	47,XX,+16	47,XX,+16
36	5BB	47,XX,+16	47,XX,+16	n/a
37	5BB	47,XY,+16	47,XY,+16	47,XY,+16
38	4BB	47,XY,+16	47,XY,+16	47,XY,+16
39	4BC	47,XY,+16	47,XY,+16	47,XY,+16
40	5BB	47,XY,+17	47,XY,+17	47,XY,−10*,+17
41	4BB	47,XY,+18	47,XY,+18	47,XY,+18
42	4CB	47,XY,+18	47,XY,+18	47,XY,+18
43	5BB	47,XY,+19	47,XY,+19	47,XY,+19
44	5AB	47,XX,+20	47,XX,+20	47,XX,+20
45	4BC	47,XX,+21	47,XX,+21	47,XX,+21

Table 1 continued

Blastocyst Study id#	Gardner Grade	Clinical TE–ICM aneuploid–aneuploid perfect concordant		
		Clinical TE Biopsy	**ICM Biopsy**	**Second TE Biopsy**
46	5CB	48,XX,+21(x2)	48,XX,+21(x2)	48,XX,+21(x2)
47	4BB	47,XX,+22	47,XX,+22	47,XX,+22
48	4AA	47,XX,+22	47,XX,+22	47,XX,+22
49	5AB	47,XX,+22	47,XX,+22	47,XX,+22
50	4BB	47,XY,+22	47,XY,+22	47,XY,+22
51	5CC	47,XY,+22	47,XY,+22	47,XY,+22
52	4BC	47,XY,+22	47,XY,+22	47,XY,+22
53	3CC	47,XY,+22	47,XY,+22	47,XY,+22,del(1)(q25.2q44)
54	3BB	44,XY,−10,−22	44,XY,−10,−22	44,XY,−10,−22
55	4BB	46,XX,−12,+16	46,XX,−12,+16	46,XX,−12,+16
56	4CC	44,XX,−14,−19	44,XX,−14,−19	44,XX,−14,−19
57	4BB	44,XY,−18,−21	44,XY,−18,−21	44,XY,−18,−21
58	4BC	46,XY,−19,+22	46,XY,−19,+22	n/a
59	5BB	46,XY,−21,+22	46,XY,−21,+22	46,XY,−21,+22
60	5CB	48,XY,+2,+3	48,XY,+2,+3	48,XY,+2,+3
61	4BB	46,XY,+3,−22	46,XY,+3,−22	n/a
62	4AA	48,XX,+5,+9	48,XX,+5,+9	48,XX,+5,+9
63	4AC	46,XX,+6,−15	46,XX,+6,−15	46,XX,+6,−15
64	5BB	48,XY,+8,+16	48,XY,+8,+16	48,XY,+8,+16,del(2)(q21.1q37.3)*
65	3BB	48,XX,+9,+16	48,XX,+9,+16	48,XX,+9,+16
66	3BB	48,XX,+9,+22	48,XX,+9,+22	48,XX,+9,+22
67	4BB	48,XX,+10,+18	48,XX,+10,+18	48,XX,+10,+18
68	5AB	48,XY,+16,+21	48,XY,+16,+21	48,XY,+16,+21
69	5BB	46,XX,+18,−22	46,XX,+18,−22	46,XX,+18,−22
70	3BA	45,XX,−11,+12,−21	45,XX,−11,+12,−21	45,XX,−11,+12,−21
71	4CB	47,XY,+1,−13,+21	47,XY,+1,−13,+21	47,XY,+1,−13,+21
72	3BB	47,XY,+11,+18,−20	47,XY,+11,+18,−20	47,XY,+11,+18,−20
73	5BC	47,XY,+14,−15,+19	47,XY,+14,−15,+19	47,XY,+14,−15,+19
74	5BC	49,XX,+16,+18,+19	49,XX,+16,+18,+19	48,XX,+16,+18,+19*
75	4AB	48,XX,−2,+3,+9,+22	48,XX,−2,+3,+9,+22	48,XX,−2,+3,+9,+22
76	5BA	46,XY,+3,+4,−18,−21	46,XY,+3,+4,−18,−21	46,XY,+3,+4,−18,−21
77	5CB	47,XY,+16,del(20)(q13.2q13.33)	47,XY,+16,del(20)(q13.2q13.33)	47,XY,−1*,+16,−20*,del(5)(q23.1q35.3)*
78	4AB	46,XY,del(6)(q16.1q27)	46,XY,del(6)(q16.1q27)	46,XY,del(6)(q16.1q27)*
79	4BC	46,XX,del(1)(q43q44)	46,XX,del(1)(q43q44)	46,XX,del(1)(q43q44)

Blastocyst Study id#	Gardner Grade	Clinical TE–ICM aneuploid–aneuploid imperfect concordant		
		Clinical TE Biopsy	**ICM Biopsy**	**Second TE Biopsy**
80	4AC	45,XX,−14	45,XX,−14,del(1)(p36.32p36.12)*	45,XX,−14
81	4BB	45,XY,−16	45,XY,−16,dup(2)(p25.3p23.1)*	45,XY,−16
82	4AA	45,XY,−18	45,XY,−18,dup(2)(q23.3q37.3)*	45,XY,−18
83	5BA	45,XY,−21	45,XY,−21,dup(18)(p11.32q12.1)*	45,XY,−21
84	3BC	45,XX,−22	45,XX,−15*,−22	45,XX,−22
85	4BC	45,X	45,X,+20*,+21*	45,X,+2*,+14*
86	4BB	47,XX,+16	47,XX,+16,dup(5)(q12.1q35.1)*	47,XX,+16

Table 1 continued

Blastocyst Study id#	Gardner Grade	Clinical TE–ICM aneuploid–aneuploid imperfect concordant		
		Clinical TE Biopsy	ICM Biopsy	Second TE Biopsy
87	5BB	47,XY,+20	47,XY,+20,del(1)(p36.33p33)*	47,XY,+20
88	5CC	46,XX,−10,+15	48,XX,−10*,+15,+17	46,XX,−10,+15
89	4BC	44,XX,−15,−22	44,XX, −15,+18*,−22,dup(1)(q12q44)*	44,XX,−15,−22
90	5BB	44,XY,−21,−22	44,XY,−21,−22,del(1)(p36.33p33)*	44,XY,−21,−22
91	5BC	47,XX,+4,+9,−13	47,XX,+3*,+4,+7*,+9,−13	47,XX,+3*,+4,+7*,+9,−13
92	5CC	47,XX,+20,del(2)(p25.3p24.1)	47,XX,+20,del(2)(p25.3p24.1)*	47,XX,+20,del(2)(p25.3p24.1)
93	5BB	46,XX,del(16)(p13.3p11.2)	45 XX,−16	46,XX,del(16)(p13.3p11.2),dup(16)(p11.2p24.3)*

Blastocyst Study id#	Gardner Grade	Clinical TE–ICM aneuploid–mosaic discordant		
		Clinical TE Biopsy	ICM Biopsy	Second TE Biopsy
94	4BC	45,XY,−19	46,XY,−19*	45,XY,−19
95	5AB	47,XY,+6	46,XY,del(4)(q32.1q35.2)*	46,XY

Blastocyst Study id#	Gardner Grade	Clinical TE–ICM aneuploid–euploid discordant		
		Clinical TE Biopsy	ICM Biopsy	Second TE Biopsy
96	4AB	47,XX,+12	46,XX	46,XX
97	4BB	46,XX,del(2)(q22.1q31.1)	46,XX	46,XX,del(2)(q22.1q31.1)
98	4BB	46,XY,dup(3)(q26.2q29)(x2)	46,XY	46,XY,dup(3)(q26.2q29)*,dup(22)(q11.1q13.31)*
99	4AB	46,XX,del(9)(q12q34.3)	46,XX	46,XX,del(9)(q12q34.3)*
100	3BB	46,XX,dup(11)(q23.2q25)	46,XX	n/a

* MOSAIC

10.5.3. Clinical TE-ICM Biopsy Discordant Blastocysts

Of the 100 blastocysts tested, we observed two cases in which the clinical TE biopsy was uniformly aneuploid but the ICM was mosaic (Figure 12, Table 1, and for the karyotypic profiles see Figure 13).

Five out of 100 blastocysts had euploid ICMs while their clinical TE biopsies contained aneuploidies (Figure 12, Table 1, and for the karyotypic profiles see Figure 13). Blastocyst

#96 was the only case in which the clinical TE biopsy had a whole chromosomal

aneuploidy (gain of chromosome 12, note that the karyotype profile enters

Figure 13. NGS-Based PGT-A Karyotype Profiles For Biopsies In Blastocysts With Discordant Clinical TE-ICM Patterns.
See Table 1 for the interpretation of each profile.
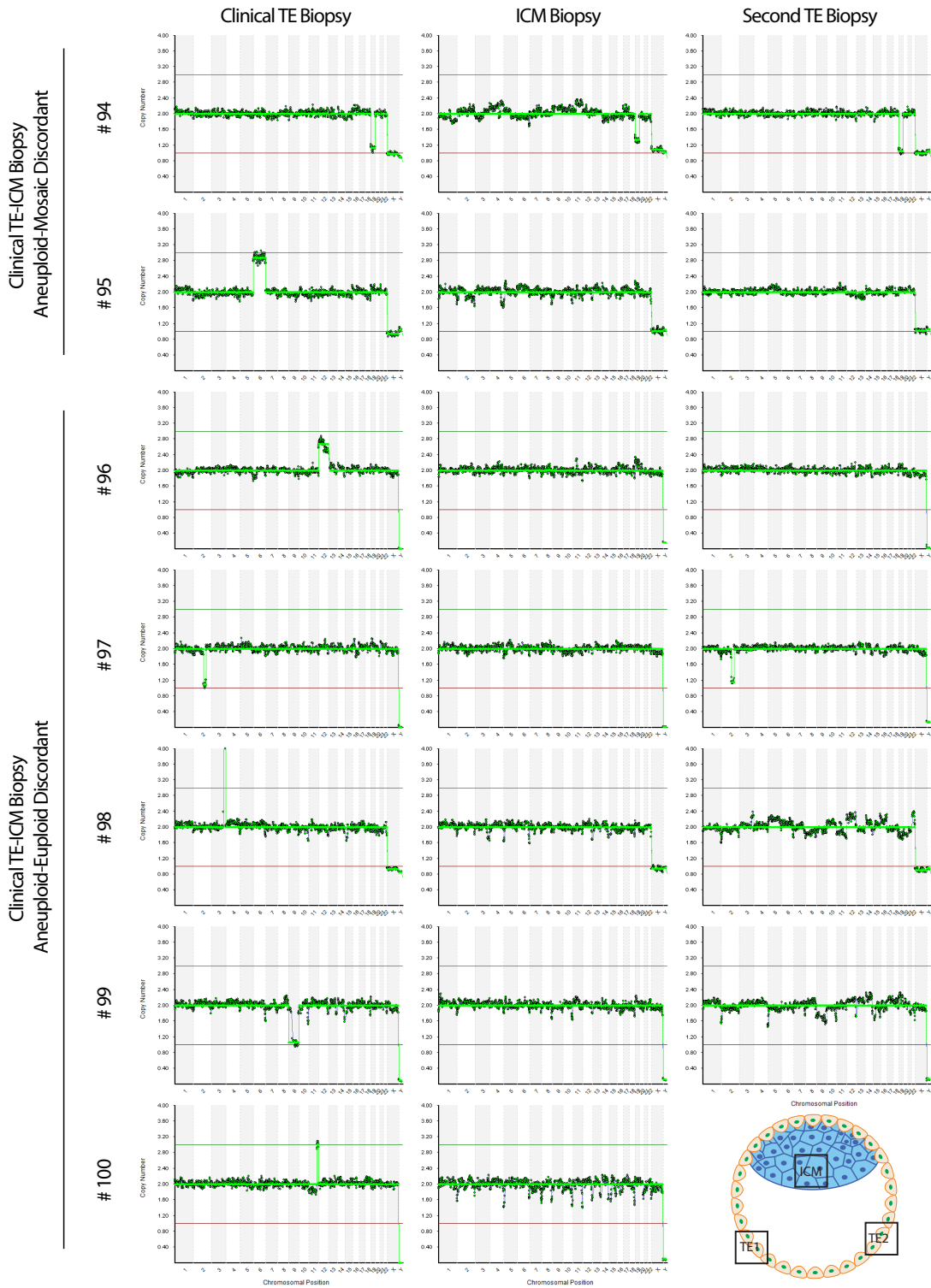
into the 2.8-3.0 copy number region) but it displayed euploidy in the ICM as well as in the second TE biopsy.

The remaining four samples (blastocysts #97-#100) contained segmental aneuploidies in their original TE biopsies, but euploid ICM biopsies. For blastocyst #97, the clinical and second TE biopsies contained the same segmental aneuploidy, thereby suggesting euploidy confined to the ICM. This would be consistent with a mitotic event happening before or at the time of lineage segregation but in the progenitor cell of a large part of the TE. Blastocysts #98 and #99 displayed mosaicism in their respective second TE biopsies, revealing the occurrence of mitotic errors in the TE lineage. For one blastocyst (#100), the second TE biopsy did not yield results due to a failed WGA reaction. (Global WGA failure rate for this study is 1 out of 221, or 0.4%). In total, of the clinical TE-ICM discordant blastocysts (aneuploid-euploid or aneuploid-mosaic) yielding information in the second TE biopsy, only 2 out of 6 (33.3%) were uniformly aneuploid.

In cases of clinical TE-ICM biopsy discordance, there existed the possibility of sample contamination or mislabeling. Notably, in the 100 embryos tested, the sex chromosomes (XX or XY) were always concordant between biopsies taken within the same blastocyst. Further, for each of the seven blastocysts that produced discordant results, we performed DNA fingerprinting to confirm that the clinical TE and ICM biopsies were derived from the same respective embryos (Figure 14, Supplementary Figure 3, Supplementary Table 1). As controls, we applied the Tilde method to 24 comparisons of presumed unrelated

embryos as well as four comparisons of full sibling (full-sib) embryos obtained from the

same patient. Results from the unrelated negative controls supported

Figure 14. Log-Likelihood Ratios Of Relatedness Between Tissues In Blastocysts With Clinical TE-ICM Discordance.

In green, controls comparing biopsies from embryos derived from patients expected to be unrelated, showing negative values. In red, comparisons between biopsies from blastocysts derived from the same patient (full-sibs) showing positive values. In purple, comparisons between clinical TE and ICM biopsies for each blastocyst classified as discordant in the study, showing highly positive log-likelihood ratios of relatedness.
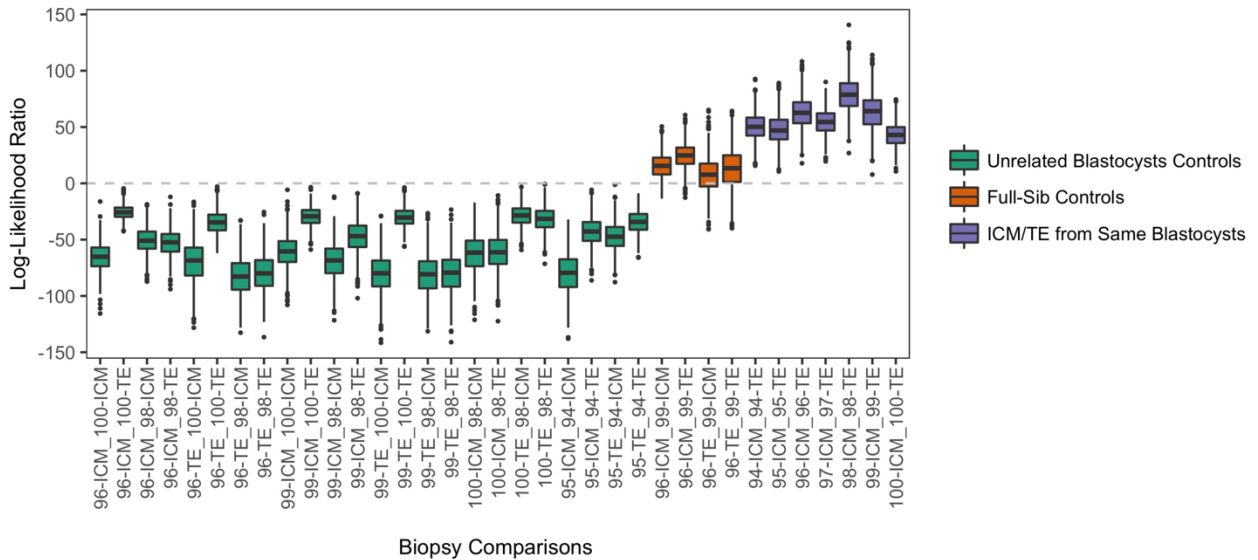
the capacity of Tilde to distinguish these samples, reflected by negative distributions of

log-likelihood ratios. For all seven embryos producing discordant TE-ICM results, the data

supported a model in which the samples were derived from the same corresponding

embryo, reflected by positive distributions of log-likelihood ratios. Meanwhile, the full-sib

samples from the same patient also produced positive distributions of log-likelihood ratios,

but intermediate between the unrelated and same-embryo comparisons, supporting the

power of tilde to distinguish varying levels of relatedness. Together, our data suggest no

evidence of cross-contamination or sample mislabeling and substantiate the conclusion

that the TE and ICM biopsies of discordant karyotype were derived from the same respective embryos.

Finally, we determined whether poor blastocyst morphology impacted karyotype discordance. The analysis indicated that neither blastocyst stage nor ICM/TE grade affected the likelihood of intra-blastocyst karyotype inconsistencies (Supplementary Figure 4).

10.6. Chapter Discussion

Some parties have argued that PGT-A should not be performed under any circumstance and one of the criticisms of the technology questions whether a clinical TE biopsy is a valid genetic representative of the embryo (198, 201, 215). A study basing its rationale on mathematical modeling has claimed that a typical TE cell biopsy cannot determine embryo ploidy accurately enough for clinical use (216). One of the ensuing concerns that has been expressed is the possibility of erroneously discarding viable embryos (199). Here however, we provide experimental evidence using NGS that a TE biopsy classified as aneuploid is commonly predictive of aneuploidy in the ICM. In our experience, a whole chromosome aneuploidy in a clinical TE biopsy is predictive of aneuploidy in the ICM in 96.8% of cases (sample size n=93), although for only a segmental aneuploidy, this decreases significantly to 42.9% (n=7).

A blastocyst with an aneuploid TE and ICM due to meiotic error is in principle exceptionally unlikely to result in healthy pregnancy (217). Although various corrective mechanisms for aneuploidies in human embryos have been proposed (differential proliferation/depletion, preferential lineage allocation, self-correction) (153, 173) and have also been conceptually demonstrated in mouse embryos (218) and human embryonic stem cells (hESC) (219), most models describe the out-competition of aneuploid cells by euploid cells in the mosaic setting, not the conversion of an entirely aneuploid embryo to an entirely euploid one.

The observation that segmentals had a drastically different rate of clinical TE-ICM discordance compared to whole chromosome aneuploids highlights the difference in mechanistic origins of these two types of aneuploidies. Whole chromosome aneuploidies can arise during meiosis or mitosis by different mechanisms that include non-disjunction, anaphase lag, and endoreplication (141), but the majority are believed to be derived from meiotic errors in the oocyte (220). The majority of segmental aneuploidies on the other hand are mitotic in origin and are thought to arise during the first few cell divisions after fertilization (136). Cell cycle control is thought to be more lax during the first days of embryogenesis due to rapid mitoses primarily controlled by maternal RNA and proteins, leading to an increased incidence of double strand breaks which upon faulty correction mechanisms result in segmental duplications or deletions when left unresolved by a strained cell cycle machinery (136). Consequently, segmental aneuploidies will often be

represented in mosaic configurations at a whole blastocyst level, likely translating in the high TE-ICM discordance rate observed for the segmental aneuploidy group in this study. Out of 93 blastocysts with whole chromosome aneuploidies (single or multiple) in a clinical TE biopsy, three embryos had a discordant ICM: two contained mosaic ICM biopsies, and one had a euploid ICM. Consequently, the karyotype of these three blastocysts should be re-classified from aneuploid to mosaic, since on a whole embryo level they contained aneuploid and euploid cells. This re-categorization would have changed the status of the blastocysts from 'not recommended for transfer' to 'possible transfer if no euploid embryos available'. Mosaic embryos have recently been considered for transfer in several clinics, producing healthy pregnancies albeit with considerably lower implantation rates than blastocysts classified as euploid (164, 171, 204, 221).

From a clinical standpoint, our findings may support re-biopsy of blastocysts in patients who have only produced embryos classified as aneuploid (particularly segmentals) by initial TE biopsy after repeated IVF cycles, an occurrence that happens with relative frequency especially with advanced maternal age (75). It could also affect those patients who have unsuccessfully transferred their embryos classified as 'euploid' and 'mosaic', and only have 'aneuploid' samples remaining. In our study, all blastocysts had an initial, clinical TE biopsy that was uniformly aneuploid. When a second TE biopsy was either mosaic or euploid, such a blastocyst had a 66% chance of containing an ICM that was either mosaic or euploid as well. On the other hand, in cases where the second TE biopsy was aneuploid, the ICM was mosaic in only 1.1% of cases, and there were no euploid

ICM instances. Therefore, our results suggest that TE re-biopsy can reveal whether the ICM is mosaic or euploid, helping to identify new blastocysts for possible clinical use when they were originally not recommended for transfer due to aneuploidy in the clinical TE biopsy. Importantly, while the act of re-biopsy might negatively affect blastocysts, re-biopsied blastocysts can lead to healthy pregnancies albeit with lower efficiency than single-biopsied blastocysts (222). Nevertheless, more research is necessary to determine the short and long term effects of TE re-biopsy, and a recommendation of routine re-biopsy of blastocysts classified as aneuploid is undoubtedly premature.

The confirmed existence of clinical TE-ICM discordant embryos could also help explain the rare accounts of healthy pregnancies resulting from transfer of embryos classified as aneuploid by PGT-A (223), although it must be pointed out that to our knowledge, there exist no reports of such events when using blastocyst stage NGS-based PGT-A.

It is important to note that our determined rates of clinical TE-ICM concordance apply specifically to blastocysts classified as 'uniform aneuploid' (no mosaics) by PGT-A. Having observed an overall 7% clinical TE-ICM discordance rate in our samples, we cannot assume the inverse: that 7% of blastocysts classified as euploid contain an aneuploid ICM. A further intriguing and clinically important question is what a clinical TE biopsy showing mosaicism says about the ICM. Unfortunately, our study cannot shed light on that point.

A further limitation of this study was that not all cells were analyzed for intra-blastocyst karyotypic concordance. The ICM biopsies isolated (averaging 7.3 cells) collected the bulk of ICM cells but invariably left residual ICM cells behind. On average, we collected 15 TE cells from the two combined TE biopsies of each blastocyst, hence a substantial portion of the TE was left unanalyzed. From the technical standpoint, we were unable to isolate more cells from a specific tissue without contamination from the other lineage. As a result, instances of karyotype discordance could remain concealed.

While highly controversial, the concept of transferring embryos testing aneuploid by PGT-A is a real subject of discussion in both scientific (223) and mainstream media (224). The upheaval created by these viewpoints has partly been bolstered by the yet unspecified capability of a single clinical TE biopsy to reflect the state of the ICM and remaining TE. With regard to this question, our findings contribute experimental validation on the practice of PGT-A at the blastocyst stage, considering the high intra-blastocyst aneuploidy concordance rates, especially in the case of whole chromosome losses or gains. If indeed the group of blastocysts analyzed in this study is representative of the general body of IVF blastocysts, it would mean that when selecting an embryo classified as 'aneuploid' by PGT-A for uterine transfer, it almost always contains aneuploidy in the entire blastocyst. Unless robust self-correction mechanisms do in fact exist, the said embryo would invariable lead to failed implantation, miscarriage or a chromosomally abnormal baby. Segmental aneuploidies on the other hand are rarely concordant; if our

observations are confirmed in a larger sample group they should be regarded as their

own distinct class when prioritising or de-selecting embryos for transfer in the clinic.

11. Specific Aim B: To test the hypothesis that embryos classified as mosaic with PGT-A have inferior clinical success rates than euploid embryos, but can nonetheless result in healthy pregnancies

The following published work is presented for this specific aim:

Victor AR, Tyndall JC, Brake AJ, Lepkowsky LT, Murphy AE, Griffin DK, McCoy RC, Barnes FL, Zouves CG, Viotti M. *One hundred mosaic embryos transferred prospectively in a single clinic: exploring when and why they result in healthy pregnancies.* Fertil Steril. 2019 Feb;111(2):280-293. doi: 10.1016/j.fertnstert.2018.10.019. PMID: 30691630.

11.1. My Personal Contribution To The Work

My personal contribution to this study includes its conceptual design and performing a large portion of the clinical work that forms its basis (embryology and molecular genetics, validation). In addition, performing most of the data collection and assisting in its analysis and manuscript preparation.

11.2. Chapter Summary

State-of-the-art PGT-A methods can identify intermediate copy numbers (ICNs) for (sub-) chromosomal regions in TE biopsies, which is consistent with mosaicism in the

multicellular sample. The appropriate clinical management of embryos producing such results is a matter of debate. Here, we investigated the clinical outcomes of embryos classified as 'mosaic' by PGT-A, and explored biological mechanisms leading to healthy pregnancies from mosaic embryo transfers.

Embryos underwent blastocyst-stage PGT-A by next-generation sequencing (NGS). Trophectoderm (TE) biopsies containing 20-80% abnormal cells were deemed mosaic, and corresponding blastocysts (n=100) were transferred into 59 patients. Globally, mosaic embryos showed inferior clinical outcomes than euploid embryos. In this sample group, aneuploid cell percentage in TE biopsies did not correlate with outcomes, but type of mosaicism did, as embryos with single mosaic segmental aneuploidies fared better than all other types. Mosaic blastocysts generated from oocytes retrieved at young maternal ages (≤ 34 years) showed better outcomes than those retrieved at older maternal ages.

Mosaic embryos donated to research were examined for karyotype concordance in multiple biopsies, and assessed for cell proliferation and death by immunofluorescence and computational quantitation. The embryos displayed low rates of karyotype concordance between multiple biopsies, and showed significant elevation of cell proliferation and death compared to euploid embryos.

In summary, after euploid embryos, mosaic embryos can be considered for transfer prioritizing those of the single segmental mosaic type. If a patient has mosaic embryos available that were generated at different ages, preference should be given to those made at younger ages. Intra-blastocyst karyotype discordance and differential cell proliferation and death might be reasons by which embryos classified as mosaic can result in healthy pregnancies and babies.

11.3. Chapter Introduction

Chromosomal mosaicism, or the presence of two or more chromosomally distinct cell lines within an individual, has clinical implications both in naturally conceived and IVF pregnancies. Among natural pregnancies it is known to affect ~2% of all gestations in the form of confined placental mosaicism (CPM). This condition entails discordance of karyotypes between fetal and placental cells and can lead to adverse obstetric outcomes including intrauterine growth retardation or placental insufficiency (141, 160). Among IVF embryos, data from a flurry of recent studies suggests that, in general, mosaicism results in decreased pregnancy rates compared to normal embryos (164, 171, 172, 204, 221). However, numerous forms of mosaicism exist, and refinement of these interpretations is needed. The contemporary IVF clinic must grapple with the question: What should be done with mosaic embryos, should they be transferred, and if so, how should they be prioritized?

Preimplantation genetic testing for aneuploidy (PGT-A) at the blastocyst stage is currently used in over 20% of all IVF treatments in the USA, and growing (204). It entails analysis of the chromosomal content of a representative 5-10 cell biopsy taken from the trophectoderm (TE) tissue and produces a readout estimating the copy number of each chromosome. For autosomes, a copy number two is indicative of a disomy (considered normal/euploid), while copy numbers of one and three are indicative monosomy and trisomy, respectively (considered abnormal/aneuploid). In such cases, the clinical decision to de-select aneuploid embryos for transfer is straightforward. A third classification category exists, namely samples with analysis readouts producing values at intermediate levels between whole numbers. Such profiles are consistent with mosaicism, which would indicate the presence of both euploid and aneuploid cells in the source blastocyst. While previous technologies for PGT-A were limited in identifying this condition, next-generation sequencing (NGS) is now widely recognized as the most accurate platform for revealing and quantifying mosaicism (225).

In order to better define the characteristics and genetic abnormalities affecting the clinical outcomes of mosaic embryos, we performed an analysis of the prospective transfer of 100 embryos classified as mosaic via NGS-based PGT-A in a single IVF center. Furthermore, we explore biological mechanisms that can lead a mosaic blastocyst to ultimately result in a healthy baby.

11.4. Methods And Materials

11.4.1. Patients And Embryos

Embryos derived from patients seeking infertility treatment at a private IVF center were generated by intracytoplasmic sperm injection (ICSI) and cultured to the blastocyst stage as previously described (206). Blastocysts were assessed with the Gardner evaluation system (207) and subjected to a 5-10 cell TE biopsy and vitrified until further use. Biopsies were processed for PGT-A (see details below). In cases where no euploid blastocysts were available, patients were counseled about the possibility of selecting blastocysts classified as mosaic for uterine transfer. All embryos described in this study were transferred in a prospective manner, meaning that prior knowledge of the mosaic status of the embryos was available in every case. In certain instances, more than one mosaic blastocyst was transferred at once, or one mosaic blastocyst was transferred along with a euploid blastocyst (generally of poorer quality), especially in patients with previous failed transfers.

Clinical outcomes were defined and collected as follows: Beta human Chorionic Gonadotropin (Beta-hCG) was measured by blood test on day 10 after transfer, with values > 5.0 mIU/mL considered positive and indicative of start of pregnancy. Presence of a gestational sac observed by endovaginal ultrasound at 3-5 weeks after transfer was considered evidence of implantation. Fetal heartbeat (FHB) was confirmed by endovaginal ultrasound 6-8 weeks after transfer. Non-Invasive Prenatal Testing (NIPT), amniocentesis, and birth information were voluntarily reported by the patient.

The experiments of serial biopsy concordance and cell proliferation and death made use of supernumerary embryos donated to research by informed consent. This study was approved by the Zouves Foundation IRB (OHRP IRB00011505).

11.4.2. PGT-A

NGS-based PGT-A was performed in-house using VeriSeq kit (Illumina) on a MiSeq system (Illumina) following the manufacturer's protocol, in 24 sample runs. Karyotype profiles were scored independently by two analysts using Bluefuse Multi Analysis Software (Illumina), which depicts the copy number for each chromosome in a sample. The platform is validated to detect segmental gains/losses of 20 Mb or larger by the manufacturer, but can occasionally detect regions smaller than 2 Mb (103). A molecular karyotype profile consistent with mosaicism was determined when a whole chromosome or sub-chromosomal segment resulted in intermediate copy number levels (in the range of 20-80% between whole numbers), following PGDIS guidelines (http://www.pgdis.org/docs/newsletter_071816.html) and as previously described (164).

11.4.3. Mosaic Study Of Cell And DNA Mixes

For cell analysis, the following cell lines were used: Coriell GM00425 (+8) and GM04435 (+16, +21). Cells were cultured in RPMI 1640 (Thermo Fisher #12633-012) containing 10% FBS (Seradigm 1500-050), GlutaMAX-I (Gibco 35050-061) and Pen-Strep (Gibco 15140-122). Cells were detached with TrypLE (Gibco 12604021) and re-suspended in

culture medium. Single cells were collected and mixed in the indicated ratios totaling 10 cells per sample and stored at -80°C until chromosomal analysis by NGS as above. Each cell ratio was performed in triplicate, and one representative karyotype profile is shown per tested ratio in Figure 15A.

For DNA analysis, we obtained genomic DNA extracted from two aneuploid fibroblast cell lines. The first DNA sample (Coriell NA02948) was purified from cells trisomic for chr13. The second DNA sample (Coriell NA00072) was purified from a cell line advertised as containing a segmental loss in chr4p. We found additional chromosomal errors (-13, mos(-5q,-11p,-12p,+17q)) in the sub-clonal line used in this study (lot 1 with original extraction date 4/28/1997) and verified them in over 40 test runs. In the singlicate mixing experiments, DNA was diluted down to represent equivalent amounts contained in single diploid cells (6.6pg), such that a 50:50 mix of DNAs contained 33pg of DNA from each cell line for a total of 66pg, equivalent to DNA from 10 diploid cells per NGS reaction.

11.4.4. Multiple Biopsy Experiment

Mosaic blastocysts as determined from the original clinical TE biopsy were further processed to isolate an ICM biopsy and a second TE biopsy as described elsewhere (226). All biopsies underwent PGT-A as described above. DNA fingerprinting using a previously described method (226) was performed on every biopsy to confirm it originated from its intended blastocyst, thereby excluding the possibility of sample mislabeling or contamination.

11.4.5. Immunofluorescence

Blastocysts were immersed in fixation buffer containing 4% paraformaldehyde (EMS #15710) and 10% fetal bovine serum (FBS) (Seradigm 1500-050) in phosphate buffered saline (PBS) (Corning MT21040CM) for 10 minutes (min) at room temperature (rt), followed by three 1 min washes at rt in stain buffer composed of 0.1% Triton X-100 (TX-100) (Sigma X100-100ML) and 10% FBS in PBS. Samples were then immersed in permeabilization buffer (0.5% TX-100, 10% FBS in PBS) for 30 min at rt, followed by three washes in stain buffer. Samples were then exposed to stain buffer containing both primary antibodies (abs) each in 1:200 concentrations over night at 4°C rocking on a nutator. Primary abs were rabbit anti-human phospho-Histone H3 (Ser10) (pHH3) AlexaFluor555 conjugated monoclonal ab (Cell Signaling #3475), rabbit anti-human Cleaved Caspase-3 (Asp175) AlexaFluor647 conjugated monoclonal ab (Cell Signaling #9602), and mouse anti-human OCT-3/4 monoclonal ab (Santa Cruz sc-5279). The next day, after three washes in stain buffer, samples were immersed in stain buffer containing the secondary antibody goat anti-mouse IgG AlexaFluor488 (Thermo Fisher A11029) at 1:500 concentrations for 2-3 hours at rt. After three washes in stain buffer, samples were exposed to nuclear stain (Hoechst 33342, Thermo Fisher H3570) diluted at 1:1000 in stain buffer for 30 min at rt, followed by three more washes in stain buffer and subsequently imaged.

11.4.6. Imaging And Computational Quantitation Of Cell Proliferation And Death

Stained blastocysts were placed in glass bottom dishes (MatTek P35G-1.5-20-C) in small drops of stain buffer overlaid with mineral oil (Sigma M5904), and imaged with a LSM 780 Confocal microscope (Zeiss). Image files in the .lsm format were uploaded into the software package Imaris 8.4.1 (Bitplane), and fluorescent channels quantified for each blastocyst. The analysis was performed in a blinded fashion, as all samples were quantified computationally with a uniform set of parameters, independently of blastocyst classification. The parameters were:

Nuclear channel: spots with estimated diameter = 8.00um, background subtraction = true, classify spots by quality above 13.6. OCT3/4 channel: spots with estimated diameter = 6.00um, background subtraction = true, classify spots by quality above 11.0. pHH3 channel: spots with estimated diameter = 8.00um, background subtraction = true, classify spots by quality above 15.5. Caspase-3 channel: surfaces with enable smooth = true, surface grain size = 0.700um, enable eliminate background = true, diameter of largest sphere = 8.00um, manual threshold value = 7.64, active threshold B = false, classify surfaces by number of voxels above 204.

11.4.7. Statistics

Analysis and graph preparation was done in Prism 6 (GraphPad). In Table 3, clinical outcome comparisons between groups (defined in the table footnotes) were performed with Fisher's exact test. Note that for the analyses in Table 3, for double embryo transfer

in which only one embryo was positive but its identity could not be resolved due to matching sexes, each embryo received a value of 0.5. When this scenario occurred in cases of triple embryo transfers, each embryo received a value of 0.33. Final numbers are shown rounded to the closest integer.

In the mitosis/apoptosis quantitation experiment (Figure 15), differences between groups were assessed by unpaired, two-tailed Student's t test with Welch's correction. For all analyses: *, $P < 0.05$; **, $P < 0.01$; ***, $P < 0.001$; ns (not significant), $P \geq 0.05$.

11.5. Results

11.5.1. Detection Of Chromosomal Mosaicism With NGS-Based PGT-A

Previous reports elegantly demonstrated that mixes of cell lines with different karyotypes resulted in mosaic profiles during PGT-A (37, 108, 164, 204), and that NGS showed superior resolution and more accurate mosaic calling than other platforms, including array comprehensive chromosome hybridization (aCGH) (108). We sought to use similar spike-in experiments to confirm the ability to detect chromosomal mosaicism in our hands, using an in-house PGT-A platform. As a first pass test, we observed that mixes of individual cells from lines with different aneuploidies yielded expected profiles consistent with mosaicism (Figure 15A). Then, in order to better establish the resolution of the technology in detecting mosaicism we performed experiments with DNA purified from cell lines. This allowed for more refined mixing ratios than with whole cells. We took advantage of cell line-derived DNA that displayed a very distinct karyotypic profile: copy number 2 for some parts of the genome (consistent with disomy), copy number 1 for other regions (consistent

with monosomy), and intermediate levels (consistent with mosaicism) for yet other regions (Figure 15B, See DNA Cell Line B). This particular profile was replicated in over 40 sequencing runs, suggesting that at the time of DNA purification the cell line was not uniform and contained sub-clones resulting in mosaic profiles in some genomic regions. Mixing experiments with DNA from a different, uniformly aneuploid cell line showed superb resolution of mosaic profiles, with resolution of differences as small as ~5% (Figure 15B). This was true for both whole chromosome and segmental (sub-chromosomal) aneuploidies. Together, these experiments confirmed the capability to detect instances of chromosomal and segmental mosaicism with our in-house NGS-based PGT-A pipeline.

11.5.2. Clinical Outcome Of Prospective Mosaic Embryo Transfers Tested By NGS-based PGT-A

Between October 2016 and June 2018, a total of 100 blastocysts classified as mosaic by NGS-based PGT-A were transferred in a prospective manner (with previous knowledge of their mosaic status) at a single IVF program as frozen embryo transfers (Table 2). 50 were replaced into patients as single embryo transfers (SET), 26 as double embryo transfers (DET), and 6 as triple embryo transfers (TET). The remaining 18 were transferred alongside one euploid embryo often of poor morphological quality (Supplementary Table 4).

Figure 15. Validation Of PGT-A Method In Accurate Identification Of Mosaicism.
(A) Results from cell mixtures using a total of 10 cells per reaction. (B) Composite image from spike-in experiments with varying ratios of purified DNA from two aneuploid cell lines. Amounts of DNA mimic contents of single cells (6.6pg), resulting in 66pg per reaction. Results depict karyotype patterns consistent with the expected presence of mosaicism using NGS-based PGT-A. Note for example that the aneuploid region on chr5 is at ~50% loss when solely using DNA from cell line B, suggesting that each incremental mix with DNA from cell line A translates into a ~5% difference.
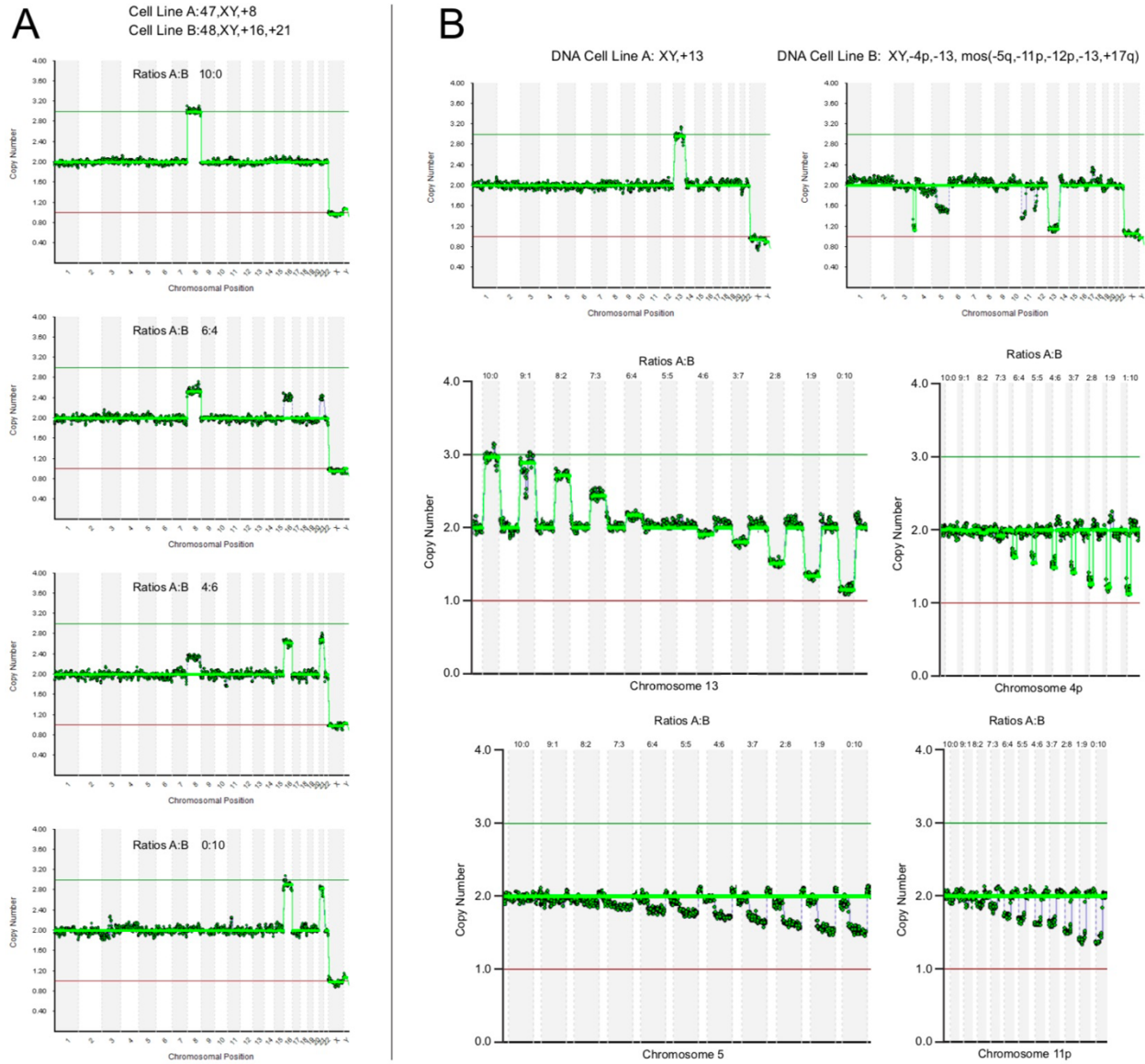
Table 2. List Of Mosaic Blastocyst Transfers.

[a] Estimated percentage of aneuploid cells in biopsy. When several chromosomes affected, highest value is indicated.

[b] Single ventricle congenital heart defect detected at 22 weeks; NIPT was normal for all whole chromosomes and microdeletions tested, including DiGeorge deletion (22q11.2).

[c] Microdeletion of one copy comprising 84.11 Kb at 2q13.

[d] Balanced translocation of 1p and 16p.

[e] Only applies to one embryo in the double frozen ET; due to equal genders it cannot be deduced which one.

[f] Microdeletion of one copy less than 100 kb (no further information available).

[g] Spontaneous rupture of membranes at 23 weeks leading to neonatal death of both babies, which showed no other physiological abnormalities upon examination.

[h] Only applies to one embryo in the triple frozen ET; due to equal genders it cannot be deduced which one.

Note: FET = frozen ET; N = no; seg = segment; Y = yes.

List of mosaic blastocyst transfers.

Embryo no.	Classification	Reported summary	Beta-hCG +	Sac (implantation)	FHB	Birth	Mosaic level[a]	Embryo evaluation	Oocyte age	Age embryo recipient	No. of previous FETs	Postimplantation testing
Single mosaic FETs												
1	Single seg	mos(+9p)	Y	Y	N	N	50	5BB	30	30	0	
2	Single seg	mos(-9p)	N	N	N	N	40	5BB	37	37	3	
3	Single seg	mos(-14q31.1q32.33)	N	N	N	N	35	6BB	37	37	1	
4	Single seg	mos(-9q21.33q34.3)	Y	Y	Y	N	50	5BC	43	43	1	
5	Single seg	mos(+5q12.3q35.3)	Y	Y	Y	N	20	5BC	40	40	0	
6	Single seg	mos(+9q21.13q34.3)	Y	Y	Y	Y	30	5BB	39	39	1	
7	Single seg	mos(-4q22.2q35.2)	Y	Y	N	N	20	5BB	36	36	0	
8	Single seg	mos(+3p24.1p21.1)	N	N	N	N	25	5CC	41	41	1	
9	Single seg	mos(+21p11.1q22.11)	Y	Y	Y	Ongoing	30	5CC	37	41	1	NIPT:Normal
10	Single seg	mos(+19p)	N	N	N	N	30	5BB	34	34	0	
11	Single seg	mos(+Xq22.3q28)	Y	Y	Y	Ongoing[b]	50	5BB	42	42	0	NIPT:Normal
12	Single seg	mos(+Xq)	Y	Y	Y	N	25	5BC	39	39	0	
13	Single seg	mos(+1p36.33p34.3)	Y	Y	Y	Ongoing	70	5BB	33	33	0	
14	Single seg	mos(-7q)	Y	Y	Y	N	35	5BB	39	39	2	
15	Single seg	mos(-Xq21.1q28)	Y	Y	Y	Ongoing	30	5BB	40	33	0	
16	Single seg	mos(-5q14.3q35.3)	Y	Y	Y	Ongoing	20	5BB	39	39	1	
17	Multiple seg	mos(-2p25.3p24.1, -21q22.1q22.3)	Y	Y	Y	Y	40	5AB	33	33	2	Amnio:Normal
18	Multiple seg	mos(+4q22.1q32.3, -4q32.3q35.2)	N	N	N	N	60	5BC	39	39	0	
19	Multiple seg	mos(-1p36.11p32.3, -5p13.3q14.3)	N	N	N	N	40	6CC	40	40	0	
20	Multiple seg	mos(-4p16.3q22.1, +4q22.1q35.2)	N	N	N	N	50	6CB	39	39	1	NIPT:Normal
21	Multiple seg	mos(-2p25.3p23.1,-8p)	N	N	N	N	30	5BC	36	42	2	
22	Multiple seg	mos(-1q,-9q21.2q31.2)	N	N	N	N	50	5BB	34	34	1	
23	Multiple seg	mos(+4q32.3qter, -10q22.2qter)	Y	Y	Y	Ongoing	40	5AB	24	36	6	NIPT:Normal
24	1 or 2 whole	mos(+14)	N	N	N	N	50	5CC	31	31	1	
25	1 or 2 whole	mos(-15)	N	N	N	N	30	5BB	36	36	0	
26	1 or 2 whole	mos(-20)	Y	Y	N	N	20	6BC	31	52	3	
27	1 or 2 whole	mos(+6)	N	N	N	N	20	5BC	38	38	1	
28	1 or 2 whole	mos(+3)	Y	Y	Y	Y	60	5BC	33	26	3	NIPT:Normal; Amnio:Normal
29	1 or 2 whole	mos(-13)	N	N	N	N	50	4BB	37	37	0	
30	1 or 2 whole	mos(+3)	N	N	N	N	25	4CC	39	39	1	
31	1 or 2 whole	mos(-3)	N	N	N	N	35	4BB	34	34	0	
32	1 or 2 whole	mos(+17)	N	N	N	N	25	5BC	42	42	0	
33	1 or 2 whole	mos(+X)	N	N	N	N	25	5BB	33	33	3	
34	1 or 2 whole	mos(-11)	Y	Y	Y	N	40	5BB	38	38	3	
35	1 or 2 whole	mos(+9)	N	N	N	N	40	4BC	44	44	0	
36	1 or 2 whole	mos(-6)	N	N	N	N	50	5BC	37	44	0	
37	1 or 2 whole	mos(+14)	N	N	N	N	20	5BB	43	37	1	
38	1 or 2 whole	mos(-18)	Y	Y	Y	Ongoing	20	6BA	43	25	0	NIPT:Normal

Table 2 continued

Continued.

Embryo no.	Classification	Reported summary	Beta-hCG +	Sac (implantation)	FHB	Birth	Mosaic level[a]	Embryo evaluation	Oocyte age	Age embryo recipient	No. of previous FETs	Postimplantation testing
39	1 or 2 whole	mos(-7,+22)	N	N	N	N	45	6AA	35	35	3	
40	1 or 2 whole	mos(+2,-15)	Y	Y	Y	Y	25	5BC	43	43	0	
41	1 or 2 whole	mos(-2,-8)	Y	Y	Y	Ongoing	30	5BB	34	34	2	Amnio: microdeletion[c]
42	1 or 2 whole	mos(+1,-20)	Y	Y	Y	Ongoing	60	5BB	39	39	2	NIPT:Normal
43	1 or 2 whole	mos(+22)	Y	Y	N	N	30	5BB	41	41	2	
44	Complex	mos(+1,+20,-22)	Y	Y	Y	Y	30	5BB	34	34	1	
45	Complex	mos(-9,-11,-18,+19)	Y	Y	Y	N	40	6BC	34	34	0	
46	Complex	mos(-3,+4,+16)	Y	N	N	N	30	5BC	35	35	0	NIPT:Normal
47	Complex	mos(-3,-6,-8,-15,-18)	Y	N	N	N	40	5BC	38	38	1	
48	Complex	mos(+3,+5p15q14.3,+19)	Y	N	N	N	35	5BC	42	42	0	
49	Complex	mos(-1p,+13,+14,+15,+20,+22)	Y	N	N	N	50	5BC	41	41	0	
50	Complex	mos(+1,-7,-16,+17,+21q22.12q22.3,+22)	Y	Y	Y	Ongoing	30	3BB	26	45	0	
Double FET (one mosaic transferred together with one euploid embryo)												
51	Single seg	mos(+11p)	Y	N	N	N	30	5CC	41	41	0	
52	Single seg	mos(+12q14.1q24.31)	Y	Y	Y	Y	30	5BC	37	37	0	
53	Single seg	mos(+5q)	N	N	N	N	45	5BB	34	34	1	
54	Single seg	mos(+1p36.33p31.1)	Y	Y	Y	Y	25	5AB	34	34	2	Amnio:Normal
55	Single seg	mos(+1p36.31p32.2)	N	N	N	N	40	5BB	35	35	1	
56	Single seg	mos(+10q23.1q26.3)	N	N	N	N	30	5BB	41	41	1	
57	Single seg	mos(+6q22.31qter)	(Y)	(Y)	(Y)	(Y)	40	5BC	37	37	1	
58	Single seg	mos(+Xq)	(Y)	(Y)	(Y)	(Ongoing)	25	3BB	42	42	1	
59	Multiple seg	mos(-1q21.3qter,-21p11.1q21.2)	N	N	N	N	30	5BB	31	31	1	
60	1 or 2 whole	mos(-17)	Y	Y	Y	Y	30	6BB	39	39	1	Amnio: translocation[d]
61	1 or 2 whole	mos(+14)	N	N	N	N	20	5BC	29	29	0	
62	1 or 2 whole	mos(+17)	Y	Y	Y	Ongoing	25	5CC	39	39	1	
63	1 or 2 whole	mos(+16)	Y	Y	Y	Ongoing	40	5BB	24	46	0	
64	1 or 2 whole	mos(+21)	N	N	N	N	25	5BB	38	38	3	
65	1 or 2 whole	mos(+15q14q22.31,+21)	N	N	N	N	35	5CC	35	35	2	
66	1 or 2 whole	mos(+17p13.2q25.3,+1p31.3p21.3)	N	N	N	N	45	6CB	40	40	2	
67	1 or 2 whole	mos(-10,+5)	Y	Y	Y	Y	20	5BB	33	33	1	Amnio:Normal
68	Complex	mos(-14,-18q,+18p)	N	N	N	N	65	4CC	40	40	0	
Double FET (two mosaic)												
69	Complex	mos(-1,+13,-20)	Y	Y	Y	Y	20	5BC	34	34	1	Amnio:Normal
70	1 or 2 whole	mos(-2)	N	N	N	N	25	5CC	34	34	1	
71	Multiple seg	mos(-3p;+21p11.1q21.2)	(Y)[e]	(Y)[e]	(Y)[e]	N	40	5BC	32	32	2	
72	1 or 2 whole	mos(-11)	(Y)[e]	(Y)[e]	N	N	25	5BC	26	26	2	
73	1 or 2 whole	mos(+3p14.3p12.1,+7)	(Y)[e]	(Y)[e]	(Y)[e]	(Y)[e]	35	5BB	33	33	1	(Amnio:Normal)[e]
74	1 or 2 whole	mos(+22)	(Y)[e]	(Y)[e]	(Y)[e]	(Y)[e]	30	5BB	33	33	1	(Amnio:Normal)[e]
75	Single seg	mos(+16p)	Y	Y	Y	Y	30	5BB	32	32	1	Amnio: microdeletion[f]

Table 2 continued

Continued.

Embryo no.	Classification	Reported summary	Beta-hCG +	Sac (implantation)	FHB	Birth	Mosaic level[a]	Embryo evaluation	Oocyte age	Age embryo recipient	No. of previous FETs	Postimplantation testing
76	1 or 2 whole	mos(−19)	Y	Y	Y	Y	30	5BC	32	32	1	
77	Multiple seg	mos(+1p,−1q)	Y	Y	Y	Y-g	30	5AB	34	35	2	
78	Single seg	mos(+11p11.2q14.1)	Y	Y	Y	Y-g	30	6BA	34	35	2	
79	Complex	mos(+12,+14,+16, +18,+19,−X)	(Y)e	(Y)e	(Y)e	(Y)e	50	3BC	36	36	5	(Amnio:Normal)e
80	1 or 2 whole	mos(+16)	(Y)e	(Y)e	(Y)e	(Y)e	40	5CB	36	36	5	(Amnio:Normal)e
81	Single seg	mos(−2q35q37.3)	(Y)e	(Y)e	N	N	50	5BC	36	42	1	
82	1 or 2 whole	mos(−4)	(Y)e	(Y)e	N	N	25	5BB	36	42	1	
83	Complex	mos(+3,+6,−14,−15,+20)	N	N	N	N	60	5CC	27	39	0	
84	Complex	mos(+8,+12,−21)	N	N	N	N	50	4BC	27	39	0	
85	Single seg	mos(+10q21.3q26.3)	Y	Y	Y	Y	45	5BB	36	36	1	Amnio:Normal
86	Single seg	mos(−1p36.33p32.3)	Y	Y	Y	Y	60	5BB	36	36	0	Amnio:Normal
87	Single seg	mos(−2p25.3p24.3)	(Y)e	(Y)e	Y	Y	25	4BB	34	34	0	
88	1 or 2 whole	mos(+2)	(Y)e	(Y)e	N	N	25	5CB	34	34	0	
89	Complex	mos(+11p11.2q12.2,+20,+22)	(Y)e	(Y)e	N	N	25	5CC	38	28	7	
90	1 or 2 whole	mos(+19)	(Y)e	(Y)e	N	N	30	5BB	38	28	7	
91	Single seg	mos(−5p)	N	N	N	N	40	3CC	39	39	0	
92	Single seg	mos(+14q32.12q32.33)	N	N	N	N	35	5CB	39	39	0	
93	Multiple seg	mos(+3p14.2p14.1, +16p13.3p12.1, +18q11.2q24.3)	(Y)e	(Y)e	(Y)e	(Onging)e	50	5CC	42	42	1	
94	1 or 2 whole	mos(−3,−X)	(Y)e	(Y)e	(Y)e	(Onging)e	20	5BC	42	42	1	
Triple FET (three mosaic)												
95	Single seg	mos(+13q13.3q33.3)	(Y)h	N	N	N	20	5CC	40	40	1	
96	Single seg	mos(+5,+20)	(Y)h	N	N	N	40	5CC	40	40	1	
97	1 or 2 whole	mos(+19)	(Y)h	N	N	N	50	5BC	40	40	1	
98	1 or 2 whole	mos(−7,−17)	(Y)h	N	N	N	50	5BB	40	40	3	
99	1 or 2 whole	mos(−4)	(Y)h	(Y)h	N	N	30	5BB	40	40	3	
100	1 or 2 whole	mos(+21)	(Y)h	(Y)h	N	N	40	5BB	40	40	3	

Compared to euploid blastocysts across all medical indications and ages transferred in the same time period, the combined mosaic cohort had significantly lower implantation rates per embryo (as determined by the presence of a gestational sac)(49.6% vs 38.0%)(Table 3). Mosaic embryos also resulted in significantly lower chances of developing a fetal heartbeat (FHB)(47.1% vs 30.0%)(Table 3). Patients who had only a single euploid blastocyst available for transfer (without the possibility of further embryo selection) experienced clinical outcomes that were inferior to the combined group of euploid blastocysts, but were appreciably superior to the mosaic blastocyst cohort (45.0% implantation, 42.2% FHB) (Table 3).

Of the 30 mosaic embryos resulting in FHB in this study, 11 were ongoing pregnancies at the time of manuscript preparation and the remaining 19 have resulted in births. One patient who had two mosaic embryos transferred simultaneously went into labor at 23 weeks with spontaneous rupture of membranes (SRM) leading to death of both newborns, which showed no other physiological abnormalities upon examination.

In 7 cases where NIPT information could be retrieved from patients, all results were normal. Amniocentesis was performed and data retrieved in 11 cases, 8 of which tested normal. One case contained a balanced translocation, and two cases showed microdeletions affecting segments smaller than the validated resolution of the PGT-A platform used (Table 2).

Hence, the combined cohort of mosaic embryos showed overall decreased implantation rates compared to euploids. Of the 30 cases showing a FHB there were no instances of clinical miscarriage to date.

11.5.3. Parameters Of Mosaicism Affecting Clinical Outcome

In our dataset, blastocysts showing mosaicism exclusively in a single segmental (sub-chromosomal) region resulted in considerably better clinical outcomes than blastocysts with other types of mosaicism (i.e. affecting multiple segments or any number of whole chromosomes) (Table 3).

The degree of mosaicism, which is an estimate of the percentage of aneuploid cells in the TE biopsy, did not correlate with clinical outcome in our dataset. We came to the same conclusion when analyzing the data using two different cutoffs for 'low' versus 'high' degree of mosaicism, and the differences between groups were statistically insignificant (Table 3).

Interestingly, we observed a significant age effect on the success of mosaic embryo transfers. When oocytes were retrieved from patients 34 years old or younger, the clinical outcomes of their resulting mosaic blastocysts were considerably better than those retrieved from patients greater than 34 years old (Table 3). This was true for all types of mosaicism (Supplementary Table 5). In the control group, euploid blastocysts fared equally well regardless of age.

Table 3. Analysis Of Mosaic Parameters Affecting Clinical Outcomes.

[a] Compared to the 'Euploid All' group.

[b] Compared to previous row (intra-group comparison)

[c] Multi-biopsy analysis. Square brackets indicate the estimated degree of mosaicism observed in the karyotype profile.

Type	Embryos Transferred	Beta-hCG +	Sac [Implantation]	Fetal Heartbeat	Beta-hCG + (%)	Sac (%) [Implantation]	Fetal Heartbeat (%)	P Value Sac [Implantation]	P Value Fetal Heartbeat	Average Age	Average Mosaicism
Euploid All	478	296	237	225	61.9%	49.6%	47.1%			37.4	N/A
Euploid No Selection	109	68	49	46	62.4%	45.0%	42.2%	0.3974 (ns) [a]	0.3949 (ns) [a]	36.9	N/A
Mosaic All	100	49	37	30	49.0%	38.0%	30.0%	0.0273 (*) [a]	0.0019 (**) [a]	36.4	36%
Mos. Single Segmental	33	19	15	13	57.6%	45.5%	39.4%	0.7203 (ns) [a]	0.4717 (ns) [a]	37.6	35%
Mos. Multiple Segmental	11	4	3	3	36.4%	36.4%	27.3%	0.5446 (ns) [a]	0.2331 (ns) [a]	34.4	42%
Mos. 1 or 2 Whole Chr.	43	18	12	10	41.9%	27.9%	23.3%	0.0067 (**) [a]	0.0035 (**) [a]	36.6	33%
Mos. Complex (>2 Chr)	13	8	6	4	61.5%	46.2%	30.8%	1.0000 (ns) [a]	0.2748 (ns) [a]	34.7	40%

Level Range of Mosaicism	Embryos Transferred	Beta-hCG +	Sac [Implantation]	Fetal Heartbeat	Beta-hCG + (%)	Sac (%) [Implantation]	Fetal Heartbeat (%)	P Value Sac [Implantation]	P Value Fetal Heartbeat	Average Age	Average Mosaicism
20% – 50%	78	39	28	23	50.0%	35.9%	29.5%			36.4	-
50% – 80%	22	10	9	7	45.5%	40.9%	31.8%	0.8031 (ns) [b]	0.7992 (ns) [b]	36.5	-
20% – 40%	58	32	21	16	55.2%	36.2%	27.5%			36.7	-
40% – 80%	42	17	16	14	40.5%	38.1%	33.3%	1.0000 (ns) [b]	0.6590 (ns) [b]	36.0	-

Age of Oocyte (years)	Embryos Transferred	Beta-hCG +	Sac [Implantation]	Fetal Heartbeat	Beta-hCG + (%)	Sac (%) [Implantation]	Fetal Heartbeat (%)	P Value Sac [Implantation]	P Value Fetal Heartbeat	Average Age	Average Mosaicism
≤34 Euploid	141	95	72	69	67.4%	51.1%	48.9%			36.4	N/A
>34 Euploid	337	201	165	156	59.6%	49.0%	46.2%	0.6893 (ns) [b]	0.6164 (ns) [b]	36.5	N/A
≤34 Mosaic All	34	21	19	16	61.8%	55.9%	47.1%	0.0082 (**) [b]	0.0111 (*) [b]	36.7	35%
>34 Mosaic All	66	28	18	14	42.4%	27.3%	21.2%			36.0	36%

Mosaic Abnormality	Embryos Transferred	Beta-hCG +	Sac [Implantation]	Fetal Heartbeat	Beta-hCG + (%)	Sac (%) [Implantation]	Fetal Heartbeat (%)	P Value Sac [Implantation]	P Value Fetal Heartbeat	Average Age	Average Mosaicism
Gain	38	18	13	12	47.4%	34.2%	31.6%			37.8	35%
Loss	42	20	16	11	47.6%	38.1%	26.2%	0.8172 (ns) [b]	0.6296 (ns) [b]	36.2	33%

[c]Blastocysts with PGT-A Classification: Mosaic Only

	Blastocyst 1	Blastocyst 2	Blastocyst 3	Blastocyst 4	Blastocyst 5
Clinical TE Biopsy	XY, mos(-10 [50%])	XX, mos(-3 [65%])	XY, mos(+3 [65%], +9 [40%], +11 [45%])	XY, mos(-12 [40%], +18 [45%], +21 [50%])	XY, euploid
ICM Biopsy	XY, euploid	XX, mos(+3 [40%])	XY, euploid	XX, euploid	XX, euploid
Second TE Biopsy	XY, mos(+10 [25%])	XX, mos(+3 [75%])	XY, euploid	XX, euploid	XY, euploid

[c]Blastocysts with PGT-A Classification: Uniform Aneuploid and Mosaic

	Blastocyst 6	Blastocyst 7	Blastocyst 8
Clinical TE Biopsy	XX,+22, mos(+1q21.2-q44 [70%])	XX, -22, mos(-10 [80%])	XX,+14,-21, mos(-16q [30%])
ICM Biopsy	XX, +22	XX, -22, mos(+1 [30%], -X [25%])	XX,+14,-21, mos(-16q [65%])
Second TE Biopsy	n/a	XX, -22, mos(+19 [35%])	XX,+14,-21, mos(-16q [50%])

Finally, we saw no difference in rates of implantation or FHB when the mosaicism affected chromosomal gains (trisomies) versus losses (monosomies)(Table 3).

11.5.4. Mosaicism in the Clinical TE Biopsy Is A Poor Predictor Of Chromosomal Content In The Remaining Blastocyst

We hypothesized that some mosaic blastocysts might lead to normal pregnancies because the clinical TE biopsy collected might not be representative of the entirety of the blastocyst and particularly the ICM, which could be euploid. To test this experimentally, we took an ICM biopsy and an additional TE biopsy from five blastocysts that were originally classified as mosaic (Table 3). In three blastocysts, the ICM biopsy was euploid, while in two blastocysts the ICM biopsy displayed mosaicism that was reciprocal to that observed in the clinical TE biopsy. The reciprocal patterns suggested incidences of chromosomal non-disjunction as the root cause of mitotic error resulting in mosaicism (141). It has been suggested that a reciprocal gain/loss in different biopsies of the same blastocyst is the strongest evidence of true mosaicism (163). In regards to the second TE biopsies collected, such reciprocal patterns were observed in three of the five blastocysts, while the two other samples were euploid.

We performed the same multi-biopsy experiment on three blastocysts with uniform aneuploidies as well as mosaic aneuploidies within their clinical TE biopsies (Table 3). The uniform aneuploidies were always present in the subsequent biopsies for all three

embryos. The mosaic aneuploidies observed in the clinical TE biopsy were replicated in subsequent biopsies in only one blastocyst (see Blastocyst 8, Table 3). For that case, the degree of mosaicism varied greatly between biopsies (30% in the clinical TE biopsy, versus 65% in the ICM and 50% in the second TE biopsy).

We performed DNA fingerprinting on all sequenced biopsies to confirm there were no sample mix-ups or contamination (Supplementary Figure 7). Notwithstanding the limited sample size, this experiment demonstrated that embryos classified as mosaic by PGT-A can be euploid in other regions of the blastocyst including the ICM, and that the degree of mosaicism observed in the clinical TE biopsy are not strongly correlated with the degree of mosaicism in subsequent biopsies.

11.5.5. Cell Proliferation And Death Rates Are Elevated In Mosaic Blastocysts Compared To Euploid Blastocysts

It has been suggested that euploid cells of mosaic embryos outcompete aneuploid cells during development, possibly leading to chromosomally normal babies. Experimental evidence for such a mechanism comes from a mouse model, in which chimeras of euploid cells and aneuploid cells showed selective apoptosis of aneuploid cells in the ICM and proliferative defects in aneuploid cells of the TE, leading to a progressive depletion of aneuploid cells from the blastocyst stage onwards (218).

If such a model were to apply in the context of human blastocysts generated by IVF, we reasoned that mosaic embryos might display different patterns of cell proliferation and

death compared to euploid embryos. In order to test this hypothesis, we performed immunofluorescence experiments on human embryos with markers of mitosis (cell proliferation) and apoptosis (programmed cell death). Serine 10 on histone H3 becomes phosphorylated specifically during mitotic chromatic condensation, making phosphohistone 3 (pHH3) an oft-used marker of mitotic activity. Caspase-3 is the central executioner of apoptosis, and its active (cleaved) form is a validated marker of apoptotic cells. In addition, we stained all blastocysts in this experiment with the nuclear dye Hoechst in order to visualize the nuclei of all cells, as well as OCT-3/4 to be able to differentiate ICM cells from TE cells. After staining euploid, mosaic, and aneuploid blastocysts, they were visualized by a confocal microscope, and fluorescent signals were quantified computationally (Figure 16A).

In general, levels of mitosis were relatively low in euploid blastocysts (Figure 16B); even though no actively dividing ICM cells were detected in all five euploid blastocysts used in our experiment, these findings do not suggest that cell proliferation does not occur in the ICM of euploid blastocysts (which would be impossible). Instead, it is important to note that immunofluorescent staining produces a static snapshot of development, and rates or levels of cell proliferation and death should be analyzed in a comparative fashion with other groups (i.e. mosaic and aneuploid). Euploid blastocysts displayed negligible levels of apoptosis in the TE as well as in the ICM (Figure 16B), agreeing with previous observations made in normal human blastocysts (227, 228).

Interestingly, a large proportion of mosaic as well as aneuploid blastocysts displayed medium or high levels of mitosis and apoptosis in the TE compared to euploid blastocysts (Figure 16B). In the ICM, some mosaic and aneuploid blastocysts displayed minimal/low levels of mitosis and apoptosis, and others displayed medium or high levels of mitosis and apoptosis (Figure 16B). Together, this data suggest that levels of cell proliferation and death are considerably higher in mosaic and aneuploid blastocysts when compared to euploid blastocysts.

Figure 16. Quantitation Of Cell Proliferation And Death In Blastocysts.
(A) Left column shows representative immunofluorescent images of a hatching blastocyst classified as mosaic by PGT-A. Right column shows method of computational detection and quantitation. Note that the image analysis software detects the concrete number (count) of nuclei, ICM cells, and cells in mitosis. Apoptosis is measured as arbitrary units (AU) of fluorescence in regions displaying the signal in order to capture all apoptotic bodies, including remaining vesicles of fractioned cells. Scale bar = 20µm. (B) Scatter dot plots depicting quantitation of mitosis and apoptosis in TE and ICM. Each symbol represents one blastocyst. Lines indicate mean with standard deviation. Sample size of each blastocyst group is n=5 Euploids, n=11 Mosaics, n=14 Aneuploids. *, $P < 0.05$; **, $P < 0.01$; ***, $P < 0.001$; ns (not significant), $P \geq 0.05$.
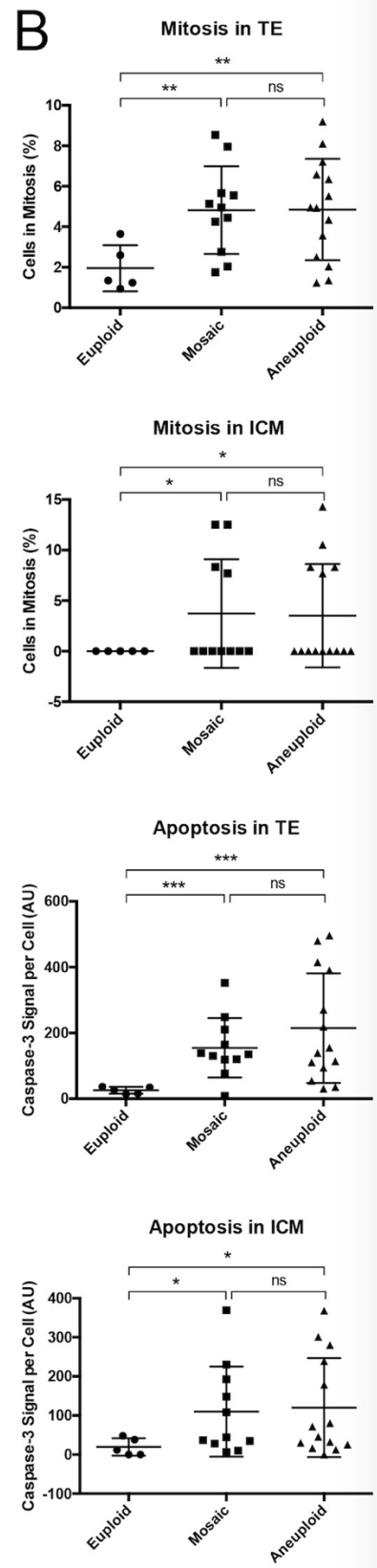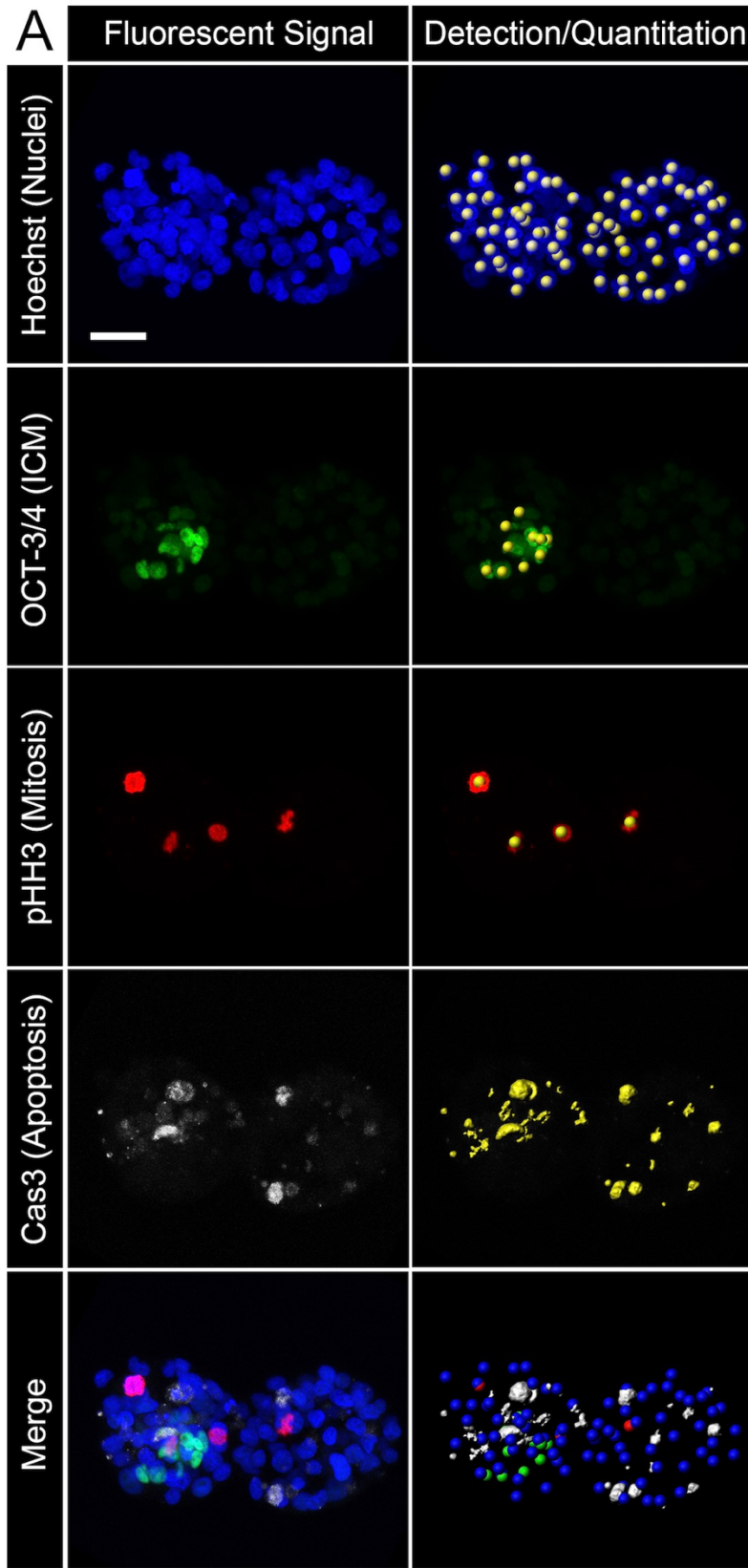
11.6. Chapter Discussion

PGT-A has undergone numerous technical advances since its inception. Compared to its initial form using FISH, which was limited to relatively few chromosomes, the most recent incarnation based on NGS permits the analysis of all chromosomes as well as detection of chromosomal mosaicism. What is more, mosaics can be further subdivided into categories by degree of mosaicism (low and high) and mosaic type (single or multiple segmental mosaics, whole chromosome mosaics, complex mosaics). This has undoubtedly added layers of complexity to the clinical interpretation of PGT-A results, and evidence-based guidelines are needed.

Preimplantation Genetic Diagnosis International Society (PGDIS) (229) and Controversies in Preconception, Preimplantation, and Prenatal Genetic Diagnosis (CoGEN) (230) provide position statements concerning prioritization of mosaic embryos for transfer, but the rationale behind them remains mainly theoretical. An alternative set of recommendations have been proposed, based on risk levels deduced from mosaic patterns observed in chorionic villus sampling (CVS) of the placenta and in products of conception (POC) (231). Nonetheless, a direct link between types of mosaicism at the blastocyst stage and clinical outcomes will only become defined over time with studies such as this one.

To date, all studies comparing euploid and mosaic embryo outcomes in IVF concur that embryos classified as mosaic can lead to babies that are healthy by routine examination,

but with decreased success rates compared to euploids (164, 171, 172, 204, 221). Nonetheless, there is some disagreement between studies about which mosaic parameters correlate with clinical outcome. For example, some have suggested that a high degree of mosaicism (i.e. high proportion of aneuploid cells in the TE biopsy) correlates with poorer outcomes. This relationship was described in a paper using a mix of PGT-A technologies to detect mosaicism (171) as well as a study analyzing NGS data in a retrospective manner, although in the latter report the trend was not statistically significant (164). To our knowledge, this is the first prospective study relying entirely on NGS, widely recognized as the most precise method to detect mosaicism in PGT-A (106, 108, 225). Our data suggests that the degree of mosaicism should not be used to prioritize mosaic embryos. This is contrary to current guidelines expressed by PGDIS or CoGEN to prioritize selection of embryos for transfer, which in our opinion should be amended.

This interesting point warrants discussion from a conceptual standpoint. Few would dispute the notion that a mosaic blastocyst with a high percentage of aneuploid cells is less likely to succeed than one with low percentage of aneuploid cells, a concept first explored in an extensive manner by Verlinsky and colleagues (155) and convincingly demonstrated experimentally in a mouse model of chimeric blastocysts (218). It follows logically that if a clinical TE biopsy were a good representative of the proportion of aneuploid cells in the remaining blastocyst, embryos with high mosaicism in the TE biopsy should fare poorly. The salient point shown in our data is that mosaicism in the TE biopsy is a poor representative of the blastocyst. Mosaic blastocysts do not distribute aneuploid cells evenly, meaning there is an inherent sampling error when collecting the TE biopsy.

Therefore, we conclude that the degree of mosaicism in the TE biopsy might be irrelevant to clinical outcome.

One parameter with a substantial effect on clinical outcome in our study was type of mosaicism: single segmental mosaics fared better than all other types, namely those affecting multiple segmental gains/losses, 1 or 2 whole chromosomes, or complex mosaics. This observation agreed with a previous retrospective study (204), although in our dataset the single segmental mosaic embryos did not fare quite as well as euploid embryos. It has been suggested that the better clinical outcomes in segmental mosaics might be due to the fact that segmental aneuploidies typically result from DNA double strand break events, which often activate checkpoint processes leading to cell cycle arrest or apoptosis (204). As a result, neighboring euploid cells could quickly and efficiently dilute out cells containing segmental gains or losses. Also, segmental aneuploidies resulting in acentric fragments do not contain a centromere and cannot attach to the spindle during mitosis, potentially leading to their loss during cell division (204). Therefore, our data supports the notion of prioritizing single segmental mosaics for transfer above other mosaic types.

Another parameter to show a significant effect was age. Mosaic blastocysts derived from oocytes retrieved from patients 34 years old or younger fared significantly better than when derived from older patients. Interestingly, the 'young' mosaic group yielded comparable results to euploid embryos, which in itself did not display an age effect upon

transfer. We can only speculate the biological reason for this. Could any of the self-correcting mechanisms that have been proposed in mosaic embryos (clonal depletion, preferential allocation, cell-endogenous rescue, see (153)) be more efficient in 'younger' blastocysts? It has been documented that, as opposed to meiotic errors and uniform aneuploidy, rates of mitotic error and consequently mosaicism at the blastocyst stage remain relatively constant with increasing age (128, 141). It is possible that 'younger' blastocysts manage to purge themselves of mosaicism, while older blastocysts more often retain their aneuploid cell load and accordingly become less likely to implant and reach birth. Another possibility is that an increasing proportion of mosaic blastocysts generated from older patients originated from trisomy rescue of uniformly aneuploid embryos, in turn possibly leading to negative outcomes. These concepts warrant further investigation and to our knowledge age has not been considered or analyzed as a mosaic parameter in previous studies. If confirmed, in cases where a patient has multiple mosaic blastocysts to choose from that were generated from different cycles at different ages, we would recommend prioritizing the 'younger' ones.

We explored two concepts that might explain why embryos classified as mosaic in PGT-A might lead to ongoing pregnancies and healthy births. The first, as mentioned above, is that mosaicism in the TE biopsy is not a good predictor of karyotype elsewhere in the blastocyst. We observed examples where the corresponding ICM as well as a second TE biopsy were euploid. Other cases had reciprocal mosaic aneuploidies in subsequent biopsies. In yet another scenario, a blastocyst had the same mosaic aneuploidy in all

three biopsies analyzed, but the degree of mosaicism was different ('low' in the clinical TE biopsy, and 'high' in the ICM and second TE biopsies The inherent degree of sampling error in isolating a biopsy from a mosaic blastocyst imposes a 'biological' source of false positive/negative calls for mosaicism in PGT-A. Ultimately, this poor predictive power of a mosaic TE biopsy vis-a-vis the remaining embryo might explain why embryos classified as mosaic do occasionally implant and lead to healthy births but do so with lower success rates than euploid embryos. Sometimes the mosaic TE biopsy will pair with euploidy, other times with mosaicism, and yet other times with aneuploidy in the remaining blastocyst. This is not to say that a mosaic TE biopsy will correspond in equal rates to euploidy, mosaicism, and aneuploidy elsewhere. Only a larger and detailed investigation analyzing serial biopsies in embryos classified as mosaic will shed light into such ratios.

It must be acknowledged that there also exists an inherent risk for technical error during PGT-A, which could produce profiles appearing mosaic when in fact the biopsy in question is uniformly euploid or aneuploid. The mixing experiments suggest that NGS-based PGT-A is excellent at identifying mosaicism when indeed present (manifested as intermediate levels of karyotype profiles), but the inverse is not necessarily true: an intermediate karyotype profile does not automatically mean that a TE biopsy contains mosaicism. Artifacts introduced during WGA or NGS could result in background noise that can produce such intermediate levels as well, falsely resulting in karyotype profiles interpretable as mosaic. Our cell mixing experiments, which were performed in biological triplicates, showed a false positive rate for mosaicism of 0% but the sample size was small and there are aspects of TE biopsy (resulting from laser use, biopsy isolation,

handling etc.) that cannot be properly modeled in cell mixes. Hence, it has been proposed that rather than categorically diagnosing blastocysts as 'mosaic', PGT-A results should indicate a pattern 'consistent with possible mosaicism' (163).

The second concept we explored that could make mosaic blastocysts result in healthy births is self-correction. It is known that the incidence of mosaicism decreases through development (164), which could be explained by the out-competition of aneuploid cells by euploid cells by differential cell proliferation and death. Indeed, a chimeric mouse model for mosaicism has shown the progressive depletion of aneuploid cells in the preimplantation embryo (218). In those experiments, aneuploid cells in the fetal lineage (ICM) were largely eliminated by apoptosis, whereas those in the placental lineage (TE) displayed severe proliferative defects. Our findings confirm that in the human embryo, the dynamics of cell proliferation and death are different, on average, between euploid, mosaic, and aneuploid blastocysts. This could correspond to the proposed self-correction mechanism, as aneuploid cells might proliferate slower or undergo apoptosis, and euploid cells compensate by elevating their rates of proliferation. Unfortunately, existing tools and reagents do not allow us to individually visualize the aneuploid and euploid cells in a mosaic human embryo, which would be required to confirm this model. Yet, and notwithstanding the limited sample size of our experiment, analysis on the blastocyst level showed statistically significant differences between groups. Importantly, not all blastocysts classified as mosaic had elevated rates of cell proliferation and death; some

showed similar levels to euploids. Presumably, those could be instances of blastocysts with mosaicism in the TE biopsy, but euploidy elsewhere.

Centers using PGT-A have reported vastly different incidences of mosaic embryos, anywhere from less than 4% up to 90% (163). Without context, such comparisons are virtually meaningless. Equal thresholds, cutoffs, and technological platforms need to be employed to make reasonable comparisons between groups. Regardless of methods used to identify mosaics, the existence of chromosomally mosaic embryos is an undisputed biological phenomenon. In our center, 18% of blastocysts analyzed by PGT-A (n=3138) are classified as 'mosaic' using the methods described in the manuscript. This is consistent with the 21% figure reported by a large reference lab using the same standards as described here (106). While biological and technical false positive/negative rates for mosaicism in PGT-A are being established, a preponderance of evidence now shows that the 'mosaic' category of blastocysts contains its own distinct set of clinical outcomes, different to the uniform euploid or aneuploid categories. Considering the importance of the mosaic group, evidence-based guidelines are vital to help prioritize them for transfer.

In summary, our findings suggest that after euploids, embryos displaying single mosaic segmental gains and losses should be prioritized for transfer, along with mosaic blastocysts derived from oocytes retrieved at younger patient age. On the other hand, degree of mosaicism in the TE biopsy is not a relevant factor, and blastocysts harboring

mosaic monosomies and trisomies result in similar clinical outcomes. Even though to our knowledge this is the largest single-center study of its kind to date, we note that the sample size is still relatively limited and future larger studies will need to corroborate or refute our findings. Finally, we provide experimental data for two possibly parallel/additive mechanisms that may explain why mosaic blastocysts can result in healthy babies, which has been a great concern when transferring embryos classified as mosaic by PGT-A.

12. Specific Aim C: To test the hypothesis that features of mosaicism detected with PGT-A are useful to rank embryos by their potential to result in pregnancy and live birth.

The following published work is presented for this specific aim:

Viotti M, **Victor AR**, Barnes FL, Zouves CG, Besser AG, Grifo JA, Cheng EH, Lee MS, Horcajadas JA, Corti L, Fiorentino F, Spinella F, Minasi MG, Greco E, Munné S. *Using outcome data from one thousand mosaic embryo transfers to formulate an embryo ranking system for clinical use.* Fertil Steril. 2021 May;115(5):1212-1224. doi: 10.1016/j.fertnstert.2020.11.041. Epub 2021 Mar 6. PMID: 33685629.

12.1. My Personal Contribution To The Work

My personal contribution to this work includes participating in its conceptualization, performing a portion of the clinical work that forms its basis (embryology and molecular genetics), data collection and analysis, assisting with the preparation and editing of the manuscript.

12.2. Chapter Summary

Contradictory data has been published on whether features of mosaicism detected with PGT-A correlate with distinct clinical outcomes. Here, we compiled a large dataset on mosaic embryo transfers from several participating centers, to assess such attributes of

mosaicism correlate with clinical outcomes, in order to formulate a ranking system of mosaic embryos for intrauterine transfer.

We analyzed 5,561 euploid blastocysts and 1,000 mosaic blastocysts used in clinical transfers in fertility patients. The euploid group had significantly more favorable rates of implantation and ongoing pregnancy/birth (OP/B) compared to the combined mosaic group or the mosaic group affecting only whole chromosomes (Implantation: 57.2% vs. 46.5% vs. 41.8%, OP/B: 52.3% vs. 37.0% vs. 31.3%), as well as lower likelihood of spontaneous abortion (8.6% vs. 20.4% vs. 25%). Whole chromosome mosaic embryos with level (percent aneuploid cells) below 50% had significantly more favorable outcomes than the ≥50% group (Implantation: 44.5% vs. 30.4%, OP/B: 36.1% vs. 19.3%). Mosaic type (nature of the aneuploidy implicated in mosaicism) affected outcomes, with a significant correlation between number of affected chromosomes and unfavorable outcomes. This ranged from mosaicism involving segmental abnormalities to complex aneuploidies affecting three or more chromosomes (Implantation: 51.6% vs. 30.4%, OP/B: 43.1% vs. 20.8%). Combining mosaic level, type, and embryo morphology revealed the order of sub-categories regarding likelihood of positive outcome.

In summary, this compiled analysis revealed traits of mosaicism identified with PGT-A that affected outcomes in a statistically significant manner, enabling the formulation of an evidence-based prioritization scheme for mosaic embryos in the clinic.

12.3. Chapter Introduction

The assemblage of cells composing a human preimplantation embryo can contain different karyotype conformations. Firstly, when all cells house the typical set of 46 chromosomes, an embryo is deemed 'euploid'. Secondly, an embryo is regarded as 'aneuploid' when all its cells contain a particular chromosomal abnormality, such as segmental or whole chromosome aneuploidy. As a third possibility, an embryo is deemed 'mosaic' when two or more cell populations with different chromosomal content are present simultaneously. This phenomenon originates from post-zygotic errors of mitosis, such as non-disjunction or anaphase lagging, where sister chromatids fail to segregate correctly among two daughter cells (141). For purposes of preimplantation genetic testing for aneuploidy (PGT-A), mosaic embryos that contain a mix of euploid and aneuploid cells (hereafter simply referred to as 'mosaic') have become highly relevant. As first described by Greco *et al.* (172) and later by others (107, 164, 171, 204, 232), embryos with a PGT-A result suggesting mosaicism can result in seemingly healthy pregnancies and births, albeit with lower success rates than euploid embryos.

Contemporary PGT-A operates on the premise that a cellular biopsy of the trophectoderm (TE) is representative of the entire blastocyst. Of the various existing molecular platforms, whole genome amplification (WGA) coupled with Next Generation Sequencing (NGS) has a comparatively high dynamic range and resolution, and is considered the most appropriate system for detecting intra-biopsy mosaicism in the 20-80% range between uniform euploidy and aneuploidy (164). Those thresholds coincide with the fact that a

typical TE biopsy can contain five cells, and therefore anywhere from 1/5 to 4/5 abnormal cells in instances of mosaicism. Numerous reports have shown accurate detection of mosaicism in cell- and DNA-mixing experiments using WGA-based NGS (37, 107, 164, 165, 171). Consequently, a PGT-A grading system that considers mosaic results as a separate category has been proposed (168) and endorsed by professional societies (PGDIS and CoGEN) (166, 230),

Nonetheless, concerns regarding the diagnosis and management of mosaicism in preimplantation embryos have been expressed. Sub-optimal blastocyst biopsies may create false mosaic results (166), and technical background noise due to artifacts of amplification or sequencing could be indistinguishable from results consistent with mosaicism (163). Furthermore, there is subjectivity in diagnosing mosaicism with PGT-A, as most contemporary analysis software is designed to classify samples as uniformly euploid or aneuploid, leaving the identification of mosaicism to the user. Other causes of artifactual mosaicism have been proposed, such as the cell cycle phase influencing readings resembling mosaic segmental abnormalities (233), although this effect appears to be minimized with contemporary, blastocyst-stage PGT-A methods (234).

Due to the above-mentioned concerns, still limited data on pregnancy outcome, and unknown potential risks associated with mosaic embryo transfer (235), some argue that mosaicism should not yet be reported (173) or that embryos classified as mosaic should not be transferred (236). In addition, doubts remain as to which characteristics of

mosaicism correlate with clinical outcomes, such as the proportion of aneuploid cells (mosaic level), nature of aneuploidy involved in the mosaicism (mosaic type), and the identity of aneuploid chromosomes present. These points can only be addressed with larger data-sets than currently published.

Here we present the analysis of one thousand embryo transfers of mosaic blastocysts, showing that the proportion of abnormal cells and type of mosaic aneuploidy significantly affect clinical outcome. Identification of these mosaic characteristics with PGT-A in a clinical TE biopsy is therefore appropriate and valuable for embryo selection. These data provide much needed evidence-based guidelines for ranking mosaic embryos in the clinic.

12.4. Methods And Materials

12.4.1. Participating Centers And Data Collection

The following IVF clinics and PGT-A laboratories contributed data to this study:

Zouves Fertility Center, Foster City, California, USA.

New York University Langone Fertility Center, New York, New York, USA

Lee Women's Hospital, Taichung, Taiwan.

IRCCS San Raffaele Scientific Institute, Milan, Italy.

Genoma, Molecular Genetics Laboratories, Rome, Italy.

European Hospital, Centre For Reproductive Medicine, Rome, Italy.

Cooper Genomics, Livingston, New Jersey, USA.

'Mosaic embryos' are defined here as those where the PGT-A analysis of a TE biopsy showed a profile consistent with mosaicism for one or more genomic regions. Participating centers contributed two data sets for a combined total of 1,000 mosaic embryos used in clinical transfers (Listed in Supplementary Table 6). One set was from previously published reports (107, 164, 171, 232), accounting for 425 mosaic embryos (comprising 42.5% of embryos in this study), each with additional unpublished information necessary for comprehensive analyses specific to this study. In one instance, samples from a previously published report were reprocessed with a different platform (NGS) for the purpose of the current study (171). The other set was new unpublished data, accounting for 575 mosaic embryos (comprising 57.5% of embryos in this study). Of the combined 1,000 mosaic embryos, 860 were used in single embryo transfers (SETs), 88 were used in double embryo transfers (DETs) together with another mosaic embryo, 50 were used in DETs together with a euploid embryo, two were used in DETs together with an untested embryo, and two mosaic embryos were used in a triple embryo transfer (TETs) together with one mosaic and one euploid. In 94.6% of cases, a mosaic embryo was selected for transfer to a patient when no euploid embryo was available. In the remaining cases, a mosaic embryo was transferred together with a euploid (5.2%) or with an untested embryo (0.2%). For DETs and TETs in which the embryos in a transfer resulted in different clinical outcomes, their identity could be deduced from the sex (through prenatal testing and/or at birth), otherwise they were excluded from the analysis. For the control group, participating centers submitted clinical outcome data on embryos categorized as euploid (n=5,561) for the same time period that mosaic embryo transfer

data was collected. A weighted average implantation rate and ongoing pregnancy or birth rate was calculated for the control group, corrected for the proportion of mosaic embryos contributed by each center.

All patients in this study receiving an embryo transfer with known mosaic PGT-A results were previously advised by certified genetic counselors on the concept of embryonic chromosomal mosaicism and its potential clinical risks and consequences. A recommendation for prenatal testing was made in each case. The participating clinics were located in countries in which laws regulating IVF treatments reference reproductive rights and emphasize patient freedom of choice. Clinics could therefore advise but not dictate decisions regarding embryo selection or pre- and postnatal testing. Due to data anonymization for this study, patients were not retroactively contacted in instances where an embryo was re-classified from 'euploid' to 'mosaic' at re-analysis of the results (constituting 16.4% of embryos in the study) to communicate the change in embryo status. In the host countries of participating centers, the task of considering the ethical implications of a research project is performed by an Institutional Review Board (IRB). The analyses presented here were approved by the Institutional Review Board of the Zouves Foundation (OHRP IRB00011505, Protocol #0002).

12.4.2. PGT-A

All embryos in this study underwent blastocyst-stage PGT-A using the same NGS-based platform VeriSeq (Vitrolife) and subsequent frozen embryo transfer (FET). TE biopsies

were collected by standard protocols and frozen until processing. Cell samples were lysed, and genomic DNA was randomly fragmented and amplified using the SurePlex DNA Amplification System (Vitrolife) according to the manufacturer's protocol. The whole genomic amplified DNA product of each sample was processed to prepare a genomic DNA library using VeriSeq PGS workflow (Vitrolife). Purified DNA libraries were normalized to equalize the quantity of each sample in the final pool by using VeriSeq's library normalization protocol. Equal volumes of normalized samples were pooled, denatured, and sequenced. The MiSeq Reagent Kit v.3 (Illumina) was used on a MiSeq System (Illumina). The sequencing data were analyzed using BlueFuse Multi Software (Vitrolife).

The participating centers in this study interpreted the resulting data uniformly: NGS profiles were defined as mosaic when displaying copy number counts in the 20-80% range between chromosome monosomy and disomy or disomy and trisomy for any genomic region, as has been previously described (164, 166). Profiles under 20% were considered euploid, and those above 80% were considered aneuploid. All participating centers performed in-house validation experiments using DNA and/or cell mixes to accurately produce intermediate copy number profiles consistent with mosaicism, as previously published (107, 108, 164, 171). VeriSeq is validated to identify segmental gains and losses of 20 Mb or larger, but is capable of detecting segments as small as 1.8 Mb (103) in some genomic regions.

12.4.3. Definitions Of Mosaic Traits, Clinical Indications, And Outcomes

Mosaic 'level' referred to the inferred percent aneuploid cells in a TE biopsy. For embryos with two or more mosaic chromosomal regions, the highest mosaic level value was considered for analysis.

Mosaic 'type' referred to the nature of the chromosomal abnormality in the aneuploid cell compartment. Mosaic embryos with exclusively segmental abnormalities were called 'single', 'double', or 'complex segmental', depending on the number of affected segments. Instances of mosaicism involving a single whole chromosome aneuploidy (monosomy or trisomy) were considered 'one chromosome' mosaics. Embryos with mosaicism in two whole chromosomes, or one whole chromosome and one segmental region, were considered 'two chromosomes' mosaic. When mosaicism was present in more than two chromosomes, the mosaicism type was considered 'complex', including combinations of whole chromosomes and segmental regions.

The clinical indications for PGT-A were defined as follows: advanced maternal age (AMA) for maternal age >37 at time of oocyte retrieval, repeat implantation failure (RIF) for cases with three or more prior failed implantation upon transfer, recurrent spontaneous abortion/miscarriage (RM) for loss of two or more clinical pregnancies prior to week 20 of gestation, 'PGT-M/-SR' for cases with familial genetic conditions undergoing concurrent PGT-A, 'Other' (including male factor infertility, unexplained infertility, etc.), and 'Good Prognosis' for cases of elective PGT-A with no specific clinical indication.

'Implantation' was defined by the presence of a gestational sac by endovaginal ultrasound at 3-5 weeks post transfer. When applicable, fetal heartbeat was monitored by endovaginal ultrasound at 6-8 weeks post transfer. Successful pregnancies were divided into 'Ongoing Pregnancy' if there was active pregnancy at the time of manuscript preparation, or 'Birth' if a baby was born. Any embryo that was positive for Implantation but negative for Ongoing Pregnancy/Birth (OP/B) before week 20 of gestation was considered to have succumbed to spontaneous abortion.

12.4.4. Statistics And Data Preparation

Statistical analysis was performed in Prism (GraphPad) and graphs assembled in Illustrator (Adobe). Comparisons between groups with categorical outcome variables were performed according to sample size with a two-tailed chi-square test with Yate's correction or a two-tailed Fisher's exact test. Comparisons with quantitative outcome variables were performed with an unpaired, two-tailed t-test. Trends were analyzed by linear regression, or in the case of ordinal variables, with a chi-square test for trend (Cochran-Armitage). For all analyses: *, $P < 0.05$; **, $P < 0.01$; ***, $P < 0.001$; ****, $P < 0.0001$; ns (not significant), $P \geq 0.05$.

For normalization of the euploid group to the mosaic group by morphology (Supplementary Figure 8), we considered every combination possible in the Gardner system (207) for stage, ICM grade, and TE grade, and counted the number of mosaic embryos in the analysis group for every permutation. Next, we matched each count with

an equal number of embryos from the euploid group, and each permutation with averaged clinical outcome rates of the euploid group (Supplementary Table 7). This led to the calculation of rates of implantation and OP/B for a putative euploid group with identical morphological characteristics as the mosaic group.

For the generation of values in the Ranking Matrix (Table 4), clinical outcome rates (listed in Supplementary Table 8) were normalized to the highest value in the euploid group. Only subgroups with n≥10 samples were included in the table, and all subgroups with n<10 samples were indicated with 'n/a'. Stage 2 is not shown, as none of the subgroups had the minimum 10 embryos for that stage.

12.5. Results

12.5.1. Mosaic Embryos Experience Less Favorable Clinical Outcomes Than Euploid Embryos

Centers contributing data to this study had incidences of mosaic embryos ranging from 11.0% to 25.7% in their general tested embryo population, with an average of 18.6% (Figure 17A). Clinical outcome data were assembled from 5,561 euploid embryos and 1,000 mosaic embryos (details for each embryo are listed in Supplementary Table 6), transferred between January 2015 and April 2020 at participating clinics. For mosaic embryos, in 83.6% of cases there was knowledge of the mosaic status prior to clinical transfer, while in 16.4% of cases the embryo was transferred under supposition of euploidy but post-transfer re-evaluation of the sequencing profile led to the embryo being

assigned to the mosaic category (Figure 17B). The following parameters showed similar overall patterns between the euploid and mosaic groups: day of biopsy, maternal age, and indication category for PGT-A (Figure 17B). Compared to the euploid group, transferred mosaic embryos tended to originate from cycles producing fewer euploid blastocysts (on average 2.2 vs. 0.8) but more mosaic blastocysts (0.9 vs. 1.7) (Figure 17B). Morphological evaluation with the Gardner system (207) indicated that, compared to the euploid group, the mosaic group had fewer grade A embryos (23.2% vs. 15.1%) and more ICM grade C embryos (14.4% vs. 19.4%), as well as more TE grade C embryos (18.9% vs. 28.9%) group (Figure 17B).

Transfer of embryos in the euploid group resulted in an implantation rate of 57.2% and a OP/B rate of 52.3% (Figure 17C). In comparison, the combined mosaic group had significantly lower rates of implantation (46.5%) and OP/B (37.0%) (Figure 17C). When only considering whole chromosome mosaic embryos (no segmental mosaics), outcome rates further declined for implantation (41.8%) as well as OP/B (31.3%) (Figure 17C). Euploid embryos that implanted had a 8.6% likelihood of spontaneously aborting, while the likelihood was significantly higher for the combined mosaic group (20.4%) as well as the whole chromosome mosaic group (25.0%) (Figure 17C). Importantly, ~72% of the documented spontaneous abortions in mosaic embryos occurred early in the pregnancy, between observation of gestational sac (3-5 weeks post transfer) and fetal heart beat monitoring (6-8 weeks post transfer).

Figure 17. Characteristics And Clinical Outcomes Of Transferred Euploid And Mosaic Embryos.

(A) Proportion of embryos by PGT-A category in participating centers. (B) Overview of data pertaining to 5,561 euploid embryos and 1,000 mosaic embryos included in this study. The 'Maternal Age' graph depicts the mean with SD. In the 'Indication for PGT-A' graph, the summed percentages exceed 100% because some embryos were in two or more categories. (C) Clinical outcomes of euploid and mosaic groups.
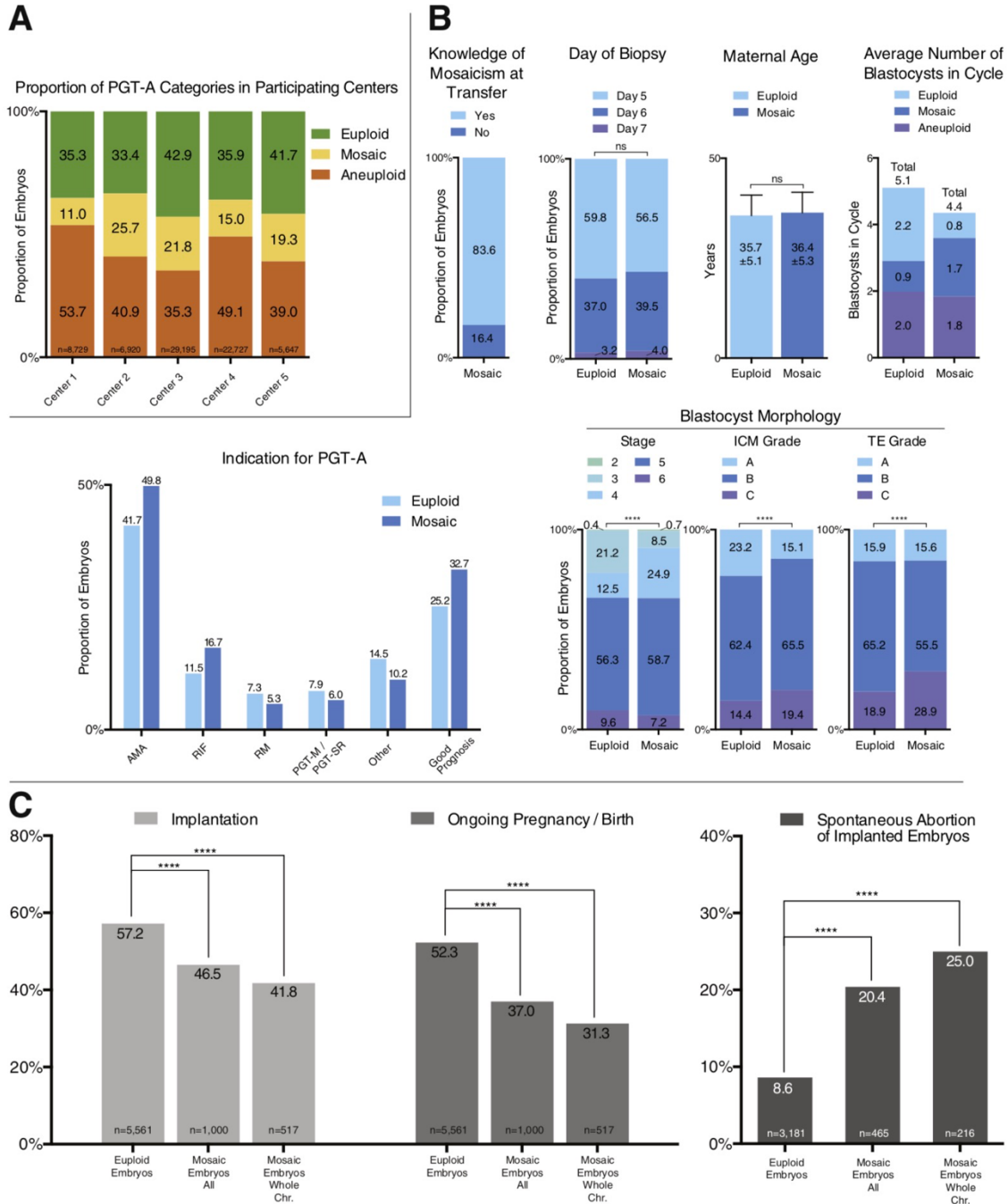
Since some mosaic embryos were transferred as DETs, we re-analyzed the data for mosaic embryos transferred exclusively as SETs (n=860), observing that they resulted in significantly inferior clinical outcomes compared to the euploids (47.7% implantation, 37.8% OP/B) (Supplementary Figure 8A). Since euploid embryos are typically given first priority for transfer amongst embryos generated in a cycle, there was a possibility that mosaic embryo transfers usually occurred in patients that had undergone one or more prior failed transfers of euploid embryos from within the same cycle, meaning that different rates of clinical outcomes could be caused by a maternal-specific effect. To investigate that possibility, we analyzed outcomes for mosaic embryo transfers from cycles with no euploid embryos, in which mosaic embryos were the first to be transferred from within a cohort. The 'no-euploid' mosaic group (n=517) experienced significantly lower rates of implantation (44.1%) and OP/B (35.4%) compared to the euploid group (Supplementary Figure 8A).

Having noted that transferred mosaic embryos were, on average, of inferior morphological grade compared to the euploid group (Figure 17A), we proceeded to determine to what extent that difference was responsible for the decreased rates of clinical outcome observed in the mosaic group. To that end, we normalized the euploid group to the mosaic group by morphology (see Materials and Methods). This lowered the rates of implantation and OP/B for euploid embryo transfers, and increased their rates of spontaneous abortion. However, comparing the morphology-normalized euploid group to the mosaic group revealed statistically significant differences in outcome, which were less favorable

for the mosaic group (Supplementary Figure 8B). This suggested that differences in morphology could not entirely account for the inferior outcomes of mosaic embryos.

12.5.2. High Level Mosaics Have Poorer Outcomes Than Low Level Mosaics

We stratified the 1,000 mosaic embryos and analyzed how the level of mosaicism (i.e. the estimated percent of abnormal cells that are mixed with normal cells) affected clinical outcomes. Data were plotted in 10% increments of mosaic level, representing a progressive increase in the proportion of aneuploid cells in the mix, and linear regression showed a statistically significant decline in rates of implantation and OP/B for whole chromosome mosaics, but not for segmental mosaics (Figure 18A). We considered four different cutoffs to group embryos into 'low' and 'high' mosaicism. For whole chromosome mosaics, neither 30% nor 40% as cutoffs yielded significant differences between the 'low' and 'high' groups (Supplementary Figure 9). However, using 50% or 60% as cutoffs resulted in significant differences, with 50% displaying the largest dissimilarities in clinical outcomes between the mosaic low and high groups (Figure 18A and Supplementary Figure 9). For segmental mosaics, none of the cutoffs yielded significant differences between mosaic low and high groups (Figure 18A and Supplementary Figure 9).

Figure 18. Effect Of Mosaicism Level And Type On Clinical Outcomes.
(A) Analysis of mosaic level (the percent aneuploid cells) in three groups: all mosaic embryos combined, embryos with whole chromosome mosaicism, and embryos with mosaicism affecting exclusively segmental abnormalities. Top graphs depict clinical outcomes by mosaic level in 10% increments, with linear regression analysis. The bottom graphs depict clinical outcomes using a cutoff of 50% to differentiate 'low' mosaics from 'high' mosaics. (B) Analysis of clinical outcomes by mosaic type (nature of aneuploidy

involved). Chi-square test for trend (blue dotted line and connected points) indicates statistically significant decreasing trend with increasing extent of mosaic aneuploidy.
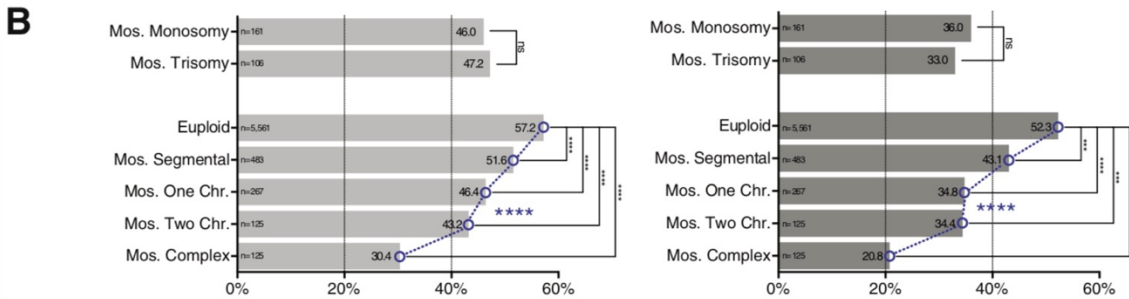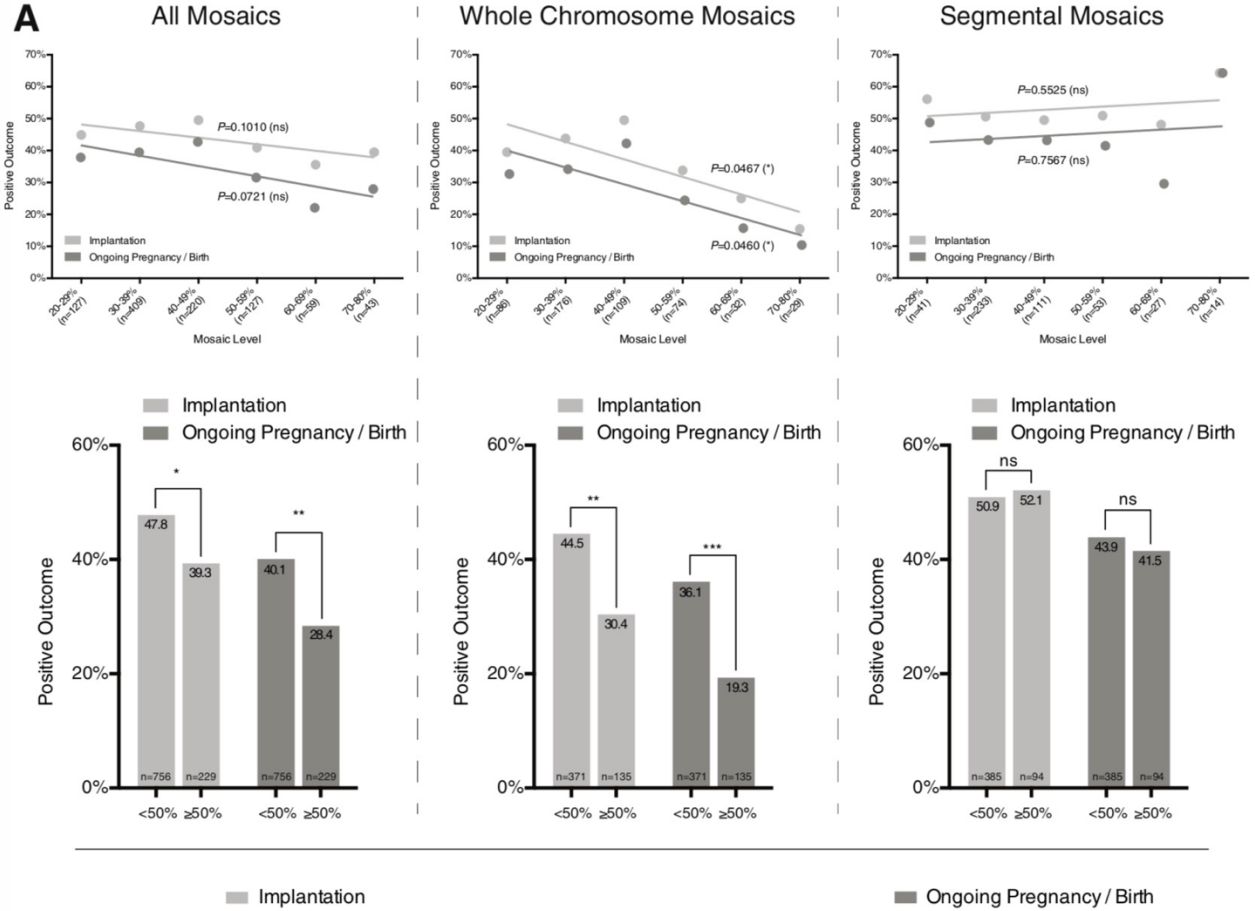
12.5.3. Number Of Affected Chromosomes In Mosaicism Correlate With Poorer Outcome

We explored whether the type of mosaicism, i.e. the kind of aneuploidy present in the abnormal cells in the mosaic mix, affected clinical outcomes. First, we considered sub-chromosomal abnormalities of segmental nature. There were no significant differences in clinical outcomes between embryos with mosaicism affecting a single, two, or more than two segmental regions (Supplementary Figure 10). However, the combined segmental mosaic group had significantly poorer outcomes compared to the euploid control group (Figure 18B).

Considering other mosaic types, a chi-square test for trend indicated that clinical outcomes were progressively poorer with increasing severity of mosaic aneuploidy in a statistically significant manner (Figure 18B). Mosaic segmentals had the best outcomes, followed by the group with one affected whole chromosome, followed by the group with two affected chromosomes, followed by the complex group, in which three or more chromosomes were affected (implantation $P<0.0001$, OP/B $P<0.0001$). There were no significant differences in outcomes between embryos with mosaic monosomies and trisomies (Figure 18B).

12.5.4. No Maternal Age Effect On Outcomes Of Mosaic Embryos

In the analyzed dataset, maternal age did not affect clinical outcomes. As in the euploid group, mosaic embryos derived from oocytes isolated at a maternal age lower than 34

had similar rates of implantation and OP/B than those isolated at maternal age 34 and higher (Supplementary Figure 11).

12.5.5. Analysis Of Mosaicism In Individual Chromosomes

We tabulated the clinical outcomes of all single, whole chromosome monosomies and trisomies in the 1,000 mosaic embryo dataset (Supplementary Table 9). There were a total of 157 and 103 embryos with a single mosaic monosomy and trisomy, respectively. Sample sizes were too small to make relevant 'per chromosome' statistical determinations, but the data indicates that blastocyst-stage mosaicism in any of the 23 chromosomes may result in viable pregnancies.

12.5.6. Combining Characteristics Of Mosaicism To Determine A Prioritization Scheme For The Clinic

Having observed that 50% was the most significant cutoff to divide embryos into mosaic low and high groups, we analyzed the clinical outcomes of each mosaic type within those two level groups. Statistical analysis indicated the most significant order in which the sub-groups correlated with clinical outcomes (Figure 19A). As noted before, the division into a low and high group was not advantageous for segmental mosaics. For embryos with mosaicism affecting at least one whole chromosome, considering mosaic level and type simultaneously revealed significantly different sub-group outcomes. On the lowest end of the spectrum, the high-level complex mosaic sub-group had the worst outcome rates, but notably those embryos still had some potential to implant and produce ongoing

pregnancies and births. Those findings can be summarized in a ranking system of mosaic traits according to clinical outcomes (Figure 19B).

Figure 19. Combined Effect Of Mosaic Traits On Clinical Outcome Reveals Ranking System For Mosaic Embryos.
(A) Clinical outcomes of the euploid group compared to mosaic groups sorted by mosaic level and type. For mosaic level, 'low' is <50%, 'high' is ≥50%. Chi-square test for trend (blue dotted line and connected points) indicates statistically significant trend. (B) Ranking of mosaic embryo sub-groups, sorted by favorable clinical outcomes.
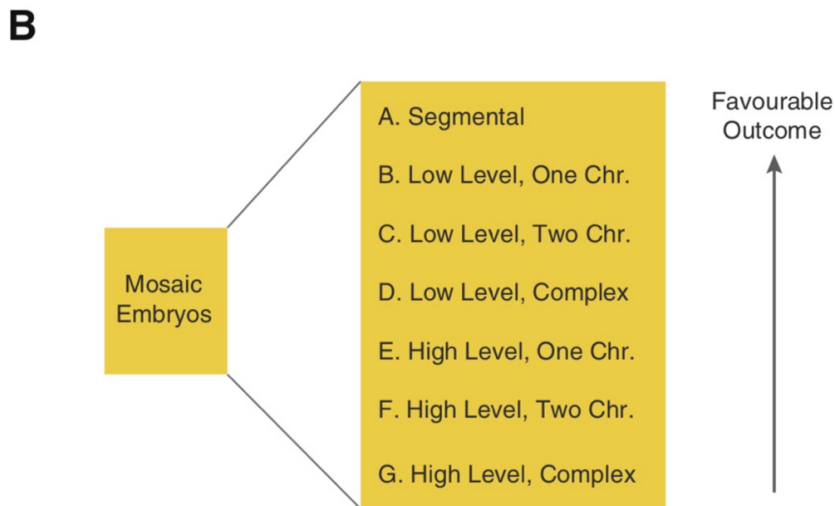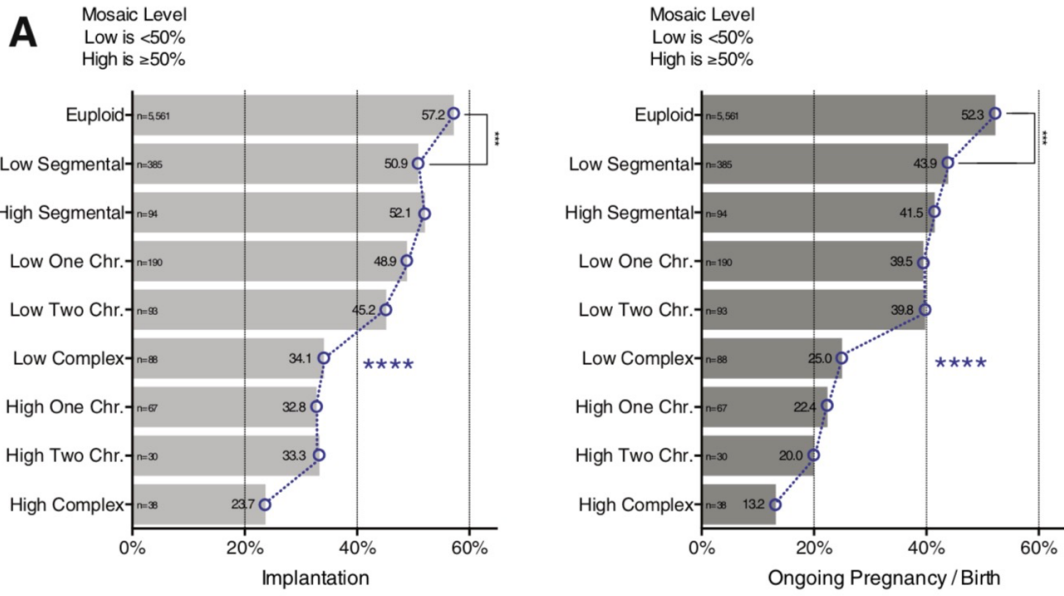
In order to consider all relevant parameters for embryo selection in the clinic, we applied an additional analysis of embryo morphology to every sub-group in the ranking scheme. Using the outcomes from the 1,000 mosaic embryo transfers, we tabulated the rates of implantation and OP/B for every permutation of morphology in the Gardner system (Supplementary Table 8). Normalizing the data to the best morphological sub-group of the euploid group (5AA) (see Materials and Methods), the resulting matrix specified the prioritization order according to mosaic embryo level, type, and Gardner stage/grade assessment (Table 4). Taking the average of the three indicated values for stage, ICM grade, and TE grade produces a ranking score for any given embryo. The table therefore provides a reference to prioritize embryos in the clinic by likelihood of favorable clinical outcome.

Table 4. Matrix Of Embryo Ranking According To Mosaicism Traits And Morphology.

Values and cell colors indicate ranking, from best (1.00/Green) to worst (0.00/Red). The table was generated using the data from 5,561 euploid embryos and 1,000 mosaic embryos analyzed in this study, and can serve as a reference to prospectively determine the order of transfer for embryos in the clinic. The combined rank value of an embryo can be assessed by considering its PGT-A (sub-) category and multiplying the three indicated values (Stage, ICM grade, and TE grade). The resulting number can be compared to that of other embryos in a cohort to establish priority for transfer.

Euploid

Euploid	Stage	Implantation	Ong. pregn./birth	ICM	Implantation	Ong. pregn./birth	TE	Implantation	Ong. pregn./birth
	3	0.66	0.70	A	1.00	1.00	A	1.00	1.00
	4	0.87	0.90	B	0.88	0.84	B	0.87	0.86
	5	1.00	1.00	C	0.39	0.33	C	0.50	0.49
	6	0.80	0.77						

Mosaic

Segmental	Stage	Implantation	Ong. pregn./birth	ICM	Implantation	Ong. pregn./birth	TE	Implantation	Ong. pregn./birth
	3	0.53	0.58	A	1.00	1.00	A	1.00	0.93
	4	0.78	0.71	B	0.84	0.74	B	0.76	0.70
	5	0.81	0.79	C	0.24	0.19	C	0.61	0.63

Low level, 1 chr	Stage	Implantation	Ong. pregn./birth	ICM	Implantation	Ong. pregn./birth	TE	Implantation	Ong. pregn./birth
	4	0.69	0.75	A	0.89	0.83	B	0.78	0.70
	5	0.62	0.53	B	0.78	0.64	C	0.52	0.41
				C	0.52	0.40			

Low level, 2 chr	Stage	Implantation	Ong. pregn./birth	ICM	Implantation	Ong. pregn./birth	TE	Implantation	Ong. pregn./birth
	4	0.67	0.73	B	0.85	0.83	A	0.89	0.96
	5	0.86	0.82	C	0.38	0.29	B	0.70	0.70
							C	0.58	0.55

Low level, complex	Stage	Implantation	Ong. pregn./birth	ICM	Implantation	Ong. pregn./birth	TE	Implantation	Ong. pregn./birth
	4	0.89	0.71	B	0.77	0.67	B	0.80	0.58
	5	0.67	0.61	C	0.53	0.22	C	0.57	0.50

High level, 1 chr	Stage	Implantation	Ong. pregn./birth	ICM	Implantation	Ong. pregn./birth	TE	Implantation	Ong. pregn./birth
	4	0.41	0.30	B	0.58	0.36	B	0.51	0.31
	5	0.45	0.39	C	0.48	0.37	C	0.45	0.38

High level, 2 chr	Stage	Implantation	Ong. pregn./birth	ICM	Implantation	Ong. pregn./birth	TE	Implantation	Ong. pregn./birth
	4	0.67	0.49	A	0.42	0.44	B	0.57	0.37
	5	0.49	0.35	B	0.64	0.44			

High level, complex	Stage	Implantation	Ong. pregn./birth	ICM	Implantation	Ong. pregn./birth	TE	Implantation	Ong. pregn./birth
	5	0.47	0.20	B	0.56	0.23	B	0.25	0.13
				C	0.31	0.32			

12.6. Chapter Discussion

The present study is the largest dataset of transferred mosaic embryo outcomes reported to date. This compiled analysis conclusively shows that embryos classified as mosaic have a distinct set of clinical outcomes and should comprise a separate PGT-A category. Maintaining PGT-A's 'classical' binary system of normal/abnormal is disadvantageous.

On one hand, grouping mosaic embryos with the normal category would result in decreased rates of implantation and increased miscarriages. On the other hand, indiscriminately lumping mosaic embryos with the abnormal category would result in discarding viable embryos. In order to further increase likelihood of positive clinical outcomes, embryos of the mosaic category should be stratified by their mosaic traits (level and type) identified with PGT-A, and ranked for transfer to a patient. The prioritization scheme outlined in this study can be applied to any embryo by considering its mosaic attributes and morphology.

Recent studies using serial biopsies have shown that uniform euploidy or whole chromosome aneuploidy are highly concordant between different regions of a blastocyst (174, 237-240). However, mounting evidence indicates that intra-biopsy mosaicism in the TE is a poor predictor of the ploidy status of the remaining embryo, and often pairs with uniform euploidy in the ICM (107, 165, 238, 241). Consequently, our findings suggest that possessing a mix of euploid and aneuploid cells in the TE alone might be sufficient to negatively influence clinical outcomes. Not only were implantation rates lowered, early spontaneous abortions (before week 8-10 of gestation) were particularly frequent with mosaic embryo transfers, possibly indicating the deleterious effects of the aneuploid cell portion in the TE-derived early placenta. That brings up a series of questions: What befalls the aneuploid cells in pregnancies that persist? What happens in cases where mosaicism is present in the ICM as well? And more broadly, how can embryos classified as mosaic by PGT-A produce seemingly healthy births?

There is substantial experimental evidence for corrective mechanisms that operate in the context of chromosomal mosaicism. They center on the well documented fact that aneuploidy often hampers cell proliferation and viability (242). Studies on murine chimeric embryos formed by mixing cell types showed that euploid cells outcompeted aneuploid cells by differential proliferation and preferential cell death (218, 243). The aneuploid cells replicated more slowly (in the TE) or underwent apoptosis (in the ICM), while euploid cells replicated rapidly and persisted. The experiments revealed a threshold of aneuploid cell load that was incompatible with viability, such that when the ratio of aneuploid to euploid cells was too high at the onset, the embryo invariably died. At mid-to-low ratios, the euploid cells were capable of 'rescuing' the embryo by diluting out the aneuploid cells (218). Correspondingly, human mosaic blastocysts subjected to extended in vitro culture frequently displayed a complete loss of the aneuploid cell constituent, and 'high' mosaics were more likely to perish during extended culture (175). Live imaging experiments showed that 'low' and 'high' mosaic embryos exhibited significantly different morphokinetics between the zygote and blastocyst stage (58). Furthermore, immunofluorescence analysis of human embryos classified as 'euploid' and 'mosaic' showed distinct global patterns of cell proliferation and programmed cell death, befitting a model of directed demise of aneuploid cells and compensatory proliferation of euploid cells (107). Our current observations with clinical outcome data build on that concept, suggesting that percent aneuploid cells and the type of aneuploidy together dictate the 'severity' of mosaicism. High abnormal cell load and/or complex aneuploidies affecting several chromosomes are more difficult for the embryo to overcome than low abnormal

cell load and/or segmental aneuploidies, resulting in distinct implantation and birth rates after transfer.

If aneuploidy can be overcome, should uniformly aneuploid embryos also be considered for transfer? It is important to note that the self-correction mechanisms described above apply specifically to mosaicism. When the chromosomal error present in an embryo is the consequence of a meiotic mistake, all of its cells are bound to contain the same aneuploidy. For such an embryo to self-correct and result in a healthy birth, individual cells would need to internally repair their chromosomal abnormalities. Putative mechanisms have been proposed in the literature: 'Endoreplication' could convert a monosomy into a disomy, or 'trisomy rescue' could revert a trisomy into a disomy by anaphase lagging (141). However, these processes would frequently result in uniparental disomy (UPD), but UPD in IVF embryos is extremely rare, estimated at 0.06% (244). Notably, intracellular corrective events have not been conclusively documented in human embryos. In fact, evidence from extended in vitro culture experiments of human embryos suggests the contrary, that uniform euploid or aneuploid embryos invariably maintain their initial ploidy in both ICM and TE lineages (175). Clinical data on this topic is limited, but one study reported the transfer of ten embryos classified as uniform aneuploid by PGT-A, resulting in nine failed pregnancies and a single ongoing pregnancy and birth of an affected baby that died at six weeks (232) and a 'non-selection study' showed no births from 102 aneuploid embryo transfers (245). The transfer of embryos classified as 'aneuploid' by PGT-A is therefore not recommended.

Unlike instances of whole chromosome mosaicism, the embryos composing the segmental mosaic group had uniform outcomes regardless of whether the segmental mosaicism was low or high level, or whether one, two, or more segments were involved in the mosaicism. This observation reflects the unique etiology and repair mechanisms related to segmental abnormalities, reviewed before (246). Unlike whole chromosome aneuploidies (which mainly arise from chromosome missegregations), segmental deletions and duplications originate from chromosomal breakage via double strand breaks (DSBs) of the DNA. DSBs are associated with a distinctive set of corrective pathways, which are dysregulated in early embryogenesis but become more established with developmental progression. Recent studies showed that segmental abnormalities are often discordant between serial biopsies in blastocysts, and are significantly more likely to originate from mitotic errors than from meiotic errors compared to whole chromosome aneuploidies (174, 237, 238, 247). Together, these observations suggest that the post-zygotic generation and correction of segmental abnormalities might be more dynamic and reversible than the processes associated with whole chromosome aneuploidies, possibly explaining why segmental mosaics are better tolerated in regards to implantation and gestation. However, while segmental mosaic embryos as a combined group had better outcomes than whole chromosome mosaics, they nonetheless had significantly poorer outcomes compared to the euploid control group.

While there is certainly a need for comprehensive analyses of neonatal outcome data of transferred mosaic embryos, as mentioned before, the newborns from our sample group have invariably been healthy by routine neonatal examination for developmental defects and gross abnormalities. Mosaicism identified by PGT-A at the blastocyst stage is generally not reflected later in gestation during prenatal genetic testing (107, 171, 172), likely because of the aforementioned corrective mechanisms operating in mosaic settings. At present, there is a singular report in the literature showing blastocyst-stage mosaicism persisting through gestation, although undergoing a substantial reduction in percent aneuploid cells: From 35% monosomy in chromosome 2 in the TE biopsy at the blastocyst stage to 2% trisomy in chromosome 2 during amniocentesis, in a reciprocal pattern (248). Birth of a healthy baby followed, in which peripheral blood analysis showed 2% mosaic monosomy in chromosome 2, however epithelial cells in a buccal smear were euploid. While that neonate had no overt phenotype, this case reinforces the need for careful genetic counselling with emphasis on prenatal testing to patients opting for mosaic embryo transfers (166, 235, 249). This precedent should also be considered when facing the choice between a poor morphology euploid embryo and a good prognosis mosaic embryo. While the ranking matrix presented in this study (Table 4) unequivocally shows that a low quality euploid embryo (e.g. ICM grade 'C' and TE grade 'C') is associated with significantly reduced rates of implantation and OP/B than several mosaic embryo sub-groups, the current outstanding questions regarding newborn chromosomal health might nonetheless motivate clinics to favor the transfer of all euploid embryos before resorting to good quality mosaic embryos. Even though newborns resulting from mosaic embryo

transfers in this study invariably appeared healthy by routine examination, concerns for long-term health cannot yet be entirely dispelled. The question must therefore be carefully considered by each clinic and patient situation.

Overall, the incidence and variability of the mosaic group at participating centers was in line with previous reports that have used NGS-based PGT-A and the guidelines set forth by PGDIS and CoGEN to define 'mosaicism'. As a reference, the STAR study reported a proportion of mosaic embryos ranging from 10.5-26.4% at participating clinics (250). While the present analysis considered numerous variables that can affect mitotic error rates and clinical outcomes, due to the multicenter nature of the study other potential confounders still persisted (such as differences in demographics, stimulation program, culture techniques and endometrial preparation methods) and must be noted as a limitation.

The results of the present study contradict the claims that mosaicism is merely an artifact of the PGT-A process. The suggestion that 'low' and 'high' mosaic profiles are respectively euploid and aneuploid profiles with technical noise is discredited by the observation that embryos in the 'low' mosaic category have significantly poorer clinical outcomes than the euploid control group. Conversely, if the 'high' mosaic group was truly no more that uniform aneuploids with technical noise, one would expect virtually no healthy pregnancies from that group. Intra-biopsy mosaicism detected with

contemporary, NGS-based PGT-A methodologies is therefore not likely a procedural fluke, but a reflection of a biological occurrence consistent with mosaicism.

The analysis of one thousand mosaic embryo transfers provides clinical, statistically significant evidence for the traits of mosaicism identified with PGT-A that affect implantation and spontaneous abortion, offering a blueprint for ranking mosaic embryos in the clinic. The field has been transferring embryos 'blindly' for 40 years, and a proportion of those have undoubtedly been of the mosaic category - now refined PGT-A tools can identify and characterize mosaics, allowing for their optimal clinical management.

13. Specific Aim D: To test the hypothesis that accurate quantitation of mitochondrial DNA (mtDNA) in human blastocysts serves as a biomarker of ploidy and/or predictor of implantation.

The following published work is presented for this specific aim:

Victor AR, Brake AJ, Tyndall JC, Griffin DK, Zouves CG, Barnes FL, Viotti M. Accurate quantitation of mitochondrial DNA reveals uniform levels in human blastocysts irrespective of ploidy, age, or implantation potential. Fertil Steril. 2017 Jan;107(1):34-42.e3. doi: 10.1016/j.fertnstert.2016.09.028. Epub 2016 Oct 25. PMID: 27793366.

13.1. My Personal Contribution to the Work

My personal contribution to this study includes study design and theoretical approach, experimental execution (NGS, qPCR), experimental oversight, data analysis and assisting with manuscript preparation.

13.2. Chapter Summary

Quantitation of mitochondrial DNA (mtDNA) copy number in blastocyst cells has been proposed as a method to identify embryos with decreased potential, despite their euploid classification with PGT-A. Accurate quantitation of mtDNA in a TE biopsy is essential to

properly evaluate its usefulness as a biomarker of ploidy or likelihood of implantation upon transfer. This study comprises two parts: 1) the optimization of mtDNA copy number quantitation in human embryos, and 2) application of that quantitation method to clinical samples to determine whether it is clinically useful. We used 1396 blastocysts derived from 259 patients for this study. TE biopsies were tested by NGS and qPCR. For each sample the mtDNA value was divided by the nuclear DNA (nDNA) value and the result was further subjected to mathematical analysis tailored to the genetic makeup of the source embryo. On average the mathematical correction factor changed the conventionally determined mtDNA score of a given blastocyst via NGS by 1.43% +/-1.59% (N=1396), with maximal adjustments of 17.42%, and via qPCR by 1.33% +/-8.08% (N=150), with maximal adjustments of 50.00%. Levels of mtDNA in euploid and aneuploid embryos showed a statistically insignificant difference by NGS (euploids N=775, aneuploids N=621) and by qPCR (euploids N=100, aneuploids N=50). Blastocysts derived from younger or older patients had comparable mtDNA levels by NGS ('young' age group N=874, 'advanced' age group N=514) and by qPCR ('young' age group N=92, 'advanced' age group N=58). Viable blastocysts did not contain significantly different mtDNA levels compared to unviable blastocysts when analyzed by NGS (implanted N=101, non-implanted N=140) and by qPCR (implanted N=49, non-implanted N=51).

We recommend implementation of the correction factor calculation to laboratories evaluating mtDNA levels in embryos by NGS or qPCR. When applied to our in-house data, the calculation reveals that overall levels of mtDNA are largely equal between blastocysts stratified by ploidy, age, or implantation potential.

13.3. Chapter Introduction

Human cells contain anywhere from 100 to 150,000+ copies of the mitochondrial DNA (mtDNA) molecules depending on cell type (251, 252), and several conditions correlate with changes in mtDNA copy number including aging, myopathies, neuropathies, diabetes, and cancer (253). In human embryos, recent studies have investigated amounts of mtDNA, generally describing a correlation of high mtDNA levels with a 'stressed' state (188, 189, 254). Conditions that deviate from the steady state such as aneuploidy, advanced maternal age, or chemically induced-stress tend to associate with higher mtDNA content. Of clinical relevance, such reports suggested that embryos with mtDNA levels above the norm showed significantly poor frequency of pregnancy when transferred (188, 189).

The described observations are in line with the 'Quiet Embryo Hypothesis', which postulates that under ideal circumstances embryos are engaged in low metabolic activity (255). Elevated mtDNA levels and by extension increased ATP production could be a compensatory mechanism providing distressed embryos with more chemical energy to overcome adverse conditions. Therefore, in the case of euploid embryos being chosen for transfer, sub-optimal intrinsic or environmental factors could elicit higher levels of mtDNA. Consequently, mtDNA content has been proposed as a biomarker for embryo viability (188, 189).

Crucial to such investigations are methods that permit precise measurements of mtDNA levels. In situ hybridization has previously been used (256), probing for a region of the mtDNA sequence, but this method has not been widely adopted possibly due to laboriousness and difficulty in interpreting results. More commonly employed technologies are quantitative real-time polymerase chain reaction (qPCR) and sequencing platforms, especially next generation sequencing (NGS). Both methods yield one value for mtDNA and one value for nuclear DNA (nDNA) quantity, and the ratio of mtDNA to nDNA is the principal mode to assess mtDNA quantity per cell (257). Crucially, using nDNA values for normalization assumes that the composition of nDNA is equal across samples.

When nDNA composition varies across samples, such as in cancer, the disparities must be accounted for. For such a purpose the use of a mathematical correction factor has been proposed in mtDNA studies of cancer (258). The correction factor takes into account characteristics of tumor biology that affect nDNA values such as genetic abnormalities of cancerous cells and tumor cell heterogeneity due to stroma and immune infiltrates (258). Only after such a mathematical adjustment are side-by-side comparisons of mtDNA levels across tumor samples appropriate. To our knowledge, such a correction factor has not been employed in studies of mtDNA levels in embryos.

In order to determine mtDNA levels in blastocysts accurately, we developed a mathematical formula adapted to the nuances of human embryology, and derived a

correction factor that accounts for genomic variation due to embryo gender and ploidy. We then undertook an analysis of mtDNA levels in biopsies from human blastocysts derived from patients with infertility at the Zouves Fertility Center (ZFC). In contrast to previous reports, our corrected values show no statistically significant differences in blastocysts grouped by ploidy, maternal age, or implantation potential.

13.4. Methods And Materials

13.4.1. Study Design

This study was a retrospective analysis of de-identified NGS workflow data and WGA product from patients consenting to preimplantation genetic screening during routine IVF procedures. It is exempt from IRB review by the U.S Department of the Health & Human Services under 45 CFR 46.101(b)(4).

13.4.2. Embryo Processing

IVF and culturing of embryos took place at ZFC using standard techniques. Briefly, fertilization was accomplished using intracytoplasmic sperm injection and zygotes were cultured for 5 to 7 days in either G1/G2 Plus medium (Vitrolife) or GTL (Vitrolife) in 5.5% CO_2, 5.5% O_2 balance N_2 at 37°C in a humidified atmosphere. Five to ten-cell trophectoderm biopsies were collected from blastocyst stage embryos and stored at -80 degrees Celsius until further processing. WGA on each biopsy was performed using the Sureplex system (Rubicon) and followed by NGS with the MiSeq sequencer (Illumina), as per the standard Veriseq protocol (Illumina). Embryo ploidy was assessed with the

Bluefuse Multi Software (BMS) (Illumina). We investigated mtDNA content in a total of 1396 embryos, 241 of which were selected for frozen embryo transfer (225 as single embryos and 16 as paired siblings).

13.4.3. Determination Of mtDNA Content By NGS

For each sample, MiSeq Reporter Software (MCS) (Illumina) files in the BAM and FASTQ format were uploaded into Geneious R9 (Biomatters Ltd) to determine number of reads aligning to the mtDNA reference genome as per Genome Reference Consortium (GRC)h37. For FASTQ files, reads were aligned under maximal stringency to avoid potential multi-mapping to NUMTs (259). The number of mtDNA mapped reads was divided by the number of nDNA mapped reads after bioinformatic processing and filtering by MCS and displayed in BMS. For Supplementary Figure 3, number reads aligning to Chromosome (Chr) 1 were determined in Geneious R9. Resulting values were further subjected to a mathematical correction factor described below.

13.4.4. Precise Calculation Of mtDNA Score From NGS Data

To calculate the mtDNA score (m_{NGS}) for each sample using NGS, the number of reads mapping to the mitochondrial genome (r_m) is divided by the number of reads mapping to the nuclear genome (r_n) to normalize for technical batch-to-batch variability during WGA and NGS as well as number of cells collected during biopsy. The resulting value is multiplied by the correction factor F_{NGS} as per formula 1.

(1)

$$m_{NGS} = \frac{r_m}{r_n} \times F_{NGS}$$

F$_{NGS}$ takes into account two parameters necessary to correctly normalize for number of cells probed: embryo gender and ploidy. Without the correction factor, the formula assumes that nuclear genomes across all samples are equal in length. According to GRCh37 (Ensembl Release 68) the diploid female human genome is comprised of 6,072,607,692 base pairs (bp), while the male counterpart is 5,976,710,698 bp long, a difference of 1.58%. Without correction, all results from male embryos are inflated by 1.58% because the denominator r_n is artificially small. To correct for this, *F$_{NGS}$* for all male embryos contains a multiplier of 0.9842, since the male genome is 98.42% the length of the female's (see Table 5A).

Similarly, an aneuploid embryo has more or less genetic material per cell compared to a euploid embryo, and without correction it would lead to inflated mtDNA counts in the case of nullisomies and monosomies, and deflated mtDNA counts in trisomies and other polysomies. To correct for this, the mtDNA value for each embryo is multiplied by a correction factor tailored to its chromosomal composition (Table 5A). The correction factors for different chromosomes should be multiplied to each other when embryos have aneuploidies in more than one chromosome. For example, a male embryo with a Chr 1 monosomy and Chr 21 trisomy with 3,000 reads mapping to mtDNA and 900,000 reads mapping to nDNA would have the following final *m$_{NGS}$* score:

$$m_{NGS} = \frac{3,000}{900,000} \times (0.9842 \times 0.9590 \times 1.0079) = 0.003171$$

Table 5. Correction Factors For Accurate mtDNA Content Determination.

A. NGS correction factor

mtDNA	16,569 bp
Diploid female (reference)	6,072,607,692 bp
Diploid male	5,976,710,698 bp
Female−male	95,896,994 bp
% Male vs. female	98.42%
% Difference	1.58%
NGS correction factor female	1
NGS correction factor male	0.984208268

Universal formula to calculate NGS correction factor	(Reference genome length ± loss or gain)/(reference genome length)
Formula for a loss (Z is the number of base pairs in the lost sequence)	(6072607692−Z)/6072607692
Formula for a gain (Z is the number of base pairs in the lost sequence)	(6072607692+Z)/6072607692

Chromosome	Length (bp)	Correction factor monosomy	Correction factor disomy	Correction factor trisomy
1	249,250,621	0.958954928	1	1.041045072
2	243,199,373	0.95995141	1	1.04004859
3	198,022,430	0.967390874	1	1.032609126
4	191,154,276	0.96852188	1	1.03147812
5	180,915,260	0.970207978	1	1.029792022
6	171,115,067	0.971821814	1	1.028178186
7	159,138,663	0.973794016	1	1.026205984
8	146,364,022	0.975897665	1	1.024102335
9	141,213,431	0.976745833	1	1.023254167
10	135,534,747	0.977680964	1	1.022319036
11	135,006,516	0.97776795	1	1.02223205
12	133,851,895	0.977958086	1	1.022041914
13	115,169,878	0.981034527	1	1.018965473
14	107,349,540	0.982322332	1	1.017677668
15	102,531,392	0.983115756	1	1.016884244
16	90,354,753	0.98512093	1	1.01487907
17	81,195,210	0.986629268	1	1.013370732
18	78,077,248	0.987142715	1	1.012857285
19	59,128,983	0.990263	1	1.009737
20	63,025,520	0.989621342	1	1.010378658
21	48,129,895	0.992074262	1	1.007925738
22	51,304,566	0.991551477	1	1.008448523
X	155,270,560	0.974430991	1	1.025569009
Y	59,373,566	0.990222723	1	1.009777277

B. qPCR correction factor

State of nDNA region probed by reference assay:	Nullisomy	Monosomy	Disomy	Trisomy	Tetrasomy
Corresponding correction factor	Use different reference assay	0.5	1	1.5	2

Note: Data based on reference genome GRCh37 Ensembl release 68. (A), NGS correction factors for complete chromosomal monosomies or trisomies. The indicated universal formula is also applicable for whole chromosome nullisomies and other polysomies, as well as segmental losses or gains. (B) Correction factor for qPCR data when the nuclear DNA reference assay probes a chromosomal region that is aneuploid.

13.4.5. Determination Of mtDNA Content By qPCR

All quantitative real time PCR (qPCR) experiments were performed using the Taqman system (Applied Biosystmems/Thermo Fisher). Surplus WGA product from the Veriseq workflow was diluted 1/10 in water, vortexed for 30-60 seconds and heated to 95 degrees Celsius for ten minutes to insure inactivation of any residual WGA polymerase activity. Two microliter of the resulting solution were used in the Taqman Fast Advance Master Mix reaction, and run with a Taqman 7500 Real-Time PCR instrument (Applied Biosystems/Thermo Fisher). All samples were run in three technical replicates. Taqman assays CYTB (Hs02596867_s1) and ND6 (Hs02596879_g1) were used for mitochondrial genes, based on consistently high qPCR experimental efficiencies compared to several other mtDNA assays tested. An assay targeting the RNase P component RPPH1 (Hs03297761_s1) was used for the nuclear gene; this is a routinely used copy number reference assay known to be present once on Chr 14 per haploid human genome (260). The qPCR efficiency was experimentally determined to exceed 95% for all three assays used in this study (Supplementary Figure 5C-E). Using standard curves for CYTB and RNase P the exact number of copies of mtDNA and nDNA was established in each sample as per the absolute quantitation methods described before: http://www6.appliedbiosystems.com/support/tutorials/pdf/quant_pcr.pdf. The ratio of the two values was determined and was further subjected to a correction factor outlined below.

Relative quantitation of mtDNA scores was performed using the qPCR Ct values from ND6 as the target assay and Ct values from RNase P as the control assay, followed by a log-to-linear conversion (2^{-dCt}).

13.4.6. Precise Calculation Of mtDNA Score From qPCR Data

When using a qPCR platform, an assay is designed that probes an mtDNA region (the target), and second assay is designed probing a nDNA region (the reference). The mtDNA score (m_{qPCR}) may be determined by absolute quantitation with a standard curve or relative quantitation.

The absolute quantitation method calculates values of unknown samples by interpolating their quantity from a previously determined standard curve. This establishes an exact count of mtDNA molecules (c_m) and nDNA molecules (c_n) for each sample. Dividing the former by the latter normalizes for technical batch-to-batch variability as well as cell numbers collected in each biopsy. A correction factor (F_{qPCR}) must be applied to account for the nuclear genomic composition of the tested embryo, resulting in formula 2.

(2)

$$m_{qPCR} = \frac{c_m}{c_n} \times F_{qPCR}$$

F_{qPCR} equals 1 for euploid embryos, as well as for aneuploid embryos with chromosomal aberrations in genetic regions other than the reference sequence. If an embryo is monosomic for the reference region, that embryo's cells only contain one copy of the

nDNA region being quantified, instead of the normal two copies. Consequently, this leads to c_n being artificially small, which in turn inflates the m_{qPCR} value. To correct this, F_{qPCR} must include the multiplier 0.5. By extension, a trisomy of the reference sequence must include F_{qPCR} with the multiplier 1.5. For example an embryo with a Chr 1 monosomy and Chr 21 trisomy with 4×10^7 counts for the mtDNA target and 2×10^4 counts to the nDNA reference, and the nDNA reference assay is located on Chr 21, would have the following final m_{qPCR} score:

$$m_{qPCR} = \frac{4 \times 10^7}{2 \times 10^4} \times (1.5) = 3000$$

The m_{qPCR} value represents the precise number of mtDNA molecules per nDNA molecules, or how many mtDNA copies there are per haploid genome. Doubling the value results in the number of mtDNA copies per diploid cell.

Similarly, when using a relative quantitation qPCR mode such as 2^{-dCt} the value must be adjusted if the reference assay is located in an aneuploid region, as per formula 3.

(3)

$$m_{qPCR} = 2^{-(Ct_m - Ct_n)} \times F_{qPCR}$$

The same correction factor (see Table 5B for details) should be applied when executing a fold change calculation such as the 2^{-ddCt} method (261).

13.4.7. Validation Of Detection Platforms

Reproducibility of the NGS platform in determining mtDNA scores was tested by re-sequenced WGA products, which yielded consistent results amongst separate runs (Supplementary Figure 2D). Also, there were unvarying mtDNA scores between multiple samples stemming from the same cell line with separate WGA and NGS runs. The starting amount of DNA for each cell line experiment was 33 pg, the equivalent DNA from a biopsy of 5 cells (assuming 6.6 pg per diploid genome). Furthermore, two separate blood samples from a single patient yielded equivalent mtDNA scores with individual DNA isolation, WGA and NGS procedures.

To attain cross-platform validation, we compared the mtDNA scores of 5 embryo biopsy WGA samples by NGS and the two different qPCR methods described above. For each case the level of mtDNA score obtained by all three platforms was comparable (Supplementary Figure 5E). From this data we deduce that mtDNA scores are highly correlative across detection platforms.

13.4.8. Statistics And Graphs

Group analyses were performed using Welch's parametric two-tailed unpaired t-test in Prism 6 (GraphPad Software). The logistic regression analysis was performed in R Statistical Software. All graphs were prepared in Prism 6 showing means with error bars indicating standard deviation.

13.5. Results

13.5.1. Applying Correction Factor Substantially Changes Mtdna Scores In Blastocyst Samples

We analyzed mtDNA scores in blastocyst embryos used in our clinic for IVF, all of which had undergone routine PGS for chromosomal abnormalities. We used three distinct platforms to determine mtDNA and nDNA levels in a biopsy sample: NGS, qPCR by absolute quantitation testing for the mitochondrial gene CYTB, and qPCR by relative quantitation assaying for the mitochondrial gene ND6. Both qPCR methods also probed for the nuclear gene RNase P, which is routinely used to quantify nuclear DNA for normalization purposes.

For each sample the mtDNA score was obtained by dividing the mtDNA value by the nDNA value to normalize for technical batch-to-batch variation and number of cells collected at biopsy. All resulting values were subjected to the mathematical correction factors that take the variability of embryonic genomes into account (See Methods for full explanation of the rationale and formulas).

The NGS correction factor changed the mtDNA score on average by 1.43% +/-1.59% (N=1396). The largest change in our samples was 17.42%. Applying the correction factor for qPCR changed the values by 1.33% +/-8.08% (N=150) on average when using the absolute quantitation method, with changes ranging up to 50.00%. When using the

relative quantitation method, the qPCR correction factor changed mtDNA scores on average by 0.575% +/-5.36% (N=87), with changes ranging up to 50.00%.

13.5.2. Euploid And Aneuploid Blastocysts Have Equal mtDNA Score Distributions

When stratified by euploid and aneuploid blastocysts, the mtDNA scores by NGS did not result in a statistically significant difference (P=0.114) (Figure 20A). Samples were randomly selected out of these groups and tested by qPCR absolute quantitation assaying the mitochondrial CYTB gene. Again, euploid and aneuploid cohorts were not statistically different (P=0.642) (Figure 20B). To probe these observations by a third method, a subset of embryos was further assayed with different mitochondrial gene (ND6) and compared by a relative quantitation method (2^{-dCt}). Once more we observed insignificant differences between euploids and aneuploids (P=0.202) (Figure 20C). Therefore, regardless of quantitation platform and downstream mathematical calculation employed, blastocysts grouped by ploidy never showed statistically significant differences in mtDNA scores. This is in stark contrast with previous reports that did not employ a correction factor in their calculations (189, 254).

Figure 20. mtDNA Scores Sorted By Euploid And Aneuploid Blastocysts Result In Statistically Insignificant Differences.
(A) Next Generation Sequencing (NGS) data. (B) Quantitative RT-PCR (qPCR) data probing for a locus in the CYTB mitochondrial gene analyzed by absolute quantitation. (C) qPCR data probing for a locus in the ND6 mitochondrial gene analyzed by relative quantitation. N. S. = not significant.
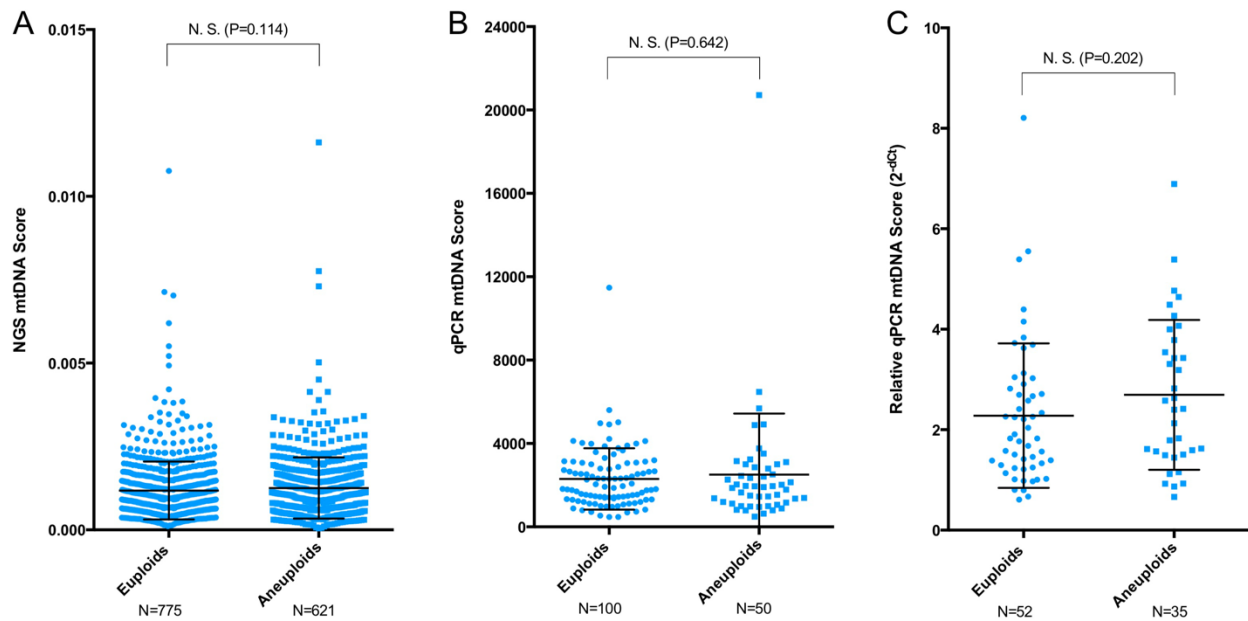
13.5.3. Maternal Age At Oocyte Retrieval Does Not Affect mtDNA Levels Of Blastocysts

We divided blastocysts into a younger maternal age group at oocyte retrieval (20-37 years) and an older group (38-46). A previous study reported a statistical difference stating that the older group had higher mtDNA levels (189). We investigated mtDNA scores by NGS amongst all embryos regardless of ploidy, and observed no difference between age groups (Figure 21A). When analyzing only euploid embryos, again there was no significant variance (Figure 21A). We confirmed this observation by re-testing a number of embryos by the two described qPCR methods, using two different mitochondrial genes CYTB and ND6 (Figure 21B,C). We further subdivided all embryos tested by NGS by individual numerical maternal age at oocyte retrieval in an effort to reveal any trends, but linear regression analysis failed to show statistically significant

tendencies (Figure 21D,E). Hence, blastocysts derived from oocytes of advanced maternal age do not contain higher mtDNA levels according to our results.

Figure 21. mtDNA Scores Of Blastocysts Sorted By Maternal Age At The Time Of Oocyte Retrieval.
(A) NGS data sorted by two age groups (20-37 and 38-46) analyzing all embryos and euploids alone, indicating no relevant differences. (B-C) mtDNA scores derived by the two described alternative qPCR methods showing no significant differences. (D-E) NGS values sorted by individual age, evaluating all embryos and euploids alone. Insets show linear regression through the means, resulting in statistically insignificant P values. N. S. = not significant.
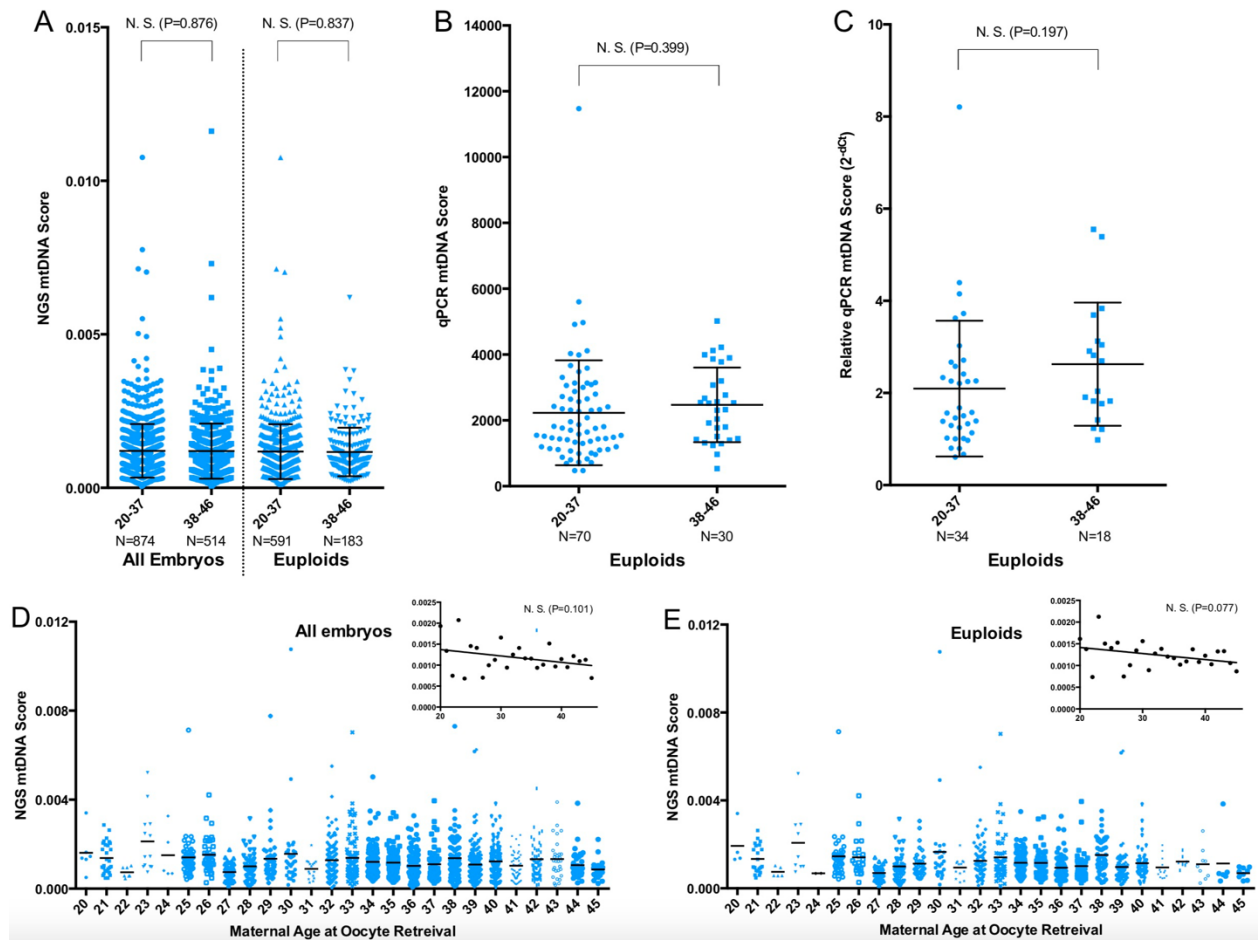
13.5.4. mtDNA Levels Show No Correlation With Viability And Do Not Predict Blastocyst Transfer Clinical Outcome

We determined the mtDNA score of embryos that had undergone frozen embryo transfer (FET) and had either implanted or had failed to do so, as determined by the presence or absence of a fetal sac at 6 weeks. Biopsies from all embryos had been collected at the blastocysts stage. NGS data from 101 implanted and 140 not implanted blastocysts showed no statistical difference in mtDNA score (P=0.510) (Figure 22A).

With these combined 241 blastocysts we carried out a logistic regression analysis to investigate whether mtDNA score could function as a predictive tool for clinical outcomes. The test is adjusted for the following confounding factors: cohort size (i.e. how many embryos produced in the cycle), embryo gender, single or paired sibling transfer, oocyte age at retrieval, patient age at transfer, embryo stage and grade. The results indicate that mtDNA score is a statistically insignificant predictor embryo viability (P=0.472) even when adjusted for confounding factors (Supplementary Table 2).

In another effort to correct for confounding factors in our study, we proceeded to compare embryos from individual cycle cohorts. We focused on patients that had undergone two or more embryo transfers in our clinic within at most 12 months. For each patient we compared mtDNA levels between embryos that resulted in pregnancy versus those that failed implantation. The NGS mtDNA score of each implanting embryo was set to 1, and the relative mtDNA score for the non-implanted embryos was calculated. This

Figure 22. mtDNA Scores And Implantation Potential Of Transferred Euploid Blastocysts.

(A) NGS data from all transferred blastocysts shows no statistically significant difference. (B) Intra-cohort analysis for 24 patients with repeat transfers results in insignificant differences. (C-D) Statistically insignificant differences resulting from absolute and relative quantitation qPCR probing two different mitochondrial genes CYTB and ND6, respectively. Only one sample in the 'not implanted' group consistently shows an mtDNA score above a possible threshold across platforms. N. S. = not significant.
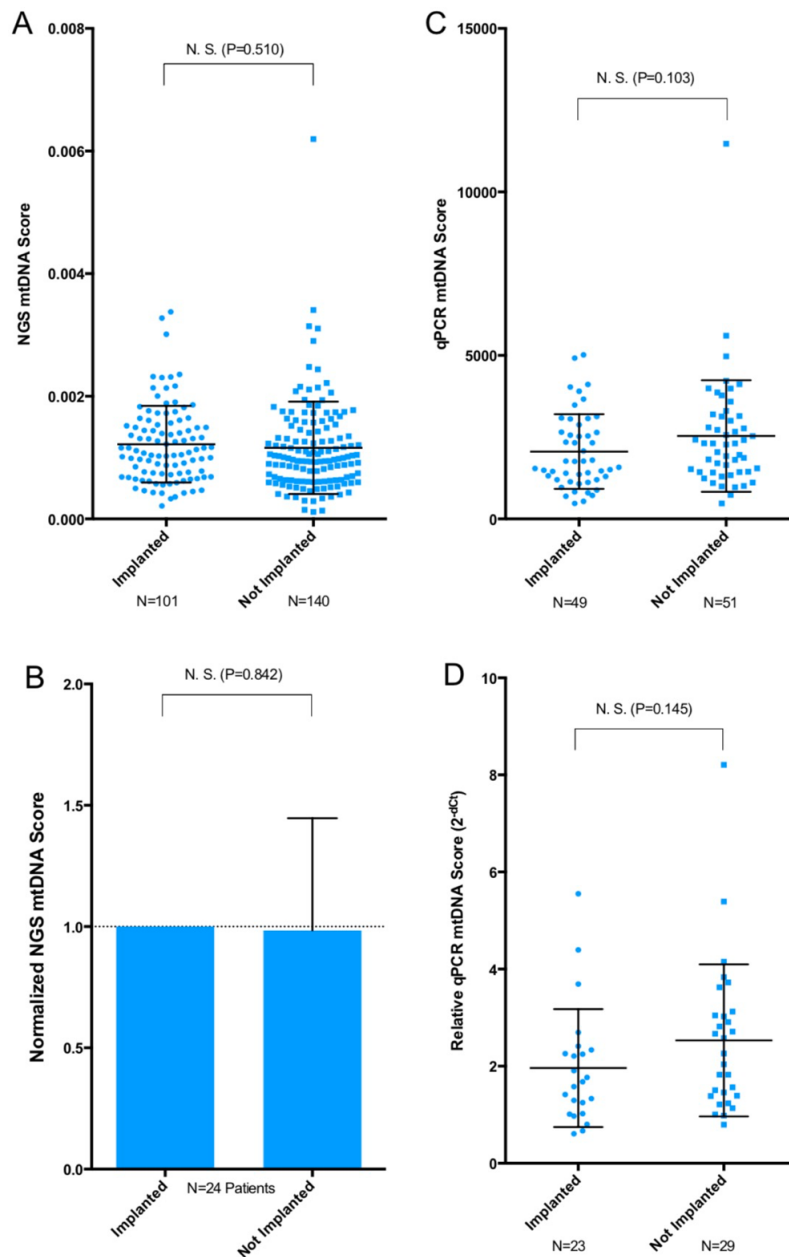
normalization step allowed us to pool data from several patients into a single graph. Results from 24 patients show a statistically insignificant difference (P=0.842) between their implanted (N=25) and non-implanted (N=34) embryos (Figure 22B). We repeated this analysis but in the second iteration we used uncorrected number of reads aligning to Chr 1 as a standardization factor. Since this particular evaluation only tests euploid embryos, the latter should be a valid alternative calculation method. Indeed, both analyses yield virtually equal results (Figure 22B and Supplementary Figure 6).

Out of all the transferred embryos tested by NGS, 49 implanted and 51 not implanted samples were re-examined by qPCR absolute quantitation assaying for CYTB, again showing no statistically significant difference (P=0.103) (Figure 22C). Finally, out of the latter set of blastocysts we re-tested 23 implanted and 29 not implanted embryos by relative quantitation (2^{-dCt}) probing the ND6 gene, once more observing no statistical difference in mtDNA score between groups (P=0.145) (Figure 22D). Two previous studies described an mtDNA value threshold that when surpassed served as a biomarker for embryos that would fail implantation (188, 189). In our data across all three detection systems we only observed a single sample in the 'not implanted' group that repeatedly showed mtDNA scores substantially above the bulk distribution (see outlier in Figure 22A, C,D), equaling 0.41% of all embryos. Hence, our data indicates that mtDNA content does not represent a statistically relevant or practical method to predict embryo viability amongst euploid blastocysts.

13.6. Chapter Discussion

Contrary to previous reports, our study finds no correlation of mtDNA content with blastocyst ploidy, age, or viability. While we detect a considerable range of mtDNA scores in the tested samples, this range is observed within all populations irrespective of criterion used to sub-group the blastocysts. The absolute quantitation method by qPCR reveals the exact mtDNA copy number in each cell of our analyzed blastocysts. This value ranges from 945 to 41,427, with a mean of 4,740, falling within the previously estimated range of mtDNA copies per human cell (252, 262-264).

We propose several explanations why our findings deviate from previous reports. Firstly, accurate determination of mtDNA levels must take the composition of the sample's nuclear genome into account. If ignored, the embryo's gender and ploidy can substantially skew the calculated mtDNA score for a given sample. For instance when comparing euploids and aneuploids by NGS, if the aneuploid group randomly contains more monosomic than trisomic cases the overall mean of the group will be artificially shifted to larger mtDNA values. Also, embryos being tested by qPCR must be corrected when the reference assay falls in a genomic region that is aneuploid, as each extra or missing copy will deflate or inflate the calculated mtDNA score by a factor of 50%. We have developed a mathematical method to accurately determine mtDNA scores of blastocysts that takes the genetic make-up of each sample into account. We propose the outlined correction factors be utilized by all laboratories investigating mtDNA levels whenever applicable. In

addition, the outlined formulas can be used for mtDNA quantitation at any stage of mammalian embryology and studies of adult patients with aneuploidies.

A further possible confounding factor between studies is that both previously published reports on embryo viability originate from reference laboratories that collected data from numerous centers, agglomerating all their numbers (188, 189). As a result, it is unclear whether their findings hold true individually within all the different clinics. Ours is the first investigation stemming from a single center, thereby correcting for several potential inter-facility variables such as culture media, temperature, biopsy technique, or equipment. Furthermore, we have amassed a number of samples unprecedented to date for this type of study in the published literature.

Lastly, It should be noted that previous reports on mtDNA levels, aside from showing interesting concordances, also show several discrepancies amongst them. For instance Fragouli et al (189) suggest a maternal age effect, while Diez-Juan et al (188) did not see a maternal age correlation. Secondary analysis of the data in Tan et al (254) also shows no age effect. Furthermore, Diez-Juan et al describes a viability effect in cleavage and blastocyst stage embryos, while Fragouli et al only detects it in blastocysts and not at the cleavage stage. These divergences remain to be explained and possibly point towards a technical or laboratory-specific effect.

The qPCR analysis in Diez-Juan's report relies on a single copy locus to normalize for nDNA, like our study. Fragouli et al utilize a multicopy Alu sequence, with the rationale that allele-drop-out (ADO) effects during WGA might be mitigated. In the context of blastocysts, where a 5-10 cell biopsy yields 10-20 initial copies of a single copy locus (in euploids), use of a multicopy sequence is unlikely to confer an advantage. The maximal estimated ~10% ADO (80) using the routinely employed Sureplex WGA system (Rubicon) would affect the initial 10-20 single locus copies or a multicopy sequence in a similar manner. Furthermore, there is well-documented variability in Alu sequence frequencies and compositions within the population (265-267), leading us to believe that a known single-copy locus such as RNAseP (260) is a superior method of standardization between embryos. Nevertheless, the potential for ADO error persists in our study as well. Another important limitation is that our NGS protocol does not permit differentiation between embryos with homogenously haploid, diploid, triploid, etc. genomes.

The Quiet Embryo Hypothesis postulates that an embryo with a calm metabolic state is more viable than another with an overactive metabolism (255). While we find no association between mtDNA content and embryonic stress, our data does not refute the proposed concept that embryos actively increase mitochondrial function and energy output as a compensatory response to overcome strained conditions. The number of mtDNA copies per mitochondrion in human cells can vary widely between 0 to 15 (268-270), meaning that the number of mtDNA copies per cell does not necessarily correlate to number of mitochondrial organelles. At least one report has demonstrated that mtDNA

copy is a poor biomarker for mitochondrial content (271). Different techniques such as immunofluorescence for direct organelle quantitation or chemical ATP detection would yield a clearer picture of mitochondrial number and function in embryos, which in turn could prove to be valid biomarkers for embryo viability.

We find an interesting historical parallel to this narrative. Within the context of the mammalian oocyte, initial studies reported that mtDNA levels might serve as a predictive biomarker for implantation (185, 272-274), but later reports rebutted these findings (252, 275, 276). Time and further studies will tell if history repeats itself, this time from the perspective of the human blastocyst.

14. Specific Aim E: To test the hypothesis that embryos with high mtDNA content can result in healthy births.

The following published work is presented for this specific aim:

Victor AR, Griffin DK, Gardner DK, Brake A, Zouves CG, Barnes FL, Viotti M. *Births from embryos with highly elevated levels of mitochondrial DNA.* Reprod Biomed Online. 2019 Sep;39(3):403-412. doi: 10.1016/j.rbmo.2019.03.214. Epub 2019 Apr 4. PMID: 31420253.

14.1. My Personal Contribution To The Work

My personal contribution to this work includes study conceptualization, as well as experimental execution (including data collection and analysis, thawing, fixing and staining of embryos for confocal imaging). I assisted with the preparation and editing of the manuscript.

14.2. Chapter Summary

Conflicting data exist on the utility of mitochondrial DNA (mtDNA) level quantitation as a predictor of blastocyst implantation in the IVF clinic. Here, we determined whether blastocysts with highly elevated mtDNA levels can result in healthy pregnancies and births, and whether mitochondrial functional output might be a readout of cell stress in the embryo.

We determined mtDNA levels in 109 blastocysts used in clinical transfers into 100 patients, noting their clinical outcomes. In a separate set of embryos, we quantified mitochondrial function in a model of embryo stress, aneuploidy. Measurement of mtDNA levels made use of surplus material from the preimplantation genetic testing for aneuploidy process, and followed recently proposed unifying guidelines for mtDNA quantitation.

In this study, we report that unusually high mtDNA levels did not preclude blastocyst implantation and healthy births. Analysis of 109 blastocysts showed no significant difference between mtDNA levels in implanted (n=55) versus non-implanted (n=54) blastocysts. We could not detect obvious differences in degree of mitochondrial functional output in a model of embryo stress.

Measurement of mtDNA copy number might therefore not provide any advantage to embryo prioritization and could lead to de-selection of blastocysts that would result in healthy pregnancies and births. Furthermore, the quantitation of mitochondrial functional output in a model of cellular stress might suggest that mitochondria are not clear targets for biomarker identification as it relates to blastocyst viability. Any suggested link between mtDNA levels, mitochondria, or their output with blastocyst transfer outcome requires further validation.

14.3. Chapter Introduction

In vitro fertilization (IVF) has made it possible for many patients experiencing infertility to achieve pregnancy, but in spite of tremendous advances since its inception 40 years ago, the process remains relatively inefficient (277). On average, only 37.1% of embryo transfers result in implantation at IVF programs based in the USA according to the Society for Assisted Reproductive Technology (278). Efforts to increase the likelihood of implantation and establishment of a healthy pregnancy include the identification of a biomarker predictive of viability. An ideal biomarker is a parameter that shows variability in the general embryo population that, when measured, provides a significant degree of predictive power of an embryo's chances to implant. Embryo metabolism has long been linked to viability and embryo health (279, 280). Using metabolism to rank embryos within a patient's cohort could effectively increase the chances of success with fewest possible attempts (281).

Mitochondria not only contribute significantly to the energy production for many cellular processes in the form of adenosine triphosphate (ATP), they also regulate apoptosis, calcium signalling, management of reactive oxygen species, pyruvate and citric acid cycle, heme and steroid synthesis, and hormonal signalling (282). Each human cell may contain a wide range in the number of mitochondrial organelles and each mitochondrion can contain numerous copies of mitochondrial DNA (mtDNA) (283). MtDNA is a circular molecule comprising 16.6 kb encoding 37 genes necessary for mitochondrial function. Due to its multicopy nature, mtDNA has typically been quantified on a per cell basis. That

value is an assessment of 'mtDNA levels' that can be compared between any discreet populations of cells, such as individual human embryos or cellular biopsies thereof. It is nevertheless important to note that the value of mtDNA levels does not necessarily reflect the actual number of mitochondria.

Four recent studies stemming from two separate groups reported that trophectoderm (TE) biopsies from blastocysts that successfully implanted showed lower mtDNA levels on average, compared with blastocysts that did not implant after transfer (188-191). Interestingly, those studies also described a threshold of mtDNA levels that, when surpassed, always resulted in implantation failure. The authors proposed that elevated mtDNA levels could be a feature of blastocysts experiencing energetic stress. It was hypothesized that stressed embryonic cells would promote mtDNA replication in a concerted effort to increase rates of cellular respiration and ATP production to meet increased energetic demands. Fragouli and colleagues suggested coupling this model to the the Quiet Embryo Hypothesis, which predicts that under ideal conditions an embryo experiences a calm metabolism (255). However, all data for the Quiet Embryo Hypothesis were collected under conditions of oxidative stress (20% oxygen), and consequently this hypothesis has been shown to be invalid for embryos cultured in physiological oxygen concentrations (5%) (280).

The interest generated by such reports encouraged numerous groups to explore the matter of mtDNA levels in their respective clinics. An independent study found no

statistically significant correlation between mtDNA levels and implantation potential in blastocysts (206). Those findings were also confirmed in a subsequent report analysing double embryo transfers (194), which revealed that blastocysts with lower mtDNA levels were just as likely to implant than their paired counterparts with higher mtDNA levels. Subsequently, a further two published studies failed to observe any statistically significant predictive power of mtDNA levels in regard to implantation in human blastocysts (192, 193), while a third published study did report a correlation (284).

Several opinions have been expressed attempting to explain the disparate results (195, 285-287). Recently, a Views and Reviews piece focused on the possibility that technical variability in methods of mtDNA quantitation might be the reason for discrepancies, proposing guidelines to promote uniformity and reducing chance of error (196). Those were: I) avoiding the use of Next Generation Sequencing platforms with low coverage of the mtDNA genome, II) using polymerase chain reaction (qPCR) targeting a mitochondrial region and a multicopy nuclear region for correct normalization to prevent allele-drop-out issues during analysis, and III) excluding samples of DNA material that may have degraded due to long-term frozen storage (196).

Consequently, we adhered to the proposed guidelines of mtDNA quantitation when analysing mtDNA levels in a set of blastocysts used for transfer. In doing so, it was possible to test whether technical variations in mtDNA quantitation were responsible for conflicting reports regarding the usefulness of mtDNA levels as a biomarker for

implantation. The clinical outcomes of all tested blastocysts through implantation, pregnancy, and birth were followed, and further it was established whether mitochondrial function in blastocysts correlated with cellular stress.

14.4. Methods And Materials

14.4.1. Patients And Embryos

Embryos derived from patients seeking infertility treatment at a private IVF center were generated by intracytoplasmic sperm injection (ICSI) and cultured to the blastocyst stage under 5% oxygen, using standard techniques, as previously described (206). Blastocysts were evaluated with the Gardner system (207) and subjected to a 5-10 cell TE biopsy and vitrified (Cryotech Vitrification Solution Set) until further use. Preimplantation genetic testing for aneuploidy (PGT-A) was performed in-house utilizing the VeriSeq kit (Illumina) following the manufacturer's protocol. Samples were sequenced on a MiSeq system (Illumina). Blastocysts classified as euploid were selected for transfer, and the presence of a gestational sac observed by endovaginal ultrasound at 3-5 weeks after transfer was considered evidence of implantation. The imaging experiments were performed on supernumerary embryos donated to research by informed consent.

This study was approved by the Zouves Foundation IRB on 22nd May 2018 (OHRP IRB00011505, Protocol #0003).

14.4.2. mtDNA Quantitation

During the PGT-A process, isolated DNA from individual TE biopsies was multiplied by whole genome amplification (WGA) and subsequently sequenced. Surplus WGA material from each sample was used to determine mtDNA levels by qPCR on a QuantStudio 3 instrument (Thermo Fisher). A 1:10 dilution of WGA product in water was vortexed for 30-60 seconds followed by heating to 95°C for 10 minutes in order to inactivate any residual WGA polymerase activity. Two microliters were used in a Taqman Fast Advanced Master Mix reaction (Thermo Fisher), with each reaction run in technical triplicates. Each reaction plate contained an equilibrator sample, used for global normalization across the entire experiment.

A mitochondrial locus was quantified with a commercially available Taqman assay for the mitochondrial *ND6* gene (Hs02596879_g1), which had been previously thoroughly validated in the context of blastocyst TE biopsies (194, 206). A multicopy nuclear DNA sequence was quantified using a previously described, custom-made Taqman assay targeting the Ya5 subfamily of *Alu* repeats (288, 289), which is present in at least 2473 copies in the human genome. Details for the *Alu-Ya5* assay were: forward primer gaccatcccggctaaaacg, reverse primer cgggttcacgccattctc, and probe ccccgtctctactaaa. *ND6* and *Alu-Ya5* assays yielded a cycle threshold (*Ct*) value, which was used to determine the normalized mtDNA level for any sample as follows:

$2^{-(Ct_{ND6}-Ct_{Alu})}$. Hence, the final value for mtDNA level is a 'per cell' measure.

14.4.3. Fluorescent Staining Of Whole Blastocysts

Supernumerary warmed blastocysts were allowed to equilibrate in an incubator for 24 h, after which media was replaced with fresh media containing 250 nM of MitoTracker Deep Red FM (Thermo Fisher #M22426). After 30 min in the incubator, blastocysts were processed for immunofluorescence following a previously described protocol (290), using the primary antibodies (abs) mouse anti-human GATA3 monoclonal ab (Thermo Fisher #MA1-028) and rabbit anti-human OCT4A monoclonal ab (Cell Signaling #2890) followed by the secondary abs goat anti-rabbit IgG AlexaFluor488 (Thermo Fisher A11008) and goat anti-mouse IgG AlexaFluor546 (Thermo Fisher A11030). Subsequently, blastocysts were exposed to nuclear stain (Hoechst 33342, Thermo Fisher H3570) and imaged.

14.4.4. Imaging And Computational Quantitation Of Mitochondrial Function

Stained blastocysts were placed in glass bottom dishes (MatTek P35G-1.5-20-C) in small drops of stain buffer overlaid with mineral oil (Sigma M5904), and imaged with an LSM 780 Confocal microscope (Zeiss). Image files in the .lsm format were uploaded into the software package Imaris 8.4.1 (Bitplane). Fluorescent channels were individually quantified in a blinded fashion computationally for each blastocyst using uniform parameters for all samples, employing background subtraction for normalization.

14.4.5. Statistics

Analysis and graph preparation were performed in Prism 6 (GraphPad). Differences between means of two groups were assessed by unpaired, two-tailed Student's t test with Welch's correction. Differences between means of three or more groups were assessed by one-way ANOVA.

14.5. Results

14.5.1. Quantifying mtDNA In Blastocysts

To conform to the recently suggested guidelines for mtDNA quantitation in TE biopsies of human embryos (196), we used qPCR on TE-derived surplus WGA material stored at -80C for less than 2 months without any vitrification-warming cycles. The qPCR targeted a region in the mtDNA sequence (*ND6*) and a multicopy region in the nuclear DNA (*Alu-Ya5*), using the latter as a reference to normalize for technical variability in the WGA run and number of cells in collected biopsy. To validate the assays, we performed 10-fold dilution series of a WGA sample from a TE biopsy of a euploid embryo to determine the following qPCR reaction efficiencies: 97.7% for *ND6* and 97.1% for *Alu-Ya5* (Figure 23).

Figure 23. Technical Validation Of qPCR Assays Used In This Study To Quantify mtDNA Levels Per Cell.
Graphs depict regression curves of serial dilution experiments.
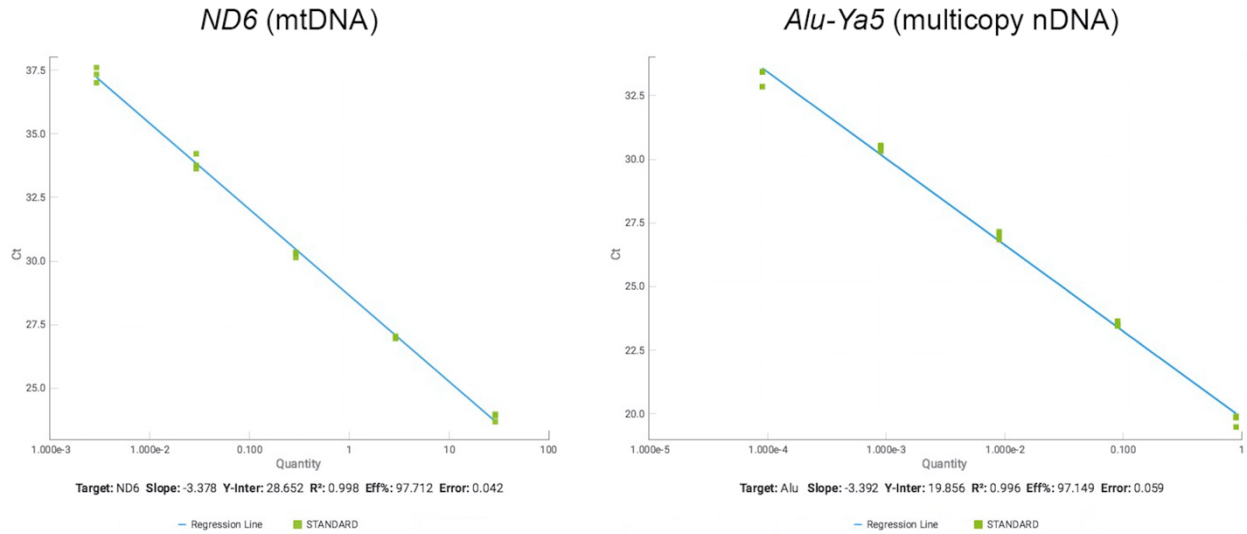
14.5.2. mtDNA Levels Have No Predictive Power Relating To Implantation

Average levels of mtDNA were not statistically different between the set of euploid blastocysts that achieved implantation and those that did not (Figure 24A). The majority of blastocysts had mtDNA levels within a range of substantial overlap between implanted and not implanted groups. Both groups also contained outliers that could be regarded as having elevated mtDNA levels. In the implanted group, there were three blastocysts with mtDNA levels just above one standard deviation of the mean, and two blastocysts with considerably higher mtDNA levels (together, those five blastocysts are labelled #1-5 in Figure 24A and Table 6).

Figure 24. mtDNA Levels Are Not Predictive Of Implantation In The Analyzed Cohort.

(A) Comparison of mtDNA levels between blastocysts that implanted and those that did not. Each data point represents the mtDNA levels of one blastocyst. Outliers above one SD of the mean are numbered in the implanted group. Each of the five outliers belongs to a different patient. Mean ± SD are indicated by the lines. There was no significant (N.S.) difference between groups Differences between groups were assessed by unpaired, two-tailed Student's t test with Welch's correction with significance determined as P < 0.05. (B) Plotted mtDNA levels of all euploid blastocysts from patient who generated blastocyst #1 in (A). (C) Images of blastocyst #1 in (A), immediately before collection of a TE biopsy and vitrification (left image, displaying target locator of laser used for biopsy), and before transfer (right image). Scale bars = 10 µm.
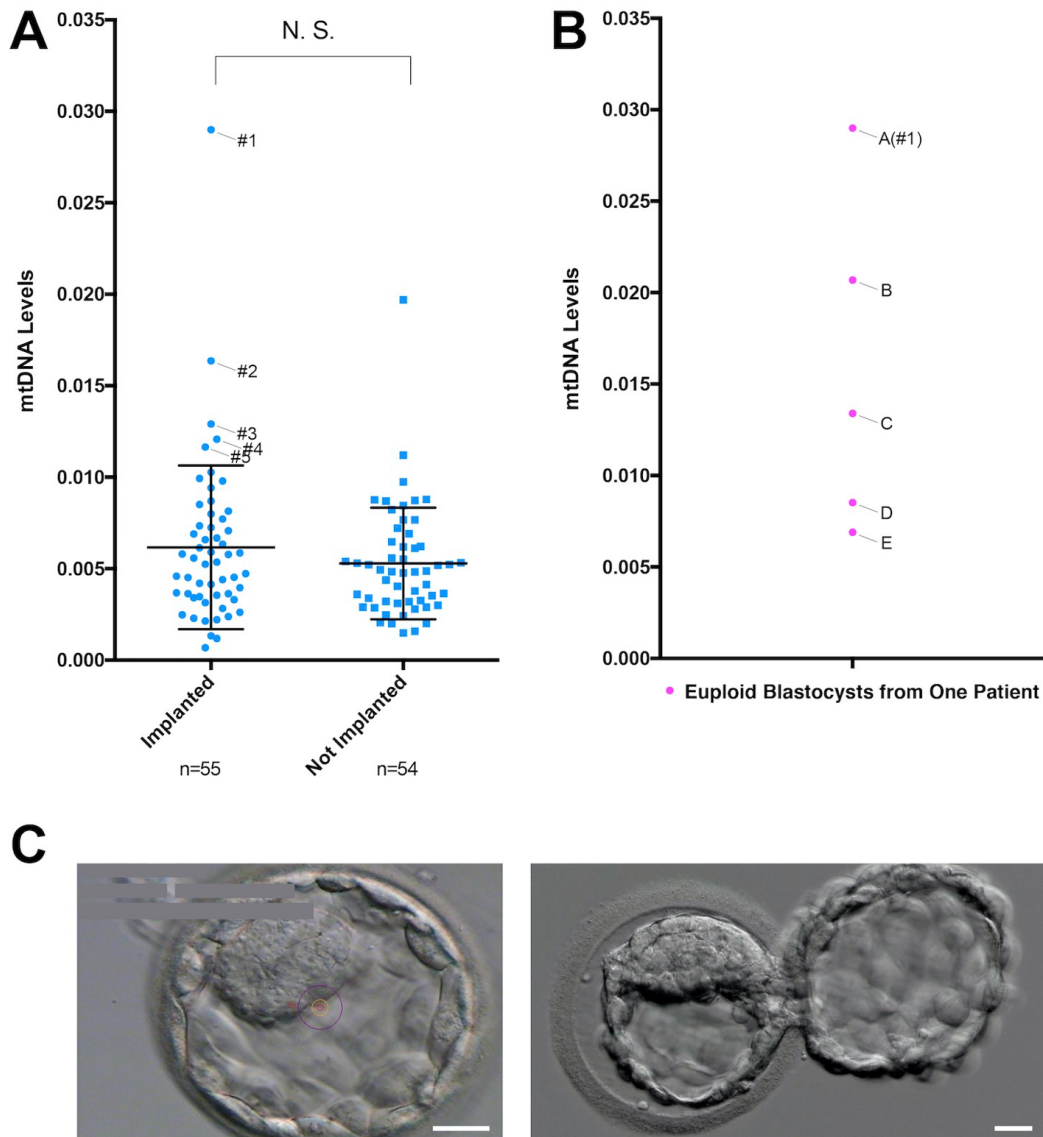
Table 6. Characteristics And Outcomes Of The Implanted Euploid Blastocysts With Highest mtDNA Levels.

Embryo Number	Grade on TE biopsy day[a]	Biopsy Day	PGT-A Result	mtDNA Level	mtDNA Level Compared with Group Mean	Implantation	Birth
#1	4AA	D5	Normal	0.02899	4.70x	Yes	Yes
#2	5BB	D6	Normal	0.01635	2.65x	Yes	Yes
#3	5BB	D6	Normal	0.01291	2.09x	Yes	Yes
#4	3AB	D5	Normal	0.01208	1.96x	Yes	Yes
#5	5BC	D6	Normal	0.01164	1.89x	Yes	Yes

[a] According to Gardner System (207). PGT-A = preimplantation genetic testing for aneuploidy; TE = trophectoderm.

14.5.3. Blastocysts With Elevated mtDNA Levels Can Result in Healthy Pregnancies and Births

The transfers of blastocysts #1-5 resulted in normal pregnancies and live births. Blastocyst #1 was particularly noteworthy for its disproportionately high mtDNA levels (~4x the group average). It was also the blastocyst with highest mtDNA levels within its respective patient cohort (Figure 24B), which means that it would not have been chosen for transfer had mtDNA levels been used for de-selection of embryos for transfer. It had good overall morphology at the time of TE biopsy (4AA) and after a vitrification-warming cycle, immediately before transfer (5AA) (Figure 24C).

All five babies resulting from this group of blastocysts with elevated mtDNA levels passed a routine neonate physical examination and were normal for a series of screened conditions by blood test, including various metabolic disorders (for a list of the 63 tested conditions see Supplementary Table 3).

14.5.4. Cellular Stress Associated With Aneuploidy Does Not Necessarily Lead To Increased Mitochondrial Activity In Blastocysts

Blastocysts were exposed to MitoTracker Deep Red (MTDR) (Figure 25A,B). This fluorescent dye is associated with active mitochondria and its accumulation is dependent upon inner mitochondrial membrane potential, which increases with cellular respiration. Quantitation of MTDR fluorescent signal is therefore an indirect indicator of mitochondrial activity (291-293). In addition, on the same blastocysts we performed immunofluorescence with antibodies targeting a TE marker (GATA3) and an ICM marker (OCT4) to be able to differentiate mitochondrial function in the two cell lineages (Figure 25B).

To model the impact of cell stress, we quantified mitochondrial function in blastocysts that had different classifications after PGT-A testing, and hence various ploidy statuses. On average, mitochondrial activity per cell in the TE was considerably higher than in the ICM. Nonetheless, we noted no statistically significant difference regarding mitochondrial activity per cell when comparing tissues in different blastocyst groups (Figure 25C).

Figure 25. Quantitation Of Mitochondrial Activity In Blastocysts.
(A) High resolution image of TE cells after exposure to Hoechst nuclear stain and MTDR, displaying fluorescent MTDR signal in characteristic punctate distribution around nuclei. Scale bar = 10µm. (B) Left column shows representative immunofluorescent images of a whole hatching blastocyst. Right column shows method of computational detection and quantitation. Note that the image analysis software detects the concrete number (count) of nuclei, ICM cells, and TE cells. The software generates a 'mask' of the MTDR signal, and quantifies the fluorescence within. The yellow number at the bottom right corner of panels indicates the computed value for the corresponding image. Scale bars = 30µm. (C) Scatter dot plots depicting quantitation of MTDR fluorescence (readout of mitochondrial function) in blastocysts. Each symbol represents one blastocyst. Lines indicate mean with standard deviation. Sample size of each blastocyst group is n=4 Euploids, n=4 Mosaics, n=8 Single Aneuploids (aneuploidy affecting a single chromosome), n=7 Multiple Aneuploids (with aneuploidy affecting multiple chromosomes). There were no significant (N.S.) differences in the TE or ICM group. Differences were assessed by one-way ANOVA with significance determined as $P < 0.05$.
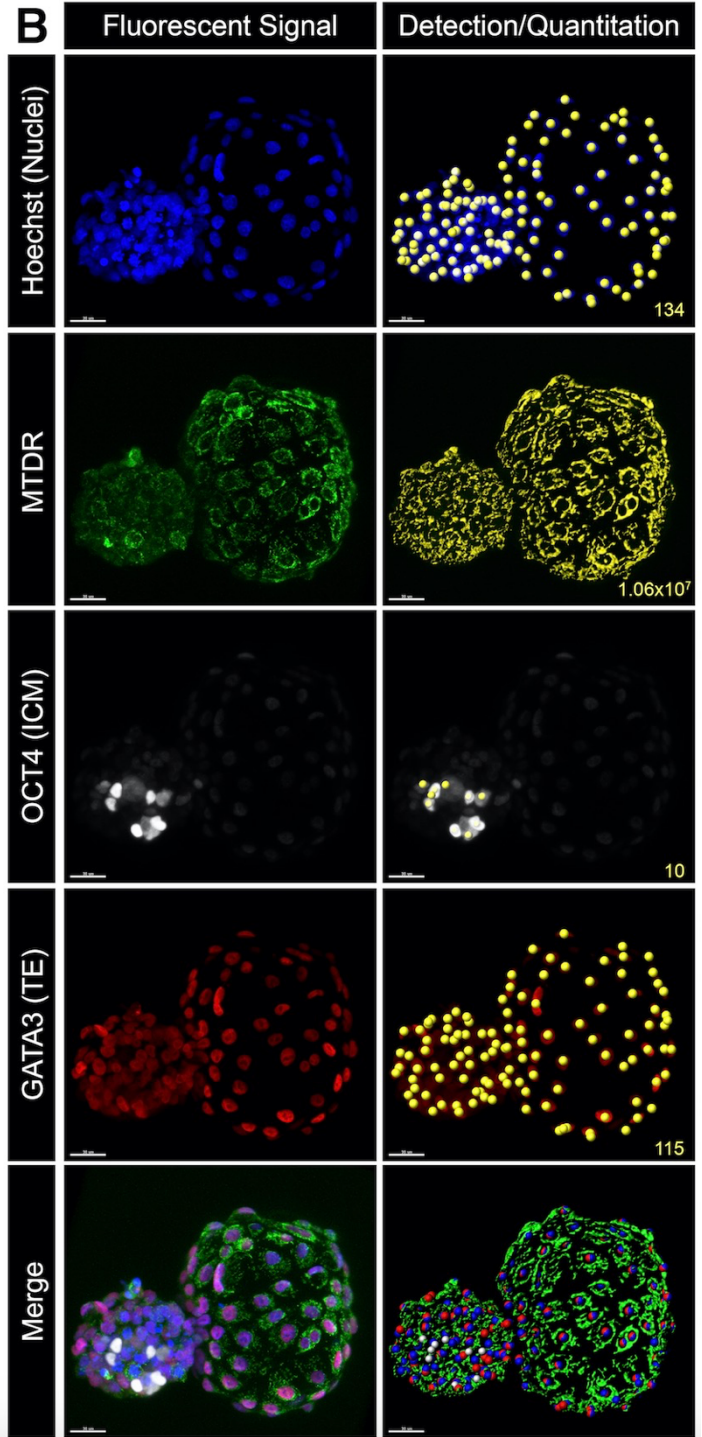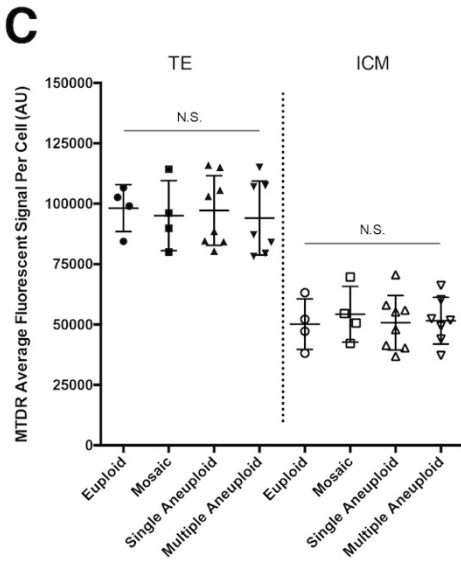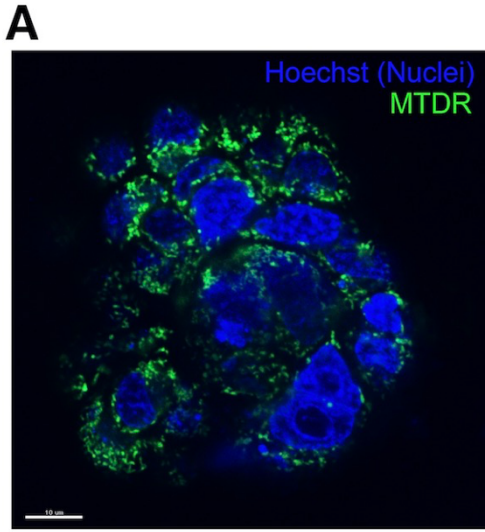
14.6. Chapter Discussion

Biomarkers predictive of implantation are urgently needed to reduce time to pregnancy and to help establish healthy pregnancies in IVF (294, 295). Here we tested whether mtDNA levels possessed prognostic qualities regarding blastocyst transfer outcome in our clinic, abiding to suggested guidelines of mtDNA quantitation (196). We found no association between mtDNA levels and blastocyst viability, and we report for the first time that blastocysts with extremely high mtDNA copy number are consistent with viable implantation, normal pregnancy, and birth. Using a unified system of mtDNA quantitation, we exclude the possibility that technical differences were responsible for reported discrepancies between our findings and those previously describing a prognostic value of mtDNA levels in blastocysts (188-191, 206).

One scenario that reconciles the conflicting reports is a laboratory-selective association between mtDNA levels and implantation. In fact, it has been reported that the incidence of blastocysts with elevated mtDNA levels varies widely amongst IVF centers (191). Out of 35 clinics participating in that study, roughly half did not produce an appreciable percentage of blastocysts with high mtDNA levels, although it must be noted that for some centers the analyzed sample size was small. In the remaining centers, incidences of blastocysts with elevated mtDNA levels ranged from 1% to 27%. Of blastocysts analyzed in this study, three out of 109 (2.8%) could be considered as containing highly elevated mtDNA levels (two implanted, one did not), and yet mtDNA quantitation was not valuable in predicting implantation in our setting.

One can only speculate why those three embryos contained highly elevated mtDNA levels. Under normal circumstances, no new mtDNA replication occurs between zygote and blastocyst stage, such that the initial set of mtDNA molecules becomes split between dividing cells and progressively diluted amongst cells of the developing embryo (296, 297). Therefore, if a cell fails to undergo one or more cell divisions, it will tend to retain its mtDNA content. It is possible that for the three blastocysts yielding highly elevated mtDNA levels the collected biopsy happened to contain a region of the TE that had undergone fewer cell divisions, resulting in concentrated mtDNA content compared with other TE regions. The blastocyst with the highest mtDNA levels, which contained fourfold the content compared with the group average, could be explained if the sampled TE cells had skipped two cell divisions compared with other TE regions of that blastocyst. What might have caused attenuated cell division in that part of the TE is another question, although to the best of our knowledge there is no clear evidence suggesting that all TE regions proliferate at equal rates under normal conditions. For example, TE cells adjacent to the section of the zona pellucida making contact with the dish during culture might experience distinct cell proliferation dynamics.

Alternatively, it has been shown in several mammalian species that once the blastocyst stage is reached, replication of mtDNA begins specifically in the TE while the ICM continues to reduce its mtDNA copy number (182, 297). Whether mtDNA replication occurs uniformly across TE cells or in a localized fashion is not well studied, and might be affected by the cell cycle stage of each individual TE cell. A spurt of mtDNA replication

in a sampled region would result in high mtDNA levels being quantified for the entire corresponding embryo.

MtDNA levels have been proposed to be a surrogate measure of mitochondrial function, which was presumed to increase in blastocysts experiencing stress as part of a compensatory mechanism (188, 189). MtDNA levels might therefore be a corollary of a larger program that increases mitochondrial organelle number, as well as mitochondrial functional output. Accordingly, mitochondrial activity should be a more direct readout of embryo stress, and could be a potentially better biomarker of viability. Nonetheless, a direct relationship between mtDNA levels and mitochondrial function in blastocysts has not been documented (298).

To shed light on this matter, mitochondrial function in euploid, mosaic, or aneuploid blastocysts were analysed. Aneuploidy is associated with global increases in cellular trauma including metabolic, proteotoxic, replicative, and mitotic cell stress (299-301). Accordingly, euploid blastocysts were expected to exhibit the least cellular stress, followed by mosaic blastocysts, then by blastocysts with aneuploidy affecting a single chromosome, and lastly by blastocysts with aneuploidy affecting multiple chromosomes, which would have the most cellular aberrations. In line with published data (182), we observed elevated mitochondrial activity per cell in the TE compared to the ICM in all blastocysts. Importantly, the ploidy status of a blastocyst did not influence its mitochondrial function in TE or ICM cells.

It is possible that aneuploidy is not representative of the type of stress that might elicit mitochondrial activation in blastocysts, such as for example changes in oxygen concentration (302). The state of aneuploidy (the model tested here) can elicit increases in various types of cell stress (299), but conceivably only a specific sub-type of energetic stress prompts mitochondrial activation, and consequently shifts in mtDNA levels. What is more, the trigger might depend on a specific threshold of that stress factor. Future studies need to test whether lab-induced variance of parameters including oxygen concentration, medium composition, pH, and/or temperature affect mitochondrial function and/or content in human embryos. This in turn could help to explain the observation that different centers generate vastly different incidences of blastocysts with highly elevated mtDNA levels (191), a phenomenon for which the underlying biological basis remains unknown. We surmise that for the time being, the suggested rationale linking increased mtDNA levels to stress remains purely speculative.

15. Specific Aim F: To test the hypothesis that PGT-M largely obviates the clinical need for germline genome editing (GGE), but that GGE might be a useful tool to correct aneuploidies detected with PGT-A in certain instances.

The following published work is presented for this specific aim:

Viotti M, **Victor AR**, Griffin DK, Groob JS, Brake AJ, Zouves CG, Barnes FL. *Estimating Demand for Germline Genome Editing: An In Vitro Fertilization Clinic Perspective.* CRISPR J. 2019 Oct;2(5):304-315. doi: 10.1089/crispr.2019.0044. PMID: 31599685.

15.1. My Personal Contribution to the Work

My personal contribution to this work includes developing suitable mathematical models to make appropriate predictions for potential demand of genome editing on human embryos and assisting with manuscript preparation.

15.2. Chapter Summary

Germline genome editing (GGE) holds the potential to mitigate or even eliminate human heritable genetic disease, but also carries genuine risks if not appropriately regulated and performed. It also raises fears in some quarters of apocalyptic scenarios of designer babies that could radically change human reproduction. Clinical need and the availability

of alternatives are key considerations in the ensuing ethical debate. Writing from the perspective of a fertility clinic, we offer a realistic projection of the demand for GGE. We lay out a framework proposing that GGE, hereditary genetic disorders, and in vitro fertilization are fundamentally entwined concepts. We note that the need for GGE to cure heritable genetic disease is typically grossly over- estimated, mainly due to the underappreciated role of preimplantation genetic testing. However, we might still find applications for GGE in the correction of chromosomal abnormalities in early embryos, but techniques for that purpose do not yet exist.

15.3. Introduction

The advent of genome editing using CRISPR-based technologies is generating tremendous enthusiasm within both the medical and public domains regarding the potential to cure the approximately 6,000 known human genetic disorders that afflict up to ~12% of the world's population (303, 304).

An important distinction should be drawn between germline genome editing (GGE) and somatic gene therapy. GGE could be used to modify all cells in the future organism and its offspring by targeting sperm, egg, or in most cases the fertilized zygote. The most likely scenario for the application of GGE is in preventing the transmission of inheritable genetic mutation(s), which would depend on prior knowledge of a genetic disorder. In the absence of a known disorder, a zygote is presumed healthy. However, mutations that arise *de novo* during embryogenesis are typically not detected until prenatal testing, during birth

or later in life, and consideration of somatic gene therapy becomes relevant in order to cure the individual.

In this article, writing from the perspective of the fertility clinic, we analyze the potential demand for GGE based on medical need, and explore the use of genetic testing in embryos as an alternative.

In practice, GGE necessitates *in vitro* fertilization (IVF) laboratory techniques to provide access to the sperm, egg, and early embryos. Successful fertilization of an egg results from either insemination with several tens of thousands prepared spermatozoa, or after intracytoplasmic sperm injection (ICSI) when a single sperm is injected directly into the oocyte with glass micropipettes. Both techniques result in an embryo that is typically cultured for 5-6 days in an incubator. The embryo is then either immediately placed into the patient by intrauterine transfer or, more commonly, frozen until future use when the recipient has had additional time to recover from the egg retrieval procedure. The embryo can subsequently be thawed and transferred, hopefully resulting in successful implantation.

The best-practice process of an IVF cycle under current international standards (305) inherently provides direct access to germ cells and embryo to deliver the CRISPR-Cas genome editing machinery (Figure 26A). In particular, the ICSI procedure provides a great avenue to co-deliver sperm and genome editing molecules into the egg, to edit the genome of the resulting zygote (306).

Figure 26. Overview Of The IVF Process.
(A) Typical workflow of an IVF cycle. (B-E) Biopsy collection for subsequent preimplantation genetic testing. (B) Human blastocyst stage embryo with inner cell mass (ICM) at the 9 o'clock position next to a holding pipette. (C) Pulses from a laser (concentric red/yellow circles show the cross hairs) create an opening in the zona pellucida at the 3 o'clock position, and a biopsy needle is inserted and guided to the trophectoderm tissue. (D) A clump of cells is extracted through the zona pellucida opening by suction applied by the biopsy pipette, and laser pulses are directed at exposed cell-cell junctions. (E) The separated 5-10 cell biopsy is collected for posterior genetic analysis. The blastocyst is vitrified until further use. ICM = Inner Cell Mass. TE = Trophectoderm. ZP = Zona Pellucida. Scale bars = 50 μm.
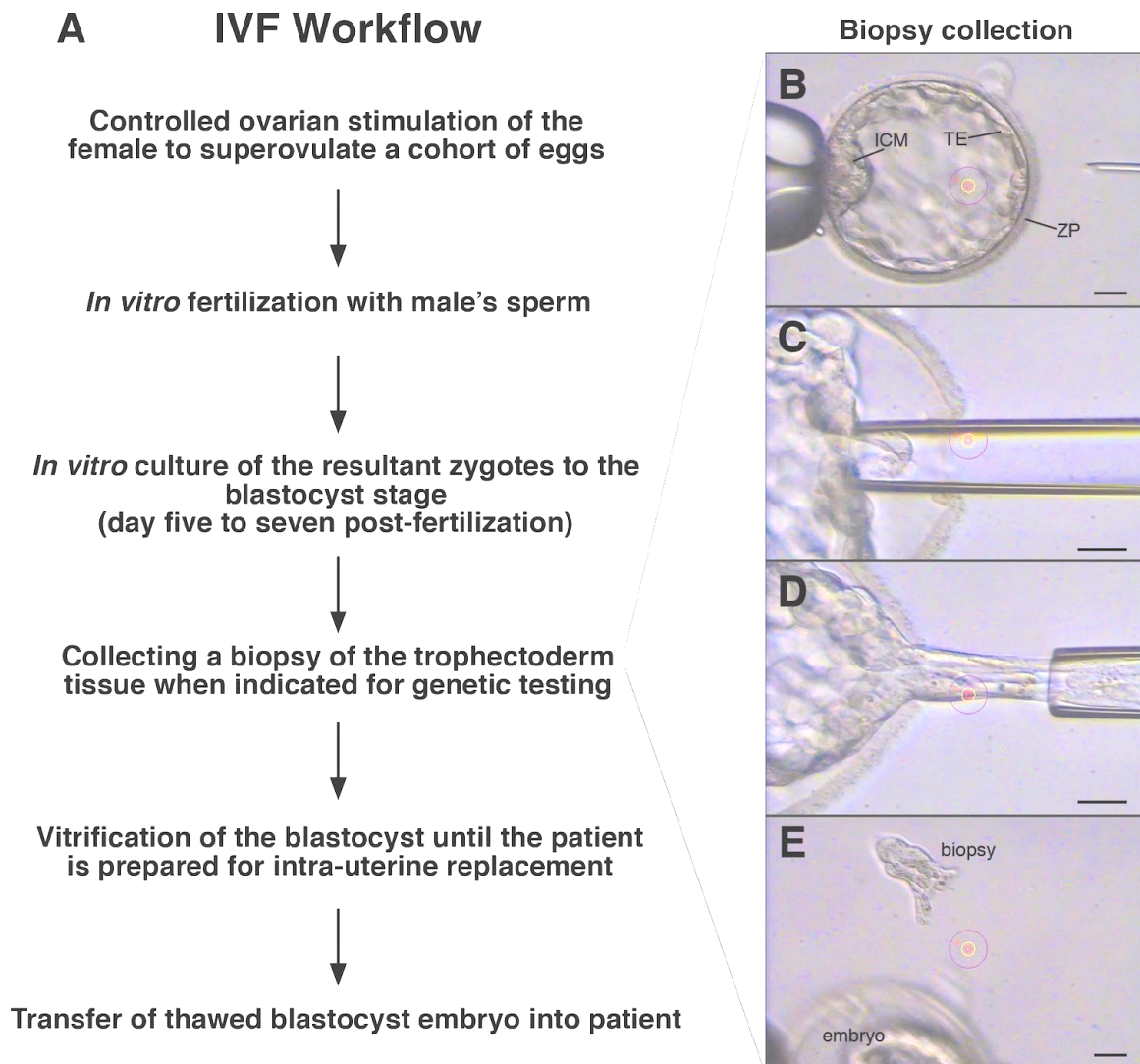
Can GGE be performed without IVF? Some hypothetical strategies for GGE have been suggested that do not involve classical IVF. For example, sperm or eggs are edited in a dish and replaced into the female reproductive system to attempt a posterior 'natural' fertilization. Alternatively, gonads are targeted directly, in hopes of modifying germ cells in their native location. In another version, germline stem cells are isolated from gonads, modified in a dish, and grafted back into ovary or testes. It is even conceivable to attempt targeting a naturally fertilized zygote by using uterine lavage to isolate it, editing the zygote *in vitro* and transferring it back into the female. Either of those methods would most likely still be performed in the setting of a fertility clinic. Ultimately, the likeliest opportunity for application of GGE techniques will occur during conventional IVF. Not surprisingly, all published studies on human GGE so far have been carried out in IVF-generated zygotes (306-312).

The field of IVF has made tremendous advances since its inception 40 years ago, perhaps none bigger than the introduction of preimplantation genetic testing (PGT, previously known as PGD/PGS). Its goal is to identify the genetically healthy embryo in a patient's cohort with highest chances of implantation.

The role of PGT in avoiding transmission of familial genetic disorders has been greatly undervalued in scientific and public discourse surrounding GGE. Conceptually it involves isolating a cell or group of cells (the biopsy) from the developing embryo to analyze its genetic content, using it as a proxy for the entire embryo (305). Common PGT techniques

currently require the isolation of a 5-10 cell biopsy at the blastocyst stage from the trophectoderm, the precursor tissue of the placenta (Figure 26B-E). The isolated cells' DNA content is subsequently amplified and analyzed. This has proven safer to the embryo (i.e. less impact on posterior viability) than earlier PGT methods collecting a single cell at the cleavage stage, and in addition provides more genetic material for analysis, which decreases the likelihood of erroneous or no results (313).

Patients with a familial disorder can apply PGT for monogenic (-M) traits to identify embryos that have inherited the causative allele amongst their cohort of IVF-generated embryos and eliminate them from consideration for intrauterine transfer and possible implantation (Figure 27A). The technique utilizes linkage analysis and/or direct sequencing of the causative mutation (123, 314). and is in principle adaptable to any monogenic disorder, gene variants with increased disease risk, late-onset disorders, and mitochondrial DNA mutations (313).

In the past two decades, PGT-M has been performed in at least 100,000 IVF cycles worldwide (313), for more than 400 different single-gene disorders (123). Most recently, PGT has been designed to identify complex (polygenic) conditions, such as congenital diabetes or cardiomyopathies, in a test involving the calculation of polygenic risk scores called PGT-P (315). This test aims to provide relative risk reduction through genetic testing and identification of significant outliers. It calculates risk scores for complex conditions in embryos, not unlike services offered by direct-to-consumer genetic profiling

companies (given the novelty of this approach, medical societies have not yet formulated ethical statements specifically addressing polygenic testing and risk score assessment in embryos). Other versions of PGT can be used to detect chromosomal abnormalities, from aneuploidy with PGT-A, to structural rearrangements with PGT-SR.

Together, these various PGT formats are being employed in 38% of the 245,000 IVF cycles taking place each year in the U.S.(316), of which 10% are PGT-M probing for monogenic disorders (317).

While the clinical goals of PGT and GGE to prevent the inheritance of genetic disease are similar, the ethics relevant to the two technologies is irrefutably different. In a recent position statement, the Ethics Committee of the American Society for Reproductive Medicine (ASRM) suggests the use of PGT is ethically justified for severe congenital as well as adult-onset conditions, and furthermore endorses the use of PGT for conditions of lesser severity or penetrance if no safe, effective interventions are available (318).

An important distinction between GGE and PGT is that the process of PGT does not create a new genetic trait. The constellation of genes present in the embryo selected for transfer after PGT screening could also have occurred if the couple had conceived naturally. Unlike the practice of GGE, PGT obviously carries no risk of undesirable off- and on-target effects and no chance of introducing genetic mosaicism. However, one possible ethical argument in favor of GGE versus PGT is that, within the IVF industry, it

remains standard practice to dispose of PGT embryos identified with a mutant allele or chromosomal defects. One could argue that GGE could repair and salvage these otherwise discarded embryos. However, utilizing GGE would not circumvent disposition of embryos, as it would remain unlikely that every embryo within an IVF cycle will always be transferred; often IVF patients give rise to supernumerary embryos that are routinely cryopreserved or discarded as part of IVF cycle management.

From a regulatory perspective, PGT in the U.S. has remained largely free from intervention by the U.S. Food and Drug Administration (FDA). Not so GGE, which clearly falls under FDA's domain as it claims "regulatory authority over genetically manipulated cells and/or their derivatives". While somatic gene therapies have already been approved by the FDA with several trials under way, an FDA-approved GGE therapy is currently impossible (319). A renewable provision of the *Consolidated Appropriation Act*, initially signed into law in 2016, explicitly prohibits the FDA from reviewing applications for "an exemption for investigational use of a drug or biological product…in which a human embryo is intentionally created or modified to include a heritable genetic modification" (320). This moratorium in effect has been renewed every year since and its short- and long-term future are unclear. Editing the genome of a human embryo without uterine transfer for research purposes is still legal in the U.S., although ineligible for public funding (320).

Numerous position statements have been issued concerning GGE (321), and different ethical ramifications are currently being explored, but here we specifically consider the unmet medical need that GGE would address. When is GGE a valid medical alternative to PGT? Which is the more appropriate treatment? Does the magnitude of the medical demand for GGE justify its practice? Given the numerous technical, regulatory and ethical concerns about the possibility of applying GGE in assisted reproduction, we should proceed very carefully. GGE would be warranted only if there is real and significant demand for the technology that could not be satisfied by other means (322).

15.4. Methods And Materials

15.4.1. Disease Prevalence Data

All disease prevalence values used for calculations pertaining to the demand of GGE were obtained from the published literature (see indicated references).

15.5. Results

15.5.1. Estimation of GGE Demand For Hereditary Disorders

Let us consider a hypothetical scenario: If a family suffers from an inherited disease, should their IVF plan be limited to PGT screening for non-affected embryos, or are there circumstances when we should consider correcting their embryos with GGE?

In recessive monogenic disorders, each embryo conceived from two heterozygous parents will have a 1-in-4 chance of inheriting two copies of the unaffected allele and a 1-

in-4 chance of being homozygous for the mutant allele. In a typical case, the unaffected embryos can be chosen for uterine transfer (Figure 27B). Statistically, there will be some instances when every embryo of such a patient's IVF cycle might carry the mutation in question. Before considering GGE to correct the existing embryos, the couple could elect to undertake another IVF cycle with the hope of producing unaffected embryos. A typical IVF cycle will produce three to five blastocysts, but eight or more are not uncommon. In our center, the average number of blastocysts per cycle is 4.2 across all ages and indications, meaning that the likelihood of conceiving an unaffected embryo increases with subsequent multiple IVF cycles. A large study from a genetic testing laboratory reported that a mere 7.1% of all cycles with PGT-M testing resulted in no genetically normal embryos available for transfer (323). Those unlucky patients could subsequently do another IVF cycle and cast the die anew.

PGT to screen embryos will probably be easier, cheaper, and safer to perform than GGE. Granted, each additional IVF cycle to generate more embryos carries its costs, as well as a physical and emotional toll on patients. Yet, when performing GGE, one would likely first perform PGT to test which embryos inherited the mutation, and then again after GGE to confirm that the correction happened. Each intervention also affects the viability of embryos, meaning a substantial increase in costs and risks. Unless methods are developed to efficiently edit all cells in a multicellular embryo, one is confined to performing the GGE intervention at the zygote stage, meaning that prior genetic testing is impossible (the process destroys the cell being analyzed). Genome editing molecules

would need to be applied 'blindly' into every zygote, affected and unaffected alike. Considering this and the possibility for off-target effects of GGE, we submit that hereditary conditions will continue to be handled preferentially by screening embryos with PGT over correcting them with GGE.

15.5.2. Scenarios Favoring GGE Over PGT

Do situations exist when PGT does not work? The answer is emphatically 'Yes'. PGT is pointless if dealing with a recessive disorder when both parents are homozygous mutants, as all resulting embryos will be homozygous mutants as well. Only GGE would prevent transmission of the disorder. Similarly, if there is a familial autosomal dominant disorder and one or both parents are homozygous for the mutant allele, every embryo will inherit at least one copy of the mutation and be affected (Figure 27B). But what is the frequency of those scenarios?

Previous commentaries have broached the subject (322, 324, 325), but a thorough analysis based on genetic epidemiology is warranted. In an effort to answer that question, we used published prevalence data for the most common genetic disorders in the U.S. to project how many conceptions would benefit from GGE per year on a national level (see Table 7).

Figure 27. Scenarios Requiring PGT Or GGE To Prevent Transmission Of Genetic Disorders.

PGT requires collecting a biopsy of the embryo, which is tested for the mutation causative of the hereditary condition. The embryos in an IVF patient's cohort that do not inherit the mutation are selected for transfer and implantation. PGT is the preferred method whenever embryos can be generated that are free of the mutation. When one of the parents is homozygous for a dominant disorder, or both parents are homozygous for a recessive disorder, all resulting embryos are affected, and GGE can be used to correct the mutation. ICM = Inner Cell Mass. TE = Trophectoderm. PGT = Preimplantation genetic testing. GGE = Germline genome editing.
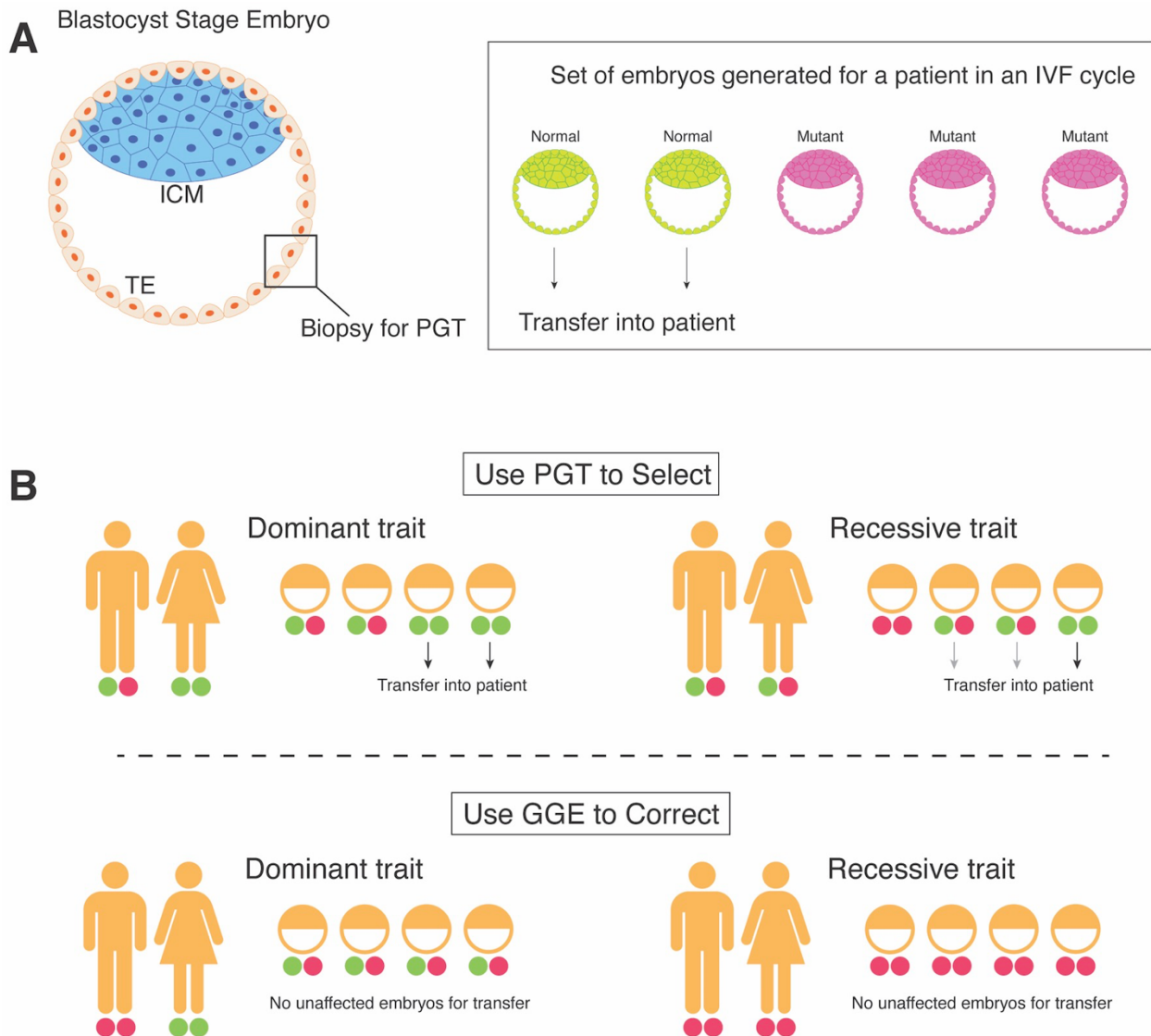
For common recessive disorders such as cystic fibrosis (CF), sickle cell disease (SCD), or Tay-Sachs, we calculated the chances of two homozygous mutant individuals forming a reproductive couple by random chance. For example, the number of people living in the U.S. with CF who are homozygous for *CFTR* mutations is estimated at 30,000, which means the prevalence in the general population is roughly 1 in ~10,000. The likelihood of two CF patients forming a couple is 1 in ~10,000^2 (assuming each affected individual pairs with a single mate). We estimate that in the U.S., there is only one couple of reproductive age at any given time where both partners are homozygous for CF mutant alleles in the U.S. (the exact calculated value is 1.26 couples). Considering the current data for the population percentage based on reproductive age, average fertility rate per woman, and range of reproductive years, we can estimate the number of conceptions each year in the U.S. for which GGE would be applicable. For CF, this number is negligible -- a mere 0.065 cases per year -- indicating we could anticipate that the need for GGE treatment to prevent the transmission of CF would occur only once every 15 years, with all other CF cases relying on PGT.

Table 7. Projected Estimates Of GGE Demand For Common Hereditary Genetic Disorders.

Genetic condition	Gene name/ symbol	Number of described mutations	Inheritance pattern[a]	Prevalence of carriers for recessive disorder population (heterozygotes)	Number of individuals affected by recessive disorder in U.S. population (homozygotes)	Prevalence of affected individuals for recessive disorder (homozygotes)	Chances two affected homozygous reproductive age individuals combine to create a reproductive couple[b]	Projected number of couples of reproductive age homozygous individuals with two affected homozygous individuals in U.S. population[c]	Total projected number of births from affected homozygous couples per year in the United States[d]	Notes
Cystic fibrosis	CFTR	>900	AR	1:31[e]	30,000[e]	1:10,964[f]	1:120,214,470	1.26	0.065	Median life expectancy is 33.4 years
Sick cell disease	HBB	1	AR	1:160 (general population)[g]	100,000 (general population)[e]	1:3,289 (general population)[f]	1:10,819,302	14.04 (general population)	0.73 (general population)	Condition negatively affects fertility in males and females. Median life expectancy is 48 years
Thalassemia (alpha)	HBA1 and HBA2	>120	AR (see Notes)	1:13 (African Americans)[h] 1:20[a]	88,000 (African Americans)[i] 36,547[i]	1:500 (African Americans)[e] ~0 (0 with homozygous mutations in both HBA genes, see Notes)[j,k]	1:250,000 (African Americans) ~0 (see Notes)	81.44 (African Americans) ~0 (see Notes)	4.22 (African Americans) ~0 (see Notes)	Complex inheritance pattern with two HBA genes. Double homozygosity of mutations is embryonic lethal.
Thalassemia (beta)	HBB	>200	AR	1:66[j,k]	5,980[j]	1:55,000[j,k]	1:3,025,000,000	0.050	0.0026	Life expectancy of beta thalassemia major is 17 years. Autosomal dominant forms exist.
Tay-Sachs disease	HEXA	>100	AR	1:250 (general population)[e] 1:27 (Ashkenazi Jews)[e] 1:27 (Cajun population)[e]	3,289 (general population)[i] 1,178 (Ashkenazi Jews)[i] 333 (Cajun Americans)[i]	1:100,000 (general population)[e] 1:3,600 (Ashkenazi Jews)[e] 1:3,600 (Cajun Americans)[e]	1:10,000,000,000 (general population) 1:12,960,000 (Ashkenazi Jews) 1:12,960,000 (Cajun Americans)	0.015 (general population) 0.15 (Ashkenazi Jews) 0.043 (Cajun Americans)	0.00079 (general population) 0.0078 (Ashkenazi Jews) 0.0022 (Cajun Americans)	Life expectancy estimated at 4–5
Spinal muscular atrophy	SMN1	>100	AR	1:50[e]	25,000[i]	1:13,100[i]	1:171,610,000	0.89	0.046	Degrees of medical severity, varying life expectancy
Phenylketonuria	PKU	>300	AR	1:50[m]	16,000[m]	1:15,000[e]	1:225,000,000	0.68	0.035	If treated, patients have normal life expectancy but experience increased rate of miscarriage
Gaucher disease	GBA	4 (most common)	AR	1:125 (general population)[n]	6,000[o]	1:75,000 (general population)[e]	1:5,625,000,000 (general population)	0.027 (general population)	0.0014 (general population)	Degrees of medical severity, varying life expectancy, depending on type
Canavan disease	ASPA	>70 (only 1 mainly in Ashkenazi Jews)	AR	1:14 (Ashkenazi Jews)[e] 1:40 (Ashkenazi Jews)[p]	5,653[i] ~400 (Ashkenazi Jews)[i]	1:750 (Ashkenazi Jews)[e] 1:10,000 (Ashkenazi Jews)[e]	1:562,500 (Ashkenazi Jews) 1:100,000,000 (Ashkenazi Jews)	3.48 (Ashkenazi Jews) 0.020	0.18 (Ashkenazi Jews) 0.0010	Majority of patients do not survive past age of 10 years
Familial dysautonomia	ELP1	2 (prevalent in Ashkenazi Jews)	AR	1:30 (Ashkenazi Jews)[e]	1,178 (Ashkenazi Jews)[i]	1:3,600 (Ashkenazi Jews)[e]	1:12,960,000 (Ashkenazi Jews)	0.15 (Ashkenazi Jews)	0.0078 (Ashkenazi Jews)	Average life expectancy is 40 years
Connexin26-related deafness	GJB2	>90	AR	1:33[q]	70,000[q]	1:4,500[q]	1:20,250,000	7.50	0.39	Assortative mating factor likely strong, see Some Caveats section in article about this point. Some autosomal dominant forms exist

Table 7 continued

Genetic condition	Gene name/symbol	Number of described mutations	Inheritance pattern[a]	Prevalence of affected individuals for dominant disorder (heterozygotes)	Number of individuals affected by dominant disorder in U.S. population (heterozygotes)	Prevalence of individuals homozygous for dominant disorder	Chances two affected homozygous reproductive age individuals combine to create a reproductive couple[b]	Projected number of couples of reproductive age with two affected homozygous individuals in U.S. population[c]	Total projected number of births from affected homozygous couples per year in the United States[d]	Notes
Huntington's disease	HTT	Trinucleotide repeat, varying number of copies	AD	1:10,964[f]	30,000[h]	~0	~0	~0	~0	Homozygosity regularly embryonic lethal
Marfan syndrome	FBN-1	>3,000	AD	1:15,000[g]	22,000[i]	~0	~0	~0	~0	Homozygosity regularly embryonic lethal
Achondroplasia	FGFR3	2 (responsible for the vast majority of cases)	AD	1:25,000[k]	13,150[i]	~0	~0	~0	~0	Homozygosity regularly embryonic lethal
Neurofibromatosis 1	NF1	>140	AD	1:3,000[e]	100,000[e]	~0	~0	~0	~0	Homozygosity regularly embryonic lethal
Myotonic dystrophy type 1	DMPK	Trinucleotide repeat, varying number of copies	AD	1:10,000[h]	32,000[j]	~0	~0	~0	~0	Homozygosity regularly embryonic lethal

Genetic condition	Gene name/symbol	Number of described mutations	Inheritance pattern[a]	Prevalence of heterozygous individuals for X-linked disorder	Number of individuals affected by X-linked disorder in U.S. population	Prevalence of women homozygous for X-linked disorder	Chances two affected homozygous/hemizygous individuals combine to create a reproductive couple[b]	Projected number of couples of reproductive age with two affected homozygous/hemizygous individuals in U.S. population[c]	Total projected number of births from affected homozygous/hemizygous couples per year in the United States[d]	Notes
Fragile X syndrome	FMR1	Trinucleotide repeat, varying number of copies	XD (incomplete penetrance)	1:1,000 (males)[o] 1:250 (females)[o]	40,000[e] 20,000[e]	~0	~0	~0	~0	Homozygosity regularly embryonic lethal
Hemophilia A	F8	>1,000	XR	1:5,000 (males)[e]	20,000[h]	~0	~0	~0	~0	Homozygosity regularly embryonic lethal
Duchenne muscular dystrophy	DMD	>2,000	XR	1:7,250 (males)[b]	22,500[i]	~0	~0	~0	~0	Homozygosity regularly embryonic lethal

Data points used for calculations (note: all numbers refer to the U.S. population), Total U.S. general population: 338,927,078.[a] Reproductive age range: 15–49 [34 years total].[b] U.S. percentage of population in reproductive age is 46.19%.[c] U.S. population in reproductive age is 151,931,417.[c] Total fertility rate per U.S. woman is 1.76.[b] U.S. real live births per year: 3,864,754.[b] Total African American population in the United States: 44,076,228.[t] African American population of reproductive age in the United States: 20,358,810.[r] Total Ashkenazi Jewish population in the United States: 4,240,000.[t] Ashkenazi Jewish population of reproductive age in the United States: 1,958,456.[r] Total Cajun population in the United States: 1,200,000.[u] Ashkenazi Cajun population of reproductive age in the United States: 554,280.[s]

[a] Autosomal recessive (AR), autosomal dominant (AD), X-linked recessive (XR), and X-linked dominant (XD).
[b] Calculated (prevalence of homozygosity for recessive mutation)[2].
[c] Calculated (population with reproductive age/chances of two affected individuals combine to create a reproductive couple).
[d] Calculated (number of couples of reproductive age with two affected individuals×fertility rate/number of fertile years).
[e] National Institutes of Health. (https://ghr.nlm.nih.gov) and (https://www.ninds.nih.gov).
[f] Calculated based on number of affected individuals and population size.
[g] World Health Organization. (https://www.who.int/genomics/public/geneticdiseases/en/index2.html) and (https://www.who.int/reproductivehealth).
[h] Centers of Disease Control and Prevention. (https://www.cdc.gov).
[i] Calculated on prevalence of affected individuals and population size.
[j] DOI: 10.1056/NEJMra1404415 (extrapolated from California data).
[k] DOI: 10.1002/pbc.21883 (extrapolated from California data).
[l] Spinal Muscular Atrophy Foundation. (https://www.smafoundation.org).
[m] National PKU alliance. (www.npkua.org).
[n] DOI: 10.1001/jama.298.11.1281.
[o] National Organization for Rare Disorders. (https://rarediseases.org).
[p] Canavan Foundation. (http://www.canavanfoundation.org).
[q] DOI: 10.1001/jama.281.23.211 (extrapolated from Midwestern U.S. data).
[r] United States Census Bureau. (https://census.gov).
[s] Calculated based on referenced data.
[t] Pew Research. (https://www.pewresearch.org).
[u] James Minahan, January 1, 2002. Encyclopedia of the Stateless Nations: A–C. Greenwood Publishing Group, p. 355. ISBN 978-0-313-32109-2.
[v] Children's Hospital of Wisconsin. (https://chw.org).

We performed calculations for other recessive genetic disorders and considered instances for which assortative mating and variable ethnical prevalence are relevant, such as SCD in the African American population and Tay-Sachs in Ashkenazi Jews (see below). The number of projected cases is remarkably small for all of the most common single-gene recessive disorders (323), totaling fewer than a dozen clinical cases of estimated children born per year in the U.S. that might hypothetically benefit from GGE (Table 7).

A more complex inheritance pattern is found in α-thalassemia, possibly the most common severe genetic disorder in the general U.S. population, due to the four alleles on two *HBA* genes. If one or two alleles are mutant, the phenotype is generally asymptomatic. When three alleles are mutant, the condition is known as hemoglobin H (HbH) disease and patients often suffer from anemia, hepatosplenomegaly, and jaundice. Harboring four mutant alleles causes the condition hemoglobin Bart's hydrops fetalis syndrome (BHFS), which is almost always lethal during gestation or shortly after birth. In the literature 69 cases of BHFS have been documented that have survived past infancy, with 18 instances of survival past 10 years of age (326). The demand for GGE for α-thalassemia is therefore virtually nil, as there will likely never be a couple with BHFS intending to procreate. In the case that two HbH patients would like to have children, 1 in 4 embryos generated would be asymptomatic carriers, 1 in 2 embryos would have HbH, and 1 in 4 embryos would die *in utero* with BHFS (327). In this case, utilizing PGT to facilitate selection of an asymptomatic carrier would likely be favored over attempting GGE.

Homozygosity for severe dominant disorders is almost always embryonically lethal, making the number of such individuals virtually non-existent in the general population. For example, the number of cases homozygous for Huntington's Disease is in the dozens (324). There have been 13 recorded patients homozygous for myotonic dystrophy Type 1 (328). Homozygotes for mutations causing neurofibromatosis type 1 have never been documented (329). Achondroplasia, one of the most common dominant disorders, is caused by a mutation in *FGFR3*. When heterozygous it causes dwarfism, but is considered uniformly fatal when homozygous, and only a handful of cases are reported to have survived into early childhood (330). Therefore, the projected annual national demand of GGE for dominant disorders approaches zero, as PGT is applicable to identify non-affected embryos in virtually all cases.

PGT is also appropriate for cases of X-linked disorders. Female carriers of a recessive X-linked disorder have a 1 in 4 chance with each pregnancy to have a carrier daughter, a 1 in 4 chance to have a non-carrier daughter, a 1 in 4 chance to have a son affected with the disease, and a 1 in 4 chance to have an unaffected son. PGT can identify affected male embryos. In cases where the mother is homozygous for the mutation, all the male offspring would inherit a mutant copy of X. Here again, just with autosomal dominant disorders, the prevalence of homozygosity for X-linked disorders is remarkably low (331). For example, Duchenne muscular dystrophy (DMD) has never been identified as homozygous (332). Hemophilia A, which affects 1:5,000 male births, has only ever been

documented as homozygous a few times (333-336). Fragile X syndrome, considered a dominant X-linked disorder, is characterized by amplification of a trinucleotide repeat, and has only been described as homozygous in the premutation form, not the fully amplified allele (337).

One clinical situation that would benefit from genome editing is a male affected by a dominant X-linked disorder that wishes to conceive children. His male embryos will be disease-free by default. But a daughter would undoubtedly inherit his affected X chromosome. Such a circumstance prompts a different ethical discussion revolving around gender selection, and specifically the justification for wanting a female child that must be genetically altered rather than choosing a healthy male. Here again, due to PGT, the number of cases that would require GGE is extremely small.

What about less severe hereditary conditions? It has been suggested that couples with congenital hearing loss, which affects 1 in 500 individuals, might consider GGE to have a hearing-enabled child (324). Deafness is genetically heterogenous with more than 1000 mutations identified in more than 90 genes, but recessively-inherited single-gene mutations in *GJB2* are responsible for over half of all cases (338). Historically, deafness has been a prime example for assortative mating. In the 1970s, 80-90% of people with profound deafness in the U.S. married another deaf person (339). It is estimated that 1 person in 4,500 is homozygous mutant for *GJB2* (340). Assuming that all *GJB2*-mutant homozygotes of reproductive age intermarried and reproduced at general rates, there

could be a potential 837 conceptions nationally per year that would benefit from editing *GJB2*, which is a sizable number.

However, the fact that deafness is a treatable condition invalidates this projection. The introduction of cochlear-implant technology has profoundly altered the mating structure of the deaf population (341). By facilitating oral communication and educational mainstreaming, practically all deaf children of hearing parents are redirected into the hearing mating pool (341). This is an example in which treatment might obviate the need for GGE and its associated risks. We predict that GGE will find little demand in less severe or treatable genetic conditions, considering medical necessity and alternative interventions. This was also one of the main criticisms of the only alleged case of human GGE resulting in births reported to date, where *CCR5* was mutated to diminish chances of possible HIV infection -- proven strategies already exist for the prevention of perinatal transmission of HIV (342).

GGE might be the only strategy for IVF patients that carry a genetic condition but have conceived only affected embryos and are precluded from initiating additional IVF cycles because of advancing age, disease, or cost. Of the annual ~100,000 IVF cycles in the U.S. accompanied by PGT (316), the fraction using PGT-M for single-gene disorders is estimated at 10% (317). Of those, 7.1% are estimated not to generate any normal embryos (323), resulting in ~7,100 cycles. Judging from observations in our IVF center, we estimate <1% of patients not being able to perform a subsequent IVF cycle for PGT-

M when desired. Hence, we project there to be at most 71 cases per year in the U.S. that would benefit from GGE for this particular scenario, if all patients elected to pursue that procedure.

It should be noted that the unicellular zygote cannot be tested for a genetic disorder without destroying it. It is therefore not feasible to screen zygotes for a mutant allele and then attempt to edit that allele. GGE at the zygote stage makes sense only when there is previous knowledge of that zygote's genetic makeup, as when the complement is deduced from homozygosity for the mutant allele in one or both parents. One exception is with maternal heterozygosity, as one can attempt deducing the status of the zygote by analyzing polar bodies, which are the products of meiosis. Although historically there has been some limited success, this practice produces notoriously high amounts of false positives and negatives. The state of heterozygosity in the mother would permit conventional PGT screening for embryos not having inherited the allele, precluding the need for GGE. Therefore, even when there would be demand for GGE, the gene editing machinery would only be administered later in development, likely at the blastocyst stage when most PGT takes places and affected embryos are identified. However, the expertise does not yet exist to deliver CRISPR-Cas to all 64-128 cells of a blastocyst and prevent any incidence of the potential medical risks associated with resultant mosaicism.

Together, our analysis suggests that the true clinical demand for GGE for single-gene hereditary disorders is exceedingly small. We estimate that GGE could at most benefit one hundred births per year in the U.S., when all eligible patients opted for the procedure.

15.5.3. Use Of GGE In Mitochondrial DNA Disease

Mitochondrial DNA (mtDNA) disease is relatively common, with an estimated prevalence of 1 in 5,000 (343), and causes severe and debilitating genetic disorders such as Leigh Syndrome, MELAS, or Kearns-Sayre Syndrome. Most mtDNA mutations occur *de novo*, and maternal transmission of mtDNA disease is rare. There are an estimated ~800 pregnancies per year in the U.S. at risk of maternal transfer of mutant mtDNA (344). Due to the multi-copy nature of mtDNA, mutant mtDNA often exists in a mix with normal mtDNA in a cell, a state known as heteroplasmy. In most cases, PGT-M can be designed to identify and quantify mutations in mtDNA to de-select embryos with high mutation load. The circumstances in which PGT-M is not useful are those in which there is homoplasmy of mutant mtDNA, or when the patient is only capable of producing heteroplasmic embryos with high mutation load. In those instances, GGE might reduce the mutation load by correcting mutations in as many mtDNA copies as possible. Even with such a treatment, GGE would need to be proven more effective and safer than the alternative treatment of mitochondrial replacement therapy (MRT) (345). Taking these factors into account, we conclude that the U.S. annual demand for GGE for mtDNA disorders might be in the low dozens.

15.5.4. Can GGE Cure Embryonic Aneuploidy And Other Chromosomal Abnormalities?

PGT-A and -SR, which tests embryos for chromosomal abnormalities, is now performed in more than 30% of IVF cycles in the U.S. and growing (316, 317). Some of those instances are for familial conditions, for which there is a risk of inheriting a chromosomal abnormality. However, PGT-A/-SR is mostly utilized as a screen, even when both parents are chromosomally normal. Chromosomal abnormalities are common *de novo* events in naturally conceived embryos as well as in those generated by IVF (313), and embryos that carry chromosomal abnormalities are developmentally compromised and often fail to implant. When implantation does occur, the pregnancy often results in miscarriage. In the few instances where they make it to birth, the offspring is bound to harbor chromosomal conditions ranging from whole chromosome monosomies or trisomies (e.g. Down, Turner, or Edwards syndromes), sub-chromosomal segmental deletions or duplications (e.g. Cri-du-Chat, Angelman, or Prader-Willi syndromes), or rearrangements that can lead to a range of conditions. PGT-A/-SR facilitates the deselection of such embryos before intrauterine transfer, and numerous RCTs and observational studies have reported a significant increase in clinical success rates when embryos classified as normal/euploid are used in comparison to blindly selecting embryos for transfer into the patient (29, 30, 346).

Importantly, the observed rates of embryo aneuploidy increase with advancing maternal age due to errors of meiosis during oocyte maturation, a process that becomes more error

prone over time (68). On average, rates of aneuploidy increase from 30% of IVF embryos in women in their early 30s to nearly 90% for women aged 44 years and above (75). This correlation between maternal age and proportion of aneuploid embryos means that classical Mendelian calculations do not apply. In contrast with hereditary single gene disorders wherein there is a high likelihood of conceiving a genetically normal embryo at each IVF cycle, a patient with advanced maternal age has an elevated risk of producing only aneuploid embryos even after multiple IVF cycles. In addition, a large study analyzing over 15,000 IVF embryos has shown that there is even a subset of younger patients also only capable of generating aneuploid embryos (75), possibly due to faulty cell cycle mechanisms in those patients. When a couple is only able to generate chromosomally abnormal embryos, even after repeated IVF cycles, the result would often be their abandonment of infertility treatment altogether.

Could GGE correct chromosomal abnormalities in embryos, such as erasure of the additional chromosome present in trisomic embryos? Even though this technology does not yet exist, intriguing new data has emerged with proof-of-concept experiments targeting and deleting of entire chromosomes (347, 348). What is the potential clinical demand for that procedure? Internal data from 1,769 IVF cycles at our IVF center indicates that ~20% of initial cycles produce only aneuploid embryos, and a subsequent cycle for those patients has ~60% chance of containing only aneuploid embryos. We also observe that nearly 100% of patients that produce only aneuploids after three cycles discontinue their IVF treatment. Extrapolating those figures to the roughly 245,000 IVF

cycles currently performed annually in the U.S. (316), we estimate that ~17,600 patients would benefit from GGE of aneuploid embryos.

A different application for this kind of GGE is for individuals with Robertsonian translocations. Such individuals are typically healthy except for their increased chances of generating embryos with aneuploidies. Robertsonian translocation 21q; 21q is particularly problematic, since 100% of resulting embryos have trisomy 21 and therefore Down's syndrome if carried to term (349). Since PGT-A for screening is not beneficial, this situation would meet the requirement for unmet medical need.

Granted, this practice would not be considered GGE under its classical definition, because the target is not the zygote but is instead a 64-128 cell blastocyst. Unless techniques are developed to target every cell in the blastocyst, the result will inevitably be mosaicism. Interestingly, recent data has shown that blastocysts classified by PGT-A as chromosomally mosaic (harboring a mix of euploid and aneuploid cells) can result in implantation and healthy pregnancies, albeit with significantly lower success rates than blastocysts classified as euploid (164, 171, 350). To date, ~300 babies born from transferred mosaic embryos have not presented medical complications of any kind (164, 171, 350). Evidence from mouse and human embryology indicates that in a mosaic embryo euploid cells dilute out aneuploid cells as the latter preferentially die off or divide at slower rates during development (218, 350).

Deleting an extra chromosome when trisomy is present would typically imply the creation of uniparental disomy, since the GGE machinery would need to target the chromosome that is dissimilar and contains differentiating DNA sequences. The implication is that the remaining two chromosomes would stem from the same parent, potentially creating epigenetic consequences with medical manifestations. Testing parental genomes, polar bodies, as well as deep sequencing of the TE biopsy in PGT-A might help identify exploitable differentiating regions between duplicated chromosomes. More research is needed in this field, and careful consideration will have to be given to what regions/chromosomes can be targeted to rid an embryo of aneuploidy.

15.6. Chapter Discussion

In summary, the prospect of GGE for chromosomal correction could have a tremendous impact on IVF patients, although many technical advances and much more research are needed. We must note some significant assumptions within our calculations. Several of the genetic disorders described here shorten life expectancies and alter life conditions to the point of skewing statistics regarding fertility for these populations. For example, the median age of survival for SCD is 48 years, for CF it is 33.4 years, and for Tay-Sachs it is 4-5 years. The likelihood of two affected individuals meeting is not entirely up to chance (as the simple calculations suggest). Having the same disorder could make it more likely for two patients to come together a form a couple (assortative mating); individuals with a particular condition are more likely to meet others with the same condition through societies, associations, and help groups. On the other hand, certain genetic disorders

affect the immune system and increase risk of infection, making it risky to interact with other patients of the same condition. For example, CF patients are recommended maintain a minimal distance of 2 meters from each other at all times due to the risk of bacterial cross-infection (351).

The incidence of genetic disorders is also altered by sociocultural and ethnicity factors such as consanguinity, endogamy, and high prevalence in certain groups, such as Tay-Sachs or SCD. Penetrance and variable expressivity have been disregarded for simplicity. Mutations causing disorders with treatable symptoms such as hemochromatosis, or mutations that increase disease risk such as *BRCA1/2* were generally excluded from this analysis as testing for those conditions is not common or remains controversial; performing GGE for those factors is even more unlikely. Importantly, our calculations using published prevalence data assume that all cases of a genetic disorder are inherited, although a substantial percentage of *de novo* mutations cases do occur for particular types of inherited disorders. Taken together, these assumptions suggest that our projections are likely inflated, and the actual demand of GGE targeting heritable genetic disorders is probably even lower than the figures presented above.

We have not considered the hypothetical demand for GGE to introduce genome edits of a non-medical nature for enhancement. The prospect of 'designer babies' whose DNA is sculpted by GGE to control features such as intelligence, height, and longevity, would

require the development of safe methods to edit dozens, hundreds, or maybe thousands of loci in the genome. Complex traits are multifactorial and the full set of involved genes remains unknown. PGT-P could potentially be used to screen embryos for such enhancements, for example ranking the embryos in a patient's cohort for predicted height. Aside from the obvious ethical concerns, we believe the actual demand for such non-medical screening will be negligible. IVF laboratories have had the capability of using PGT to select for traits such as eye color for example, but this has not become common practice (317).

Our calculations should not be considered exact predictions of the potential demand for GGE. They are intended to provide some calibration of expectations. GGE is inevitably entwined with IVF, a medical field that has long dealt with screening for familial genetic disorders using PGT. Couples in which one or both partners are affected by a genetic disorder would necessarily need to undergo IVF whether the strategy to prevent propagation of the causative allele involved GGE or PGT. Given the choice, we believe that PGT will always be preferred.

Our projections show there are extremely few instances for which GGE will be the only option, such as when both parents are homozygotes for a recessive condition or at least one parent is homozygous for a dominant condition. We do not intend to downplay the importance of those rare cases and patients. Nonetheless, the actual magnitude of the demand for GGE must be part of the conversation when debating ethical and legal

frameworks. However, we suggest that aneuploidy might be a much larger issue than previously considered, as we predict there will be many potential beneficiaries of chromosomal editing in embryos if safe technologies for that purpose can be developed.

16. Specific Aim G: To test the hypothesis that SARS-CoV-2, the virus responsible for COVID-19, can infect human embryos and affect their viability.

The following published work is presented for this specific aim:

Victor AR*, Mauricio M*, Griffin DK, Duong T, Bolduc N, Farmer A, Garg V, Hadjantonakis AK, Coates A, Barnes FL, Zouves CG, Greene WC, Viotti M. SARS-CoV-2 Can Infect Human Embryos. bioRxiv 2021.01.21.427501. doi: https://doi.org/10.1101/2021.01.21.427501. * equal contribution

16.1. My Personal Contribution to the Work

My personal contribution to this study includes structuring its original design, experimental oversight, and coordination with our virology collaborators. Executing all embryology aspects of the study, including thawing, culturing, fixing and staining embryos for confocal imaging. Assisting with data analysis and manuscript preparation.

16.2. Chapter Summary

The spread of SARS-CoV-2 has led to a devastating pandemic, with infections resulting in a range of symptoms collectively known as COVID-19. The full repertoire of human tissues and organs susceptible to infection is an area of active investigation, and some studies have implicated the reproductive system. The effects of COVID-19 on human

reproduction remain poorly understood, and particularly the impact on early embryogenesis and establishment of a pregnancy are not known. In this work, we explore the susceptibility of early human embryos to SARS-CoV-2 infection. We note that ACE2 and TMPRSS2, two canonical cell entry factors for SARS-CoV-2, are co-expressed in cells of the trophectoderm in blastocyst-stage preimplantation embryos. Using fluorescent reporter virions pseudotyped with Spike (S) glycoprotein from SARS-CoV-2, we observe robust infection of trophectoderm cells, and this permissiveness could be attenuated with blocking antibodies targeting S or ACE2. When exposing human blastocysts to the live, fully infectious SARS-CoV-2, we detected cases of infection that compromised embryo health. Therefore, we identify a new human target tissue for SARS-CoV-2 with potential medical implications for reproductive health during the COVID-19 pandemic and its aftermath.

16.3. Chapter Introduction

Coronavirus disease 2019 (COVID-19) has emerged as an unexpected and devastating pandemic upending life around the globe (352). Entry of severe acute respiratory syndrome coronavirus 2 (SARS-CoV-2), the infectious agent responsible for COVID-19 (353), requires interactions of its surface glycoprotein Spike (S) with two entry factors on the target cell including the angiotensin-converting enzyme 2 (ACE2) receptor bound by S and a priming cleavage of S by the serine protease TMPRSS2 (354, 355). These binding and processing steps promote virion fusion at the plasma membrane (356), or alternatively subsequent endocytosis of virions and fusion within the late endosome (357).

The full repertoire of cell and tissue types that SARS-CoV-2 can infect is now being better defined (352, 358). Expression of SARS-CoV-2 cell entry factors has been described in a wide assortment of human cells (358), and in COVID-19 patients, SARS-CoV-2 virus has been detected in various organs (359-361). Infected individuals can exhibit a range of symptoms spanning beyond lung-related problems, to include disease in the intestine, heart, kidney, vasculature, and liver (359, 361-365). Within the female and male reproductive systems, expression of SARS-CoV-2 entry factors is present in cells of the ovaries, uterus, vagina, testis, and prostate (358, 366-369). Some studies showed detectable virus in the semen of infected males (370, 371) and vaginal secretions of infected females (372).

The possibility of vertical transmission of SARS-CoV-2 to embryos during or shortly after fertilization is concerning, but is contingent on cells of the embryo being permissive to the virus. Here, we explore whether the factors required for SARS-CoV-2 entry are present and functional in cells of the preimplantation embryo, and using S pseudotyped reporter viruses and the fully infectious version of the virus, we assess if SARS-CoV-2 can infect human embryos.

16.4. Methods And Materials

16.4.1. Ethical Approval

The study was conducted in adherence with the Declaration of Helsinki. Ethical approval for this project was obtained through the IRB of the Zouves Foundation for Reproductive

Medicine (OHRP IRB00011505) and the UCSF Human Gamete, Embryo and Stem Cell Research (GESCR) Committee (Study # 21-34579). Furthermore, the UCSF IRB exempted the study from full review because it does not involve human subjects as defined by federal regulation 45 CFR 46.102(e) of the U.S. Department of Health & Human Services.

16.4.2. Human Embryos

All embryos used in this study were surplus samples from fertility treatment and *in vitro* fertilization, donated strictly for research by signed informed consent. Embryos were generated using standard industry procedures as previously described (206), vitrified and cryopreserved until thaw and experimental use. For the RNA-seq experiment, embryos were of various ethnic backgrounds and comprised a mix of euploid and aneuploid samples based on evaluation by preimplantation genetic testing for aneuploidy (PGT-A) (246) (Supplementary Table 10). For the pseudotyped virion infection experiments, embryos were either untested or assessed by PGT-A, and included a mix of embryos classified as euploid, mosaic, and aneuploid (samples with aneuploidies in chromosomes X or 21, respectively encoding *ACE2* and *TMPRSS2*, were excluded). For the live virus infection experiments, embryos were used that had not been previously tested by PGT-A. All embryo experiments included a range of initial developmental stages spanning from early to hatched blastocysts.

16.4.3. RNA-seq And Expression Analysis

Trophectoderm biopsies containing 5-10 cells from blastocyst-stage embryos (n=24) were processed for RNA-seq using a commercial kit (Takara Bio, USA, SMART-Seq v4 Ultra Low Input RNA Kit for Sequencing) following the user manual. The resulting cDNAs were converted to libraries using a Nextera XT kit (Illumina, USA), with a modified protocol according to SMART-Seq v4 user manual. These libraries were pooled and sequenced using a NextSeq 550 instrument (Illumina, USA) with a MidOutput cartridge at 2x75 cycles. The sequencing reads in Fastq files were down-sampled to 6M total reads, aligned to the human genome assembly (hg38), and the number of transcripts per million (TPM) was determined using the CLC Genomics Workbench 12 (Qiagen, USA). Results were mined for expression of factors implicated in SARS-CoV-2 infection. Violin plots were prepared with PlotsOfData (373).

16.4.4. Immunostaining

Blastocysts were immersed in fixation buffer containing 4% paraformaldehyde (EMS, USA, no. 15710) and 10% fetal bovine serum (FBS; Seradigm, USA, 1500-050) in phosphate-buffered saline (PBS; Corning, USA, MT21040CM) for 10 minutes (min) at room temperature (rt), followed by three 1-min washes at rt in PBS with 10% FBS. To inhibit non-specific protein interactions, embryos were cultured in 2% horse serum (Sigma, USA, H0146) diluted in PBS (blocking solution) followed by addition of 0.1% saponin (Sigma, USA, S7900) for gentle permeabilization. After 1 h incubation at rt, primary antibodies diluted in blocking solution were added and incubated overnight at 4

°C. Embryos were then washed three times for 5 min each in PBS at rt prior to incubation with secondary antibodies. Secondary antibodies diluted in blocking solution were applied for 1 h at 4 °C. Embryos were then washed twice for 5 min each in PBS and subsequently incubated with 5 μg/ml Hoechst 33342 (Invitrogen, USA) in PBS for 5 min to stain the nuclei. Finally, embryos were washed twice for 5 min each in PBS prior to mounting for imaging. The following primary antibodies were used: goat anti-ACE2 (R&D Systems, USA, AF933, 1:100), mouse anti-TMPRSS2 (Developmental Hybridoma Bank, USA, P5H9-A3, 3.2 μg/ml). The following secondary Alexa Fluor-conjugated antibodies (Invitrogen, USA) were used at a dilution of 1:500: donkey anti-goat Alexa Fluor 568 (A10042), donkey anti-mouse Alexa Fluor 488 (A21202). DNA was visualized using Hoechst 33342. For all immunofluorescence experiments, five independent experiments were performed and analyzed.

16.4.5. Pseudotyped Virion Preparation

For production of HIV-1 NL-43ΔEnv-eGFP SARS CoV-2 S pseudotyped virus particles, 293T cells were plated at 3.75 x10^6 cells in a T175 flask. 24 h post plating the cells were transfected using a PEI transfection reagent (Sigma, USA). 90 μg of PEI, 30 μg of HIV-1 NL-4ΔEnv-eGFP expression vector DNA (NIH AIDS Reagent Program, USA) and 3.5 μg of pCAGGS SARS CoV-2 S Glycoprotein expression vector DNA (NR52310, BEI, USA) in a total of 10 ml of Opti-MEM media (Invitrogen). The day following transfection the media was changed to DMEM10 complete media and samples were placed at 37 °C and 5% CO_2 for 48 h. At 48 h, the supernatants were harvested, filtered through 0.22 μm

Steriflip filters (EMD, Millipore, USA) and concentrated by ultracentrifugation for 1.5 h at 4 °C at 25K rpm. After concentration, the supernatant was removed and pellets containing virus particle pellets were resuspended in cold 1xPBS containing 1% FBS, and aliquots stored at -80 °C. For production of control virus particles not expressing the SARS CoV-2 S glycoprotein (Bald), the same procedure was followed except the pCAGGS SARS CoV-2 S vector DNA was omitted from the transfection. SARS and MERS pseudotyped virus particles were produced using the same procedure, substituting the SARS CoV-2 S expression vector with either pcDNA3.1(+) SARS S or pcDNA3.1(+) MERS S.

For production of VSVΔG SARS CoV-2 S pseudotyped virus particles, 293T cells were plated at 1.8 x10^6 cells in a T175 flask. 24 h post plating, the cells were transfected by PEI transfection reagent (Sigma, USA) with 90 μg of PEI, 30 μg of pCAGGS SARS CoV-2 S Glycoprotein expression vector DNA (NR52310, BEI, USA) in a total of 10 mL of Opti-MEM media (Invitrogen, USA). One day after transfection the media was removed, the cells were washed with 1xPBS and DMEM10 complete media was added. Once the media was changed the cells were infected with VSVΔG VSVg virus (Sandia, USA) at an MOI of 1 or higher. The infection media was changed after 4 h, the cells were washed with 1xPBS and DMEM10 supplemented with 20% anti-VSVg hybridoma supernatant (ATCC, USA, CRL-2700). At 24 h the supernatant was harvested, filtered by 0.22 μm Steriflip filter (EMD, Millipore, USA) and then concentrated by ultracentrifugation for 1.5 h at 4 °C and 25K rpm. Supernatant was removed and virus particle pellets were resuspended in cold 1xPBS containing 1% FBS, aliquots were stored at -80 °C. For

production of control virus particles not expressing the SARS CoV-2 S glycoprotein (Bald), the same procedure was used but with the omission of the pCAGGS SARS CoV-2 S vector transfection on day 2.

SARS and MERS S pseudotyped virus particles were produced using the same procedures, substituting the SARS CoV-2 S expression vector with either pcDNA3.1(+) SARS S or pcDNA3.1(+) MERS S vectors respectively.

16.4.6. Pseudotyped Virion Infection Assay

Blastocyst-stage embryos were hatched from zona pellucidas mechanically (except for samples that were already fully hatched), and transferred to flat bottom 96 well plates in 100 μl embryo culture media. Either HIV-1 NL-43ΔEnv-eGFP SARS CoV-2 S pseudotyped virions (100ng/p24), or VSVΔG SARS CoV-2 S pseudotyped virions (MOI=0.1), were added to the embryos. Bald (not expressing S glycoprotein) virions and mock infection conditions were included in each pseudotyping experiment. After the addition of the virions, the embryos were spinoculated with virus by centrifugation at 200 g for 2 h at rt. Upon completion of the spinoculation, an additional 100 μl of embryo culture media was added to each well and the cultures were placed at 37 °C and 5% CO_2. For the HIV-1 NL-43ΔEnv-eGFP based infections, embryos were monitored for fluorescence at 24-48 h post-spinoculation. For the VSVΔG based infections embryos were monitored for fluorescence at 12-24 h post-spinoculation. Additional controls included the addition of 10 μg of anti-ACE2 antibody (AF933, R&D Systems, USA) that blocks SARS-CoV-2 S

binding to ACE2, anti-SARS CoV-2 S Neutralizing antibody (SAD-S35, ACRO, USA) that

interacts with the receptor binding domain on Spike that blocks Spike engagement of the

ACE2 receptor, or anti-Human IgG Kappa (STAR 127, Bio-Rad, USA) control antibody

16.4.7. Live SARS-CoV-2 Viral Infection Assay

Viral stocks were prepared using Vero E6 cells using an infectious molecular clone of

SARS-CoV-2 expressing an mNeonGreen reporter (icSARS-CoV-2-mNeonGreen) (374).

For the infection assay, blastocyst-stage embryos were placed in 96 well flat bottom

plates in 100 μl of embryo culture media. A viral preparation at a concentration of 100

$TCID_{50}$ in culture media was added to the embryos. Control embryos were additionally

incubated with either 10ug of anti-ACE2 antibody (AF933, R&D Systems, USA), anti-

SARS CoV-2 Spike Neutralizing antibody (SAD-S35, ACRO, USA) or anti-Human IgG

Kappa (STAR 127, Bio-Rad, USA) antibody. The plates were spinoculated at 200g for 1

hour at room temperature. Upon completion of the spinoculation an additional 100uLs of

embryo culture media was added to each well and the cultures were placed at 37°c and

5% CO_2. At 12 to 16 hours post-spinoculation the embryos were assessed for infection.

All experiments were performed in the Gladstone Institutes ABSL3 facility, adhering to

BSL3 protocols.

16.4.8. Microscopy

Embryos were placed into 35-mm glass-bottom dishes (MatTek, USA). For

epifluorescence microscopy, embryos were imaged with an Echo Revolve fluorescent

microscope (Echo, USA) or an EVOS M5000 Imaging System (ThermoFisher, USA) employing a LPanFL PH2 20X/0.40 lens, and fluorescence light cube for GFP (470/525 nm) and transmitted light. For confocal microscopy of immunostained embryos, samples were suspended in small quantities of a 4 mg/ml solution of BSA (Sigma, USA) in PBS. Images were acquired using a LSM880 (Zeiss, Germany) laser-scanning confocal microscope, equipped with an oil-immersion Zeiss EC Plan-Neofluar 40x/NA1.3/WD0.17mm. Z-stacks were acquired through whole embryos with an optical section thickness of 1 μm. Fluorescence was excited with a 405-nm laser diode (Hoechst), a 488-nm Argon laser (Alexa Fluor 488), and a 561-nm DPSS laser (Alexa Fluor 568). For confocal microscopy of infected embryos, samples were stained with Hoechst 33342, and images were acquired using an Olympus FV3000RS laser-scanning microscope using a 40X UPLXAPO (NA=0.95). Embryos were simultaneously scanned for Hoechst and GFP using the 405-nm and 488-nm lasers. Rapid Z series were taken through the entire volume of the imaged embryos in 3 μm steps.

16.5. Results

16.5.1. Embryo Cells Express Genes Required For SARS-CoV-2 Infection

We reasoned that within the preimplantation period of human development, embryos in the blastocyst stage may become vulnerable to SARS-CoV-2 as they lose their protective zona pellucida. This structure counters the threat of many foreign agents (375). The trophectoderm, which is the precursor of the placenta (376), is located at the surface of the blastocyst and may be an early target for infecting viruses. Hence, we focused our

attention on the trophectoderm and evaluated its permissiveness to SARS-CoV-2 infection.

Two prior publications have described *ACE2* and *TMPRSS2* expression in blastocyst-stage preimplantation embryos (358, 377), albeit based on analysis of publicly available RNA-seq datasets from a single ethnic group (East Asian/Chinese) (378-380). To determine whether this pattern of gene expression is observed in more diverse populations, we performed RNA-seq on a group of 24 human blastocysts from multiple ethnic backgrounds (Supplementary Table 10). *ACE2* transcripts were detected in trophectoderm biopsies comprising 5-10 cells in 23 of 24 embryos (95.8%), and *TMPRSS2* transcripts in biopsies from all 24 embryos (Figure 28A). The group of tested embryos ranged in developmental stage from early blastocyst to hatched blastocyst, meaning that *ACE2* and *TMPRSS2* transcripts were present throughout this developmental window. We evaluated the expression of 22 additional human genes proposed to be involved in the SARS-CoV-2 life cycle (358) (Figure 28B). Positive expression was confirmed for genes encoding some putative alternate receptors (*BSG/CD147*, *ANPEP*) but not for others (*CD209*, *CLEC4G*, *CLEC4M*). There was also detectable expression of genes encoding some alternative proteases (*CTSB, CTSL, TMPRSS4*), but not others (*TMPRSS11A* and *TMPRSS11B*). Transcripts for *DPP4*, encoding the receptor used by MERS-CoV S for entry, were either absent or expressed at very low levels in our samples.

We noted expression of genes for three factors apparently required for SARS-CoV-2 genome replication (*FURIN, TOP3B* and *ZCRB1/MADP1*). Among the genes encoding factors proposed to control trafficking and/or assembly of viral components and which are known to interact with SARS-CoV-2 proteins, *RHOA, RAB10, RAB14, RAB1A, AP2M1*, and *CHMP2A* exhibited high levels of expression while *AP2A2* and *TAPT1* were expressed at lower levels. Together, these transcriptomic profiling data indicate that trophectoderm cells express many key factors required for SARS-CoV-2 entry and subsequent replication.

Figure 28. Expression Of Genes Involved In SARS-CoV-2 Infection In Embryo Cells.
Violin plots showing log10-normalized expression profiles obtained by RNA-seq performed on trophectoderm biopsies of blastocysts. Each data point represents one embryo (n=24). Each trophectoderm biopsy consisted of 5-10 cells. (A) Canonical SARS-CoV-2 entry factors *ACE2* and *TMPRSS2*. (B) Proposed alternative/ancillary mediators of SARS-CoV-2 entry, replication, traffic, and assembly.
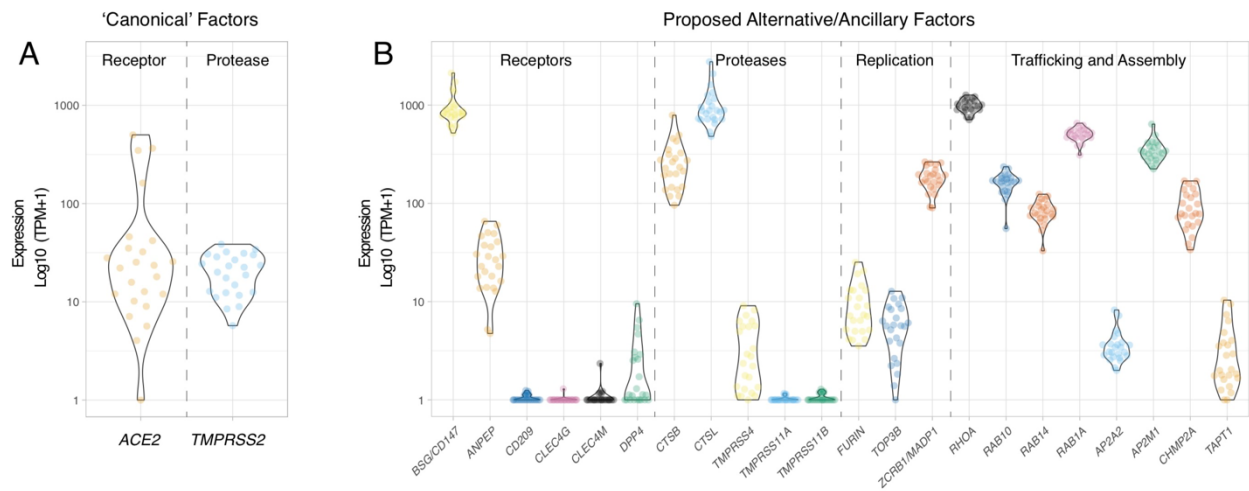
16.5.2. SARS-CoV-2 Entry Factors Localize To The Membrane Of Trophectoderm Cells

To evaluate the presence and localization of entry factors in trophectoderm cells, we performed immunofluorescence and confocal imaging for ACE2 and TMPRSS2 in blastocysts. Both factors were readily detectable in cells of the trophectoderm; ACE2 was enriched on cellular membranes, as evidenced by strong signal at cell-cell junctions (Figure 29A), while the TMPRSS2 presence was more diffuse, localizing to both cell membranes and within the cytoplasm but not nucleus (Figure 29B). The inner cell mass (ICM) was not evaluated, since the immunofluorescence protocol was not optimized for penetration of antibodies into deeper cell layers. Based on the localization of ACE2 and TMPRSS2 proteins, at least trophectoderm cells of preimplantation embryos contain the requisite entry factors needed for SARS-CoV-2 infection.

16.5.3. S-Pseudotyped Virions Utilize ACE2 For Entry Into Trophectoderm Cells

To test whether the standard S protein-mediated SARS-CoV-2 cell-entry process was functional in embryo cells, we evaluated the entry of pseudotyped reporter virions expressing S in zona pellucida-free blastocysts. In the first series of experiments (see summary on Table 8), we used an HIV-ΔEnv virus encoding a green fluorescence protein (GFP) reporter. Embryos exposed to control media or media containing the original non-pseudotyped 'bald' reporter virus displayed no fluorescence and appeared healthy 24-48 hours after mock spinoculation (inoculation by centrifugation) (Supplementary Figure 12).

Figure 29. Localization Of ACE2 And TMPRSS2 In Embryos.
Maximum intensity projections (MIPs) of confocal z-stacks of blastocysts, showing nuclei (blue) and ACE2 or TMPRSS2 (white). Pink arrowheads point to cell membranes. Scale bars represent 50 μm in low magnification panels, and 10 μm in high magnification panels. Representative images from independent biological replicates (n=5 embryos for each factor).
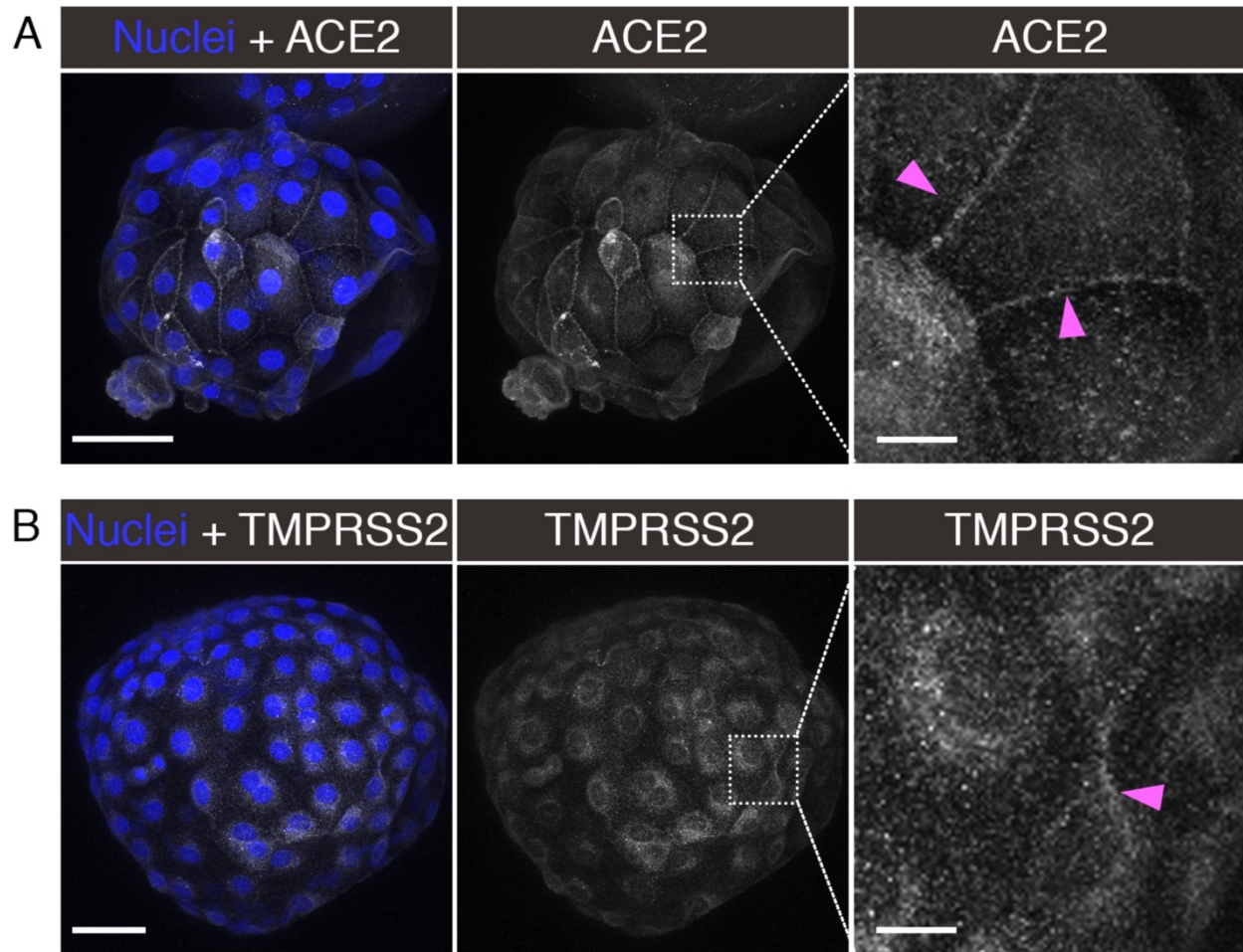
However, when embryos were exposed to the reporter virus pseudotyped with the S protein from SARS-CoV-2, several showed robust GFP signal in numerous trophectoderm cells (Figure 30A and Supplementary Figure 12). Treatment of the

blastocysts with neutralizing anti-S antibodies markedly decreased GFP fluorescence to a limited number of puncta (Supplementary Figure 12).

Table 8. Summary Of Experiments Using Pseudotyped Reporter Virions.
For each reporter virion (HIV- or VSVΔG -based), the table indicates the experimental condition, the number of embryos used, and the number/percent of infected embryos as evidenced by GFP signal.

HIV-based Reporter

Treatment	Number of Embryos Tested	GFP Positive Embryos
No Treatment	15	0
No Pseudotype ('Bald') Virus	15	0
SARS-CoV-2 Pseudotyped Virus	15	6 (40%)
SARS-CoV-2 Pseudotyped Virus + anti-S neutralizing Antibody	7	1 (14.3%) with limited puncta

VSVΔG -based Reporter

Treatment	Number of Embryos Tested	GFP Positive Embryos
No Treatment	4	0
No Pseudotype ('Bald') Virus	5	0
SARS-CoV-2 S Pseudotyped Virus	7	4 (57.1%)
SARS-CoV-2 S Pseudotyped Virus + anti-S neutralizing Antibody	4	0
SARS-CoV-2 S Pseudotyped Virus + anti-ACE2 neutralizing Antibody	4	2 (50%) with limited puncta
SARS-CoV-2 S Pseudotyped Virus + anti-IgG neutralizing Antibody	6	4 (66.7%)
SARS-CoV-1 S Pseudotyped Virus	5	4 (80%)
MERS-CoV S Pseudotyped Virus	5	0

In the second experimental series (see summary on Table 8), we used a vesicular stomatitis virus lacking the cell entry factor G glycoprotein (VSVΔG), and encoding GFP as a reporter. No fluorescence was detected when embryos were exposed to control media or media containing the non-pseudotyped 'bald' virions . Conversely, several

samples exhibited GFP when exposed to the reporter virus pseudotyped with the SARS-CoV-2 S protein (Figure 30B and Supplementary Figure 12). Addition of a neutralizing antibody targeting either S or ACE2 strongly reduced GFP expression, while addition of a control non-specific anti-IgG antibody resulted in undiminished GFP expression in several embryos (Supplementary Figure 12). When the VSVΔG-based reporter virus was pseudotyped with the S protein from SARS-CoV-1, which also utilizes the ACE2 receptor for cell entry, embryos again displayed GFP signal. Conversely, reporter virus pseudotyped with the S protein from MERS-CoV, which depends on the dipeptidyl peptidase 4 (DPP4) receptor for cell entry, produced no GFP signal (Supplementary Figure 12).

In these experiments using pseudotyped reporter virions, embryos with evidence of infection displayed occasional cell degradation, likely due to expression of native genes in the HIV- and VSV-based reporter virions (Supplementary Figure 12).

Together, these pseudotyped-virion experiments indicate that trophectoderm cells present in preimplantation embryos are permissive to SARS-CoV-2 entry involving interactions between S and the ACE2 receptor.

16.5.4. Live SARS-CoV-2 Infects Human Embryos

We next tested the susceptibility of embryos to live SARS-CoV-2 infection.

Figure 30. Embryo Infection By Reporter Virions Pseudotyped With The S Protein Of SARS-CoV-2.
Sample confocal MIP images of embryos infected with (A) HIV- based or (B) VSVΔG -based reporter virions pseudotyped with the S protein from SARS-CoV-2. Pink arrowheads point to cells displaying robust signal. Scale bars represent 20 *μ*m. Representative images from independent biological replicates (n=15 embryos with HIV-based virion, n=7 embryos with VSVΔG -based virion).
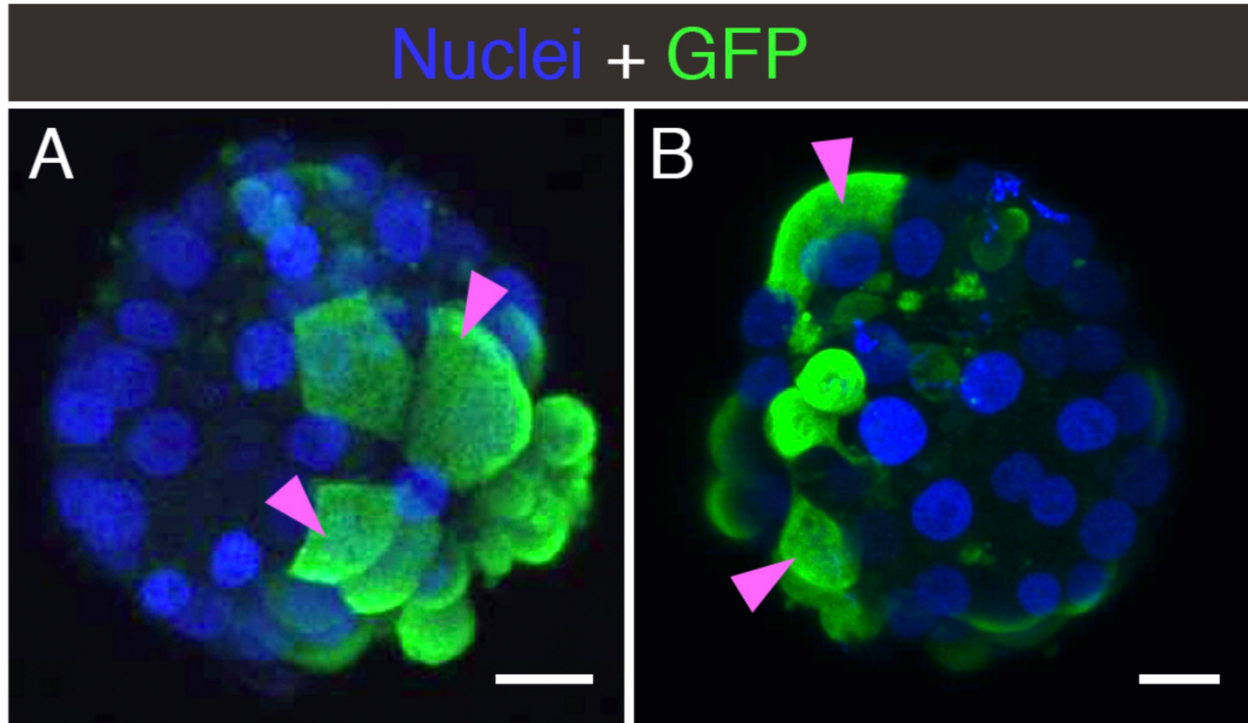
Embryos were exposed to a version of SARS-CoV-2 that, in addition to possessing its full native infectivity, also expresses a fluorescent reporter protein facilitating visualization of infected cells (374). For this experiment, we did not remove the zona pellucida from blastocysts growing in vitro. As a result, the samples contained a mix of embryos at different stages of blastocyst development, ranging from non-hatched (fully encapsulated by the zona pellucida), to hatching (some cells herniating out of an opening in zona pellucida), to fully hatched (all embryo cells have fully emerged from the zona pellucida).

Some embryos readily displayed evidence of infection when exposed to the virus (Figure 31A and
Table 9), which could be prevented with neutralizing antibodies targeting S or ACE2, but not with a non-specific anti-IgG antibody (Supplementary Figure 13 and
Table 9). Infected cells were predominantly in the trophectoderm, but in some instances,

there was also evidence of infection in the ICM (Figure 31B).

Figure 31. Embryos Exposed To Live SARS-CoV-2 Are Susceptible To Infection.
Fluorescent signal indicates cells infected with icSARS-CoV-2-mNeonGreen. (A) Four sample blastocysts exposed to the virus. One blastocyst has not initiated hatching and shows no evidence of infection, two blastocysts are at early stages of hatching (one shows evidence of infection in the herniating cells), and one blastocyst is in advanced hatching phase showing high incidence of infected cells. (B) High magnification of blastocyst with high incidence of positive cells, with two panels showing the mNeonGreen channel at different focus depths (z-axis). White arrowheads point to positive herniating cells in hatching blastocysts, pink arrowhead points to positive cells in the zona pellucida compartment of a hatching blastocyst. Representative images from independent biological replicates (n=19 embryos). icm = inner cell mass. bc = blastocoel cavity. zp = zona pellucida. Scale bar represents 100 μm.
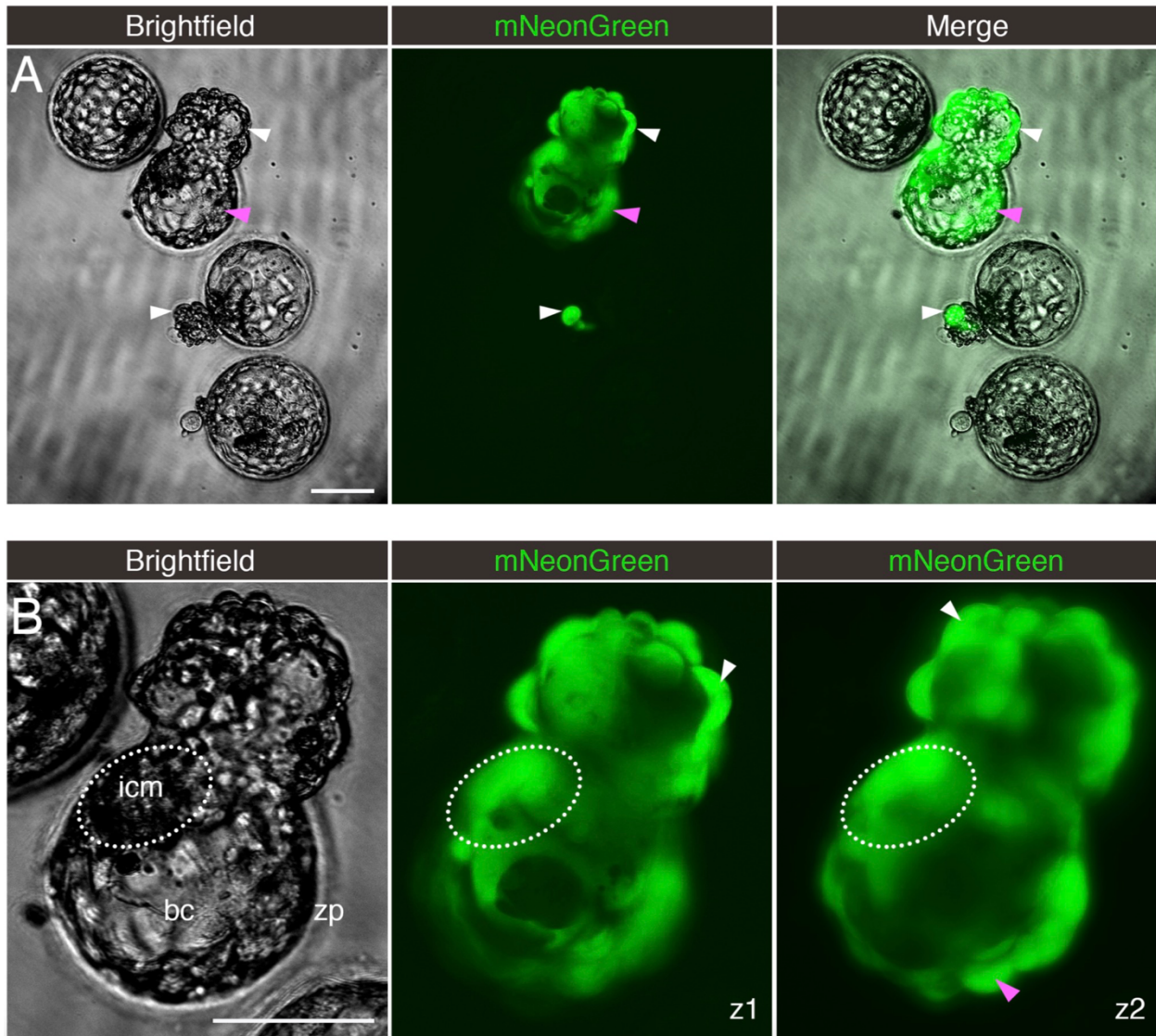
Table 9. Summary Of Experiments Using Live, Fully-Infectious SARS-CoV-2.
The table indicates the experimental condition, the number of embryos used, and the number/percent of infected embryos as evidenced by fluorescent signal.

SARS-CoV-2-mNeonGreen Virus

Treatment	Number of Embryos Tested	Embryos w/ Fluorescent Cells
No Treatment	9	0
Virus	19	14 (73.7%)
Virus + anti-S neutralizing Antibody	4	0
Virus + anti-ACE2 neutralizing Antibody	4	0
Virus + anti-IgG neutralizing Antibody	7	4 (57.1%)

Infection was uncommon in non-hatching blastocysts, common in hatching blastocysts, and frequent in fully hatched blastocysts (Figure 32A). Only one non-hatching blastocyst displayed evidence of infection (Figure 32B). Some hatching blastocysts only contained infected cells in the herniating (zona pellucida-free) compartment (Figure 32C). Others had infected cells in both herniating and non-herniating compartments, however cells proximal to the zona opening were more readily infected than cells distal to the zona opening (Figure 32D-E). We confirmed that experimental groups showing no infection (no virus, anti-S, and anti-ACE2) did not contain a overrepresentation of non-hatching embryos (Supplementary Table 11).

These live SARS-CoV-2 virus experiments show that embryos are susceptible to infection, and the zona pellucida might confer protection.

Figure 32. The Zona Pellucida Might Confer Protection Against SARS-CoV-2 Infection.
(A) Pie charts indicating the proportion of blastocysts displaying evidence of infection at three separate stages of development (before, during, and after hatching), when exposed to live SARS-CoV-2 expressing a fluorescent reporter (in the presence or absence of control IgG blocking antibody). Non-hatching blastocysts have an intact zona pellucida, hatching blastocysts have some cells herniating out of the zona pellucida opening as well as some cells confined in the zona pellucida compartment, and fully hatched blastocysts have emerged completely out of the zona pellucida. (B) Only example of a non-hatching blastocyst with zona pellucida-encapsulated positive cells (orange arrowhead). (C) Example of a hatching blastocyst with positive cells exclusively in the herniating compartment. (D, E) Examples of hatching blastocysts, with positive cells in the herniating compartment (white arrowheads) as well as in cells proximal to the zona pellucida opening (pink arrowheads). zp = zona pellucida. Scale bars represent 50 μm.
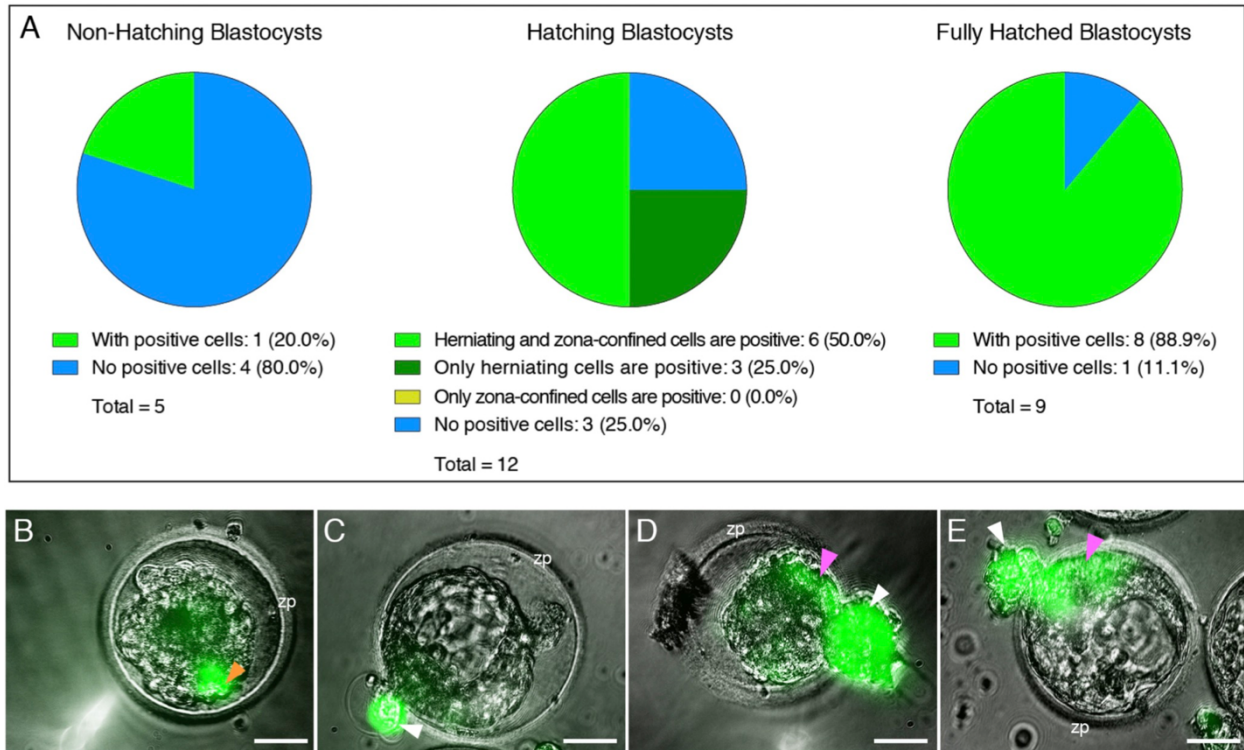
16.5.5. Infection By SARS-CoV-2 Induces Cytopathicity And Affects Embryo Health

In the course of the SARS-CoV-2 live virus experiments we noted an impact on embryo health. Embryos with evidence of infection (with visible reporter signal) often displayed signs of cell degeneration. This ranged from focal cell degradation, particularly in infected (fluorescent) areas of the embryo, to severely affected embryo health, and at times to embryo collapse and global cell death (Figure 33A-F). On average, infected embryos exhibited morphologic signs of considerably poorer health and morphology at 12-16 hours post-infection compared to embryos that had gone through the same spinoculation protocol but had not been infected. Out of 18 embryos with evidence of infection, only one appeared in good health, while four displayed focal damage, five exhibited severe cellular degeneration (but were still alive), and eight embryos had completely collapsed and were dead (Figure 33G). Out of the 25 embryos with no evidence of infection, 16 appeared in good health, while eight showed some cell damage, and one had severe cytopathic changes (likely due to the stress of spinoculation and subsequent culturing) (Figure 33G). These findings suggest a cytopathic effect of infection, which can at times lead to embryo demise.

Figure 33. Embryo Health Is Negatively Affected By SARS-CoV-2 Infection.
Sample images of infected embryos with various degrees of cytopathic effects. (A-B) Embryo with cell damage (yellow arrowheads) in fluorescent (infected) cells in the herniating and zona pellucida compartments. (C) Infected herniating embryo (bottom) with severely affected health, and non-infected embryo (top) with good health. (D) Hatched infected embryo next to empty zona pellucida, displaying global cell death. (E-F) Examples of infected embryos displaying total collapse and death. (G) Summary of embryo health 12-16 hours after exposure to SARS-CoV-2. Top bar includes all embryos

with evidence of infection (fluorescent cells). Bottom bar includes all embryos with no evidence of infection (no fluorescent cells). Scale bars represent 50 *µ*m.
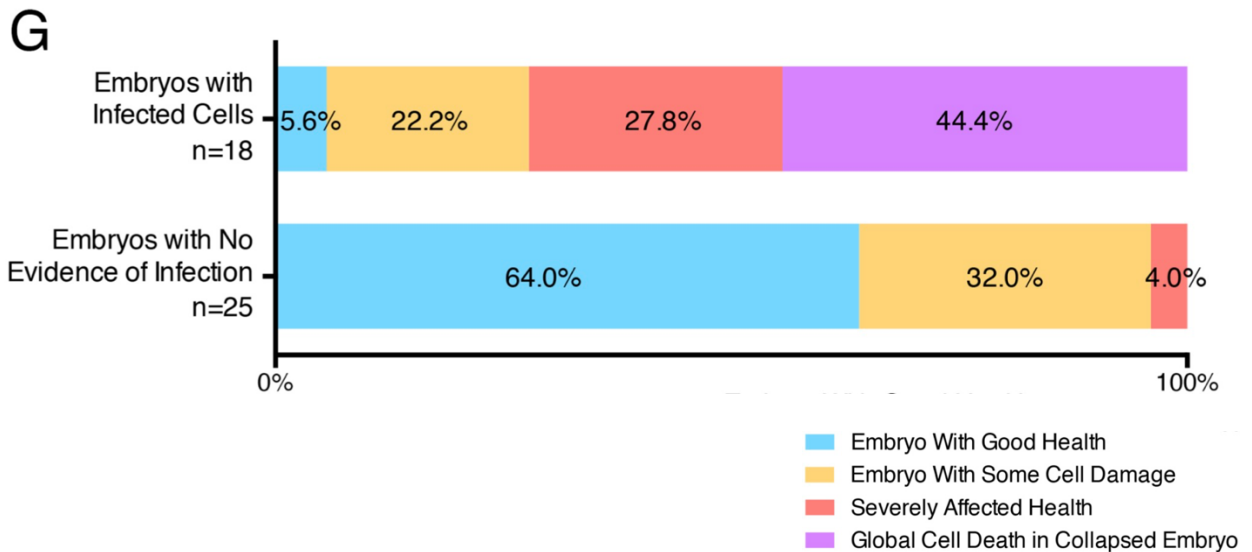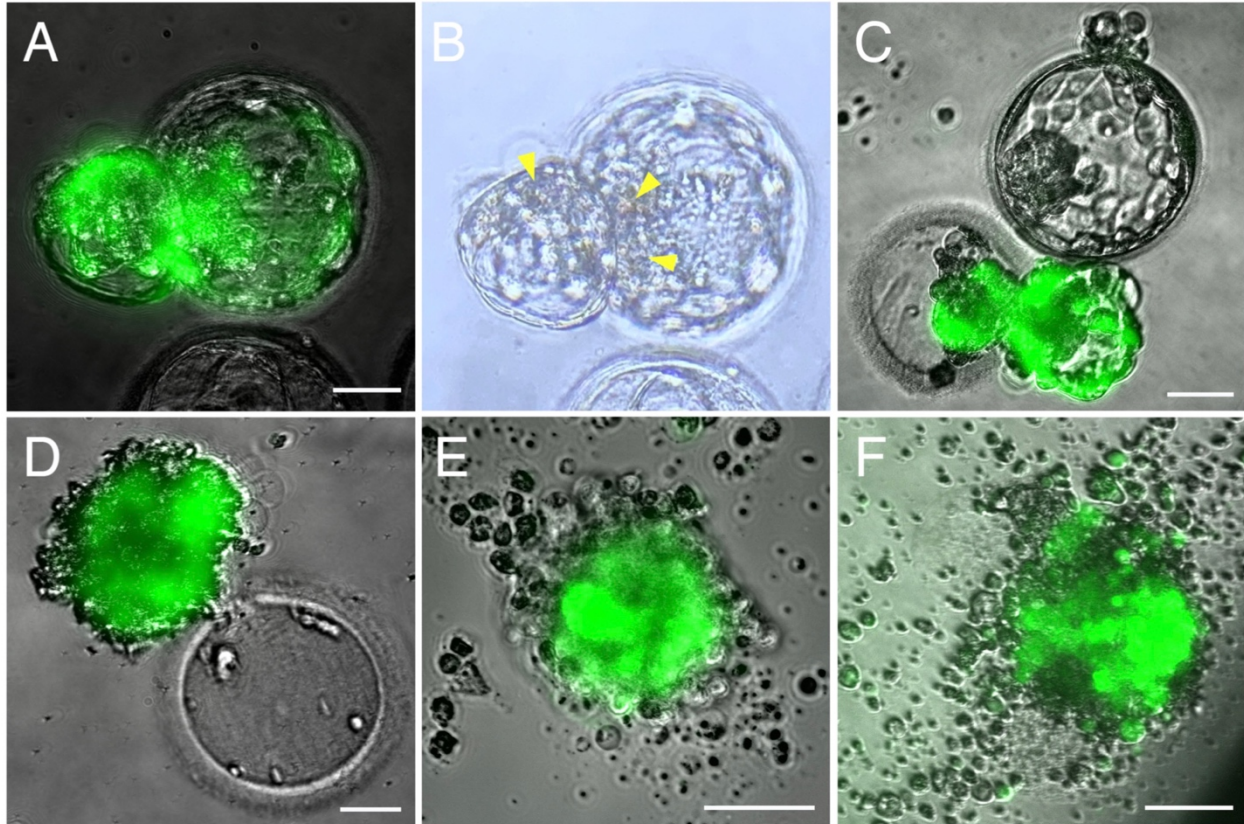
16.6. Chapter Discussion

This study shows that some cells within the human embryo 1) express and correctly localize factors required for SARS-CoV-2 entry, 2) are permissive to viral entry via the S-ACE2 ligand-receptor system, 3) are susceptible to live virus infection, which can produce cytopathic effects, and 5) may be protected against SARS-CoV-2 infection by the zona pellucida. Together, these findings confirm that human embryos at the blastocyst stage prior to implantation are susceptible to SARS-CoV-2 infection, which can impact their viability.

The RNA-seq experiments show that embryos from multiple ethnic backgrounds express the canonical entry factor genes *ACE2* and *TMPRSS2* in trophectoderm cells (conceptually the most vulnerable cell lineage to viral infection as these cells form the outer cell layer of the embryo and ultimately give rise to the placenta). These findings confirm and extend prior reports of *ACE2* and *TRMPRSS2* embryonic expression in a single ethnic group (East Asian/China) (378-380). Membrane localization of the SARS-CoV-2 receptor ACE2 observed on trophectoderm cells confirms and extends a previous immunofluorescence microscopy study employing a different commercially-available anti-ACE2 antibody (381). In addition, we further detect TMPRSS2 protein localization in these same cells. TMPRSS2 cleavage of S primes the S2 component for effective virion fusion (354, 355).

The experiments using reporter virions corroborate involvement of S and ACE2. Only virions pseudotyped with the SARS-COV-2 S protein could infect cells of the embryo. Addition of blocking antibodies reactive with either S or ACE2 reduces infection by the pseudotyped virions, implicating a functional interplay between S and ACE2 for virion entry. Embryos also displayed evidence of infection by reporter virions pseudotyped with the S protein from SARS-CoV-1 (which similarly uses ACE2 for entry) but not with the S protein from MERS-CoV (which uses DPP4 for entry). These findings further support the conclusion that ACE2 functions as an effective SARS-CoV-2 receptor in trophectoderm cells.

Finally, using live SARS-CoV-2, we confirm that trophectoderm cells of the embryos are susceptible to viral infection. Infection may also extend to the ICM (the precursor of the fetus). Of note, not all embryos exposed to SARS-CoV-2 showed evidence of infection and when infection occurred, not all of the cells uniformly expressed the viral reporter. Infection is likely dependent on numerous factors, including: grade of an embryo at the time of exposure, timing of infection, and effective titers of the virus (viral copy numbers to which cells are exposed). Our goal was not to achieve maximum infection efficiency, but rather to determine whether cells of the embryo are at all permissive to infection. The observation that the zona pellucida confers protection from infection was reinforced in studies showing preferential infection of cells herniating from the zona during hatching. Embryos infected with live virus displayed evidence of viral cytopathic effects ranging

from focal changes to death of the entire embryo likely determined by the overall levels of infection achieved in each embryo.

The finding that preimplantation embryos are susceptible to SARS-CoV-2 infection raises the possibility of viral transmission from either the mother or father to the developing embryo. Vertical transmission of SARS-CoV-2 between pregnant mothers and fetuses has been reported (382-387), albeit considerably later in pregnancy. Of note, these studies implicate the placenta, which develops from the trophectoderm, as the principal site of viral infection and subsequent transmission (384, 387-389). It is estimated that placental infection occurs in 21% of COVID-19 pregnancies, while 2% of neonates show SARS-CoV-2 positivity (390). A placenta infected by SARS-CoV-2 often shows signs of injury characterized by trophoblast necrosis (391, 392). Studies analyzing the delivered placentas of SARS-CoV-2 positive pregnant women revealed widespread and diffuse trophoblastic damage sufficient to undermine fetal health (387, 393).

Could vertical transmission of SARS-CoV-2 occur whereby preimplantation embryos are infected? Numerous studies have failed to identify virus in male and female reproductive organs of infected patients (394-396). However, a more recent study detected the virus in vaginal swabs of two out of 35 women with COVID-19 (372), and two groups have reported virus in semen of infected men (370, 371). For example, a study by Li and colleagues found that six of 38 male COVID-19 patients had detectable levels of SARS-CoV-2 in their semen (370). Virus in vaginal fluid or semen could potentially infect a newly

conceived embryo prior to implantation, potentially compromising establishment or maintenance of the pregnancy. In view of this, our data highlights the need for expectant mothers or couples considering pregnancy to fully vaccinate to help prevent SARS-CoV-2 infection that could jeopardize their health and their pregnancy (397-399).

In comparison to embryos from natural conceptions, embryos generated by assisted reproductive technologies (ART) for treatment of infertility, such as *in vitro* fertilization (IVF), face additional risks of potential viral exposure. These include exposure to virus shed by asymptomatically infected medical and laboratory personnel during various procedures (handling of gametes, assisted conception, embryo culture, biopsy, vitrification, and thawing), or by infected patients (for example, a male patient contaminating a sample vial during sperm collection, via regular exhalation). The data presented here should inform best practices in the ART clinic during the COVID-19 pandemic, further building on existing recommendations for safety and risk mitigation (400-404).

SARS-CoV-2 infection in pregnant women is associated with increased risk of miscarriage, prematurity, and impaired fetal growth (405). Such adverse fetal outcomes have mainly been attributed to COVID-19-related complications in pregnant patients (405), but could reflect infection of the placenta or fetus during pregnancy (382-385, 389, 393). The present study raises the possibility of vertical transmission during preimplantation stages. Of note, the zona pellucida appears to protect the embryo from

infection (likely starting at the zygote stage) but inevitably the blastocyst becomes exposed at hatching, which is a necessary event prior to implantation into the maternal endometrium. Given the trophectoderm's central role in implantation, compromised health of trophectoderm cells due to SARS-CoV-2 infection could altogether impede establishment of a pregnancy. The same result (no pregnancy) would inevitably occur in the the case of complete embryo collapse, as we observed in a substantial proportion of infected blastocysts. Alternatively, lasting detrimental effects on the trophectoderm-derived placenta could affect the clinical outcome of an established pregnancy by increasing the risk of spontaneous abortion, intrauterine growth restriction (IUGR), or stillbirth, as has been noted in instances of placental infection (387, 393).

Noting that our transcriptomic analysis revealed RNA presence of various factors associated with downstream steps of the SARS-CoV-2 viral life cycle, such as genome replication, trafficking and assembly (358), the possibility of trophectoderm cells infecting surrounding tissues (maternal or fetal) after additional viral shedding cannot be excluded. Our observation that the ICM might itself be vulnerable to infection further highlights this risk. Ultimately, population effects of the COVID-19 pandemic on fertility may become apparent when epidemiological data on pregnancies and birth rates become more readily available.

A weakness of the study is that it primarily focuses on one embryonic tissue, namely the trophectoderm: 1) the RNA-seq experiment specifically probed trophectoderm cells, 2)

The immunostaining experiments used a protocol optimized for cell membrane-bound factors on the surface of the embryo (precluding analysis of deeper cell layers), 3) The pseudotyped virion experiments made use of non-replicative agents, meaning that even with entry into the outer cell layer, subsequent infection of deeper layers was not possible. Only the live, fully infectious (and replicative) SARS-CoV-2 experiment was informative regarding potential infection of the ICM. It should be noted however, that by forming the outside layer of the blastocyst, the trophectoderm constitutes the primary site of exposure to viral infection. This means we assessed the likeliest first step of an embryo infection by SARS-CoV-2. A further caveat of the study is that it exclusively used *in vitro*-generated embryos, and the findings might not be entirely applicable to preimplantation embryos derived from natural conceptions.

Future experiments will need to define the presence/absence of virus in the setting of natural conceptions and IVF treatment around embryos, to better understand the risks and take appropriate measures. Also, future work should continue addressing the direct consequences of infection on individual cells, embryo viability, and pregnancy outcomes. In summary, our finding that preimplantation embryos are susceptible to SARS-CoV-2 infection *in vitro* raises the potential vulnerability of these embryos *in vivo*. Additionally, the data presented here should prompt careful review of procedures surrounding assisted reproduction during the COVID-19 pandemic and its aftermath.

17. General Discussion

Methods to evaluate embryos have been used since the early days of IVF. The goal is to select those embryo(s) for transfer with the highest chance of achieving implantation, ongoing pregnancy, and healthy live birth. The main goal of the project constituting this thesis was to perform a thorough and unbiased evaluation of current methods of embryos selection. It was largely successful in the fulfilment of its specific aims, namely, that I determined the following:

- A clinical TE biopsy is a good predictor of the remaining blastocyst's chromosomal status for whole chromosome aneuploidy, but not segmental aneuploidy; i.e. there is good concordance between biopsy and blastocyst (specific Aim A - see chapter 10)
- Embryos classified as mosaic by PGT-A (TE biopsy) do indeed have inferior clinical success rates than euploid embryos, but can nonetheless result in healthy pregnancies (specific Aim B - see chapter 11)
- Features of mosaicism detected with PGT-A can serve to sub-rank mosaic embryos to increase likelihood of achieving live birth (specific Aim C - see chapter 12)
- Accurate quantitation of mitochondrial DNA (mtDNA) in human blastocysts is not a biomarker of ploidy nor a predictor of implantation (specific Aim D - see chapter 13)

- Embryos with high mtDNA content can result in healthy births (specific Aim E - see chapter 14)

- PGT largely obviates the clinical need for germline genome editing (GGE), but GGE might still become a useful tool to correct aneuploidies detected by PGT-A in certain instances (specific Aim F - see chapter 15)

- SARS-CoV-2, the virus responsible for COVID-19, can infect human embryos, affect their viability and thus impact PGT-A strategies for embryo selection (specific Aim G - see chapter 16)

One of the most significant advancements in the field of ART has been the vetting of embryos for chromosomal abnormalities prior to embryo transfer. Collectively known as PGT-A (previously PGS, PGD-A, or CCS), its implementation is widespread among IVF clinics across the world. Nonetheless, the determination of which blastocysts should be tested, and its overall success in improving birth rates are current topics of debate. Furthermore, the basic premise of the method is that an embryo biopsy (a small group of cells removed from the embryo), can be a valuable representative of the whole embryo's chromosomal content. However, at the onset of my project this assumption remained to be confirmed. Mosaicism can theoretically be a root cause for many miscalls of aneuploidy, because the biopsy being probed might contain a different chromosomal set compared to the other cells in the embryo. Concerns have been expressed in the scientific literature as well as in popular media about the possibility that blastocysts testing 'aneuploid' might be incorrectly de-selected for IVF and discarded.

In Specific Aim A (Chapter 10) we asked a simple yet important question: How well does a clinical TE biopsy predict chromosomal aneuploidy in the remaining embryo, and specifically the ICM? Previous studies exploring this issue have analyzed small sample sizes or have relied on technologies that have been superseded by Next Generation Sequencing (NGS), currently the most accurate method to quantify all chromosomes in a cellular sample. The concordance study presented in this thesis is the largest study to date and the first to use NGS for this analysis.

Our results show that whole chromosome aneuploidy in the ICM is efficiently predicted by a TE biopsy, but segmental aneuploidy is not well correlated between TE and ICM. The clinical implications of these findings are twofold. One, the high concordance rate between TE and ICM in cases involving whole chromosome aneuploidy provides experimental validation for the practice of PGT-A at the blastocyst stage. Two, a PGT-A result indicating segmental aneuploidy is potentially false, and a re-biopsy might be recommended because the second TE biopsy can reveal the true status of the ICM.

Therefore, a TE biopsy with uniform whole chromosome aneuploidy by PGT-A is rarely discordant with the ploidy of the ICM (something that could have been caused by mosaicism). This, however, was not informative for cases in which evidence of mosaicism is present within the biopsy itself, which is the subject of Specific Aims B and C (Chapters 11 and 12, respectively).

Chromosomal mosaicism detected during PGT-A is currently a hotly debated topic in the ART community. A handful of studies have described the clinical transfer of such mosaic embryos (164, 171, 172), but to our knowledge, the work described in Specific Aim B (Chapter 11) is the first report to satisfy two conditions: the prospective transfer of embryos (with previous knowledge of the classification of mosaicism) and the exclusive use of next-generation sequencing (NGS) in PGT-A, which is now recognized as the most accurate method to detect mosaicism in a trophectoderm biopsy (108). Previous studies in the field, while tremendously valuable, have either been conducted in a retrospective manner, or have relied partly or fully on previous technologies of PGT-A. In addition, analyzing the outcome of 100 mosaic embryos, it is the largest single-clinic study yet.

The results indicate that mosaic embryos (those with evidence of mosaicism in the TE biopsy) have lower rates of implantation than embryos with uniformly euploid results. We also addressed a question that many have asked: How are mosaic embryos, which clearly contain a component of aneuploid cells, capable of resulting in seemingly healthy pregnancies and babies? Interesting models of self-correction have been suggested and tested in model organisms or cell lines, but we investigate these concepts experimentally for the first time in human embryos. My data shows a clear difference between mosaic and euploid embryos regarding rates of cell proliferation and death. Mosaic embryos are more active on both counts, which likely reflects the ongoing process of self-correction;

Aneuploid cells selectively undergo apoptosis, while euploid cells proliferate faster than usual to compensate and achieve a normal total cell count in the embryo.

To develop evidence-based recommendations regarding mosaic embryo transfers, we initiated a large international collaboration between six centers to compile genetic and clinical outcome data for 1,000 mosaic embryo transfers. The ensuing analysis, discussed in Chapter 12 (Specific Aim C) reveals with statistical significance what parameters of mosaicism detected during PGT-A affect success rates in the IVF clinic. The data shows that the level of mosaicism, which is the putative percent aneuploid cells in the TE biopsy, significantly influences the chances of success. Embryos with low level mosaicism (<50%) on average have higher rates of implantation, achieving ongoing pregnancy and live birth, and lower rates of spontaneous abortions compared to high level mosaics (≥ 50%). Also, the type of mosaicism (i.e. what type of aneuploidy is involved in the mosaicism) significantly affects chances of success. Segmental abnormalities have significantly better average clinical outcomes than whole chromosome aneuploidies, which in turn are favorable to complex aneuploidies affecting more than 2 chromosomes.

I believe these findings to be of importance for two reasons:

1) This report will serve as a reference for clinics worldwide, as it provides an evidence-based ranking system for embryos classified as mosaic by PGT-A.

2) The manuscript makes an important technical point. The observation that different sub-classes of mosaic embryos have distinct patterns of clinical outcomes clearly argues in

favor of mosaicism being a true biological phenomenon rather than an artifact of the PGT-A process, as some have argued.

Because embryo selection also involves the consideration of morphology, we further refined the outcome data through integration of PGT-A sub-category and embryo stage and grade. Again, further sub-trends became apparent within the various groups. The resulting matrix of values can serve prospectively in the clinic to rank embryos. We developed a freely accessible online tool that allows the user to input the characteristics of two or more embryos and determine their relative potential for clinical success, based on the experience gathered from the one-thousand mosaic embryo study (https://embryo-score.web.app/).

The hesitation to transfer embryos in which mosaicism is detected is obvious and justified. After all, chromosomal mosaicism is one underlying cause of human disorders and confined placental mosaicism (CPM), which can lead to placental dysfunction (406). Of the 247 babies born in the thousand mosaic embryo study, none had notable birth defects. A more complete set of data was collected for 162 newborns, each with a matching baby born from a euploid embryo transfer. The average birth weight and length of gestation was equal between the two groups, and no overt symptoms associated with chromosomal abnormalities were reported in the babies from mosaic embryos (407). After mosaic embryo transfers, in over 100 amniocentesis results and over 200 prenatal testing results across all platforms (amniocentesis, CVS, and NIPT), there were five instances of

abnormalities (407, 408). All five were amniocentesis cases, which identified segmental imbalances smaller than the resolution of contemporary PGT-A NGS platforms and were unrelated to the mosaicism detected with PGT-A. Therefore, in this sample group, the mosaicism observed at the blastocyst stage never persisted through gestation.

How could blastocyst-stage mosaicism 'disappear'? Data from mosaic embryo transfers represents indirect clinical evidence for 'self-correction' via a mechanism of 'clonal depletion' (409), whereby aneuploid cells of mosaic embryos are outcompeted by euploid cells through differential proliferation and/or directed apoptosis. Indeed, there is a well-documented, universal link between aneuploidy and attenuated cell proliferation in humans and other organisms (242) (with the notable exception of cancer, where aneuploidy is common, but increased proliferation is primarily a consequence of mutations in oncogenes and tumor suppressor genes). Thus, mosaic embryos could develop into healthy babies if aneuploid cells are sufficiently diluted out during pregnancy, such that by the time of delivery (or much earlier, judging by prenatal testing results) there is no observable trace. In further support of this point, a study profiling the genomic landscape of fetal and placental tissues postpartum from both IVF and naturally conceived children showed that mosaicism was not preserved at later stages of prenatal development and that *de novo* numerical aberrations or large structural DNA imbalances occur at similar rates in IVF and naturally conceived neonates (410).

There is mounting experimental evidence for self-correction of embryonic mosaicism. Single-cell RNA-seq in mosaic embryos indicates that aneuploid cells downregulate proliferation genes, and the average incidence of aneuploid cells steadily decreases between the cleavage stage and the late blastocyst stage of development (411, 412). Extended *in vitro* culture assays show that mosaic blastocysts tend to become fully euploid in what is equivalent to the early stages post-implantation (175). Human gastruloids (models of gastrulation-stage embryos derived from embryonic stem cells), in which mosaicism was chemically induced, are prone to losing the aneuploid compartment over time due to directed apoptosis (412). Mouse chimeric blastocysts composed of euploid and aneuploid cells usually become fully euploid when the initial aneuploid-to-euploid ratio is equal or low but tend to perish if the initial proportion of aneuploid cells is high (218). This mouse model of mosaicism shows attenuated proliferation and preferential apoptosis of aneuploid cells, which is compensated by increased proliferation of euploid cells (243).

It is therefore logical that a disconnect should exist between mosaicism at the blastocyst stage and the (typically normal) karyotype later in pregnancy. There has only been one report to date of an amniocentesis reflecting the mosaicism detected with PGT-A (248). The pregnancy resulted in a live birth, and the phenotypically healthy baby showed evidence of mosaicism in a blood sample (but not in a buccal swab). The measured level of mosaicism declined over time from 35% with PGT-A to 2% with amniocentesis and 2% in one tissue at birth. This case argues for continued heightened surveillance of

pregnancies from mosaic embryo transfers by careful monitoring of fetal growth and prenatal testing. Time and additional data will tell whether that single case is an outlier, or if persistence of mosaicism throughout gestation is more common than the bulk of the data currently indicates.

Considering the data in our study, the original binary classification system of embryos into 'normal' and 'abnormal' groups seems obsolete. If this system is retained, embryos that should be classified as 'mosaic' would be included in either the 'normal' or the 'abnormal group', over- or under-valuing their developmental potential, respectively. Failure to differentiate between 'euploids' and 'mosaics' may impact clinical success rates, considering the poorer outcomes of the latter. Conversely, grouping the mosaic category with the aneuploid category would mean discarding viable embryos, and if no euploids are available, denying patients a potential pregnancy. The mosaic category should be further stratified into sub-groups according to mosaicism level and type, such that, when given the choice, the embryo with the best chances of clinical success can be prioritized.

It is also important to note the distinction between self-correction in a mosaic setting (described above), and cell-intrinsic forms of self-correction (so called aneuploidy-rescue). In the latter, aneuploidies would be corrected within cells, and would allow a fully aneuploid embryo (arising from a meiotic error) to amend itself, at least in part. This could lead to the idea of transferring embryos with a PGT-A result indicating a uniform aneuploidy, with the hope that they would self-correct. However, the evidence for this

mechanism in human IVF embryos remains scarce. Intracellular correction by endoreplication (for a monosomy) or trisomy rescue (141) would often result in uniparental disomy (UPD), an extremely rare occurrence in IVF-generated blastocysts (244). If by that stage the aneuploidy has not been corrected, the embryo is unlikely to result in a healthy pregnancy. In fact, transfers of embryos classified as uniformly aneuploid (non-mosaic) with PGT-A have virtually no chance of resulting in a healthy pregnancy, let alone a normal baby (232, 245). Therefore, under no circumstances should embryos with a mosaic result be conflated with those of an aneuploid result into one single 'abnormal' group.

It is crucial to assess the accuracy of each individual PGT-A platform for calling mosaicism. Specifically, platform validation should be performed in such a way to ensure that particular features of mosaicism (level and type) can be accurately assessed.

This can be accomplished with experiments in which cells or extracted DNA of euploid and aneuploid control samples are mixed in known proportions, subjected to the complete PGT-A protocol, and results compared with expectations. The reaction should contain 5-10 cells or amounts of DNA equivalent to that cell range, thereby mimicking a clinical TE biopsy. Using cell lines with different aneuploidies (both whole chromosome and segmental abnormalities) and preparing various mixture ratios (1:9, 2:8. 3:7, etc.) allows for thorough assessment of detection accuracy.

Several groups have successfully validated NGS-based PGT-A platforms for accurate ICN identification with such mixing experiments (37, 107, 108, 164, 165, 171, 204, 413). One study compared two widely adopted commercial platforms, confirming high resolution between mosaic intervals (20% for Veriseq, Illumina/Vitrolife and 30% for Reproseq, ThermoFisher) (414). This demonstrated degree of accuracy contradicts the notion that the intermediate outcomes for 'mosaic' embryos observed in clinical studies may be attributed to the fact that they are actually a combination of misdiagnosed uniform euploid and aneuploid embryos (a concept that also neglects the vast data documenting the common existence of mosaicism in embryos). It is equally important for each PGT-A platform and center to define appropriate quality control cutoffs with the noise-quantifying metrics of the analysis software to preclude 'messy' karyotype profiles (consequence of technical noise) from being classified as 'mosaic' simply because values fall in the ICN range. In such cases, the source blastocysts should be managed as undiagnosed embryos or be considered for re-biopsy.

It follows that given appropriate validation, a 'high complex' mosaic sample, for example, should produce the same results across laboratories, and so on for all mosaic sub-categories. Any PGT-A technology that correctly identifies mosaicism should ultimately produce similar clinical outcome associations to those observed in the thousand mosaic embryo study, and the ranking system should therefore be transferrable across clinics.

Regarding the predictive value of the embryo biopsy, PGT-A is very different from its cousin, diagnostic preimplantation genetic testing for monogenic disorders (PGT-M). In PGT-M, the biopsy serves as an ideal genetic representation of the remaining blastocyst, as well as the future fetus. In the case of chromosomal analysis with PGT-A, the phenomenon of mosaicism complicates the role of the biopsy as 'representative'. Aneuploidies derived from meiotic errors are present in the oocyte (or occasionally, the sperm), affect the resulting zygote, and thus uniformly impact all cells of the blastocyst (except in the unlikely event of aneuploidy rescue). Indeed, fully 'euploid' or 'aneuploid' PGT-A results from a TE biopsy tend to be perfectly concordant with the remaining blastocyst (174, 415, 416), though noting that meiotic and mitotic errors are not mutually exclusive and may co-occur. In contrast, a result indicating mosaicism in the TE biopsy is a poor predictor of the embryo's global chromosomal make-up (415), due to randomness in the sampling of cells. Furthermore, considering mosaic self-correction discussed above, a mosaic PGT-A result at the blastocyst stage will rarely (if ever) be predictive of the karyotype of the placenta or fetus later in the pregnancy. Hence, it might seem highly counterintuitive that mosaicism detected in the biopsy should be predictive in any capacity.

Nevertheless, the results of the thousand mosaic embryo transfer study are unequivocal; mosaic profiles, and what is more, levels and types of mosaicism detected with PGT-A strongly associate with specific outcomes (408). Therefore, while fully acknowledging the limitations of a biopsy, the data suggest it would be unwise to ignore the information

regarding mosaicism provided by the biopsy to guide decisions of embryo prioritization according to their probabilities of clinical success.

How common is embryonic mosaicism? Can we determine the incidence of mosaicism from data gathered from biopsies? Not without contrived mathematical extrapolations. The biopsy can only directly inform us about the percentage of embryos classified as mosaic (as opposed to euploid or aneuploid). If, for example, 15% of embryos tested by PGT-A are classified in the mosaic category, it does not say much about the true incidence of mosaicism in all blastocysts from IVF—and yet the two values are often taken to be one and the same. To know the actual incidence, we would need to dissociate individual blastocysts and assess ploidy at the single-cell level in all their cells. Such an experiment has simply not yet been performed systematically in a large blastocyst sample size with modern DNA copy number quantitation methods, due to obvious limitations related to technology, cost, and sample availability. The data generated from aforementioned whole embryo FISH studies and analyses of single-cell RNA-seq information suggest that low level mosaicism (even as low as a single aneuploid cell being present amidst euploid cells) is quite frequent in early embryos and might even be present in the majority of human embryos. However, such latent (ultra-) low level mosaicism is not likely detected by PGT-A due to sample randomness and is likely inconsequential to embryo viability. This differs from cases with evidence of 'high' level mosaicism in the TE biopsy, which implies an early mitotic error event with clonal expansion.

Should we then use the terminology 'mosaic' embryos at all? Again, it must be understood that the categories in which we place embryos with PGT-A are solely based on the biopsy, not as a global assessment of the whole embryo. It follows then, that when we call an embryo 'mosaic', we are really saying that the embryo produced a PGT-A result that is consistent with mosaicism. In the same vein, a 'euploid' embryo is one with a biopsy producing results consistent with euploidy, and an 'aneuploid' embryo one with aneuploidy. It follows that those terms are used as short hand to classify and manage embryos in the clinic.

Advances in modern PGT-A have ignited the debate around mosaicism in embryos: should it be diagnosed, and how should such embryos be managed in the clinic? Many opinions, preferences, and beliefs have been expressed regarding this topic. The current data suggest that 1) Embryos with a mosaic diagnosis have poorer clinical outcomes than those with a euploid result, 2) Features of mosaicism detected with PGT-A are associated with specific clinical outcomes, 3) Babies born from embryo transfers following a mosaic diagnosis by PGT-A are largely indistinguishable from babies born following a euploid diagnosis.

More data is urgently needed to solidify, refine, or refute these current findings, and to dig deeper into the next set of questions, such as: Is mosaicism in different chromosomes associated with variable clinical success rates? Does the size or genomic content of mosaic segmental imbalances matter? Do rates or characteristics of mosaicism vary

across cell types and tissues? Do products of conception from miscarried mosaic embryo transfers display chromosomal mosaicism? What other follow-up work should be done on neonates? Future studies will need to address these questions.

In recent years, a new factor was proposed as a potentially useful biomarker to prioritize embryos, namely mitochondrial DNA (mtDNA) copy number. That is the subject of Specific Aims D and E (Chapters 13 and 14, respectively). Two publications from 2015, described correlations between mtDNA levels and embryo viability (188, 189). This sparked immense interest in using mtDNA content as a ranking tool in IVF.

In our studies, a method is outlined for determining embryonic mtDNA content in a more precise manner than previously described. Numerous groups across the world are examining mtDNA levels in their respective laboratories, and it is crucial they do so accurately. We provide a blueprint to achieve high precision in mtDNA level quantitation using NGS or qPCR. Surprisingly, when applied to our in-house embryos, the analysis reveals that blastocysts did not contain statistically significant differences in mtDNA content regardless of their ploidy status, maternal age, or implantation potential, starkly contrasting previous reports.

The two previous reports originated from reference laboratories that collected data from numerous centers, agglomerating all their numbers (188, 189). As a result, it is unclear whether their findings hold true individually within all of the different centers. Ours is the

first investigation stemming from a single center, thereby correcting for several potential inter-facility factors. We confirm our observations using three independent quantitation platforms, and amass a number of samples unprecedented to date for this type of study. My findings therefore call into question the use of mtDNA quantitation as a ranking tool, and highlights the need to properly validate new methods of embryo selection before clinical implementation.

A specific claim made by the original groups proposing mtDNA quantitation was that embryos with very high mtDNA copy number at the blastocyst stage were invariably destined for implantation failure. One of the original groups proposing this concept subsequently published two more reports on the use of mtDNA level quantitation in the IVF clinic to improve overall implantation rates (190, 191). However, we report for the first time the births of babies derived from blastocysts with highly elevated mtDNA levels. Those newborns are healthy by physical assessment and test normal for an extensive panel of metabolic conditions. This data demonstrates that in our setting, deselection of blastocysts with high mtDNA levels for transfer (as has been proposed) would result in discarding healthy future babies. Considering that numerous groups across the world are examining mtDNA levels and evaluating its implementation in routine embryo selection decisions in the clinic, I believe that the findings of this study will have substantial and direct impact in the clinical ART landscape.

One of the central considerations in the debate on ethics and policy surrounding germline genome editing (GGE) is clinical demand and the availability of medical alternatives. In Specific Aim F (Chapter 15) we explore this topic from the perspective of an IVF clinic. The IVF industry is uniquely familiar with the concept of preventing transmission of hereditary disease, as it currently routinely employs PGT for that purpose in the clinic. The question ensues whether PGT or GGE is preferred from a technical, ethical, and medical perspective. We propose that PGT is generally advantageous, but we also identify scenarios in which only GGE is applicable. We build on that observation and use mathematical frameworks and data on genetic disease prevalence to estimate the realistic clinical demand for GGE. We find that demand for GGE to cure hereditary conditions is much smaller than previously estimated. While familial genetic disorders are quite common, PGT is appropriate in the vast majority of cases, resulting in our calculated projection of less than one hundred cases benefitting from GGE in the U.S. per year.

Our study's second finding pertains to chromosomal abnormalities: GGE might be highly requested to correct *de novo* aneuploidies in IVF embryos, although CRISPR techniques for that purpose are still being developed. Therefore, there might be a future application for chromosomal editing in cases where, for example, a patient only has fully aneuploid embryos at their disposal. Such cases are quite common, especially amongst patients of advanced maternal age. By 'correcting' an aneuploid embryo, for example by excising a trisomic chromosome, a patient that had previously abandoned treatment due to absence

of transferrable embryos could suddenly be awarded renewed opportunities to use autologous embryos.

While the projects described above were ongoing, the sudden and devastating appearance of COVID-19 prompted me to shift focus from evaluating methods of embryo selection to exploring risks to embryos during the COVID-19 pandemic (Specific Aim G, Chapter 16). I asked if embryos are vulnerable to infection by SARS-CoV-2, the virus responsible for COVID-19. Defining the range of tissues that can be infected by SARS-CoV-2 is an area of current investigation, and existing data shows an association between the virus and the human reproductive system (370, 372). The implications for reproductive medicine are evident: SARS-CoV-2 infection could affect embryo viability, as well as its potential to implant and result in a healthy pregnancy.

Our findings indicate that human preimplantation embryos are susceptible to SARS-CoV-2 infection. Two independent methods show this: 1) The live, fully infectious SARS-CoV-2 virus expressing a fluorescent reporter molecule, and 2) Reporter virions pseudotyped with the Spike (S) glycoprotein of SARS-CoV-2. In both cases, exposure of preimplantation embryos displays robust evidence of infection. Efficiency of infection can be attenuated using blocking antibodies targeting S or ACE2, directly implicating the canonical S-ACE2 cell entry mechanism. We also confirm the presence and correct localization of the key SARS-CoV-2 cell entry factors ACE2 and TMPRSS2 on cells of the embryo by RNA-seq and immunostaining.

Notably, we observe cell degradation in embryos infected with SARS-CoV-2, and sometimes complete embryo demise. From a public health standpoint, this means that early vertical transmission from parents to embryos could compromise establishment or maintenance of a pregnancy.

To date, the prospect of human embryos being infected by SARS-CoV-2 has not been thoroughly considered. I believe our study is an inflection point in our understanding of risk to human reproduction during the pandemic and should be of broad interest to the scientific and medical communities, as well the general public. Furthermore, experimental evidence is urgently needed by professional societies issuing guidelines concerning reproduction and vaccination of couples considering (or during) pregnancy, both in natural conceptions and ART practice.

As the technologies of embryo selection allow us to gain invaluable insights into early human embryonic development, we may also gain insight into the populations we treat. Combining our findings with those from companies like Previvo that have developed techniques to recover embryos conceived in-vivo in order to perform PGT, may help further the discussions of the dissonance between in-vitro and in-vivo conceptuses, and fertile vs infertile populations. Potentially this will lead to improvements in ways we perform IVF and treat different subsets of patients.

For the foreseeable future, however, given an ageing population and trends towards reproduction later in life, the demand for PGT-A will likely continue to increase as female age is one of the significant genetic problems facing reproduction. It is, of course, never acceptable to be reckless in the application of any medical genetic test, especially one as high stakes as PGT that determines the fate of embryos, and ongoing RCTs are crucial checkpoints – *primum non nocere*. However, refusal to lend at least some credibility to its potential seems equally as reckless; possibly causing patients to confer significant physiological and psychological stress due to miscarriages, failed implantation and delays in establishing a viable pregnancy. A reminder that benefits from a test as unique as PGT-A may be more complex than what previous and current RCTs are after, and perhaps additional criteria need to be included in the discussion and quantification of its efficacy.

In summary, the findings of this project were intended to confirm, refute, or refine current methods of embryo selection. My work has resulted in data that: 1) Validates the central tenet of PGT-A at the blastocyst stage, namely that a TE biopsy is a useful representative of an embryo's chromosomal status in the case of whole chromosome aneuploidy, 2) Refines the ranking system pertaining to mosaic embryos, identifying features of mosaicism that correlate with specific clinical outcomes, 3) Refutes the use of mtDNA copy number quantitation to rank embryos, and 4) Defines a potential need for genome editing in settings where PGT-A identifies aneuploidy. Since, in the course of these studies, the emergence of COVID-19 affected every aspect of everyday life, my focus and experiments pivoted and I discovered that human pre-implantation embryos are

vulnerable to SARS-CoV-2 infection. Together, the findings presented in this thesis should improve the way in which embryos are profiled and selected for transfer, ultimately benefitting the patient population struggling with fertility.

18. Bibliography

1.   Edwards RG, Gardner RL. Sexing of live rabbit blastocysts. Nature 1967;214:576-7.

2.   Verlinsky Y, Ginsberg N, Lifchez A, Valle J, Moise J, Strom CM. Analysis of the first polar body: preconception genetic diagnosis. Hum Reprod 1990;5:826-9.

3.   Magli MC, Montag M, Koster M, Muzi L, Geraedts J, Collins J *et al.* Polar body array CGH for prediction of the status of the corresponding oocyte. Part II: technical aspects. Hum Reprod 2011;26:3181-5.

4.   Geraedts J, Collins J, Gianaroli L, Goossens V, Handyside A, Harper J *et al.* What next for preimplantation genetic screening? A polar body approach! Hum Reprod 2010;25:575-7.

5.   Geraedts J, Montag M, Magli MC, Repping S, Handyside A, Staessen C *et al.* Polar body array CGH for prediction of the status of the corresponding oocyte. Part I: clinical results. Hum Reprod 2011;26:3173-80.

6.   Hardarson T, Hanson C, Lundin K, Hillensjo T, Nilsson L, Stevic J *et al.* Preimplantation genetic screening in women of advanced maternal age caused a decrease in clinical pregnancy rate: a randomized controlled trial. Hum Reprod 2008;23:2806-12.

7.   Mastenbroek S, Twisk M, van Echten-Arends J, Sikkema-Raddatz B, Korevaar JC, Verhoeve HR *et al.* In vitro fertilization with preimplantation genetic screening. N Engl J Med 2007;357:9-17.

8.   Fishel S, Gordon A, Lynch C, Dowell K, Ndukwe G, Kelada E *et al.* Live birth after polar body array comparative genomic hybridization prediction of embryo ploidy-the future of IVF? Fertil Steril 2010;93:1006 e7- e10.

9.   Capalbo A, Bono S, Spizzichino L, Biricik A, Baldi M, Colamaria S *et al.* Sequential comprehensive chromosome analysis on polar bodies, blastomeres and trophoblast: insights into female meiotic errors and chromosomal segregation in the preimplantation window of embryo development. Hum Reprod 2013;28:509-18.

10.   Salvaggio CN, Forman EJ, Garnsey HM, Treff NR, Scott RT, Jr. Polar body based aneuploidy screening is poorly predictive of embryo ploidy and reproductive potential. J Assist Reprod Genet 2014;31:1221-6.

11.   Forman EJ, Treff NR, Stevens JM, Garnsey HM, Katz-Jaffe MG, Scott RT, Jr. *et al.* Embryos whose polar bodies contain isolated reciprocal chromosome aneuploidy are almost always euploid. Hum Reprod 2013;28:502-8.

12.   Feichtinger M, Stopp T, Gobl C, Feichtinger E, Vaccari E, Madel U *et al.* Correction: Increasing Live Birth Rate by Preimplantation Genetic Screening of Pooled Polar Bodies Using Array Comparative Genomic Hybridization. PLoS One 2015;10:e0133334.

13.   Verpoest W, Staessen C, Bossuyt PM, Goossens V, Altarescu G, Bonduelle M *et al.* Preimplantation genetic testing for aneuploidy by microarray analysis of polar bodies in advanced maternal age: a randomized clinical trial. Hum Reprod 2018;33:1767-76.

14.   Brown S. Still in highESTEEM. Focus on Reproduction - ESHRE Magazine Blog https://focusonreproductioneu/ July 4, 2017.

15.   Harper JC, Wilton L, Traeger-Synodinos J, Goossens V, Moutou C, SenGupta SB *et al.* The ESHRE PGD Consortium: 10 years of data collection. Hum Reprod Update 2012;18:234-47.

16.   Cohen J, Wells D, Munné S. Removal of 2 cells from cleavage stage embryos is likely to reduce the efficacy of chromosomal tests that are used to enhance implantation rates. Fertil Steril 2007;87:496-503.

17.   Munné S, Lee A, Rosenwaks Z, Grifo J, Cohen J. Diagnosis of major chromosome aneuploidies in human preimplantation embryos. Hum Reprod 1993;8:2185-91.

18.   Gianaroli L, Magli MC, Ferraretti AP, Tabanelli C, Trengia V, Farfalli V *et al.* The beneficial effects of preimplantation genetic diagnosis for aneuploidy support extensive clinical application. Reprod Biomed Online 2005;10:633-40.

19.   Schoolcraft WB, Katz-Jaffe MG, Stevens J, Rawlins M, Munné S. Preimplantation aneuploidy testing for infertile patients of advanced maternal age: a randomized prospective trial. Fertil Steril 2009;92:157-62.

20.   Scott RT, Jr., Upham KM, Forman EJ, Zhao T, Treff NR. Cleavage-stage biopsy significantly impairs human embryonic implantation potential while blastocyst biopsy does not: a randomized and paired clinical trial. Fertil Steril 2013;100:624-30.

21.   Duncan FE, Stein P, Williams CJ, Schultz RM. The effect of blastomere biopsy on preimplantation mouse embryo development and global gene expression. Fertil Steril 2009;91:1462-5.

22.   Kirkegaard K, Hindkjaer JJ, Ingerslev HJ. Human embryonic development after blastomere removal: a time-lapse analysis. Hum Reprod 2012;27:97-105.

23.   McArthur SJ, Leigh D, Marshall JT, de Boer KA, Jansen RP. Pregnancies and live births after trophectoderm biopsy and preimplantation genetic testing of human blastocysts. Fertil Steril 2005;84:1628-36.

24.   Forman EJF, K.M.; Gueye, N.-A.; Smith, R.D.; Stevens, J.; Scott Jr., R.T.;. Trophectoderm biopsy for single-gene disorder preimplantation genetic diagnosis (PGD) is significantly more reliable than day 3 blastomere biopsy. Fertil Steril 2011;96:S222.

25.   Kokkali G, Traeger-Synodinos J, Vrettou C, Stavrou D, Jones GM, Cram DS *et al.* Blastocyst biopsy versus cleavage stage biopsy and blastocyst transfer for preimplantation genetic diagnosis of beta-thalassaemia: a pilot study. Hum Reprod 2007;22:1443-9.

26.   Forman EJ, Hong KH, Ferry KM, Tao X, Taylor D, Levy B *et al.* In vitro fertilization with single euploid blastocyst transfer: a randomized controlled trial. Fertil Steril 2013;100:100-7 e1.

27.   Ubaldi FM, Capalbo A, Colamaria S, Ferrero S, Maggiulli R, Vajta G *et al.* Reduction of multiple pregnancies in the advanced maternal age population after implementation of an elective single embryo transfer policy coupled with enhanced embryo selection: pre- and post-intervention study. Hum Reprod 2015;30:2097-106.

28.   Capalbo A, Ubaldi FM, Cimadomo D, Maggiulli R, Patassini C, Dusi L *et al.* Consistent and reproducible outcomes of blastocyst biopsy and aneuploidy screening across different biopsy practitioners: a multicentre study involving 2586 embryo biopsies. Hum Reprod 2016;31:199-208.

29.   Yang Z, Liu J, Collins GS, Salem SA, Liu X, Lyle SS *et al.* Selection of single blastocysts for fresh transfer via standard morphology assessment alone and with array CGH for good prognosis IVF patients: results from a randomized pilot study. Mol Cytogenet 2012;5:24.

30.   Scott RT, Jr., Upham KM, Forman EJ, Hong KH, Scott KL, Taylor D *et al.* Blastocyst biopsy with comprehensive chromosome screening and fresh embryo transfer significantly increases in vitro fertilization implantation and delivery rates: a randomized controlled trial. Fertil Steril 2013;100:697-703.

31.   Munne S, Kaplan B, Frattarelli JL, Child T, Nakhuda G, Shamma FN *et al.* Preimplantation genetic testing for aneuploidy versus morphology as selection criteria for single frozen-thawed embryo transfer in good-prognosis patients: a multicenter randomized clinical trial. Fertil Steril 2019.

32.   Rubio C, Bellver J, Rodrigo L, Castillon G, Guillen A, Vidal C *et al.* In vitro fertilization with preimplantation genetic diagnosis for aneuploidies in advanced maternal age: a randomized, controlled study. Fertil Steril 2017;107:1122-9.

33.   Jensen PL, Beck HC, Petersen J, Hreinsson J, Wanggren K, Laursen SB *et al.* Proteomic analysis of human blastocoel fluid and blastocyst cells. Stem Cells Dev 2013;22:1126-35.

34.   Zhang Y, Li N, Wang L, Sun H, Ma M, Wang H *et al.* Molecular analysis of DNA in blastocoele fluid using next-generation sequencing. J Assist Reprod Genet 2016;33:637-45.

35.   Gianaroli L, Magli MC, Pomante A, Crivello AM, Cafueri G, Valerio M *et al.* Blastocentesis: a source of DNA for preimplantation genetic testing. Results from a pilot study. Fertil Steril 2014;102:1692-9 e6.

36.   Magli MC, Pomante A, Cafueri G, Valerio M, Crippa A, Ferraretti AP *et al.* Preimplantation genetic testing: polar bodies, blastomeres, trophectoderm cells, or blastocoelic fluid? Fertil Steril 2016;105:676-83 e5.

37.   Tsuiko O, Zhigalina DI, Jatsenko T, Skryabin NA, Kanbekova OR, Artyukhova VG *et al.* Karyotype of the blastocoel fluid demonstrates low concordance with both trophectoderm and inner cell mass. Fertil Steril 2018;109:1127-34 e1.

38.   Magli MC, Albanese C, Crippa A, Tabanelli C, Ferraretti AP, Gianaroli L. Deoxyribonucleic acid detection in blastocoelic fluid: a new predictor of embryo ploidy and viable pregnancy. Fertil Steril 2019;111:77-85.

39.   Brison DR, Houghton FD, Falconer D, Roberts SA, Hawkhead J, Humpherson PG *et al.* Identification of viable embryos in IVF by non-invasive measurement of amino acid turnover. Hum Reprod 2004;19:2319-24.

40.   Houghton FD, Hawkhead JA, Humpherson PG, Hogg JE, Balen AH, Rutherford AJ *et al.* Non-invasive amino acid turnover predicts human embryo developmental capacity. Hum Reprod 2002;17:999-1005.

41.   Huang L, Bogale B, Tang Y, Lu S, Xie XS, Racowsky C. Noninvasive preimplantation genetic testing for aneuploidy in spent medium may be more reliable than trophectoderm biopsy. Proc Natl Acad Sci U S A 2019;116:14105-12.

42.   Jiao J, Shi B, Sagnelli M, Yang D, Yao Y, Li W *et al.* Minimally invasive preimplantation genetic testing using blastocyst culture medium. Hum Reprod 2019;34:1369-79.

43.   Kuznyetsov V, Madjunkova S, Antes R, Abramov R, Motamedi G, Ibarrientos Z *et al.* Evaluation of a novel non-invasive preimplantation genetic screening approach. PLoS One 2018;13:e0197262.

44.   Xu J, Fang R, Chen L, Chen D, Xiao JP, Yang W *et al.* Noninvasive chromosome screening of human embryos by genome sequencing of embryo culture medium for in vitro fertilization. Proc Natl Acad Sci U S A 2016;113:11907-12.

45.   Rubio C, Rienzi L, Navarro-Sanchez L, Cimadomo D, Garcia-Pascual CM, Albricci L *et al.* Embryonic cell-free DNA versus trophectoderm biopsy for aneuploidy testing: concordance rate and clinical implications. Fertil Steril 2019;112:510-9.

46.   Ferreux L, Bourdon M, Sallem A, Santulli P, Barraud-Lange V, Le Foll N *et al.* Live birth rate following frozen-thawed blastocyst transfer is higher with blastocysts expanded on Day 5 than on Day 6. Hum Reprod 2018;33:390-8.

47.   Vera-Rodriguez M, Diez-Juan A, Jimenez-Almazan J, Martinez S, Navarro R, Peinado V *et al.* Origin and composition of cell-free DNA in spent medium from human embryo culture during preimplantation development. Hum Reprod 2018;33:745-56.

48.   Basile N, Nogales Mdel C, Bronet F, Florensa M, Riqueiros M, Rodrigo L *et al.* Increasing the probability of selecting chromosomally normal embryos by time-lapse morphokinetics analysis. Fertil Steril 2014;101:699-704.

49.   Campbell A, Fishel S, Bowman N, Duffy S, Sedler M, Hickman CF. Modelling a risk classification of aneuploidy in human embryos using non-invasive morphokinetics. Reprod Biomed Online 2013;26:477-85.

50.   Chavez SL, Loewke KE, Han J, Moussavi F, Colls P, Munne S *et al.* Dynamic blastomere behaviour reflects human embryo ploidy by the four-cell stage. Nat Commun 2012;3:1251.

51.   Del Carmen Nogales M, Bronet F, Basile N, Martinez EM, Linan A, Rodrigo L *et al.* Type of chromosome abnormality affects embryo morphology dynamics. Fertil Steril 2017;107:229-35 e2.

52.   Yang Z, Zhang J, Salem SA, Liu X, Kuang Y, Salem RD *et al.* Selection of competent blastocysts for transfer by combining time-lapse monitoring and array CGH testing for patients undergoing preimplantation genetic screening: a prospective study with sibling oocytes. BMC Med Genomics 2014;7:38.

53.   Patel DV, Shah PB, Kotdawala AP, Herrero J, Rubio I, Banker MR. Morphokinetic behavior of euploid and aneuploid embryos analyzed by time-lapse in embryoscope. J Hum Reprod Sci 2016;9:112-8.

54.   Reignier A, Lammers J, Barriere P, Freour T. Can time-lapse parameters predict embryo ploidy? A systematic review. Reprod Biomed Online 2018;36:380-7.

55.   Meseguer M, Herrero J, Tejera A, Hilligsoe KM, Ramsing NB, Remohi J. The use of morphokinetics as a predictor of embryo implantation. Hum Reprod 2011;26:2658-71.

56.   Campbell A, Fishel S, Bowman N, Duffy S, Sedler M, Thornton S. Retrospective analysis of outcomes after IVF using an aneuploidy risk model derived from time-lapse imaging without PGS. Reprod Biomed Online 2013;27:140-6.

57.   Mumusoglu S, Ozbek IY, Sokmensuer LK, Polat M, Bozdag G, Papanikolaou E *et al.* Duration of blastulation may be associated with ongoing pregnancy rate in single euploid blastocyst transfer cycles. Reprod Biomed Online 2017;35:633-9.

58.   Lee CI, Chen CH, Huang CC, Cheng EH, Chen HH, Ho ST *et al.* Embryo morphokinetics is potentially associated with clinical outcomes of single-embryo transfers in preimplantation genetic testing for aneuploidy cycles. Reprod Biomed Online 2019;39:569-79.

59.   Cobo A, de los Santos MJ, Castello D, Gamiz P, Campos P, Remohi J. Outcomes of vitrified early cleavage-stage and blastocyst-stage embryos in a cryopreservation program: evaluation of 3,150 warming cycles. Fertil Steril 2012;98:1138-46 e1.

60.   Roy TK, Bradley CK, Bowman MC, McArthur SJ. Single-embryo transfer of vitrified-warmed blastocysts yields equivalent live-birth rates and improved neonatal outcomes compared with fresh transfers. Fertil Steril 2014;101:1294-301.

61.   Koot YE, van Hooff SR, Boomsma CM, van Leenen D, Groot Koerkamp MJ, Goddijn M *et al.* An endometrial gene expression signature accurately predicts recurrent implantation failure after IVF. Sci Rep 2016;6:19411.

62.   Mahajan N. Endometrial receptivity array: Clinical application. J Hum Reprod Sci 2015;8:121-9.

63.   Altmae S, Tamm-Rosenstein K, Esteban FJ, Simm J, Kolberg L, Peterson H *et al.* Endometrial transcriptome analysis indicates superiority of natural over artificial cycles in recurrent implantation failure patients undergoing frozen embryo transfer. Reprod Biomed Online 2016;32:597-613.

64.   Handyside AH, Kontogianni EH, Hardy K, Winston RM. Pregnancies from biopsied human preimplantation embryos sexed by Y-specific DNA amplification. Nature 1990;344:768-70.

65.   Griffin DK, Wilton LJ, Handyside AH, Winston RM, Delhanty JD. Dual fluorescent in situ hybridisation for simultaneous detection of X and Y chromosome-specific probes for the sexing of human preimplantation embryonic nuclei. Hum Genet 1992;89:18-22.

66.   Griffin DK, Wilton LJ, Handyside AH, Atkinson GH, Winston RM, Delhanty JD. Diagnosis of sex in preimplantation embryos by fluorescent in situ hybridisation. BMJ 1993;306:1382.

67.   Schrurs BM, Winston RM, Handyside AH. Preimplantation diagnosis of aneuploidy using fluorescent in-situ hybridization: evaluation using a chromosome 18-specific probe. Hum Reprod 1993;8:296-301.

68.   Hassold T, Hunt P. To err (meiotically) is human: the genesis of human aneuploidy. Nat Rev Genet 2001;2:280-91.

69.   Findikli N, Kahraman S, Saglam Y, Beyazyurek C, Sertyel S, Karlikaya G *et al.* Embryo aneuploidy screening for repeated implantation failure and unexplained recurrent miscarriage. Reprod Biomed Online 2006;13:38-46.

70.   Kahraman S, Findikli N, Biricik A, Oncu N, Ogur C, Sertyel S *et al.* Preliminary FISH studies on spermatozoa and embryos in patients with variable degrees of teratozoospermia and a history of poor prognosis. Reprod Biomed Online 2006;12:752-61.

71.   Coates A, Hesla JS, Hurliman A, Coate B, Holmes E, Matthews R *et al.* Use of suboptimal sperm increases the risk of aneuploidy of the sex chromosomes in preimplantation blastocyst embryos. Fertil Steril 2015;104:866-72.

72.   Ioannou D, Meershoek EJ, Thornhill AR, Ellis M, Griffin DK. Multicolour interphase cytogenetics: 24 chromosome probes, 6 colours, 4 layers. Mol Cell Probes 2011;25:199-205.

73.   Ioannou D, Fonseka KG, Meershoek EJ, Thornhill AR, Abogrein A, Ellis M *et al.* Twenty-four chromosome FISH in human IVF embryos reveals patterns of post-zygotic chromosome segregation and nuclear organisation. Chromosome Res 2012;20:447-60.

74.   Munné S, Fragouli E, Colls P, Katz-Jaffe M, Schoolcraft W, Wells D. Improved detection of aneuploid blastocysts using a new 12-chromosome FISH test. Reprod Biomed Online 2010;20:92-7.

75.   Franasiak JM, Forman EJ, Hong KH, Werner MD, Upham KM, Treff NR *et al.* The nature of aneuploidy with increasing age of the female partner: a review of 15,169

consecutive trophectoderm biopsies evaluated with comprehensive chromosomal screening. Fertil Steril 2014;101:656-63 e1.

76.   Twisk M, Mastenbroek S, Hoek A, Heineman MJ, van der Veen F, Bossuyt PM *et al.* No beneficial effect of preimplantation genetic screening in women of advanced maternal age with a high risk for embryonic aneuploidy. Hum Reprod 2008;23:2813-7.

77.   Delhanty JD, Griffin DK, Handyside AH, Harper J, Atkinson GH, Pieters MH *et al.* Detection of aneuploidy and chromosomal mosaicism in human embryos during preimplantation sex determination by fluorescent in situ hybridisation, (FISH). Hum Mol Genet 1993;2:1183-5.

78.   Munné S, Sandalinas M, Magli C, Gianaroli L, Cohen J, Warburton D. Increased rate of aneuploid embryos in young women with previous aneuploid conceptions. Prenat Diagn 2004;24:638-43.

79.   Turner K, Fowler K, Fonseka G, Griffin D, Ioannou D. Multicolor detection of every chromosome as a means of detecting mosaicism and nuclear organization in human embryonic nuclei. Panminerva Med 2016;58:175-90.

80.   Deleye L, De Coninck D, Christodoulou C, Sante T, Dheedene A, Heindryckx B *et al.* Whole genome amplification with SurePlex results in better copy number alteration detection using sequencing data compared to the MALBAC method. Sci Rep 2015;5:11711.

81.   Blagodatskikh KA, Kramarov VM, Barsova EV, Garkovenko AV, Shcherbo DS, Shelenkov AA *et al.* Improved DOP-PCR (iDOP-PCR): A robust and simple WGA method for efficient amplification of low copy number genomic DNA. PLoS One 2017;12:e0184507.

82.   Babayan A, Alawi M, Gormley M, Muller V, Wikman H, McMullin RP *et al.* Comparative study of whole genome amplification and next generation sequencing performance of single cancer cells. Oncotarget 2017;8:56066-80.

83.   Chen M, Song P, Zou D, Hu X, Zhao S, Gao S *et al.* Comparison of multiple displacement amplification (MDA) and multiple annealing and looping-based amplification cycles (MALBAC) in single-cell sequencing. PLoS One 2014;9:e114520.

84.   Deleye L, Tilleman L, Vander Plaetsen AS, Cornelis S, Deforce D, Van Nieuwerburgh F. Performance of four modern whole genome amplification methods for copy number variant detection in single cells. Sci Rep 2017;7:3422.

85.   Li W, Ma Y, Yu S, Sun N, Wang L, Chen D *et al.* The mutation-free embryo for in vitro fertilization selected by MALBAC-PGD resulted in a healthy live birth from a family carrying PKD 1 mutation. J Assist Reprod Genet 2017;34:1653-8.

86.   Kallioniemi A, Kallioniemi OP, Sudar D, Rutovitz D, Gray JW, Waldman F *et al.* Comparative genomic hybridization for molecular cytogenetic analysis of solid tumors. Science 1992;258:818-21.

87.   Spelcher MR, Du Manoir S, SchrÖck E, Holtgreve-Grez H, Schoell B, Lengauer C *et al.* Molecular cytogenetic analysis of formalin-fixed, paraffin-embedded solid tumors by comparative genomic hybridization after universal DNA-amplification. Human Molecular Genetics 1993;2:1907-14.

88.   Forozan F, Karhu R, Kononen J, Kallioniemi A, Kallioniemi O-P. Genome screening by comparative genomic hybridization. Trends in Genetics 1997;13:405-9.

89.   Wilton L. Preimplantation genetic diagnosis and chromosome analysis of blastomeres using comparative genomic hybridization. Hum Reprod Update 2005;11:33-41.

90.   Wells D, Escudero T, Levy B, Hirschhorn K, Delhanty JD, Munné S. First clinical application of comparative genomic hybridization and polar body testing for preimplantation genetic diagnosis of aneuploidy. Fertil Steril 2002;78:543-9.

91.   Kirchhoff M, Gerdes T, Rose H, Maahr J, Ottesen AM, Lundsteen C. Detection of chromosomal gains and losses in comparative genomic hybridization analysis based on standard reference intervals. Cytometry Part A 1998;31:163-73.

92.   Lichter P, Joos S, Bentz M, Lampel S. Comparative genomic hybridization: uses and limitations. In: Seminars in hematology: Elsevier, 2000:348-57.

93.   De Ravel TJ, Devriendt K, Fryns J-P, Vermeesch JR. What's new in karyotyping? The move towards array comparative genomic hybridisation (CGH). European journal of pediatrics 2007;166:637-43.

94.   Le Caignec C, Spits C, Sermon K, De Rycke M, Thienpont B, Debrock S *et al.* Single-cell chromosomal imbalances detection by array CGH. Nucleic Acids Res 2006;34:e68.

95.   Traversa MV, Marshall J, McArthur S, Leigh D. The genetic screening of preimplantation embryos by comparative genomic hybridisation. Reprod Biol 2011;11 Suppl 3:51-60.

96.   Vanneste E, Voet T, Melotte C, Debrock S, Sermon K, Staessen C *et al.* What next for preimplantation genetic screening? High mitotic chromosome instability rate provides the biological basis for the low success rate. Hum Reprod 2009;24:2679-82.

97.   Fiorentino F, Spizzichino L, Bono S, Biricik A, Kokkali G, Rienzi L *et al.* PGD for reciprocal and Robertsonian translocations using array comparative genomic hybridization. Hum Reprod 2011;26:1925-35.

98.   Johnson DS, Gemelos G, Baner J, Ryan A, Cinnioglu C, Banjevic M *et al.* Preclinical validation of a microarray method for full molecular karyotyping of blastomeres in a 24-h protocol. Hum Reprod 2010;25:1066-75.

99.   Keltz MD, Vega M, Sirota I, Lederman M, Moshier EL, Gonzales E *et al.* Preimplantation genetic screening (PGS) with Comparative genomic hybridization (CGH) following day 3 single cell blastomere biopsy markedly improves IVF outcomes while lowering multiple pregnancies and miscarriages. J Assist Reprod Genet 2013;30:1333-9.

100.   Mamas T, Gordon A, Brown A, Harper J, Sengupta S. Detection of aneuploidy by array comparative genomic hybridization using cell lines to mimic a mosaic trophectoderm biopsy. Fertil Steril 2012;97:943-7.

101.   Fiorentino F, Biricik A, Bono S, Spizzichino L, Cotroneo E, Cottone G *et al.* Development and validation of a next-generation sequencing-based protocol for 24-chromosome aneuploidy screening of embryos. Fertil Steril 2014;101:1375-82.

102.   Wells D, Kaur K, Grifo J, Glassner M, Taylor JC, Fragouli E *et al.* Clinical utilisation of a rapid low-pass whole genome sequencing technique for the diagnosis of aneuploidy in human embryos prior to implantation. J Med Genet 2014;51:553-62.

103.   Zheng H, Jin H, Liu L, Liu J, Wang WH. Application of next-generation sequencing for 24-chromosome aneuploidy screening of human preimplantation embryos. Mol Cytogenet 2015;8:38.

104.   Knapp M, Stiller M, Meyer M. Generating barcoded libraries for multiplex high-throughput sequencing. Methods Mol Biol 2012;840:155-70.

105.   Treff NR, Zimmerman R, Bechor E, Hsu J, Rana B, Jensen J *et al.* Validation of concurrent preimplantation genetic testing for polygenic and monogenic disorders, structural rearrangements, and whole and segmental chromosome aneuploidy with a single universal platform. Eur J Med Genet 2019;62:103647.

106.   Munné S, Wells D. Detection of mosaicism at blastocyst stage with the use of high-resolution next-generation sequencing. Fertil Steril 2017;107:1085-91.

107.   Victor AR, Tyndall JC, Brake AJ, Lepkowsky LT, Murphy AE, Griffin DK *et al.* One hundred mosaic embryos transferred prospectively in a single clinic: exploring when and why they result in healthy pregnancies. Fertil Steril 2019;111:280-93.

108.   Maxwell SM, Colls P, Hodes-Wertz B, McCulloh DH, McCaffrey C, Wells D *et al.* Why do euploid embryos miscarry? A case-control study comparing the rate of aneuploidy within presumed euploid embryos that resulted in miscarriage or live birth using next-generation sequencing. Fertil Steril 2016;106:1414-9 e5.

109.   Scott RT, Upham KM, Forman EJ, Hong KH, Scott KL, Taylor D *et al.* Blastocyst biopsy with comprehensive chromosome screening and fresh embryo transfer significantly increases in vitro fertilization implantation and delivery rates: a randomized controlled trial. Fertility and sterility 2013b;100:697-703.

110.   Treff NR, Scott RT. Four-hour quantitative real-time polymerase chain reaction–based comprehensive chromosome screening and accumulating evidence of accuracy, safety, predictive value, and clinical efficacy. Fertility and sterility 2013b;99:1049-53.

111.   Treff NR, Tao X, Ferry KM, Su J, Taylor D, Scott RT. Development and validation of an accurate quantitative real-time polymerase chain reaction–based assay for human blastocyst comprehensive chromosomal aneuploidy screening. Fertility and sterility 2012;97:819-24. e2.

112.   Dahdouh EM, Balayla J, Audibert F, Genetics C, Wilson RD, Audibert F *et al.* Technical Update: Preimplantation Genetic Diagnosis and Screening. J Obstet Gynaecol Can 2015;37:451-63.

113.   Treff NR, Tao X, Ferry KM, Su J, Taylor D, Scott RT, Jr. Development and validation of an accurate quantitative real-time polymerase chain reaction-based assay for human blastocyst comprehensive chromosomal aneuploidy screening. Fertil Steril 2012;97:819-24.

114.   Dahdouh EM, Balayla J, Audibert F, Wilson RD, Brock J-A, Campagnolo C *et al.* Technical update: preimplantation genetic diagnosis and screening. Obstetrical & Gynecological Survey 2015;70:557-8.

115.   LaFramboise T. Single nucleotide polymorphism arrays: a decade of biological, computational and technological advances. Nucleic Acids Res 2009;37:4181-93.

116.   Treff NR, Northrop LE, Kasabwala K, Su J, Levy B, Scott RT. Single nucleotide polymorphism microarray–based concurrent screening of 24-chromosome aneuploidy and unbalanced translocations in preimplantation human embryos. Fertility and sterility 2011;95:1606-12. e2.

117.   Handyside AH. Live births following karyomapping - a "key" milestone in the development of preimplantation genetic diagnosis. Reprod Biomed Online 2015;31:307-8.

118.   Rabinowitz M, Ryan A, Gemelos G, Hill M, Baner J, Cinnioglu C *et al.* Origins and rates of aneuploidy in human blastomeres. Fertil Steril 2012;97:395-401.

119.   Natesan SA, Bladon AJ, Coskun S, Qubbaj W, Prates R, Munne S *et al.* Genome-wide karyomapping accurately identifies the inheritance of single-gene defects in human preimplantation embryos in vitro. Genetics in Medicine 2014a.

120.   Kubicek D, Hornak M, Horak J, Navratil R, Tauwinklova G, Rubes J *et al.* Incidence and origin of meiotic whole and segmental chromosomal aneuploidies detected by karyomapping. Reprod Biomed Online 2019;38:330-9.

121.   Zamani Esteki M, Dimitriadou E, Mateiu L, Melotte C, Van der Aa N, Kumar P *et al.* Concurrent whole-genome haplotyping and copy-number profiling of single cells. Am J Hum Genet 2015;96:894-912.

122.   Wolstenholme J. Confined placental mosaicism for trisomies 2, 3, 7, 8, 9, 16, and 22: their incidence, likely origins, and mechanisms for cell lineage compartmentalization. Prenat Diagn 1996;16:511-24.

123.   Kuliev A, Rechitsky S. Preimplantation genetic testing: current challenges and future prospects. Expert Rev Mol Diagn 2017;17:1071-88.

124.   Jarvis GE. Estimating limits for natural human embryo mortality. F1000Res 2016;5:2083.

125.   Benkhalifa M, Kasakyan S, Clement P, Baldi M, Tachdjian G, Demirol A *et al.* Array comparative genomic hybridization profiling of first-trimester spontaneous abortions that fail to grow in vitro. Prenat Diagn 2005;25:894-900.

126.   Hodes-Wertz B, Grifo J, Ghadir S, Kaplan B, Laskin CA, Glassner M *et al.* Idiopathic recurrent miscarriage is caused mostly by aneuploid embryos. Fertil Steril 2012;98:675-80.

127.   Munne S. Preimplantation genetic diagnosis for aneuploidy and translocations using array comparative genomic hybridization. Curr Genomics 2012;13:463-70.

128.   McCoy RC, Demko ZP, Ryan A, Banjevic M, Hill M, Sigurjonsson S *et al.* Evidence of Selection against Complex Mitotic-Origin Aneuploidy during Preimplantation Development. PLoS Genet 2015;11:e1005601.

129.   Penrose LS. The relative effects of paternal and maternal age in mongolism. 1933. J Genet 2009;88:9-14.

130.   Rubio C, Rodrigo L, Garcia-Pascual C, Peinado V, Campos-Galindo I, Garcia-Herrero S *et al.* Clinical application of embryo aneuploidy testing by NGS. Biol Reprod 2019.

131.   Tarin JJ, Vendrell FJ, Ten J, Blanes R, van Blerkom J, Cano A. The oxidizing agent tertiary butyl hydroperoxide induces disturbances in spindle organization, c-meiosis, and aneuploidy in mouse oocytes. Mol Hum Reprod 1996;2:895-901.

132.   Tatone C, Heizenrieder T, Di Emidio G, Treffon P, Amicarelli F, Seidel T *et al.* Evidence that carbonyl stress by methylglyoxal exposure induces DNA damage and spindle aberrations, affects mitochondrial integrity in mammalian oocytes and contributes to oocyte ageing. Hum Reprod 2011;26:1843-59.

133.   Battaglia DE, Goodwin P, Klein NA, Soules MR. Influence of maternal age on meiotic spindle assembly in oocytes from naturally cycling women. Hum Reprod 1996;11:2217-22.

134.   Munne S, Ary J, Zouves C, Escudero T, Barnes F, Cinioglu C *et al.* Wide range of chromosome abnormalities in the embryos of young egg donors. Reprod Biomed Online 2006;12:340-6.

135.   Vickers AD. Delayed fertilization and chromosomal anomalies in mouse embryos. J Reprod Fertil 1969;20:69-76.

136.   Babariya D, Fragouli E, Alfarawati S, Spath K, Wells D. The incidence and origin of segmental aneuploidy in human oocytes and preimplantation embryos. Hum Reprod 2017;32:2549-60.

137.   Vera-Rodriguez M, Michel CE, Mercader A, Bladon AJ, Rodrigo L, Kokocinski F *et al.* Distribution patterns of segmental aneuploidies in human blastocysts identified by next-generation sequencing. Fertil Steril 2016;105:1047-55 e2.

138.   Martinez MC, Mendez C, Ferro J, Nicolas M, Serra V, Landeras J. Cytogenetic analysis of early nonviable pregnancies after assisted reproduction treatment. Fertil Steril 2010;93:289-92.

139.   Wellesley D, Dolk H, Boyd PA, Greenlees R, Haeusler M, Nelen V *et al.* Rare chromosome abnormalities, prevalence and prenatal diagnosis rates from population-based congenital anomaly registers in Europe. Eur J Hum Genet 2012;20:521-6.

140.   Munné S, Weier HU, Grifo J, Cohen J. Chromosome mosaicism in human embryos. Biol Reprod 1994;51:373-9.

141.   Taylor TH, Gitlin SA, Patrick JL, Crain JL, Wilson JM, Griffin DK. The origin, mechanisms, incidence and clinical consequences of chromosomal mosaicism in humans. Hum Reprod Update 2014;20:571-81.

142.   Vazquez-Diez C, FitzHarris G. Causes and consequences of chromosome segregation error in preimplantation embryos. Reproduction 2018;155:R63-R76.

143.   Kort DH, Chia G, Treff NR, Tanaka AJ, Xing T, Vensand LB *et al.* Human embryos commonly form abnormal nuclei during development: a mechanism of DNA damage, embryonic aneuploidy, and developmental arrest. Hum Reprod 2016;31:312-23.

144.   Capalbo A, Wright G, Elliott T, Ubaldi FM, Rienzi L, Nagy ZP. FISH reanalysis of inner cell mass and trophectoderm samples of previously array-CGH screened blastocysts shows high accuracy of diagnosis and no major diagnostic impact of mosaicism at the blastocyst stage. Hum Reprod 2013;28:2298-307.

145.   Coonen E, Derhaag JG, Dumoulin JC, van Wissen LC, Bras M, Janssen M *et al.* Anaphase lagging mainly explains chromosomal mosaicism in human preimplantation embryos. Hum Reprod 2004;19:316-24.

146.   Vazquez-Diez C, Yamagata K, Trivedi S, Haverfield J, FitzHarris G. Micronucleus formation causes perpetual unilateral chromosome inheritance in mouse embryos. Proc Natl Acad Sci U S A 2016;113:626-31.

147.   Robinson WP. Mechanisms leading to uniparental disomy and their clinical consequences. Bioessays 2000;22:452-9.

148.   Lightfoot DA, Kouznetsova A, Mahdy E, Wilbertz J, Hoog C. The fate of mosaic aneuploid embryos during mouse development. Dev Biol 2006;289:384-94.

149.   Yuan L, Liu JG, Hoja MR, Wilbertz J, Nordqvist K, Hoog C. Female germ cell aneuploidy and embryo death in mice lacking the meiosis-specific protein SCP3. Science 2002;296:1115-8.

150.   Los FJ, Van Opstal D, van den Berg C. The development of cytogenetically normal, abnormal and mosaic embryos: a theoretical model. Hum Reprod Update 2004;10:79-94.

151. van Echten-Arends J, Mastenbroek S, Sikkema-Raddatz B, Korevaar JC, Heineman MJ, van der Veen F *et al.* Chromosomal mosaicism in human preimplantation embryos: a systematic review. Hum Reprod Update 2011;17:620-7.

152. Mertzanidou A, Wilton L, Cheng J, Spits C, Vanneste E, Moreau Y *et al.* Microarray analysis reveals abnormal chromosomal complements in over 70% of 14 normally developing human embryos. Hum Reprod 2013;28:256-64.

153. McCoy RC. Mosaicism in Preimplantation Human Embryos: When Chromosomal Abnormalities Are the Norm. Trends Genet 2017;33:448-63.

154. Rubio C, Bellver J, Rodrigo L, Bosch E, Mercader A, Vidal C *et al.* Preimplantation genetic screening using fluorescence in situ hybridization in patients with repetitive implantation failure and advanced maternal age: two randomized trials. Fertil Steril 2013;99:1400-7.

155. Evsikov S, Verlinsky Y. Mosaicism in the inner cell mass of human blastocysts. Hum Reprod 1998;13:3151-5.

156. Sandalinas M, Sadowy S, Alikani M, Calderon G, Cohen J, Munne S. Developmental ability of chromosomally abnormal human embryos to develop to the blastocyst stage. Hum Reprod 2001;16:1954-8.

157. Bolton H, Graham SJL, Van der Aa N, Kumar P, Theunis K, Fernandez Gallardo E *et al.* Mouse model of chromosome mosaicism reveals lineage-specific depletion of aneuploid cells and normal developmental potential. Nat Commun 2016;7:11165.

158. Ledbetter DH, Zachary JM, Simpson JL, Golbus MS, Pergament E, Jackson L *et al.* Cytogenetic results from the U.S. Collaborative Study on CVS. Prenat Diagn 1992;12:317-45.

159. Griffin DK, Millie EA, Redline RW, Hassold TJ, Zaragoza MV. Cytogenetic analysis of spontaneous abortions: comparison of techniques and assessment of the incidence of confined placental mosaicism. Am J Med Genet 1997;72:297-301.

160. Kalousek DK, Dill FJ. Chromosomal mosaicism confined to the placenta in human conceptions. Science 1983;221:665-7.

161.   Palermo GD, Colombero LT, Rosenwaks Z. The human sperm centrosome is responsible for normal syngamy and early embryonic development. Rev Reprod 1997;2:19-27.

162.   Baart EB, Martini E, Eijkemans MJ, Van Opstal D, Beckers NG, Verhoeff A *et al.* Milder ovarian stimulation for in-vitro fertilization reduces aneuploidy in the human preimplantation embryo: a randomized controlled trial. Hum Reprod 2007;22:980-8.

163.   Capalbo A, Ubaldi FM, Rienzi L, Scott R, Treff N. Detecting mosaicism in trophectoderm biopsies: current challenges and future possibilities. Hum Reprod 2017;32:492-8.

164.   Munné S, Blazek J, Large M, Martinez-Ortiz PA, Nisson H, Liu E *et al.* Detailed investigation into the cytogenetic constitution and pregnancy outcome of replacing mosaic blastocysts detected with the use of high-resolution next-generation sequencing. Fertil Steril 2017;108:62-71 e8.

165.   Popovic M, Dheedene A, Christodoulou C, Taelman J, Dhaenens L, Van Nieuwerburgh F *et al.* Chromosomal mosaicism in human blastocysts: the ultimate challenge of preimplantation genetic testing? Hum Reprod 2018;33:1342-54.

166.   Cram DS, Leigh D, Handyside A, Rechitsky L, Xu K, Harton G *et al.* PGDIS Position Statement on the Transfer of Mosaic Embryos 2019. Reprod Biomed Online 2019;39 Suppl 1:e1-e4.

167.   CoGEN. CoGEN Position Statement on Chromosomal Mosaicism Detected in Preimplantation Blastocyst Biopsies. In, Accessed 2019:https://ivf-worldwide.com/cogen/general/cogen-statement.html.

168.   Munné S, Grifo J, Wells D. Mosaicism: "survival of the fittest" versus "no embryo left behind". Fertil Steril 2016;105:1146-9.

169.   Treff NR, Franasiak JM. Detection of segmental aneuploidy and mosaicism in the human preimplantation embryo: technical considerations and limitations. Fertil Steril 2017;107:27-31.

170.	Munne S, Spinella F, Grifo J, Zhang J, Beltran MP, Fragouli E *et al.* Clinical outcomes after the transfer of blastocysts characterized as mosaic by high resolution Next Generation Sequencing- further insights. Eur J Med Genet 2019:103741.

171.	Spinella F, Fiorentino F, Biricik A, Bono S, Ruberti A, Cotroneo E *et al.* Extent of chromosomal mosaicism influences the clinical outcome of in vitro fertilization treatments. Fertil Steril 2018;109:77-83.

172.	Greco E, Minasi MG, Fiorentino F. Healthy Babies after Intrauterine Transfer of Mosaic Aneuploid Blastocysts. N Engl J Med 2015;373:2089-90.

173.	Capalbo A, Rienzi L. Mosaicism between trophectoderm and inner cell mass. Fertil Steril 2017;107:1098-106.

174.	Victor AR, Griffin DK, Brake AJ, Tyndall JC, Murphy AE, Lepkowsky LT *et al.* Assessment of aneuploidy concordance between clinical trophectoderm biopsy and blastocyst. Hum Reprod 2019;34:181-92.

175.	Popovic M, Dhaenens L, Taelman J, Dheedene A, Bialecka M, De Sutter P *et al.* Extended in vitro culture of human embryos demonstrates the complex nature of diagnosing chromosomal mosaicism from a single trophectoderm biopsy. Hum Reprod 2019;34:758-69.

176.	Grati FR, Ferreira J, Benn P, Izzi C, Verdi F, Vercellotti E *et al.* Outcomes in pregnancies with a confined placental mosaicism and implications for prenatal screening using cell-free DNA. Genet Med 2019.

177.	Harton GL, Cinnioglu C, Fiorentino F. Current experience concerning mosaic embryos diagnosed during preimplantation genetic screening. Fertil Steril 2017;107:1113-9.

178.	May-Panloup P, Vignon X, Chretien MF, Heyman Y, Tamassia M, Malthiery Y *et al.* Increase of mitochondrial DNA content and transcripts in early bovine embryogenesis associated with upregulation of mtTFA and NRF1 transcription factors. Reprod Biol Endocrinol 2005;3:65.

179. Pawlak P, Chabowska A, Malyszka N, Lechniak D. Mitochondria and mitochondrial DNA in porcine oocytes and cumulus cells--A search for developmental competence marker. Mitochondrion 2016;27:48-55.

180. Jansen RP, de Boer K. The bottleneck: mitochondrial imperatives in oogenesis and ovarian follicular fate. Mol Cell Endocrinol 1998;145:81-8.

181. Michaels GS, Hauswirth WW, Laipis PJ. Mitochondrial DNA copy number in bovine oocytes and somatic cells. Dev Biol 1982;94:246-51.

182. Van Blerkom J. Mitochondrial function in the human oocyte and embryo and their role in developmental competence. Mitochondrion 2011;11:797-813.

183. Spikings EC, Alderson J, St John JC. Regulated mitochondrial DNA replication during oocyte maturation is essential for successful porcine embryonic development. Biol Reprod 2007;76:327-35.

184. Mao J, Whitworth KM, Spate LD, Walters EM, Zhao J, Prather RS. Regulation of oocyte mitochondrial DNA copy number by follicular fluid, EGF, and neuregulin 1 during in vitro maturation affects embryo development in pigs. Theriogenology 2012;78:887-97.

185. El Shourbagy SH, Spikings EC, Freitas M, St John JC. Mitochondria directly influence fertilisation outcome in the pig. Reproduction 2006;131:233-45.

186. Cagnone GL, Tsai TS, Makanji Y, Matthews P, Gould J, Bonkowski MS *et al.* Restoration of normal embryogenesis by mitochondrial supplementation in pig oocytes exhibiting mitochondrial DNA deficiency. Sci Rep 2016;6:23229.

187. Scantland S, Tessaro I, Macabelli CH, Macaulay AD, Cagnone G, Fournier E *et al.* The adenosine salvage pathway as an alternative to mitochondrial production of ATP in maturing mammalian oocytes. Biol Reprod 2014;91:75.

188. Diez-Juan A, Rubio C, Marin C, Martinez S, Al-Asmar N, Riboldi M *et al.* Mitochondrial DNA content as a viability score in human euploid embryos: less is better. Fertil Steril 2015;104:534-41 e1.

189. Fragouli E, Spath K, Alfarawati S, Kaper F, Craig A, Michel CE *et al.* Altered levels of mitochondrial DNA are associated with female age, aneuploidy, and provide an independent measure of embryonic implantation potential. PLoS Genet 2015;11:e1005241.

190. Fragouli E, McCaffrey C, Ravichandran K, Spath K, Grifo JA, Munné S *et al.* Clinical implications of mitochondrial DNA quantification on pregnancy outcomes: a blinded prospective non-selection study. Hum Reprod 2017;32:2340-7.

191. Ravichandran K, McCaffrey C, Grifo J, Morales A, Perloe M, Munné S *et al.* Mitochondrial DNA quantification as a tool for embryo viability assessment: retrospective analysis of data from single euploid blastocyst transfers. Hum Reprod 2017;32:1282-92.

192. Klimczak AM, Pacheco LE, Lewis KE, Massahi N, Richards JP, Kearns WG *et al.* Embryonal mitochondrial DNA: relationship to embryo quality and transfer outcomes. J Assist Reprod Genet 2018;35:871-7.

193. Shang W, Zhang Y, Shu M, Wang W, Ren L, Chen F *et al.* Comprehensive chromosomal and mitochondrial copy number profiling in human IVF embryos. Reprod Biomed Online 2018;36:67-74.

194. Treff NR, Zhan Y, Tao X, Olcha M, Han M, Rajchel J *et al.* Levels of trophectoderm mitochondrial DNA do not predict the reproductive potential of sibling embryos. Hum Reprod 2017;32:954-62.

195. Viotti M, Victor AR, Zouves CG, Barnes FL. Is mitochondrial DNA quantitation in blastocyst trophectoderm cells predictive of developmental competence and outcome in clinical IVF? J Assist Reprod Genet 2017;34:1581-5.

196. Wells D. Mitochondrial DNA quantity as a biomarker for blastocyst implantation potential. Fertil Steril 2017;108:742-7.

197. Viotti M, Victor AR, Griffin DK, Groob JS, Brake AJ, Zouves CG *et al.* Estimating Demand for Germline Genome Editing: An In Vitro Fertilization Clinic Perspective. CRISPR J 2019;2:304-15.

198.   Sermon K, Capalbo A, Cohen J, Coonen E, De Rycke M, De Vos A *et al.* The why, the how and the when of PGS 2.0: current practices and expert opinions of fertility specialists, molecular biologists, and embryologists. Mol Hum Reprod 2016;22:845-57.

199.   Practice Committees of the American Society for Reproductive M, the Society for Assisted Reproductive Technology. Electronic address Aao, Practice Committees of the American Society for Reproductive M, the Society for Assisted Reproductive T. The use of preimplantation genetic testing for aneuploidy (PGT-A): a committee opinion. Fertil Steril 2018;109:429-36.

200.   Gleicher N, Orvieto R. Is the hypothesis of preimplantation genetic screening (PGS) still supportable? A review. J Ovarian Res 2017;10:21.

201.   Esfandiari N, Bunnell ME, Casper RF. Human embryo mosaicism: did we drop the ball on chromosomal testing? J Assist Reprod Genet 2016;33:1439-44.

202.   Schoolcraft W, Meseguer M, Global Fertility Alliance. Electronic address atic. Paving the way for a gold standard of care for infertility treatment: improving outcomes through standardization of laboratory procedures. Reprod Biomed Online 2017;35:391-9.

203.   Vera-Rodriguez M, Rubio C. Assessing the true incidence of mosaicism in preimplantation embryos. Fertil Steril 2017;107:1107-12.

204.   Fragouli E, Alfarawati S, Spath K, Babariya D, Tarozzi N, Borini A *et al.* Analysis of implantation and ongoing pregnancy rates following the transfer of mosaic diploid-aneuploid blastocysts. Hum Genet 2017;136:805-19.

205.   Lai HH, Chuang TH, Wong LK, Lee MJ, Hsieh CL, Wang HL *et al.* Identification of mosaic and segmental aneuploidies by next-generation sequencing in preimplantation genetic screening can improve clinical outcomes compared to array-comparative genomic hybridization. Mol Cytogenet 2017;10:14.

206.   Victor AR, Brake AJ, Tyndall JC, Griffin DK, Zouves CG, Barnes FL *et al.* Accurate quantitation of mitochondrial DNA reveals uniform levels in human blastocysts irrespective of ploidy, age, or implantation potential. Fertil Steril 2017;107:34-42 e3.

207.   Gardner DK, Schoolcraft WB. In vitro culture of human blastocysts. . In: R. J, D. M, eds. Towards reproductive certainty: fertility and genetics beyond. Camforth, UK: Parthenon Publishing, 1999:378-88.

208.   Taylor TH, Griffin DK, Katz SL, Crain JL, Johnson L, Gitlin S. Technique to 'Map' Chromosomal Mosaicism at the Blastocyst Stage. Cytogenet Genome Res 2016;149:262-6.

209.   Vohr SH, Buen Abad Najar CF, Shapiro B, Green RE. A method for positive forensic identification of samples from extremely low-coverage sequence data. BMC Genomics 2015;16:1034.

210.   Li H, Durbin R. Fast and accurate short read alignment with Burrows-Wheeler transform. Bioinformatics 2009;25:1754-60.

211.   Wang C, Zhan X, Liang L, Abecasis GR, Lin X. Improved ancestry estimation for both genotyping and sequencing data using projection procrustes analysis and genotype imputation. Am J Hum Genet 2015;96:926-37.

212.   Genomes Project C, Auton A, Brooks LD, Durbin RM, Garrison EP, Kang HM *et al.* A global reference for human genetic variation. Nature 2015;526:68-74.

213.   Li JZ, Absher DM, Tang H, Southwick AM, Casto AM, Ramachandran S *et al.* Worldwide human relationships inferred from genome-wide patterns of variation. Science 2008;319:1100-4.

214.   Deglincerti A, Croft GF, Pietila LN, Zernicka-Goetz M, Siggia ED, Brivanlou AH. Self-organization of the in vitro attached human embryo. Nature 2016;533:251-4.

215.   Mastenbroek S, Repping S. Preimplantation genetic screening: back to the future. Hum Reprod 2014;29:1846-50.

216.   Gleicher N, Metzger J, Croft G, Kushnir VA, Albertini DF, Barad DH. A single trophectoderm biopsy at blastocyst stage is mathematically unable to determine embryo ploidy accurately enough for clinical use. Reprod Biol Endocrinol 2017;15:33.

217.   Adashi EY, McCoy RC. Technology versus biology: the limits of pre-implantation genetic screening: Better methods to detect the origin of aneuploidy in pre-implantation embryos could improve the success rate of artificial reproduction. EMBO Rep 2017;18:670-2.

218.   Bolton H, Graham SJ, Van der Aa N, Kumar P, Theunis K, Fernandez Gallardo E *et al.* Mouse model of chromosome mosaicism reveals lineage-specific depletion of aneuploid cells and normal developmental potential. Nat Commun 2016;7:11165.

219.   Munné S, Velilla E, Colls P, Garcia Bermudez M, Vemuri MC, Steuerwald N *et al.* Self-correction of chromosomally abnormal embryos in culture and implications for stem cell production. Fertil Steril 2005;84:1328-34.

220.   Nagaoka SI, Hassold TJ, Hunt PA. Human aneuploidy: mechanisms and new insights into an age-old problem. Nat Rev Genet 2012;13:493-504.

221.   Lledo B, Morales R, Ortiz JA, Blanca H, Ten J, Llacer J *et al.* Implantation potential of mosaic embryos. Syst Biol Reprod Med 2017;63:206-8.

222.   Bradley CK, Livingstone M, Traversa MV, McArthur SJ. Impact of multiple blastocyst biopsy and vitrification-warming procedures on pregnancy outcomes. Fertil Steril 2017;108:999-1006.

223.   Gleicher N, Vidali A, Braverman J, Kushnir VA, Barad DH, Hudson C *et al.* Accuracy of preimplantation genetic screening (PGS) is compromised by degree of mosaicism of human embryos. Reprod Biol Endocrinol 2016;14:54.

224.   Hall SS. A new last chance. In: New York Magazine, 2017.

225.   Kane SC, Willats E, Bezerra Maia EHMS, Hyett J, da Silva Costa F. Pre-Implantation Genetic Screening Techniques: Implications for Clinical Prenatal Diagnosis. Fetal Diagn Ther 2016;40:241-54.

226.   Victor AR, Griffin DK, Brake AJ, Tyndall JC, Murphy AE, Lepkowsky LT *et al.* Assessment of aneuploidy concordance between clinical trophectoderm biopsy and blastocyst. Hum Reprod In press.

227.   Lalitkumar S, Boggavarapu NR, Menezes J, Dimitriadis E, Zhang JG, Nicola NA *et al.* Polyethylene glycated leukemia inhibitory factor antagonist inhibits human blastocyst implantation and triggers apoptosis by down-regulating embryonic AKT. Fertil Steril 2013;100:1160-9.

228.   Ptak G, Zacchini F, Czernik M, Fidanza A, Palmieri C, Della Salda L *et al.* A short exposure to polychlorinated biphenyls deregulates cellular autophagy in mammalian blastocyst in vitro. Hum Reprod 2012;27:1034-42.

229.   PGDIS. PGDIS position statement on chromosome mosaicism and preimplantation aneuploidy testing at the blastocyst stage. In: http://www.pgdis.org/docs/newsletter_071816.html, Accessed July 26, 2018, Online Statement.

230.   CoGEN. CoGEN position statement on chromosomal mosaicism detected in preimplantation blastocyst biopsies In: https://ivf-worldwide.com/index.php?option=com_content&view=article&id=733&Itemid=464 Accessed July 26, 2018, Online Statement.

231.   Grati FR, Gallazzi G, Branca L, Maggi F, Simoni G, Yaron Y. An evidence-based scoring system for prioritizing mosaic aneuploid embryos following preimplantation genetic screening. Reprod Biomed Online 2018;36:442-9.

232.   Munné S, Spinella F, Grifo J, Zhang J, Beltran MP, Fragouli E *et al.* Clinical outcomes after the transfer of blastocysts characterized as mosaic by high resolution Next Generation Sequencing- further insights. Eur J Med Genet 2020;63:103741.

233.   Van der Aa N, Cheng J, Mateiu L, Zamani Esteki M, Kumar P, Dimitriadou E *et al.* Genome-wide copy number profiling of single cells in S-phase reveals DNA-replication domains. Nucleic Acids Res 2013;41:e66.

234.   Ramos L, del Rey J, Daina G, Martinez-Passarell O, Rius M, Tunon D *et al.* Does the S phase have an impact on the accuracy of comparative genomic hybridization profiles in single fibroblasts and human blastomeres? Fertil Steril 2014;101:488-95.

235.   Besser AG, Mounts EL. Counselling considerations for chromosomal mosaicism detected by preimplantation genetic screening. Reprod Biomed Online 2017;34:369-74.

236.   Murtinger M, Wirleitner B, Schuff M. Scoring of mosaic embryos after preimplantation genetic testing: a rollercoaster ride between fear, hope and embryo wastage. Reprod Biomed Online 2018;37:120-1.

237.   Girardi L, Serdarogullari M, Patassini C, Poli M, Fabiani M, Caroselli S *et al.* Incidence, Origin, and Predictive Model for the Detection and Clinical Management of Segmental Aneuploidies in Human Embryos. Am J Hum Genet 2020.

238.   Navratil R, Horak J, Hornak M, Kubicek D, Balcova M, Tauwinklova G *et al.* Concordance of various chromosomal errors among different parts of the embryo and the value of re-biopsy in embryos with segmental aneuploidies. Mol Hum Reprod 2020.

239.   Huang J, Yan L, Lu S, Zhao N, Qiao J. Re-analysis of aneuploidy blastocysts with an inner cell mass and different regional trophectoderm cells. J Assist Reprod Genet 2017;34:487-93.

240.   Lawrenz B, El Khatib I, Linan A, Bayram A, Arnanz A, Chopra R *et al.* The clinicians dilemma with mosaicism-an insight from inner cell mass biopsies. Hum Reprod 2019;34:998-1010.

241.   Sachdev NM, McCulloh DH, Kramer Y, Keefe D, Grifo JA. The reproducibility of trophectoderm biopsies in euploid, aneuploid, and mosaic embryos using independently verified next-generation sequencing (NGS): a pilot study. J Assist Reprod Genet 2020.

242.   Sheltzer JM, Amon A. The aneuploidy paradox: costs and benefits of an incorrect karyotype. Trends Genet 2011;27:446-53.

243.   Singla S, Iwamoto-Stohl LK, Zhu M, Zernicka-Goetz M. Autophagy-mediated apoptosis eliminates aneuploid cells in a mouse model of chromosome mosaicism. Nat Commun 2020;11:2958.

244.   Gueye NA, Devkota B, Taylor D, Pfundt R, Scott RT, Jr., Treff NR. Uniparental disomy in the human blastocyst is exceedingly rare. Fertil Steril 2014;101:232-6.

245.   Tiegs AW, Tao X, Zhan Y, Whitehead C, Kim J, Hanson B *et al.* A multicenter, prospective, blinded, nonselection study evaluating the predictive value of an aneuploid diagnosis using a targeted next-generation sequencing-based preimplantation genetic testing for aneuploidy assay and impact of biopsy. Fertil Steril 2020.

246.   Viotti M. Preimplantation Genetic Testing for Chromosomal Abnormalities: Aneuploidy, Mosaicism, and Structural Rearrangements. Genes (Basel) 2020;11.

247.   Ou Z, Chen Z, Yin M, Deng Y, Liang Y, Wang W *et al.* Re-analysis of whole blastocysts after trophectoderm biopsy indicated chromosome aneuploidy. Hum Genomics 2020;14:3.

248.   Kahraman S, Cetinkaya M, Yuksel B, Yesil M, Pirkevi Cetinkaya C. The birth of a baby with mosaicism resulting from a known mosaic embryo transfer: a case report. Hum Reprod 2020;35:727-33.

249.   Besser AG, McCulloh DH, Grifo JA. What are patients doing with their mosaic embryos? Decision making after genetic counseling. Fertil Steril 2019;111:132-7 e1.

250.   Munné S, Kaplan B, Frattarelli JL, Child T, Nakhuda G, Shamma FN *et al.* Preimplantation genetic testing for aneuploidy versus morphology as selection criteria for single frozen-thawed embryo transfer in good-prognosis patients: a multicenter randomized clinical trial. Fertil Steril 2019;112:1071-9 e7.

251.   Seli E. Mitochondrial DNA as a biomarker for in-vitro fertilization outcome. Curr Opin Obstet Gynecol 2016;28:158-63.

252.   Wai T, Ao A, Zhang X, Cyr D, Dufort D, Shoubridge EA. The role of mitochondrial DNA copy number in mammalian fertility. Biol Reprod 2010;83:52-62.

253.   Clay Montier LL, Deng JJ, Bai Y. Number matters: control of mammalian mitochondrial DNA copy number. J Genet Genomics 2009;36:125-31.

254.   Tan Y, Yin X, Zhang S, Jiang H, Tan K, Li J *et al.* Clinical outcome of preimplantation genetic diagnosis and screening using next generation sequencing. Gigascience 2014;3:30.

255.   Leese HJ. Quiet please, do not disturb: a hypothesis of embryo metabolism and viability. Bioessays 2002;24:845-9.

256.   Hirai K, Aliev G, Nunomura A, Fujioka H, Russell RL, Atwood CS *et al.* Mitochondrial abnormalities in Alzheimer's disease. J Neurosci 2001;21:3017-23.

257.   Phillips NR, Sprouse ML, Roby RK. Simultaneous quantification of mitochondrial DNA copy number and deletion ratio: a multiplex real-time PCR assay. Sci Rep 2014;4:3887.

258.   Reznik E, Miller ML, Senbabaoglu Y, Riaz N, Sarungbam J, Tickoo SK *et al.* Mitochondrial DNA copy number variation across human cancers. Elife 2016;5.

259.   Richly E, Leister D. NUMTs in sequenced eukaryotic genomes. Mol Biol Evol 2004;21:1081-4.

260.   Baer M, Nilsen TW, Costigan C, Altman S. Structure and transcription of a human gene for H1 RNA, the RNA component of human RNase P. Nucleic Acids Res 1990;18:97-103.

261.   Livak KJ, Schmittgen TD. Analysis of relative gene expression data using real-time quantitative PCR and the 2(-Delta Delta C(T)) Method. Methods 2001;25:402-8.

262.   Moraes CT. What regulates mitochondrial DNA copy number in animal cells? Trends Genet 2001;17:199-205.

263.   Shadel GS, Clayton DA. Mitochondrial DNA maintenance in vertebrates. Annu Rev Biochem 1997;66:409-35.

264.   D'Erchia AM, Atlante A, Gadaleta G, Pavesi G, Chiara M, De Virgilio C *et al.* Tissue-specific mtDNA abundance from exome data and its correlation with mitochondrial transcription, mass and respiratory activity. Mitochondrion 2015;20:13-21.

265.   Hormozdiari F, Alkan C, Ventura M, Hajirasouliha I, Malig M, Hach F *et al.* Alu repeat discovery and characterization within human genomes. Genome Res 2011;21:840-9.

266.   Mills RE, Bennett EA, Iskow RC, Devine SE. Which transposable elements are active in the human genome? Trends Genet 2007;23:183-91.

267.   Wildschutte JH, Baron A, Diroff NM, Kidd JM. Discovery and characterization of Alu repeat sequences via precise local read assembly. Nucleic Acids Res 2015;43:10292-307.

268.   Cavelier L, Johannisson A, Gyllensten U. Analysis of mtDNA copy number and composition of single mitochondrial particles using flow cytometry and PCR. Exp Cell Res 2000;259:79-85.

269.   Satoh M, Kuroiwa T. Organization of multiple nucleoids and DNA molecules in mitochondria of a human cell. Exp Cell Res 1991;196:137-40.

270.   Navratil M, Poe BG, Arriaga EA. Quantitation of DNA copy number in individual mitochondrial particles by capillary electrophoresis. Anal Chem 2007;79:7691-9.

271.   Larsen S, Nielsen J, Hansen CN, Nielsen LB, Wibrand F, Stride N *et al.* Biomarkers of mitochondrial content in skeletal muscle of healthy young human subjects. J Physiol 2012;590:3349-60.

272.   Reynier P, May-Panloup P, Chretien MF, Morgan CJ, Jean M, Savagner F *et al.* Mitochondrial DNA content affects the fertilizability of human oocytes. Mol Hum Reprod 2001;7:425-9.

273.   Hua S, Zhang Y, Li XC, Ma LB, Cao JW, Dai JP *et al.* Effects of granulosa cell mitochondria transfer on the early development of bovine embryos in vitro. Cloning Stem Cells 2007;9:237-46.

274.   Santos TA, El Shourbagy S, St John JC. Mitochondrial content reflects oocyte variability and fertilization outcome. Fertil Steril 2006;85:584-91.

275.   Tamassia M, Nuttinck F, May-Panloup P, Reynier P, Heyman Y, Charpigny G *et al.* In vitro embryo production efficiency in cattle and its association with oocyte adenosine triphosphate content, quantity of mitochondrial DNA, and mitochondrial DNA haplogroup. Biol Reprod 2004;71:697-704.

276.   Chiaratti MR, Bressan FF, Ferreira CR, Caetano AR, Smith LC, Vercesi AE *et al.* Embryo mitochondrial DNA depletion is reversed during early embryogenesis in cattle. Biol Reprod 2010;82:76-85.

277.   Niederberger C, Pellicer A, Cohen J, Gardner DK, Palermo GD, O'Neill CL *et al.* Forty years of IVF. Fertil Steril 2018;110:185-324 e5.

278.   SART. Society for Reproductive Technology, National Summary Report. https://wwwsartcorsonlinecom/rptCSR_PublicMultYearaspx?reportingYear=2016.

279.   Gardner DK, Leese HJ. Assessment of embryo viability prior to transfer by the noninvasive measurement of glucose uptake. J Exp Zool 1987;242:103-5.

280.   Gardner DK, Wale PL. Analysis of metabolism to select viable human embryos for transfer. Fertil Steril 2013;99:1062-72.

281.   Gardner DK, Wale PL, Collins R, Lane M. Glucose consumption of single post-compaction human embryos is predictive of embryo sex and live birth outcome. Hum Reprod 2011;26:1981-6.

282.   Harvey AJ. Mitochondria in early development: linking the microenvironment, metabolism and the epigenome. Reproduction 2019;157:R159-R79.

283.   Lima A, Burgstaller J, Sanchez-Nieto JM, Rodriguez TA. The Mitochondria and the Regulation of Cell Fitness During Early Mammalian Development. Curr Top Dev Biol 2018;128:339-63.

284.   Lledo B, Ortiz JA, Morales R, Garcia-Hernandez E, Ten J, Bernabeu A *et al.* Comprehensive mitochondrial DNA analysis and IVF outcome. Hum Reprod Open 2018;2018:hoy023.

285.   Barnes FL, Victor AR, Zouves CG, Viotti M. Mitochondrial DNA quantitation-making sense of contradictory reports. Hum Reprod 2017;32:2149-50.

286.   Wells D, Ravichandran K, McCaffrey C, Grifo J, Morales A, Perloe M *et al.* Reply: Mitochondrial DNA Quantification-the devil in the detail. Hum Reprod 2017;32:2150-1.

287.   Humaidan P, Kristensen SG, Coetzee K. Mitochondrial DNA, a new biomarker of embryonic implantation potential: fact or fiction? Fertil Steril 2018;109:61-2.

288.   Nicklas JA, Buel E. Simultaneous determination of total human and male DNA using a duplex real-time PCR assay. J Forensic Sci 2006;51:1005-15.

289.   Treff NR, Su J, Taylor D, Scott RT, Jr. Telomere DNA deficiency is associated with development of human embryonic aneuploidy. PLoS Genet 2011;7:e1002161.

290.   Victor AR, Griffin DK, Brake AJ, Tyndall JC, Murphy AE, Lepkowsky LT *et al.* Assessment of aneuploidy concordance between clinical trophectoderm biopsy and blastocyst. Hum Reprod 2018.

291.   Hallap T, Nagy S, Jaakma U, Johannisson A, Rodriguez-Martinez H. Mitochondrial activity of frozen-thawed spermatozoa assessed by MitoTracker Deep Red 633. Theriogenology 2005;63:2311-22.

292.   Kanno C, Kang SS, Kitade Y, Yanagawa Y, Takahashi Y, Nagano M. Simultaneous evaluation of plasma membrane integrity, acrosomal integrity, and mitochondrial membrane potential in bovine spermatozoa by flow cytometry. Zygote 2016;24:529-36.

293.   Kodiha M, Pie B, Wang YM, Flamant E, Boppana NB, Young JC *et al.* Detecting changes in the mitochondrial membrane potential by quantitative fluorescence microscopy. Protocol Exchange 2015.

294.   Gardner DK, Meseguer M, Rubio C, Treff NR. Diagnosis of human preimplantation embryo viability. Hum Reprod Update 2015;21:727-47.

295.   Ferrick L, Lee YSL, Gardner DK. Reducing time to pregnancy and facilitating the birth of healthy children through functional analysis of embryo physiology. Biol Reprod 2019.

296.   Cecchino GN, Seli E, Alves da Motta EL, Garcia-Velasco JA. The role of mitochondrial activity in female fertility and assisted reproductive technologies: overview and current insights. Reprod Biomed Online 2018;36:686-97.

297.   St John JC, Facucho-Oliveira J, Jiang Y, Kelly R, Salah R. Mitochondrial DNA transmission, replication and inheritance: a journey from the gamete through the embryo and into offspring and embryonic stem cells. Hum Reprod Update 2010;16:488-509.

298.   Van Blerkom J. Mitochondria in human oogenesis and preimplantation embryogenesis: engines of metabolism, ionic regulation and developmental competence. Reproduction 2004;128:269-80.

299.   Zhu J, Tsai HJ, Gordon MR, Li R. Cellular Stress Associated with Aneuploidy. Dev Cell 2018;44:420-31.

300.   Sheltzer JM. A transcriptional and metabolic signature of primary aneuploidy is present in chromosomally unstable cancer cells and informs clinical prognosis. Cancer Res 2013;73:6401-12.

301.   Stingele S, Stoehr G, Peplowska K, Cox J, Mann M, Storchova Z. Global analysis of genome, transcriptome and proteome reveals the response to aneuploidy in human cells. Mol Syst Biol 2012;8:608.

302.   Gardner DK, Harvey AJ. Blastocyst metabolism. Reprod Fertil Dev 2015;27:638-54.

303.   . Online Mendelian Inheritance in Man (OMIM). McKusick-Nathans Institute of Genetic Medicine, Johns Hopkins University (Baltimore, MD), accessed 06/03/2019. https://omim.org/.

304.   Assembly of Life Sciences (U.S.). Committee on the Biological Effects of Ionizing Radiations. The Effects on populations of exposure to low levels of ionizing radiation, 1980. Washington, D.C.: National Academy Press, 1980.

305.   Maxwell SM, Grifo JA. Should every embryo undergo preimplantation genetic testing for aneuploidy? A review of the modern approach to in vitro fertilization. Best Pract Res Clin Obstet Gynaecol 2018;53:38-47.

306.   Ma H, Marti-Gutierrez N, Park SW, Wu J, Lee Y, Suzuki K *et al.* Correction of a pathogenic gene mutation in human embryos. Nature 2017;548:413-9.

307.   Fogarty NME, McCarthy A, Snijders KE, Powell BE, Kubikova N, Blakeley P *et al.* Genome editing reveals a role for OCT4 in human embryogenesis. Nature 2017;550:67-73.

308.   Liang P, Xu Y, Zhang X, Ding C, Huang R, Zhang Z *et al.* CRISPR/Cas9-mediated gene editing in human tripronuclear zygotes. Protein Cell 2015;6:363-72.

309.   Zeng Y, Li J, Li G, Huang S, Yu W, Zhang Y *et al.* Correction of the Marfan Syndrome Pathogenic FBN1 Mutation by Base Editing in Human Cells and Heterozygous Embryos. Mol Ther 2018;26:2631-7.

310.   Liang P, Ding C, Sun H, Xie X, Xu Y, Zhang X *et al.* Correction of beta-thalassemia mutant by base editor in human embryos. Protein Cell 2017;8:811-22.

311.   Tang L, Zeng Y, Du H, Gong M, Peng J, Zhang B *et al.* CRISPR/Cas9-mediated gene editing in human zygotes using Cas9 protein. Mol Genet Genomics 2017;292:525-33.

312.   Kang X, He W, Huang Y, Yu Q, Chen Y, Gao X *et al.* Introducing precise genetic modifications into human 3PN embryos by CRISPR/Cas-mediated genome editing. J Assist Reprod Genet 2016;33:581-8.

313.   Griffin DK, Ogur C. Chromosomal analysis in IVF: just how useful is it? Reproduction 2018;156:F29-F50.

314.   Grace J, El-Toukhy T, Scriven P, Ogilvie C, Pickering S, Lashwood A *et al.* Three hundred and thirty cycles of preimplantation genetic diagnosis for serious genetic disease: clinical considerations affecting outcome. BJOG 2006;113:1393-401.

315.   Treff NR, Zimmerman R, Bechor E, Hsu J, Rana B, Jensen J *et al.* Validation of concurrent preimplantation genetic testing for polygenic and monogenic disorders, structural rearrangements, and whole and segmental chromosome aneuploidy with a single universal platform. Eur J Med Genet 2019.

316.   . Society for Assisted Reproductive Technology (SART), accessed 06/04/2019. htpps://www.sart.org.

317.   Munné S. Status of preimplantation genetic testing and embryo selection. Reprod Biomed Online 2018;37:393-6.

318.   Ethics Committee of the American Society for Reproductive Medicine. Electronic address Aao, Ethics Committee of the American Society for Reproductive M. Use of preimplantation genetic testing for monogenic defects (PGT-M) for adult-onset conditions: an Ethics Committee opinion. Fertil Steril 2018;109:989-92.

319.   Gleicher N. Expected advances in human fertility treatments and their likely translational consequences. J Transl Med 2018;16:149.

320.   Cohen IG, Adashi EY. SCIENCE AND REGULATION. The FDA is prohibited from going germline. Science 2016;353:545-6.

321.   Brokowski C. Do CRISPR Germline Ethics Statements Cut It? CRISPR J 2018;1:115-25.

322.   Dance A. Better beings? Nat Biotechnol 2017;35:1006-11.

323.   Gutierrez-Mateo C, Sanchez-Garcia JF, Fischer J, Tormasi S, Cohen J, Munné S *et al.* Preimplantation genetic diagnosis of single-gene disorders: experience with more than 200 cycles conducted by a reference laboratory in the United States. Fertil Steril 2009;92:1544-56.

324.   Lander ES. Brave New Genome. N Engl J Med 2015;373:5-8.

325.   Araki M, Ishii T. International regulatory landscape and integration of corrective genome editing into in vitro fertilization. Reprod Biol Endocrinol 2014;12:108.

326.   Songdej D, Babbs C, Higgs DR, Consortium BI. An international registry of survivors with Hb Bart's hydrops fetalis syndrome. Blood 2017;129:1251-9.

327.   Piel FB, Weatherall DJ. The alpha-thalassemias. N Engl J Med 2014;371:1908-16.

328.   Carroll JM, Quaid KA, Stone K, Jones R, Schubert F, Griffith CB. Two is better than one: a case of homozygous myotonic dystrophy type 1. Am J Med Genet A 2013;161A:1763-7.

329.   Jouhilahti EM, Peltonen S, Heape AM, Peltonen J. The pathoetiology of neurofibromatosis 1. Am J Pathol 2011;178:1932-9.

330.   Pauli RM, Conroy MM, Langer LO, Jr., McLone DG, Naidich T, Franciosi R *et al.* Homozygous achondroplasia with survival beyond infancy. Am J Med Genet 1983;16:459-73.

331. Germain DP. General aspects of X-linked diseases. In: Mehta A, Beck M, Sunder-Plassmann G, eds. Fabry Disease: Perspectives from 5 Years of FOS. Oxford, 2006.

332. Fujii K, Minami N, Hayashi Y, Nishino I, Nonaka I, Tanabe Y *et al.* Homozygous female Becker muscular dystrophy. Am J Med Genet A 2009;149A:1052-5.

333. Nair PS, Shetty S, Ghosh K. A homozygous female hemophilia A. Indian J Hum Genet 2012;18:134-6.

334. Morita H, Kagami M, Ebata Y, Yoshimura H. The occurrence of homozygous hemophilia in the female. Acta Haematol 1971;45:112-9.

335. Pola V, Svojitka J. [Classic hemophilia in women]. Folia Haematol Int Mag Klin Morphol Blutforsch 1957;75:43-51.

336. Sie P, Caranobe C, Benalioua M, Boneu B. Homozygous hemophilia A in a female. Thromb Haemost 1985;54:728.

337. Mazzocco MM, Holden JJ. Neuropsychological profiles of three sisters homozygous for the fragile X premutation. Am J Med Genet 1996;64:323-8.

338. Martinez AD, Acuna R, Figueroa V, Maripillan J, Nicholson B. Gap-junction channels dysfunction in deafness and hearing loss. Antioxid Redox Signal 2009;11:309-22.

339. Schein JD, Delk MT, National Association of the Deaf. The deaf population of the United States. Silver Spring, Md.: National Association of the Deaf, 1974.

340. Green GE, Scott DA, McDonald JM, Woodworth GG, Sheffield VC, Smith RJ. Carrier rates in the midwestern United States for GJB2 mutations causing inherited deafness. JAMA 1999;281:2211-6.

341. Arnos KS, Welch KO, Tekin M, Norris VW, Blanton SH, Pandya A *et al.* A comparative analysis of the genetic epidemiology of deafness in the United States in two sets of pedigrees collected more than a century apart. Am J Hum Genet 2008;83:200-7.

342. Zhang L, Zhong P, Zhai X, Shao Y, Lu S, signatories. Open letter from Chinese HIV professionals on human genome editing. Lancet 2019;393:26-7.

343. Gorman GS, Schaefer AM, Ng Y, Gomez N, Blakely EL, Alston CL *et al.* Prevalence of nuclear and mitochondrial DNA mutations related to adult mitochondrial disease. Ann Neurol 2015;77:753-9.

344. Gorman GS, Grady JP, Turnbull DM. Mitochondrial donation--how many women could benefit? N Engl J Med 2015;372:885-7.

345. Zhang J, Liu H, Luo S, Lu Z, Chavez-Badiola A, Liu Z *et al.* Live birth derived from oocyte spindle transfer to prevent mitochondrial disease. Reprod Biomed Online 2017;34:361-8.

346. Dahdouh EM, Balayla J, Garcia-Velasco JA. Comprehensive chromosome screening improves embryo selection: a meta-analysis. Fertil Steril 2015;104:1503-12.

347. Adikusuma F, Williams N, Grutzner F, Hughes J, Thomas P. Targeted Deletion of an Entire Chromosome Using CRISPR/Cas9. Mol Ther 2017;25:1736-8.

348. Zuo E, Huo X, Yao X, Hu X, Sun Y, Yin J *et al.* CRISPR/Cas9-mediated targeted chromosome elimination. Genome Biol 2017;18:224.

349. Kolgeci S, Azemi M, Ahmeti H, Dervishi Z, Sopjani M, Kolgeci J. Recurrent abortions and down syndrome resulting from Robertsonian translocation 21q; 21q. Med Arch 2012;66:350-2.

350. Victor AR, Tyndall JC, Brake AJ, Lepkowsky LT, Murphy AE, Griffin DK *et al.* One Hundred Mosaic Embryos Transferred Prospectively In A Single Clinic: Exploring When And Why They Result In Healthy Pregnancies. Fertil Steril In press.

351. . Cystic Fibrosis Foundation, accessed 06/03/2019. https://www.cff.org.

352. Morens DM, Fauci AS. Emerging Pandemic Diseases: How We Got to COVID-19. Cell 2020;182:1077-92.

353.   Zhu N, Zhang D, Wang W, Li X, Yang B, Song J *et al.* A Novel Coronavirus from Patients with Pneumonia in China, 2019. N Engl J Med 2020;382:727-33.

354.   Zhou P, Yang XL, Wang XG, Hu B, Zhang L, Zhang W *et al.* A pneumonia outbreak associated with a new coronavirus of probable bat origin. Nature 2020;579:270-3.

355.   Hoffmann M, Kleine-Weber H, Schroeder S, Kruger N, Herrler T, Erichsen S *et al.* SARS-CoV-2 Cell Entry Depends on ACE2 and TMPRSS2 and Is Blocked by a Clinically Proven Protease Inhibitor. Cell 2020;181:271-80 e8.

356.   Tang T, Bidon M, Jaimes JA, Whittaker GR, Daniel S. Coronavirus membrane fusion mechanism offers a potential target for antiviral development. Antiviral Res 2020;178:104792.

357.   Jackson CB, Farzan M, Chen B, Choe H. Mechanisms of SARS-CoV-2 entry into cells. Nat Rev Mol Cell Biol 2021.

358.   Singh M, Bansal V, Feschotte C. A Single-Cell RNA Expression Map of Human Coronavirus Entry Factors. Cell Rep 2020;32:108175.

359.   Gao QY, Chen YX, Fang JY. 2019 Novel coronavirus infection and gastrointestinal tract. J Dig Dis 2020;21:125-6.

360.   Puelles VG, Lutgehetmann M, Lindenmeyer MT, Sperhake JP, Wong MN, Allweiss L *et al.* Multiorgan and Renal Tropism of SARS-CoV-2. N Engl J Med 2020;383:590-2.

361.   Xiao F, Tang M, Zheng X, Liu Y, Li X, Shan H. Evidence for Gastrointestinal Infection of SARS-CoV-2. Gastroenterology 2020;158:1831-3 e3.

362.   Goyal P, Choi JJ, Pinheiro LC, Schenck EJ, Chen R, Jabri A *et al.* Clinical Characteristics of Covid-19 in New York City. N Engl J Med 2020;382:2372-4.

363.   Zhang C, Shi L, Wang FS. Liver injury in COVID-19: management and challenges. Lancet Gastroenterol Hepatol 2020;5:428-30.

364.	Ellul MA, Benjamin L, Singh B, Lant S, Michael BD, Easton A *et al.* Neurological associations of COVID-19. Lancet Neurol 2020;19:767-83.

365.	Moriguchi T, Harii N, Goto J, Harada D, Sugawara H, Takamino J *et al.* A first case of meningitis/encephalitis associated with SARS-Coronavirus-2. Int J Infect Dis 2020;94:55-8.

366.	Henarejos-Castillo I, Sebastian-Leon P, Devesa-Peiro A, Pellicer A, Diaz-Gimeno P. SARS-CoV-2 infection risk assessment in the endometrium: viral infection-related gene expression across the menstrual cycle. Fertil Steril 2020;114:223-32.

367.	Stanley KE, Thomas E, Leaver M, Wells D. Coronavirus disease-19 and fertility: viral host entry protein expression in male and female reproductive tissues. Fertil Steril 2020;114:33-43.

368.	Wang Z, Xu X. scRNA-seq Profiling of Human Testes Reveals the Presence of the ACE2 Receptor, A Target for SARS-CoV-2 Infection in Spermatogonia, Leydig and Sertoli Cells. Cells 2020;9.

369.	Jing Y, Run-Qian L, Hao-Ran W, Hao-Ran C, Ya-Bin L, Yang G *et al.* Potential influence of COVID-19/ACE2 on the female reproductive system. Mol Hum Reprod 2020;26:367-73.

370.	Li D, Jin M, Bao P, Zhao W, Zhang S. Clinical Characteristics and Results of Semen Tests Among Men With Coronavirus Disease 2019. JAMA Netw Open 2020;3:e208292.

371.	Delaroche L, Bertine M, Oger P, Descamps D, Damond F, Genauzeau E *et al.* Evaluation of SARS-CoV-2 in semen, seminal plasma, and spermatozoa pellet of COVID-19 patients in the acute stage of infection. PLoS One 2021;16:e0260187.

372.	Schwartz A, Yogev Y, Zilberman A, Alpern S, Many A, Yousovich R *et al.* Detection of severe acute respiratory syndrome coronavirus 2 (SARS-CoV-2) in vaginal swabs of women with acute SARS-CoV-2 infection: a prospective study. BJOG 2021;128:97-100.

373.	Postma M, Goedhart J. PlotsOfData-A web app for visualizing data together with their summaries. PLoS Biol 2019;17:e3000202.

374.   Xie X, Muruato A, Lokugamage KG, Narayanan K, Zhang X, Zou J *et al.* An Infectious cDNA Clone of SARS-CoV-2. Cell Host Microbe 2020;27:841-8 e3.

375.   Litscher ES, Wassarman PM. Zona Pellucida Proteins, Fibrils, and Matrix. Annu Rev Biochem 2020;89:695-715.

376.   Turco MY, Moffett A. Development of the human placenta. Development 2019;146.

377.   Weatherbee BAT, Glover DM, Zernicka-Goetz M. Expression of SARS-CoV-2 receptor ACE2 and the protease TMPRSS2 suggests susceptibility of the human embryo in the first trimester. Open Biol 2020;10:200162.

378.   Yan L, Yang M, Guo H, Yang L, Wu J, Li R *et al.* Single-cell RNA-Seq profiling of human preimplantation embryos and embryonic stem cells. Nat Struct Mol Biol 2013;20:1131-9.

379.   Xiang L, Yin Y, Zheng Y, Ma Y, Li Y, Zhao Z *et al.* A developmental landscape of 3D-cultured human pre-gastrulation embryos. Nature 2020;577:537-42.

380.   Zhou F, Wang R, Yuan P, Ren Y, Mao Y, Li R *et al.* Reconstituting the transcriptome and DNA methylome landscapes of human implantation. Nature 2019;572:660-4.

381.   Essahib W, Verheyen G, Tournaye H, Van de Velde H. SARS-CoV-2 host receptors ACE2 and CD147 (BSG) are present on human oocytes and blastocysts. J Assist Reprod Genet 2020.

382.   Flaherman VJ, Afshar Y, Boscardin J, Keller RL, Mardy A, Prahl MK *et al.* Infant Outcomes Following Maternal Infection with SARS-CoV-2: First Report from the PRIORITY Study. Clin Infect Dis 2020.

383.   Turan O, Hakim A, Dashraath P, Jeslyn WJL, Wright A, Abdul-Kadir R. Clinical characteristics, prognostic factors, and maternal and neonatal outcomes of SARS-CoV-2 infection among hospitalized pregnant women: A systematic review. Int J Gynaecol Obstet 2020.

384. Vivanti AJ, Vauloup-Fellous C, Prevot S, Zupan V, Suffee C, Do Cao J *et al.* Transplacental transmission of SARS-CoV-2 infection. Nat Commun 2020;11:3572.

385. Patane L, Morotti D, Giunta MR, Sigismondi C, Piccoli MG, Frigerio L *et al.* Vertical transmission of coronavirus disease 2019: severe acute respiratory syndrome coronavirus 2 RNA on the fetal side of the placenta in pregnancies with coronavirus disease 2019-positive mothers and neonates at birth. Am J Obstet Gynecol MFM 2020;2:100145.

386. Gurol-Urganci I, Jardine JE, Carroll F, Draycott T, Dunn G, Fremeaux A *et al.* Maternal and perinatal outcomes of pregnant women with SARS-CoV-2 infection at the time of birth in England: national cohort study. Am J Obstet Gynecol 2021;225:522 e1-e11.

387. Schwartz DA, Avvad-Portari E, Babal P, Baldewijns M, Blomberg M, Bouachba A *et al.* Placental Tissue Destruction and Insufficiency from COVID-19 Causes Stillbirth and Neonatal Death from Hypoxic-Ischemic Injury: A Study of 68 Cases with SARS-CoV-2 Placentitis from 12 Countries. Arch Pathol Lab Med 2022.

388. Hosier H, Farhadian SF, Morotti RA, Deshmukh U, Lu-Culligan A, Campbell KH *et al.* SARS-CoV-2 infection of the placenta. J Clin Invest 2020;130:4947-53.

389. Gioia CD, Zullo F, Vecchio RCB, Pajno C, Perrone G, Galoppi P *et al.* Stillbirth and fetal capillary infection by SARS-CoV-2. Am J Obstet Gynecol MFM 2021:100523.

390. Sharps MC, Hayes DJL, Lee S, Zou Z, Brady CA, Almoghrabi Y *et al.* A structured review of placental morphology and histopathological lesions associated with SARS-CoV-2 infection. Placenta 2020;101:13-29.

391. Debelenko L, Katsyv I, Chong AM, Peruyero L, Szabolcs M, Uhlemann AC. Trophoblast damage with acute and chronic intervillositis: disruption of the placental barrier by severe acute respiratory syndrome coronavirus 2. Hum Pathol 2021;109:69-79.

392. Linehan L, O'Donoghue K, Dineen S, White J, Higgins JR, Fitzgerald B. SARS-CoV-2 placentitis: An uncommon complication of maternal COVID-19. Placenta 2021;104:261-6.

393.   Garrido-Pontnou M, Navarro A, Camacho J, Crispi F, Alguacil-Guillen M, Moreno-Baro A *et al.* Diffuse trophoblast damage is the hallmark of SARS-CoV-2-associated fetal demise. Mod Pathol 2021;34:1704-9.

394.   Segars J, Katler Q, McQueen DB, Kotlyar A, Glenn T, Knight Z *et al.* Prior and novel coronaviruses, Coronavirus Disease 2019 (COVID-19), and human reproduction: what is known? Fertil Steril 2020;113:1140-9.

395.   Madjunkov M, Dviri M, Librach C. A comprehensive review of the impact of COVID-19 on human reproductive biology, assisted reproduction care and pregnancy: a Canadian perspective. J Ovarian Res 2020;13:140.

396.   Barragan M, Guillen JJ, Martin-Palomino N, Rodriguez A, Vassena R. Undetectable viral RNA in oocytes from SARS-CoV-2 positive women. Hum Reprod 2020.

397.   Ory S, Veiga A, Horton M, Gianaroli L. Joint IFFS/ESHRE statement on COVID-19 vaccination for pregnant women and those considering pregnancy(). Hum Reprod Open 2021;2021:hoab016.

398.   Theiler RN, Wick M, Mehta R, Weaver AL, Virk A, Swift M. Pregnancy and birth outcomes after SARS-CoV-2 vaccination in pregnancy. Am J Obstet Gynecol MFM 2021;3:100467.

399.   Aharon D, Lederman M, Ghofranian A, Hernandez-Nieto C, Canon C, Hanley W *et al.* In Vitro Fertilization and Early Pregnancy Outcomes After Coronavirus Disease 2019 (COVID-19) Vaccination. Obstet Gynecol 2022.

400.   Maggiulli R, Giancani A, Fabozzi G, Dovere L, Tacconi L, Amendola MG *et al.* Assessment and management of the risk of SARS-CoV-2 infection in an IVF laboratory. Reprod Biomed Online 2020;41:385-94.

401.   Rajput SK, Khan SA, Goheen BB, Engelhorn HJ, Logsdon DM, Grimm CK *et al.* Absence of SARS-CoV-2 (COVID-19 virus) within the IVF laboratory using strict patient screening and safety criteria. Reprod Biomed Online 2021;42:1067-74.

402.   Simopoulou M, Sfakianoudis K, Giannelou P, Rapani A, Siristatidis C, Bakas P *et al.* Navigating assisted reproduction treatment in the time of COVID-19: concerns and considerations. J Assist Reprod Genet 2020;37:2663-8.

403.   Veiga A, Gianaroli L, Ory S, Horton M, Feinberg E, Penzias A. Assisted reproduction and COVID-19: a joint statement of ASRM, ESHRE and IFFS. Hum Reprod Open 2020;2020:hoaa033.

404.   Ata B, Gianaroli L, Lundin K, McHeik S, Mocanu E, Rautakallio-Hokkanen S *et al.* Outcomes of SARS-CoV-2 infected pregancies after medically assisted reproduction. Hum Reprod 2021;36:2883-90.

405.   Boushra MN, Koyfman A, Long B. COVID-19 in pregnancy and the puerperium: A review for emergency physicians. Am J Emerg Med 2020.

406.   Biesecker LG, Spinner NB. A genomic view of mosaicism and human disease. Nat Rev Genet 2013;14:307-20.

407.   Viotti M, Victor AR, Barnes FL, Zouves CG, Besser AG, Grifo J *et al.* New insights from one thousand mosaic embryo transfers: features of mosaicism dictating rates of implantation, spontaneous abortion, and neonate health. Fertil Steril 2020;114:e1 - e2 .

408.   Viotti M, Victor AR, Barnes FL, Zouves CG, Besser AG, Grifo JA *et al.* Using outcome data from one thousand mosaic embryo transfers to formulate an embryo ranking system for clinical use. Fertil Steril 2021;115:1212-24.

409.   Coticchio G, Barrie A, Lagalla C, Borini A, Fishel S, Griffin D *et al.* Plasticity of the human preimplantation embryo: developmental dogmas, variations on themes and self-correction. Hum Reprod Update 2021.

410.   Zamani Esteki M, Viltrop T, Tsuiko O, Tiirats A, Koel M, Noukas M *et al.* In vitro fertilization does not increase the incidence of de novo copy number alterations in fetal and placental lineages. Nat Med 2019;25:1699-705.

411.   Starostik MR, Sosina OA, McCoy RC. Single-cell analysis of human embryos reveals diverse patterns of aneuploidy and mosaicism. Genome Res 2020;30:814-25.

412.   Yang M, Rito T, Metzger J, Naftaly J, Soman R, Hu J *et al.* Depletion of aneuploid cells in human embryos and gastruloids. Nat Cell Biol 2021;23:314-21.

413.   Zhou S, Xie P, Zhang S, Hu L, Luo K, Gong F *et al.* Complex mosaic blastocysts after preimplantation genetic testing: prevalence and outcomes after re-biopsy and re-vitrification. Reprod Biomed Online 2021.

414.   Biricik A, Cotroneo E, Minasi MG, Greco PF, Bono S, Surdo M *et al.* Cross-Validation of Next-Generation Sequencing Technologies for Diagnosis of Chromosomal Mosaicism and Segmental Aneuploidies in Preimplantation Embryos Model. Life (Basel) 2021;11.

415.   Marin D, Xu J, Treff NR. Preimplantation genetic testing for aneuploidy: A review of published blastocyst reanalysis concordance data. Prenat Diagn 2021;41:545-53.

416.   Popovic M, Dhaenens L, Boel A, Menten B, Heindryckx B. Chromosomal mosaicism in human blastocysts: the ultimate diagnostic dilemma. Hum Reprod Update 2020;26:313-34.

19. Supplementary Figures

Supplementary Figure 1. Validation Of Contamination-Free ICM And TE Biopsy Technique.
Nuclear counterstain (Hoechst) and immunofluorescent stains for the TE marker GATA3 and ICM marker OCT4 in matched isolated TE and ICM biopsies. Numbers in nuclear stain panels indicate total number of cells for each biopsy. Numbers in TE stain panels indicate incidence of cells positive for GATA3. Numbers in ICM stain panels indicate incidence of cells with high nuclear signal for OCT4. Scale bars = 25µm.
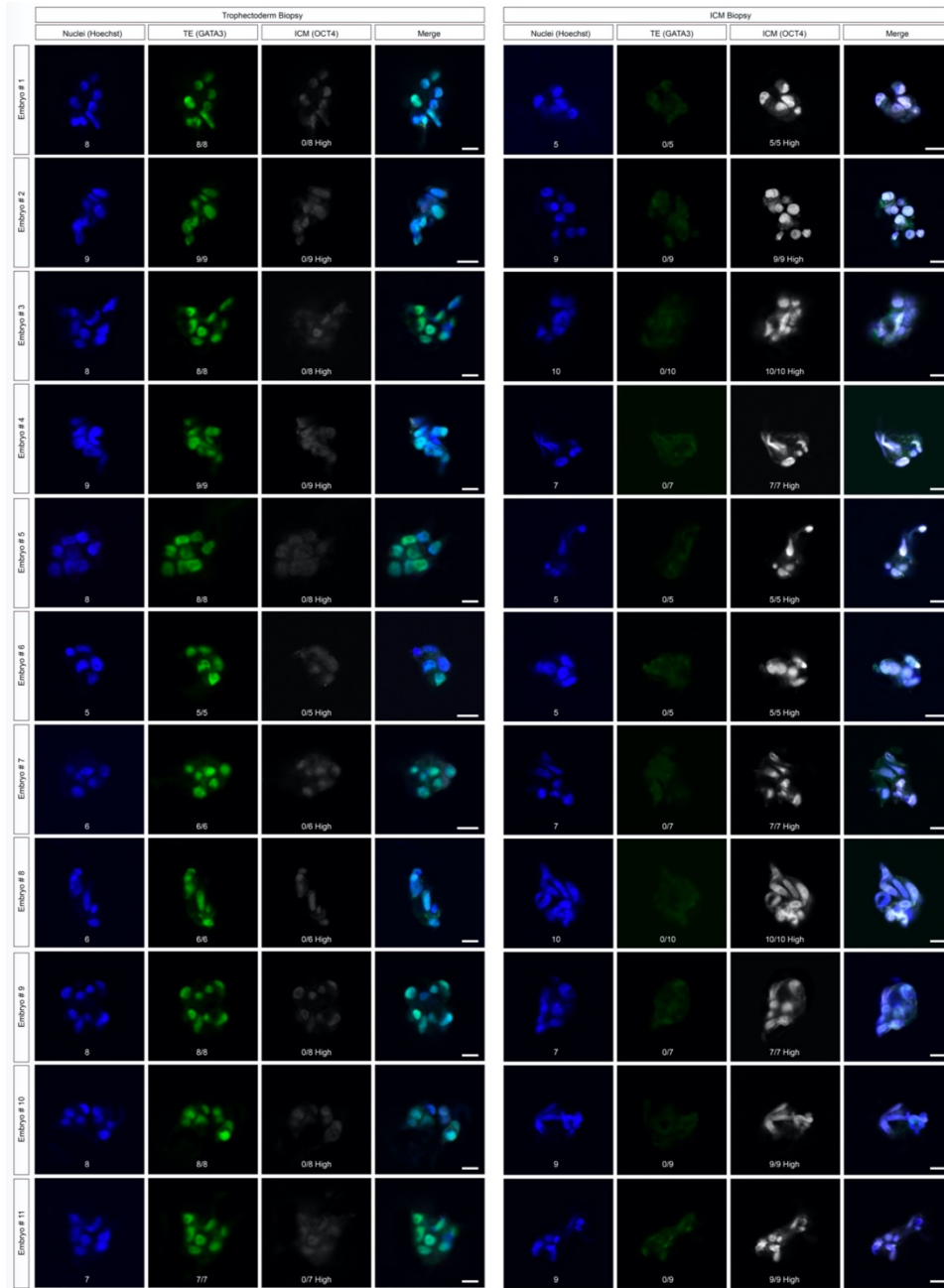
Supplementary Figure 2. Karyotype Profiles Analyzed In This Study (Continued From Figure 13).
Use Table 1 as a reference for resulting analysis.

To access the data, please use the following link:

https://drive.google.com/file/d/17eZO12wR2E6Gyou0au8l5bnTaVZS9Hns/view?usp=sharing

Supplementary Figure 3. Genotypes Of Discordant Blastocysts Visualized In Reference Ancestry Space.
See also Supplementary Table 1.
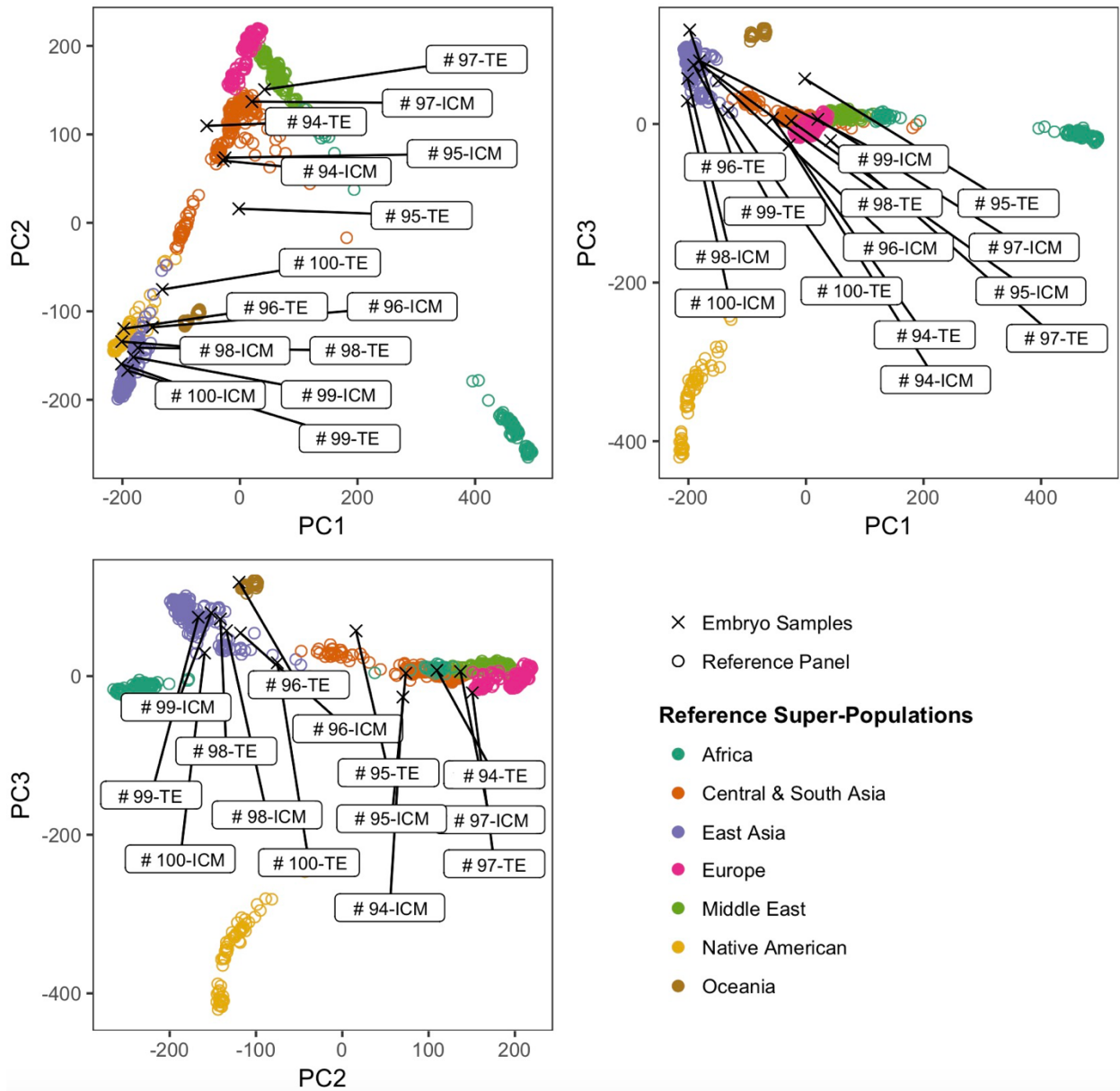
Supplementary Figure 4. Analysis Of Correlation Between Morphology And Intra-Blastocyst Karyotype Discordance.

Blastocysts were evaluated using the Gardner system, that assigns a number score for blastocyst expansion stage (1-6 from least to most progressed), and letter scores for ICM and TE grades (C-A from worst to best quality) (207). Stage of blastocyst was analyzed when there was any intra-blastocyst karyotype inconsistency (A), when an inconsistency was specific to the ICM (B), and when an inconsistency was specific to the TE (C). Grade of the ICM was analyzed when there was any karyotype inconsistency between clinical TE biopsy and the ICM (D). Grade of the TE was analyzed when there was any karyotype inconsistency between clinical TE and second TE biopsy (E). Note that in graphs A, C, and D, sample numbers do not add up to 100 because in six cases the second TE biopsy was not processed (in five cases the biopsy could not be collected, and in one case there was a failed WGA reaction).
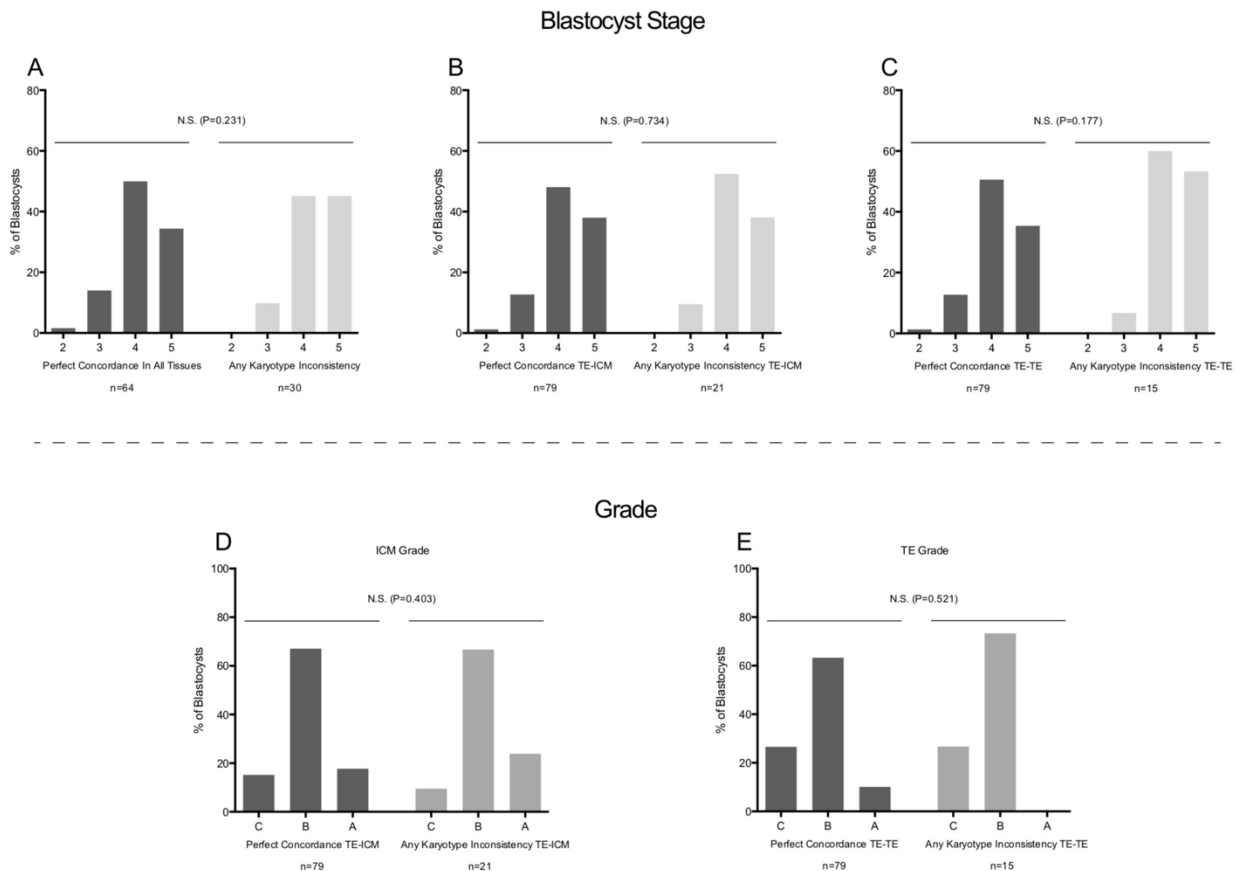
Supplementary Figure 5. Validation Of mtDNA Quantitation Platforms.

(A-C) Standard curves for the three qPCR assays used, showing high experimental efficiency. (D) NGS validation for mtDNA score reproducibility. Blastocyst biopsy-derived WGA samples were sequenced in duplicates (full circles) or triplicates (full diamonds) showing consistent mtDNA scores in repeated runs. Each sample from a-l represents one embryo WGA biopsy and numbers represent number of replicate NGS runs. Cell samples from two different cell lines (m and n) underwent repeated WGA and subsequent NGS. Half circles represent two replicates for cell line m, and half squares represent four replicates for cell line n. The consistent values for each cell line indicate that neither WGA nor NGS introduce variability in the mtDNA score determination. Full triangles (o) depict a duplicate run of blood isolated from a patient, for which DNA isolation, WGA, and NGS were run separately, and resulted in consistent mtDNA scores. (E) WGA samples from five blastocysts (Controls A-E) were used to determine mtDNA scores by NGS (purple circles), qPCR assaying the mitochondrial CYTB gene by absolute quantitation (blue circles), and qPCR assaying the mitochondrial ND6 gene by relative quantitation (orange circles). Raw values for each technique (indicated above the circles) were normalized to Control A. Fold changes of mtDNA scores A<B<C<D<E for all three techniques, indicating cross-platform consistency of mtDNA score ranking.
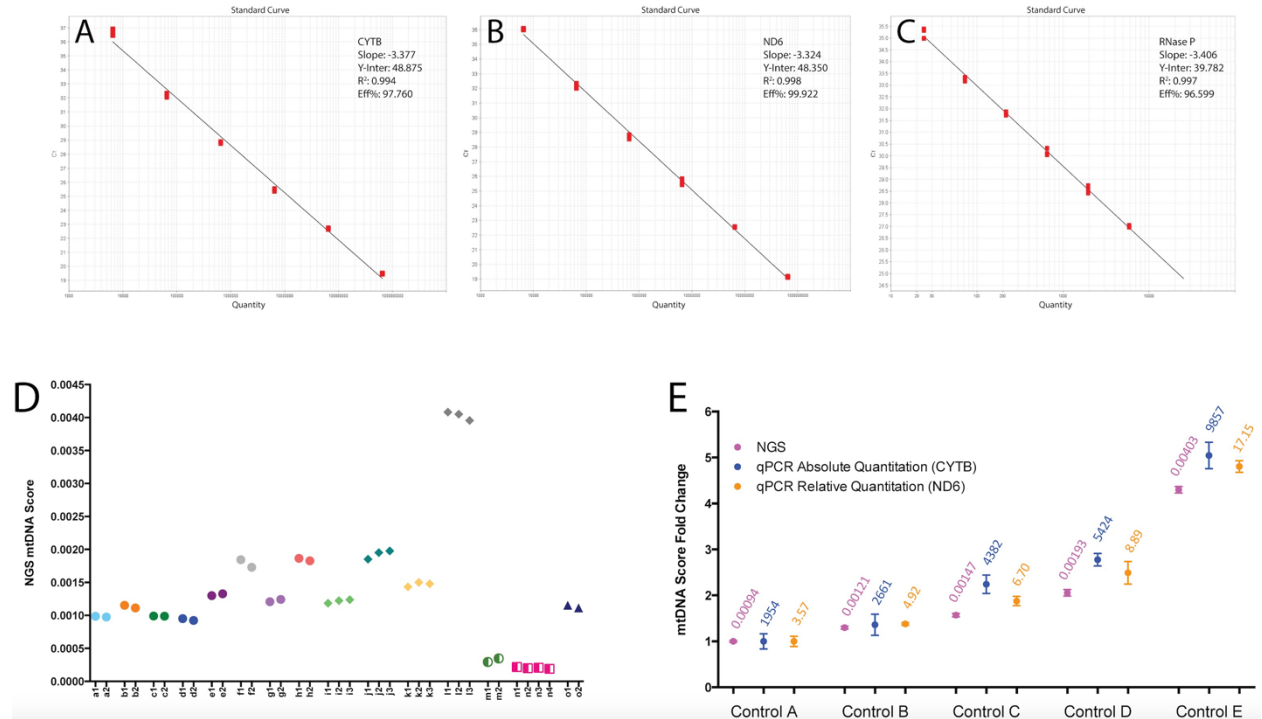
Supplementary Figure 6. Intra-Cohort Analysis Of mtDNA Scores For 24 Patients With Repeat Transfers Sorted By Blastocyst Viability, Showing A Statistically Insignificant Difference.

Intra-cohort analysis of mtDNA scores for 24 patients with repeat transfers sorted by blastocyst viability, showing a statistically insignificant difference. For this NGS analysis only reads aligning to Chr 1 were used for standardization. N. S. = not significant.
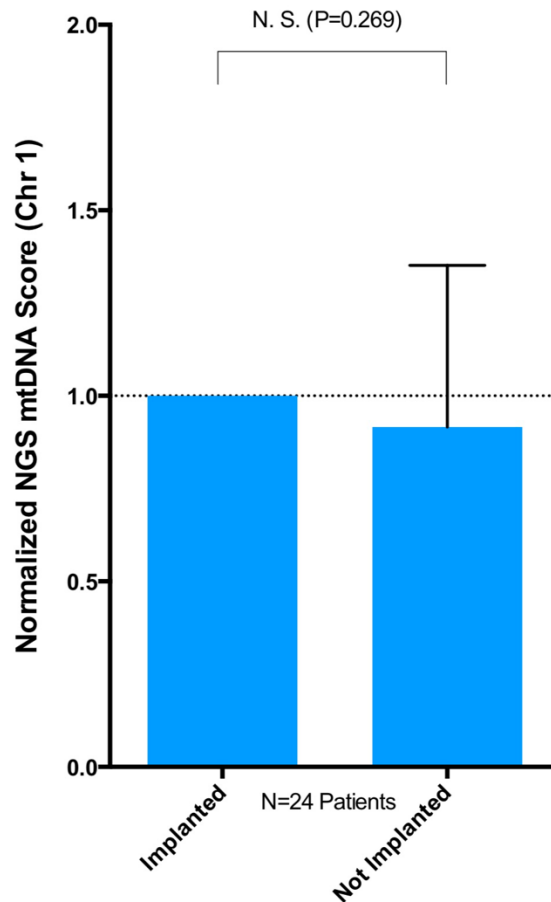
Supplementary Figure 7. Analysis Of Tissue Relatedness In Serial Biopsies Of Blastocysts.

Graph depicting log-likelihood ratios of relatedness. In green, controls comparing biopsies from embryos derived from unrelated patients, showing negative values. In red, control comparison between biopsies from blastocysts derived from the same patient (full-sibs)

showing positive values. In purple, comparisons between paired biopsies for each blastocyst analyzed in the study, showing positive log-likelihood ratios of relatedness.
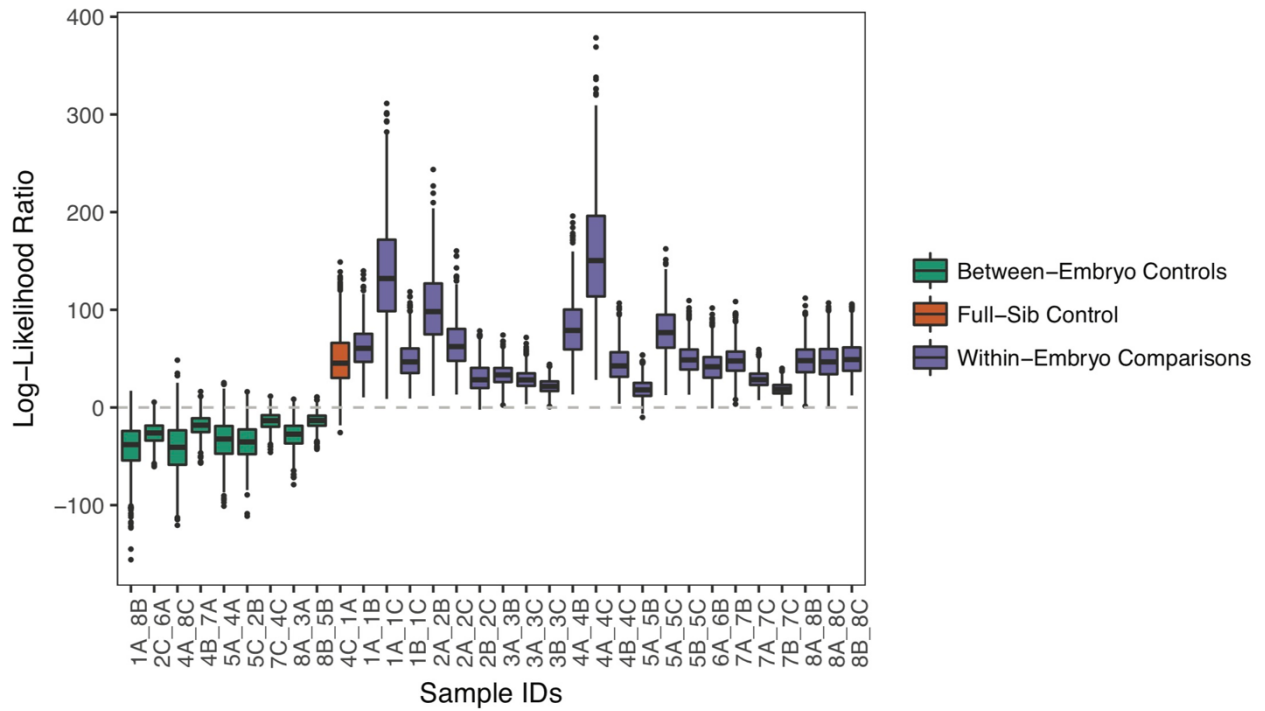
Supplementary Figure 8. Clinical Outcomes Of Transferred Euploid And Mosaic Embryos, With Controls.
(A) Comparison of the euploid group to various mosaic sub-groups. (B) Comparison of the morphology-normalized euploid group to various mosaic sub-groups.
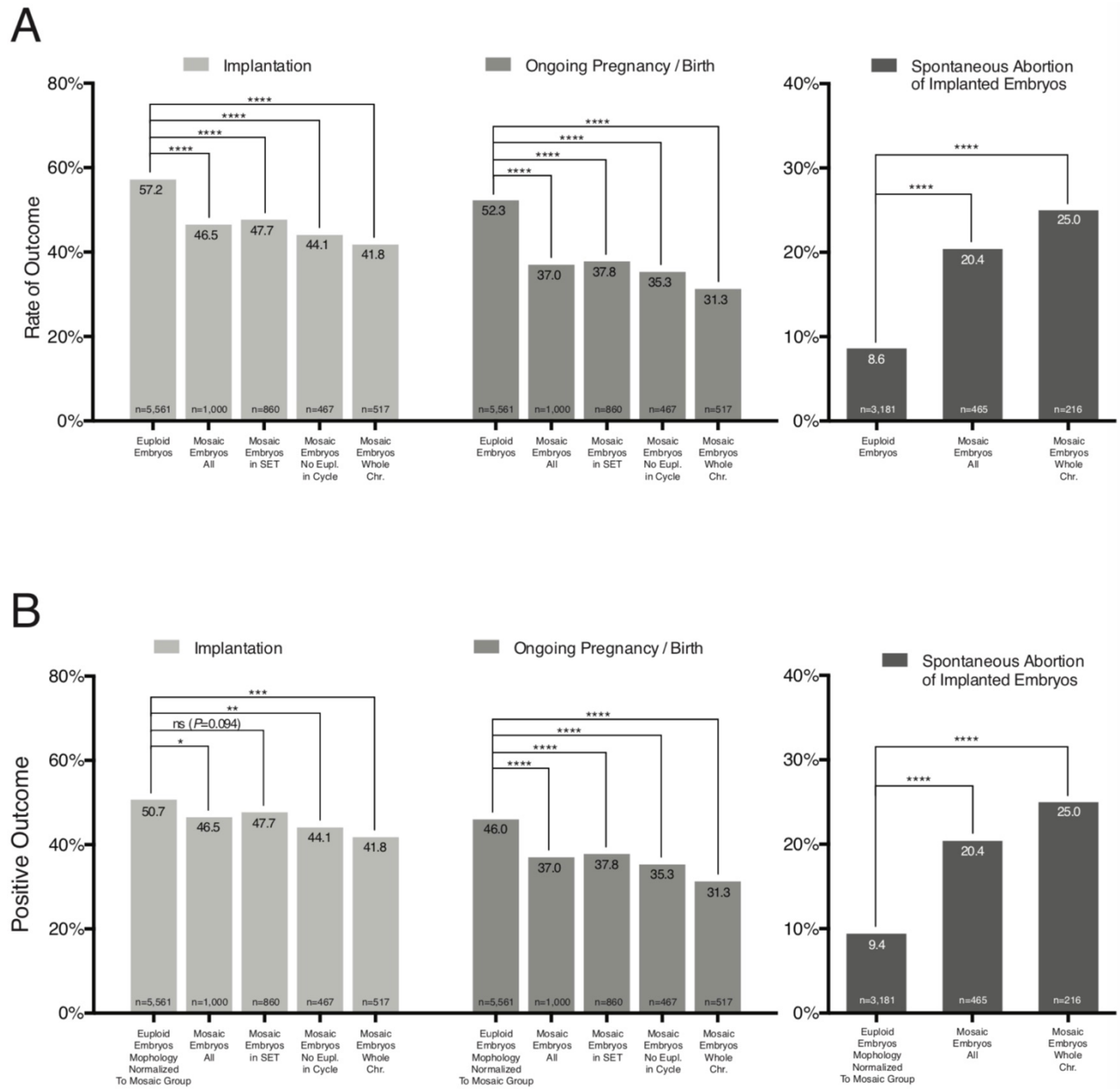
Supplementary Figure 9. Effect Of Mosaicism Level On Clinical Outcomes.
Analysis of outcomes with different cutoffs defining low and high levels of mosaicism.
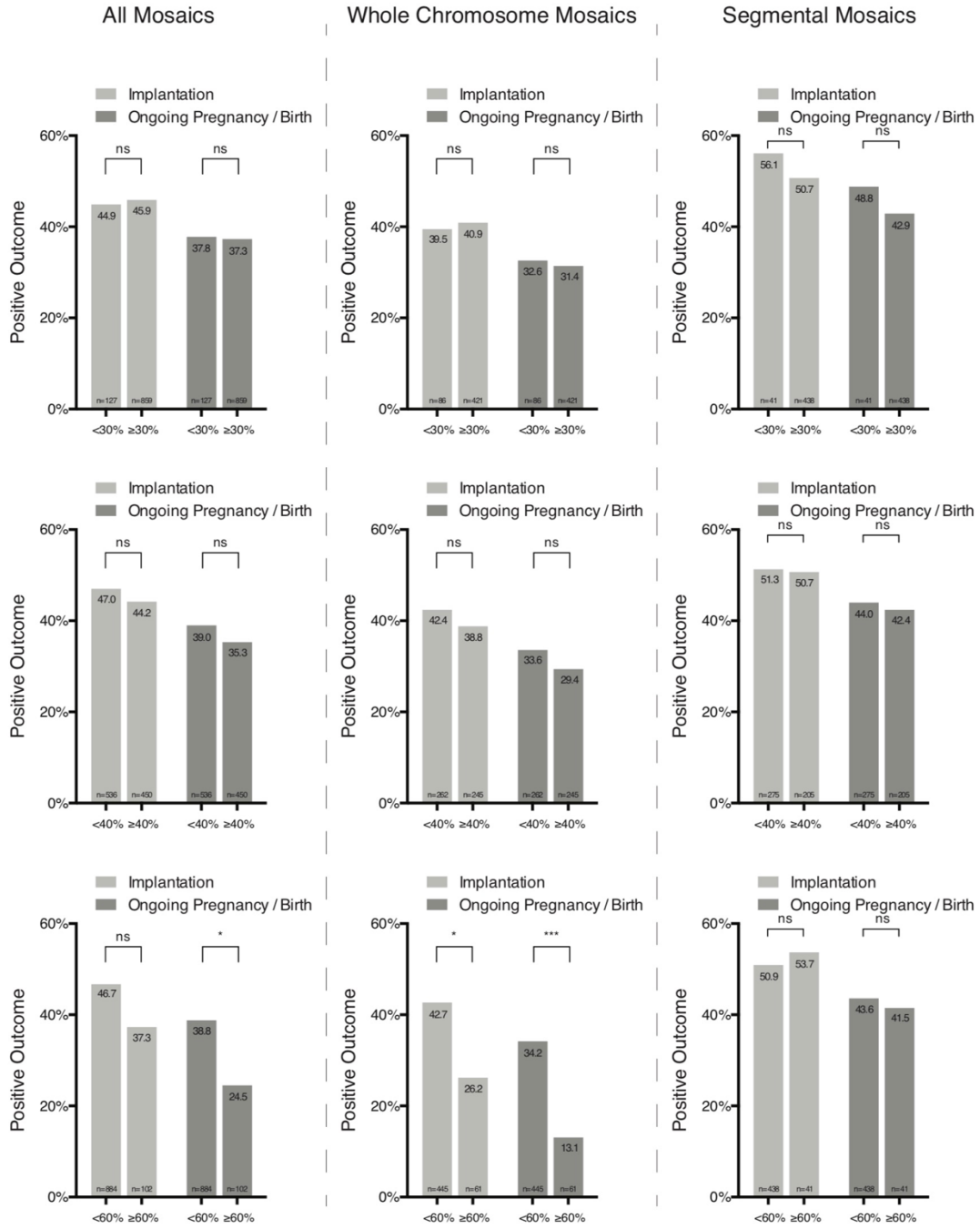
Supplementary Figure 10. Effect Of Mosaicism Type On Clinical Outcomes.
Effect Of Mosaicism Type On Clinical Outcomes. Segmental mosaic sub-type analysis.
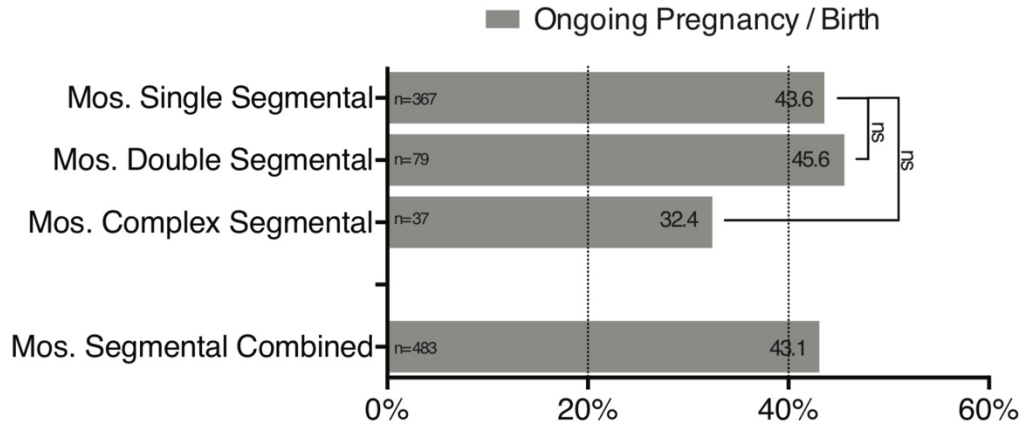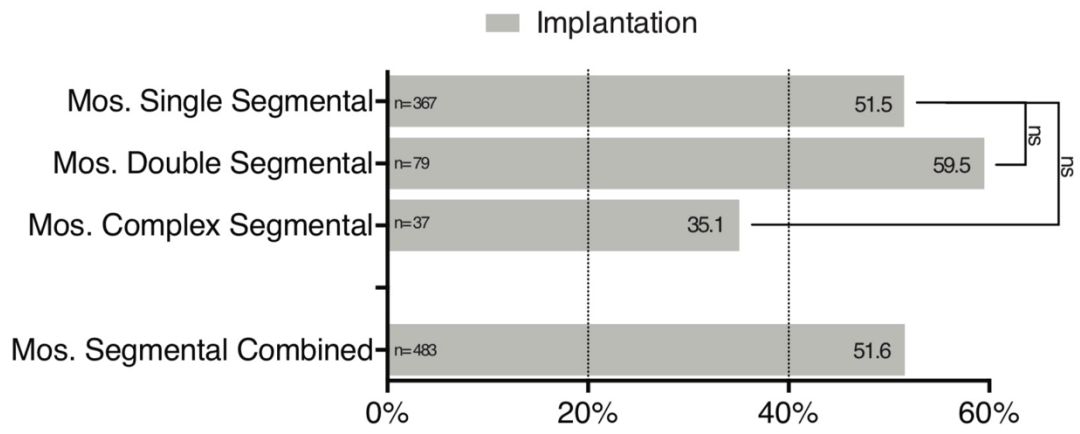
Supplementary Figure 11. Effect Of Maternal Age On Clinical Outcomes Of Mosaic Embryo Transfers.
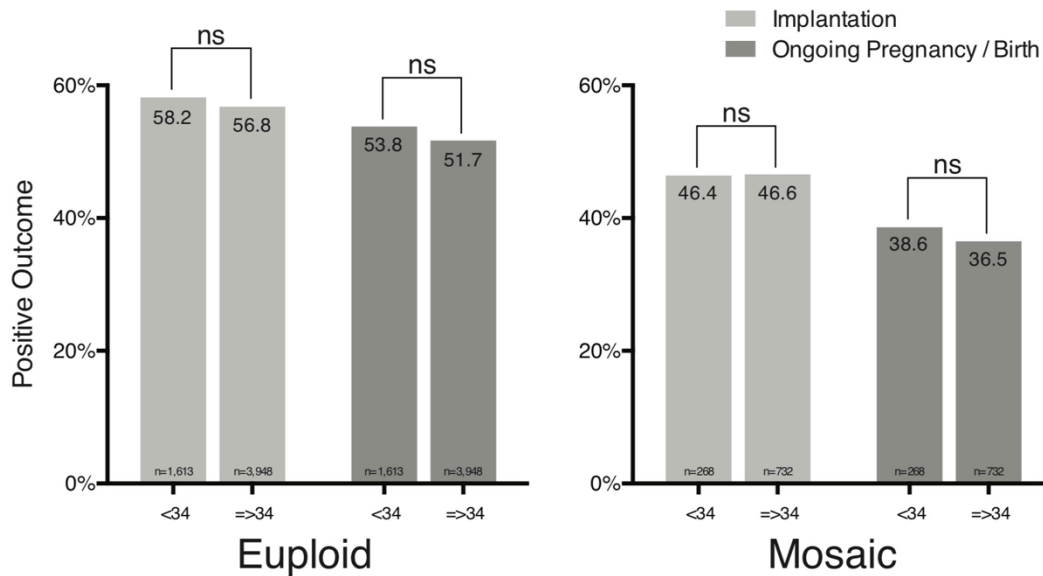
Supplementary Figure 12. Reporter Virion Experiments Indicate Entry Into Cells Of The Embryo Occurs Via S And ACE2.
Sample images from GFP reporter virion experiments, displaying merged brightfield with epifluorescence signal. Top set shows results from HIV-based virus, bottom set shows results from the VSVΔG-based virus. Two representative images are shown per condition. The sample size of each condition is indicated in Table 1. Pink arrowheads point to cells displaying robust GFP signal, yellow arrowheads point to punctate GFP signal, and white asterisks indicate embryos manifesting poor health (likely due to expression of native genes in the reporter virions). Scale bars represent 50 µm.
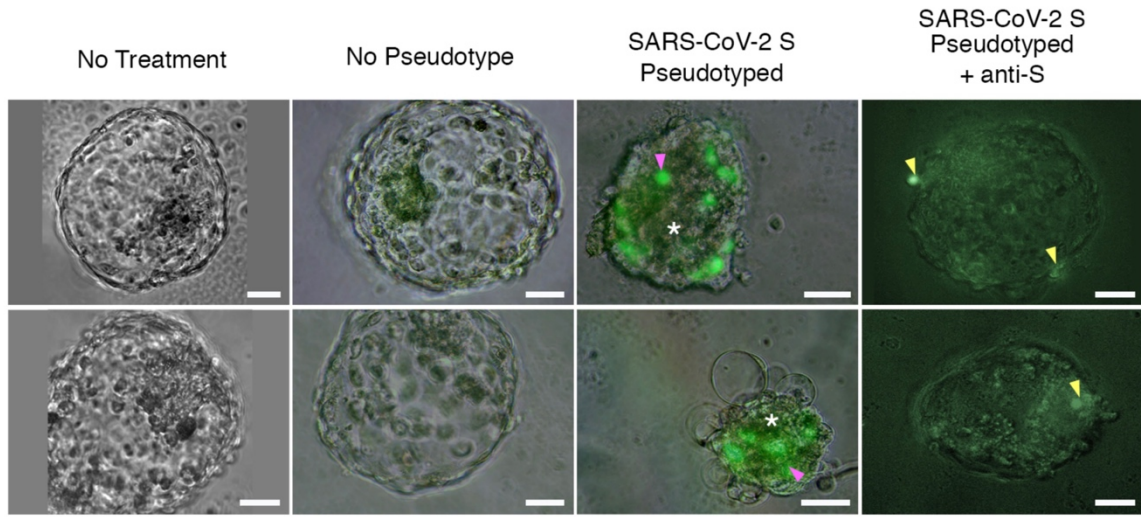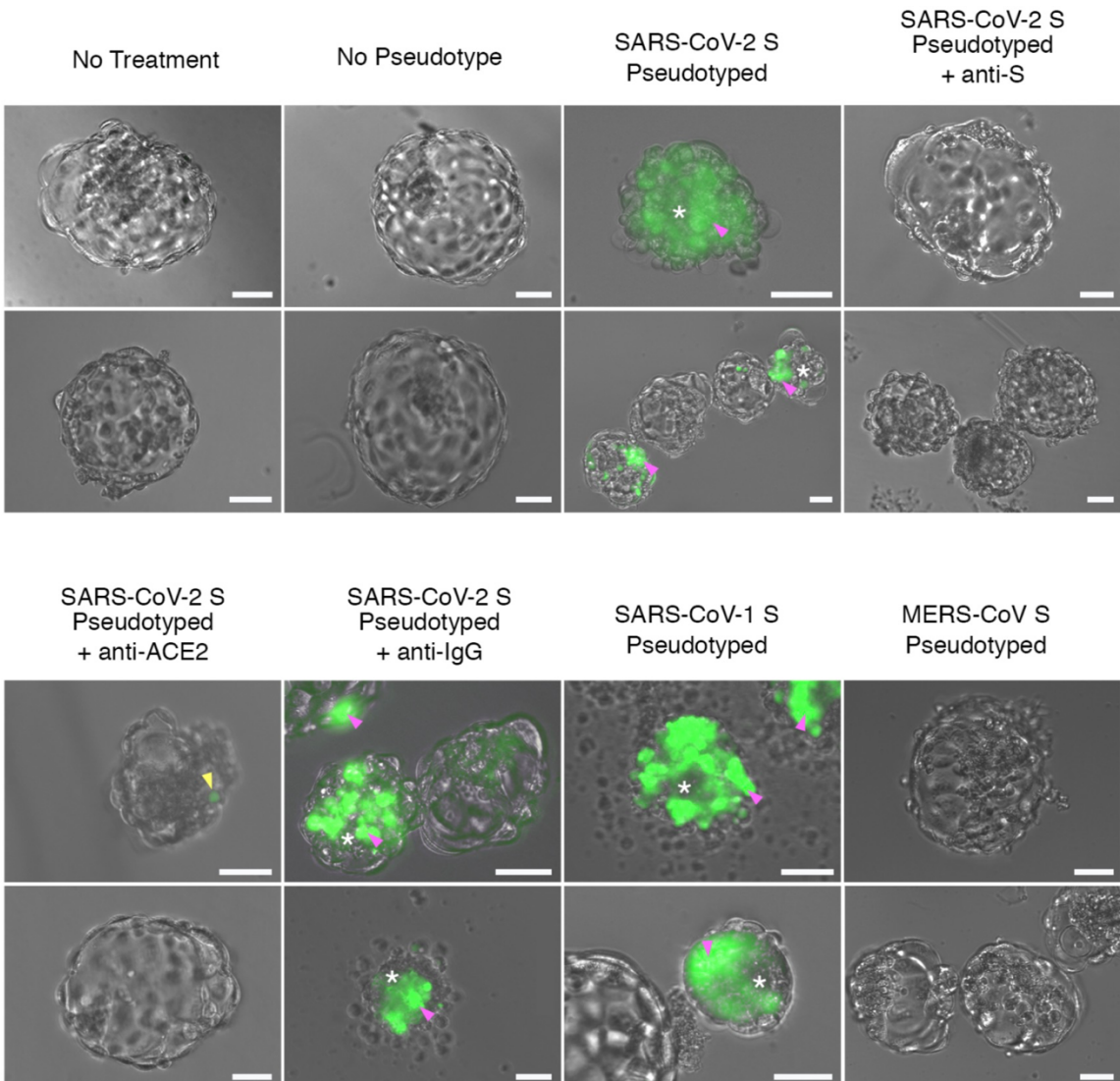
Supplementary Figure 13. Live SARS-CoV-2 Experiments Indicate Susceptibility To Infection By Cells Of The Embryo Through S And ACE2.
Sample images from SARS-CoV-2-mNeonGreen experiments, displaying merged brightfield with epifluorescence signal. The sample size of each condition is indicated in
Table 9 and Supplementary Table 11. Scale bars represent 100 μm.

20. Supplementary Tables

Supplementary Table 1. Blastocysts And Assigned 1000 Genomes Super-populations.

Blastocyst ID	Primary Ancestry Composition of K = 10 Nearest Neighbors		1000 Genomes Reference Panel Super-Population
	ICM	**TE**	
#94	C/S Asia	C/S Asia	SAS
#95	C/S Asia	C/S Asia	SAS
#96	East Asia	East Asia	EAS
#97	Europe	Middle East	EUR
#98	East Asia	East Asia	EAS
#99	East Asia	East Asia	EAS
#100	East Asia	East Asia	EAS

Supplementary Table 2. Logistic Regression Analysis For mtDNA Score.
Calculation assesses the mtDNA score predicts clinical outcome (implanted or not implanted) upon blastocyst transfer, adjusted for potential confounding factors. Factors included in the analysis are oocyte age at retrieval, single or paired sibling transfer, patient age at transfer, embryo gender, cohort size (i.e. how many embryos produced in the cycle), embryo stage and grade.

Coefficient	Estimate	SE	z value	Pr(> |z|) (*P* value)
(Intercept)	−16.99957	1693.53420	−0.010	.992
mtDNA Score	141.66159	196.88366	0.720	.472
Oocyte_Age	0.02358	0.02760	0.854	.393
Single_Double	0.14068	0.50621	0.278	.781
Age_Recipient	−0.01523	0.02999	−0.508	.612
Embryo_Gender	0.12338	0.28737	0.429	.668
Cohort_Size	0.02848	0.03575	0.797	.426
Embryo_StageGradeBIII	−0.16203	2936.98335	0.000	1.000
Embryo_StageGradeFHBII	16.85901	1693.53392	0.010	.992
Embryo_StageGradeFHBIII	−0.21243	2936.98334	0.000	1.000
Embryo_StageGradeHBI	−0.25392	2385.32511	0.000	1.000
Embryo_StageGradeHBII	16.09310	1693.53370	0.010	.992
Embryo_StageGradeHBIII	16.06627	1693.53382	0.009	.992
Embryo_StageGradeXBI	16.80955	1693.53369	0.010	.992
Embryo_StageGradeXBII	16.11707	1693.53365	0.010	.992
Embryo_StageGradeXBIII	14.86599	1693.53372	0.009	.993

Note: Factors included in the analysis are oocyte age at retrieval, single or paired sibling transfer, patient age at transfer, embryo gender, cohort size (i.e., how many embryos produced in the cycle), embryo stage, and grade.
Deviance residuals: Min: −1.468; 1Q: −1.079; Median: −0.632; 3Q: 1.229; Max: 1.799.
(Dispersion parameter for binomial family taken to be 1.)
Null deviance: 326.67 on 239 degrees of freedom.
Residual deviance: 306.18 on 224 degrees of freedom.
(538 observations deleted because of missingness.)
Akaike Information Criterion: 338.18.
Number of Fisher scoring iterations: 15.

Supplementary Table 3. Conditions Tested In Newborns Resulting From Transfers Of Blastocysts With Elevated mtDNA Levels.

Category	Condition
Amino Acid	Argininemia (ARG)
Disorders	Argininosuccinic Aciduria (ASA)
	Benign Hyperphenylalaninemia (H-PHE)
	Biopterin Defect in Cofactor Biosynthesis (BIOPT-BS)
	Biopterin Defect in Cofactor Regeneration (BIOPT-REG)
	Carbamoyl Phosphate Synthetase I Deficiency (CPS)
	Citrullinemia, Type I (CIT)
	Citrullinemia, Type II (CIT II)
	Classic Phenylketonuria (PKU)
	Homocystinuria (HCY)
	Hypermethioninemia (MET)
	Hyperornithine with Gyrate Deficiency (Hyper ORN)

	Maple Syrup Urine Disease (MSUD)
	Ornithine Transcarbamylase Deficiency (OTC)
	Prolinemia (PRO)
	Tyrosinemia, Type I (TYR I)
	Tyrosinemia, Type II (TYR II)
	Tyrosinemia, Type III (TYR III)
Endocrine	Congenital Adrenal Hyperplasia (CAH)
Disorders	Primary Congenital Hypothyroidism (CH)
Fatty Acid	Carnitine Acylcarnitine Translocase Deficiency (CACT)
Oxidation Disorders	Carnitine Palmitoyltransferase I Deficiency (CPT-IA)
	Carnitine Palmitoyltransferase Type II Deficiency (CPT-II)
	Carnitine Uptake Defect (CUD)
	Glutaric Acidemia, Type II (GA-2)
	Long-Chain L-3 Hydroxyacyl-CoA Dehydrogenase Deficiency (LCHAD)
	Medium-Chain Acyl-CoA Dehydrogenase Deficiency (MCAD)
	Medium/Short-Chain L-3 Hydroxyacyl-CoA Dehydrogenase Deficiency (M/SCHAD)
	Short-Chain Acyl-CoA Dehydrogenase Deficiency (SCAD)
	Trifunctional Protein Deficiency (TFP)
	Very Long-Chain Acyl-CoA Dehydrogenase Deficiency (VLCAD)
Hemoglobin	Hemoglobinopathies (Var Hb)
Disorders	S, Beta-Thalassemia (Hb S/ßTh)
	S, C Disease (Hb S/C)
	Sickle Cell Anemia (Hb SS)
Lysosomal Storage	Mucopolysaccharidosis Type-I (MPS I)
Disorders	Pompe (POMPE)
Organic Acid	2-Methyl-3-Hydroxybutyric Acidemia (2M3HBA)
Conditions	2-Methylbutyrylglycinuria (2MBG)

3-Hydroxy-3-Methylglutaric Aciduria (HMG)

3-Methylcrotonyl-CoA Carboxylase Deficiency (3-MCC)

3-Methylglutaconic Aciduria (3MGA)

Beta-Ketothiolase Deficiency (BKT)

Ethylmalonic Encephalopathy (EME)

Glutaric Acidemia, Type I (GA-1)

Holocarboxylase Synthetase Deficiency (MCD)

Isobutyrylglycinuria (IBG)

Isovaleric Acidemia (IVA)

Malonic Acidemia (MAL)

Methylmalonic Acidemia (Cobalamin Disorders) (Cbl A,B)

Methylmalonic Acidemia (Methymalonyl-CoA Mutase Deficiency) (MUT)

Methylmalonic Acidemia with Homocystinuria (Cbl C, D, F)

Propionic Acidemia (PROP)

Other Disorders Adrenoleukodystrophy (ALD)

Biotinidase Deficiency (BIOT)

Classic Galactosemia (GALT)

Critical Congenital Heart Disease (CCHD)

Cystic Fibrosis (CF)

Formiminoglutamic Acidemia (FIGLU)

Hearing loss (HEAR)

Hyperornithinemia-Hyperammonemia-Homocitrullinuria Syndrome (HHH)

Severe Combined Immunodeficiency (SCID)

T-cell Related Lymphocyte Deficiencies

Supplementary Table 4. List Of Double Embryo Transfers Using One Mosaic And One Euploid Blastocyst.

Transfer #	Mosaic Embryo Grade	Euploid Embryo Grade	Beta-hCG	Mosaic Sac	Euploid Sac	Mosaic Heartbeat	Euploid Heartbeat
1	5BC	5AB	+	Y	Y	Y	Y
2	5AB	5BB	+	Y	Y	Y	Y
3	5BB	5BB	+	Y	Y	Y	Y
4	6BB	4CC	+	Y	N	Y	N
5	5BB	5CC	+	Y	N	Y	N
6	5CC	5CB	+	N	N	N	N
7	3BB	6CB	+	(Y)	(Y)	(Y)	(Y)
8	5BC	5BC	+	N	N	N	N
9	5BB	5BB	+	(Y)	(Y)	N	N
10	5CC	5CC	-	N	N	N	N
11	6CB	5BB	-	N	N	N	N
12	5BB	5CC	-	N	N	N	N
13	5BB	5CC	-	N	N	N	N
14	4CC	5CC	-	N	N	N	N
15	5CC	5BB	-	N	N	N	N
16	5BB	5BB	-	N	N	N	N
17	5BC	4CC	-	N	N	N	N
18	5BB	5BC	-	N	N	N	N

Supplementary Table 5. Age Of Oocyte At Retrieval Affects Clinical Outcome In All Types Of Mosaic Embryo Transfers.

Age of Oocyte (years)	Embryos Transferred	Beta-hCG +	Sac [Implantation]	Fetal Heartbeat	Beta-hCG + (%)	Sac (%) [Implantation]	Fetal Heartbeat (%)	P Value Sac [Implantation]	P Value Fetal Heartbeat	Average Mosaicism
≤34 Euploid	141	95	72	69	67.4%	51.1%	48.9%	N/A	N/A	N/A
>34 Euploid	337	201	165	156	59.6%	49.0%	46.2%	0.6893 (ns) [b]	0.6164 (ns) [b]	N/A
≤34 Mosaic All	34	21	19	16	61.8%	55.9%	47.1%			35%
>34 Mosaic All	66	28	18	14	42.4%	27.3%	21.2%	0.0082 (**) [b]	0.0111 (*) [b]	36%
≤34 Mos. Single Segm.	7	6	5	4	85.7%	71.4%	57.1%			39%
>34 Mos. Single Segm.	26	13	10	9	50.0%	38.5%	34.6%	0.2028 (ns) [b]	0.3926 (ns) [b]	34%
≤34 Mos. Multi Segm.	6	3	3	3	50.0%	50.0%	50.0%			38%
>34 Mos. Multi Segm.	5	1	1	1	20.0%	20.0%	20.0%	0.5455 (ns) [b]	0.5455 (ns) [b]	46%
≤34 Mos. 1 or 2 Whole Chr.	15	9	7	6	60.0%	46.7%	40.0%			31%
>34 Mos. 1 or 2 Whole Chr.	28	9	5	4	32.1%	17.9%	13.0%	0.0739 (ns) [b]	0.0726 (ns) [b]	34%
≤34 Mos. Complex	6	4	4	3	66.7%	66.7%	50.0%			38%
>34 Mos. Complex	7	4	2	1	57.1%	28.5%	14.3%	0.2861 (ns) [b]	0.2657 (ns) [b]	42%

Supplementary Table 6. List Of Mosaic Embryos Analyzed In This Study With Associated Information.

The entry 'n/a' indicates data not available.

To access the data, please use the following link:

https://docs.google.com/spreadsheets/d/1yDjXszbD0cvUA6xGFhLD4MAMX-bPxGoy/edit?usp=sharing&ouid=110580616696492711817&rtpof=true&sd=true

Supplementary Table 7. Table For Normalization Of The Euploid Group To The Mosaic Group By Morphology.

Gardner Grade	Mosaic Group Incidence	Matched Euploid Group Incidence	Rate of Implantation in Euploid Group	Rate of OP/B in Euploid Group	Euploid Group Implanted Samples	Euploid Group OP/B Samples
2CC	3	3	0.0000	0.0000	0.00	0.00
2CB	0	0	0.0000	0.0000	0.00	0.00
2BC	2	2	0.0000	0.0000	0.00	0.00
2BB	0	0	0.0000	0.0000	0.00	0.00
2AC	0	0	0.0000	0.0000	0.00	0.00
2AB	0	0	0.0000	0.0000	0.00	0.00
2AA	0	0	0.0000	0.0000	0.00	0.00
3CC	20	20	0.4831	0.4356	9.66	8.71
3CB	1	1	0.6786	1.1387	0.68	1.14
3BC	12	12	0.3058	0.3057	3.67	3.67
3BB	20	20	0.5847	0.5226	11.69	10.45
3AC	0	0	0.0000	0.0000	0.00	0.00
3AB	3	3	0.6589	0.7457	1.98	2.24
3AA	3	3	0.6119	0.7047	1.84	2.11
4CC	29	29	0.3277	0.2958	9.50	8.58
4CB	4	4	0.2195	0.2994	0.88	1.20
4BC	21	21	0.4208	0.4203	8.84	8.83
4BB	78	78	0.5418	0.5092	42.26	39.72
4BA	5	5	0.7498	0.6420	3.75	3.21
4AC	1	1	1.0992	0.0000	1.10	0.00
4AB	6	6	0.7972	0.7895	4.78	4.74
4AA	29	29	0.7279	0.5877	21.11	17.04
5CC	52	52	0.1915	0.1604	9.96	8.34
5CB	13	13	0.1043	0.1060	1.36	1.38

5CA	2	2	0.1402	0.3761	0.28	0.75
5BC	52	52	0.3136	0.2764	16.31	14.37
5BB	210	210	0.6196	0.5465	130.11	114.77
5BA	23	23	0.5758	0.5486	13.24	12.62
5AC	2	2	0.0000	0.0000	0.00	0.00
5AB	24	24	0.5385	0.4920	12.92	11.81
5AA	30	30	0.7790	0.6782	23.37	20.35
6CC	5	5	0.2555	0.3287	1.28	1.64
6CB	5	5	0.1390	0.1847	0.69	0.92
6CA	1	1	1.1842	1.6669	1.18	1.67
6BC	2	2	0.2664	0.5287	0.53	1.06
6BB	19	19	0.5367	0.4634	10.20	8.80
6BA	11	11	0.5151	0.4536	5.67	4.99
6AC	0	0	0.0000	0.0000	0.00	0.00
6AB	3	3	0.5063	0.6153	1.52	1.85
6AA	4	4	0.5753	0.6673	2.30	2.67
Total		**695**			**352.66**	**319.62**
					% Implanted	%OP/B
					50.74%	**45.99%**

Supplementary Table 8. Matrix Of Clinical Outcomes According To Mosaicism Traits And Morphology.

Values and cell colors indicate ranking, from best (Green) to worst (Red).

Euploid

Stage	Implantation	Ongoing Pregnancy/I	ICM	Implantation	Ongoing Pregnancy/Bi	TE	Implantation	Ongoing Pregnancy/Birth %
3	38.9	36.7	A	61.6	58.4	A	65.1	59.2
4	50.9	47.6	B	54.2	49.3	B	56.4	51.0
5	58.6	52.7	C	24.0	19.4	C	32.5	28.8
6	46.6	40.4						

Segmental

Stage	Implantation	Ongoing Pregnancy/I	ICM	Implantation	Ongoing Pregnancy/Bi	TE	Implantation	Ongoing Pregnancy/Birth %
3	31.3	30.7	A	61.6	58.4	A	65.1	54.9
4	45.8	37.3	B	51.9	43.4	B	49.5	41.5
5	47.5	41.5	C	14.5	11.4	C	39.5	37.3
6	n/a	n/a						

Low Level, One Chr

Stage	Implantation	Ongoing Pregnancy/I	ICM	Implantation	Ongoing Pregnancy/Bi	TE	Implantation	Ongoing Pregnancy/Birth %
3	n/a	n/a	A	54.7	48.7	A	n/a	n/a
4	40.4	39.6	B	48.3	37.5	B	50.7	41.3
5	36.3	28.2	C	32.1	23.7	C	34.1	24.2
6	n/a	n/a						

Low Level, Two Chr

Stage	Implantation	Ongoing Pregnancy/I	ICM	Implantation	Ongoing Pregnancy/Bi	TE	Implantation	Ongoing Pregnancy/Birth %
3	n/a	n/a	A	n/a	n/a	A	58.0	56.9
4	39.1	38.4	B	52.2	48.5	B	45.7	41.6
5	50.6	43.4	C	23.2	17.1	C	38.0	32.6
6	n/a	n/a						

Low Level, Complex

Stage	Implantation	Ongoing Pregnancy/I	ICM	Implantation	Ongoing Pregnancy/Bi	TE	Implantation	Ongoing Pregnancy/Birth %
3	n/a	n/a	A	n/a	n/a	A	n/a	n/a
4	52.2	37.3	B	47.1	39.0	B	52.2	34.1
5	39.1	32.1	C	32.6	12.8	C	37.0	29.7
6	n/a	n/a						

High Level, One Chr

Stage	Implantation	Ongoing Pregnancy/I	ICM	Implantation	Ongoing Pregnancy/Bi	TE	Implantation	Ongoing Pregnancy/Birth %
3	n/a	n/a	A	n/a	n/a	A	n/a	n/a
4	24.1	15.8	B	36.0	21.2	B	33.5	18.3
5	26.1	20.5	C	29.8	21.9	C	29.0	22.5
6	n/a	n/a						

High Level, Two Chr

Stage	Implantation	Ongoing Pregnancy/I	ICM	Implantation	Ongoing Pregnancy/Bi	TE	Implantation	Ongoing Pregnancy/Birth %
3	n/a	n/a	A	26.1	25.6	A	n/a	n/a
4	39.1	25.6	B	39.1	25.6	B	37.2	21.9
5	28.5	18.6	C	n/a	n/a	C	n/a	n/a
6	n/a	n/a						

High Level, Complex

Stage	Implantation	Ongoing Pregnancy/I	ICM	Implantation	Ongoing Pregnancy/Bi	TE	Implantation	Ongoing Pregnancy/Birth %
3	n/a	n/a	A	n/a	n/a	A	n/a	n/a
4	n/a	n/a	B	34.7	13.6	B	16.1	7.9
5	27.4	10.8	C	19.0	18.6	C	n/a	n/a

Supplementary Table 9. Clinical Outcomes Of Embryos With Mosaicism.

Samples involving a single monosomy or trisomy, per chromosome. Only embryos with single, whole chromosome monosomy or trisomy are included.

Chromosome	Monosomies	Implantation	% Implantation	OP/B	% OP/B	Trisomies	Implantation	% Implantation	OP/B	% OP/B
1	4	4	100%	4	100%	4	3	75%	3	75%
2	12	8	67%	6	50%	1	0	0%	0	0%
3	5	0	0%	0	0%	7	2	29%	2	29%
4	6	1	17%	1	17%	4	3	75%	2	50%
5	8	3	38%	3	38%	5	1	20%	1	20%
6	9	5	56%	4	44%	8	1	13%	1	13%

7	10	5	50%	5	50%	3	2	67%	1	33%
8	4	2	50%	1	25%	4	2	50%	2	50%
9	5	2	40%	2	40%	3	2	67%	2	67%
10	5	2	40%	2	40%	3	1	33%	0	0%
11	3	3	100%	2	67%	2	1	50%	0	0%
12	3	2	67%	1	33%	2	0	0%	0	0%
13	7	4	57%	2	29%	2	1	50%	1	50%
14	4	3	75%	3	75%	7	2	29%	2	29%
15	3	1	33%	0	0%	5	3	60%	3	60%
16	4	1	25%	1	25%	6	4	67%	3	50%
17	8	3	38%	2	25%	4	1	25%	0	0%
18	13	7	54%	7	54%	4	1	25%	1	25%
19	11	1	9%	1	9%	12	5	42%	3	25%
20	7	3	43%	2	29%	2	2	100%	1	50%
21	6	5	83%	3	50%	2	2	100%	0	0%
22	14	3	21%	1	7%	11	8	73%	5	45%
X	6	4	67%	2	33%	2	1	50%	0	0%
Total	157	72	46%	55	35%	103	48	47%	33	32%
1-12	74	37	50%	31	42%	46	18	39%	14	30%
13-22	77	31	40%	22	29%	55	29	53%	19	35%

Supplementary Table 10. Features Of Embryos Used In RNA-seq Experiment.
Chromosomal status (euploid/aneuploid) as determined by PGT-A and background (ethnicity/region) of embryos tested.

Embryo Number	Ploidy	Affected Chromosomes	Ethnicity/Region
1	Euploid	-	Central American (Mexico)
2	Euploid	-	South Asian (India)
3	Euploid	-	African/Mediterranean
4	Euploid	-	European
5	Euploid	-	African/Mediterranean
6	Euploid	-	Middle Eastern (Jewish)
7	Euploid	-	European
8	Euploid	-	African/Mediterranean
9	Aneuploid	+21	East Asian (China)
10	Aneuploid	+7,-21	Central American/European
11	Aneuploid	-15	Central American/European
12	Aneuploid	+5	European
13	Aneuploid	-17	South Asian (India)
14	Aneuploid	-21,-22	Central American/European
15	Aneuploid	+7,+22	East Asian (China)
16	Aneuploid	+4	East Asian (Japan)/European
17	Aneuploid	+16,+20	East Asian (China)
18	Aneuploid	-15,+21	South-/East Asian (Vietnam/China)
19	Aneuploid	+6	South East Asian (Indonesia)/European
20	Aneuploid	+15,+16	East Asian (China)
21	Aneuploid	+11,+12,-22	East Asian (China)
22	Aneuploid	-2	East-/South Asian (China/India)
23	Aneuploid	+16	South Asian (India)
24	Aneuploid	+15	European

Supplementary Table 11. Representation Of Non-Hatching Embryos In Experimental Groups Of The Live SARS-CoV-2 Experiments.
Breakdown of embryos by their (non-)hatching status.

SARS-CoV-2-mNeonGreen Virus

Treatment	Number of Embryos Tested	Embryos w/ Fluorescent Cells
No Treatment	9	0
No Treatment, No Hatching	1	0
Virus	19	14 (73.7%)
Virus, No Hatching	4	1 (25.0%)
Virus + anti-S neutralizing Antibody	4	0
Virus + anti-S neutralizing Antibody, No Hatching	0	0
Virus + anti-ACE2 neutralizing Antibody	4	0
Virus + anti-ACE2 neutralizing Antibody, No Hatching	1	0
Virus + anti-IgG neutralizing Antibody	7	4 (57.1%)
Virus + anti-IgG neutralizing Antibody, No Hatching	1	0